

Pricing Discretely Monitored Barrier Options and Credit Default Swaps under Lévy Processes

THESIS SUBMITTED FOR THE DEGREE OF

DOCTOR OF PHILOSOPHY

AT THE UNIVERSITY OF LEICESTER

BY

MARCO DE INNOCENTIS

DEPARTMENT OF MATHEMATICS

UNIVERSITY OF LEICESTER

DECEMBER 2012

Pricing discretely monitored barrier options and credit default swaps under Lévy processes

Marco de Innocentis

Abstract

We introduce a new, fast and accurate method to calculate prices and sensitivities of European vanilla and digital options under the Variance Gamma model. For near at-the-money options of short maturity, our method is much faster than those based on discretization and truncation of the inverse Fourier transform integral (iFT method). We show that the results calculated with our method agree with those obtained with the iFT algorithm using very long and fine grids. Taking the results of our method as a benchmark, we show that the parabolic modification of the iFT method (Boyarchenko and Levendorskii, 2012) is much more efficient than the standard (flat) version. Based on this conclusion, we consider an approach which uses a combination of backward induction and parabolic iFT to price discretely monitored barrier options, as well as credit default swaps, under wide classes of Lévy models. At each step of backward induction, we use piece-wise polynomial interpolation and parabolic iFT, which allows for efficient error control. We derive accurate recommendations for the choice of parameters of the numerical scheme, and produce numerical examples showing that oversimplified prescriptions in other methods can result in large errors.

Acknowledgements

I am greatly indebted to my supervisor, Sergei Levendorskiĭ, for his invaluable guidance and advice during the time of my research studies. I would also like to thank Wilhelm Klingenberg, Jimmy Law, Jeremy Levesley, Enzo Michelangeli, and Jiayao Xie for their support, insights, and useful discussions. All errors and omissions in this thesis are the sole responsibility of the author.

Finally, special thanks to my wife, my parents, my brother and my sister for their support and understanding during the last three years.

Contents

Abstract	i
Acknowledgements	ii
Chapter 1. Introduction	1
1.1. The inverse Fourier transform pricing method for European options	1
1.2. Discretely monitored barrier options	2
1.3. Organisation of the thesis	4
Chapter 2. European option pricing under Lévy models	6
2.1. Financial modelling under Lévy processes	6
2.2. The iFT pricing method	10
2.3. Parabolic iFT method for European vanilla options	15
Chapter 3. Fast pricing of European options under VG	23
3.1. General remarks	23
3.2. ATM case	24
3.3. Non-ATM case	33
3.4. Algorithms and numerical results	39
3.5. Analysis of relative performance of flat and parabolic iFT	50
Chapter 4. Pricing discretely monitored barrier options under Lévy processes	55
4.1. General remarks	55
4.2. General scheme for pricing down-and-out put options	57

4.3. Error estimates	65
4.4. Comparison of relative performance of different methods	71
Chapter 5. Pricing credit default swaps under Lévy processes	81
5.1. General remarks	81
5.2. Numerical results	86
Chapter 6. Conclusions	90
Appendix A. Lévy processes: general background and results	92
A.1. Main definitions	92
A.2. Regular Lévy processes of exponential type	95
A.3. Measure changes for Lévy processes	97
Appendix B. Algorithms for vanilla option pricing using flat iFT	101
B.1. Calculation of option price as function of strike using FFT	101
B.2. Calculation of option price as function of spot using iFFT	102
B.3. Calculation of option price as function of strike using refined FFT	102
B.4. Calculation of option price as function of spot using refined FFT	104
Appendix C. Truncation error bounds for the VG option price	105
C.1. Flat iFT case	105
C.2. Parabolic iFT (ATM case)	107
Appendix D. A put-call symmetry	111
Appendix E. Comparison of different quadrature methods	113
E.1. ATMVG case	113
E.2. FastVG case	114
Appendix F. Deltas and digitals	116

Appendix G. Discretization error bound for $\Psi_1(x; \sigma, 0; \Lambda)$.	118
Appendix H. Pricing algorithm for discretely monitored barrier options	121
Appendix I. Other interpolation methods	124
I.1. Piece-wise linear interpolation	124
I.2. Piece-wise cubic interpolation	124
Appendix J. Additional numerical results for Chapter 4	126
Appendix K. Other types of barrier options	128
K.1. Down-and-out call option	128
K.2. Up-and-out put and call options	128
K.3. Down-and-in and up-and-in options	128
K.4. Options with rebate and first-touch digitals	128
K.5. Double barrier options	129
Appendix L. Fast convolution algorithm	130
Appendix M. Technical calculations	132
M.1. Proof of Lemma 4.1	132
M.2. Proof of Lemma 4.3	135
M.3. Proof of Lemma 4.4	136
M.4. Proof of Proposition 4.6	138
M.5. Proof of Lemma 4.7	140
M.6. Error bounds for the CDS price	142
Appendix N. Benchmark prices used in numerical examples	145
Appendix O. The iFT method for put-like options	146
O.1. Flat iFT method	146

O.2. Parabolic iFT method (case $x' \geq 0, \omega > 0$)	152
O.3. General implementation scheme for parabolic iFT	157
Appendix P. Hilbert transform method	160
P.1. General idea	160
P.2. Algorithms	161
Appendix Q. COS method	165
Q.1. Main details	165
Q.2. Algorithm	169
Appendix. Bibliography	172

CHAPTER 1

Introduction

1.1. The inverse Fourier transform pricing method for European options

The Fourier Transform (FT) method, a standard tool in applied mathematics, was introduced to option pricing by Heston [51] and Eydeland [41] for the case of diffusion models, by Boyarchenko and Levendorskiĭ [16, 17, 18] and Carr and Madan [28] for the case of Lévy models, and was later extended for term structure models in [38, 30, 40, 15]. It is now one of the most popular methods used by practitioners to price European options under Lévy¹ and stochastic volatility models. As will be shown in Chapter 2, for European options under Lévy processes, the FT method reduces the option pricing problem to the simplified trapezoid rule for an integral involving the inverse Fourier transform of the payoff. Following [19, 36], we call this sequence *inverse Fourier Transform (iFT) method*. In [19], several new efficient variations of the iFT method were developed and analyzed, one of which, parabolic iFT, was applied in [36] to price barrier options. As shown in [19], all versions of the iFT pricing method for European options face the greatest difficulties when dealing with at-the-money or near at-the-money options of short maturity, especially under Lévy processes of order close to zero. In Chapter 3 we present a new method, introduced in [35], for the pricing of short maturity options under the Variance Gamma model, and show that it is much more accurate for (near) at-the-money options than either ordinary (flat) or parabolic iFT. Using the prices obtained with the new method as a benchmark, we show that parabolic iFT can be much faster and more accurate than

¹For some background on Lévy processes, see Appendix A.

flat iFT, especially for short maturity and near at-the-money options, confirming the results in [19].

1.2. Discretely monitored barrier options

A discretely monitored (or discrete) barrier option differs from one with continuous monitoring in that the breaching of the barrier level is only observed at a finite set of times (e.g., once a day). In the foreign exchange (FX) market, discrete monitoring has become increasingly popular in recent years, especially for pairs against the euro and daily frequency linked to European Central Bank (ECB) fixing. The monitoring officially takes place at 14:15 CET every working day, although the underlying rate is only released 5-10 minutes later, upon publication by the ECB, on Reuters page ECB37, of an average of quotes from a pool of market makers for FX spot rates against the euro [6, 29].

From the point of view of option pricing, continuous monitoring is an advantage in the Black-Scholes framework, since it leads to simple analytical formulas for the option price (the interested reader may wish to consult, for example, the bibliography lists in [24] and [20]). However, in a more realistic setting in which the underlying follows a jump-diffusion or a pure jump process, no closed form solutions are available, except for particular model classes. Nevertheless, continuously monitored barrier options with one or two barriers can be priced very efficiently using the BBL method, introduced by S. Boyarchenko, M. Boyarchenko and Levendorskiĭ [18, 13, 11]. The BBL method and a closely related method developed by Kudryavtsev and Levendorskiĭ [57] are based on Carr's randomization [25] and an efficient realization of the Wiener-Hopf factorization [84].

For the most difficult case of pure jump processes, the BBL method is extremely accurate even near the barrier, unlike other methods, such as jump-diffusion approximations [12]. However, it cannot be used for the pricing of discrete barrier options. We present an alternative technique for the discrete monitoring case, introduced in [36], based on a backward induction procedure, together with piece-wise polynomial interpolation at each step and parabolic iFT.

The backward induction approach for discrete barrier options was used by Eydeland in the context of discrete path-dependent options in the gaussian framework [41]. At each step, going backwards from maturity, one computes the convolution of the value function of the option at the next monitoring date with the transition probability density between the two dates. An approximation to the discretized and truncated version of the integral is then calculated using the Toeplitz matrix-vector multiplication algorithm (cf. Appendix P.2.4). Thus, the problem of pricing a barrier option is reduced to pricing a sequence of European options. The method requires $O(NM \log_2 M)$ operations, where N is the number of monitoring dates and M the number of points in the discretized and truncated version of the integral. This approach was subsequently extended by Feng and Linetsky in [45] to the case of non-gaussian Lévy processes, using the fact that the multiplication of a function by the indicator function in the state space can be expressed in terms of the Hilbert transform in the dual space (cf. Appendix P). This observation, together with the powerful approximation theory of analytical functions in Hardy spaces, allowed the authors of *op. cit.* to develop a remarkably efficient procedure (HT method) for pricing discrete barrier options, together with a set of estimates for the discretization and truncation errors. The method requires $O(NM \log_2 M)$ operations, where M is now the number of points in the discretized and truncated dual space grid used to compute the Hilbert transform at each step.

A different generalization of the Eydeland method for discrete barrier options to the case of Lévy processes was introduced in [64] (convolution, or CONV method), in which an FFT-based approach is used to calculate the convolution of the modified option price and the transition probability density. The cosine or COS method uses a similar approach, based on the Fourier cosine expansion of the option price at each time step [44]. Both methods require $O(NM \log_2 M)$ operations, where M is the number of grid points (CONV method) or the number of terms in the cosine expansion (COS method).

Finally, the Fast Gaussian Transform (FGT) method, introduced to finance by Broadie and Yamamoto in [21] for European options, was used by the same authors in [22] for the pricing of discrete barrier options under models in which the distribution of the underlying is a mixture of independent gaussians (as in Merton's jump diffusion model [72]). The method requires only $O(NM)$ operations, where M is the number of sample points at each date used in the computation of the FGT. However, this approach does not generalize to the case of non-gaussian distributions.

We show that, while the HT and COS methods can be efficient if the numerical parameters of each scheme are chosen close to optimally, the error control in either case is non-trivial, especially for options of longer maturity, due to the presence of several interacting sources of errors. Our method, on the other hand, behaves as if the interpolation at each step, which is easier to control, were the only source of error. We also show that, in some cases, our method is much faster than the HT method.

1.3. Organisation of the thesis

In Chapter 2 we include some background on option pricing under Lévy models, and describe in detail the iFT pricing method, as well as its modification (parabolic iFT), introduced in [19]. In Chapter 3 we describe a new method, introduced in [35],

which can be used to price European vanilla and digital options under the Variance Gamma model, and calculate their sensitivities. We show that the new method is much faster and more accurate in the case of at-the-money and near at-the-money options, in which the application of iFT techniques faces the greatest difficulties, especially for short times to maturity. Using the prices calculated with the new method as benchmarks, we show that the parabolic iFT method is much more accurate than flat iFT. In Chapter 4 we introduce a new method, based on backward induction, piece-wise polynomial interpolation at each step, and parabolic iFT, to price discretely monitored barrier options. We derive error bounds and recommendations for the choice of numerical parameters, and show that the prescriptions in other methods can produce large errors. Finally, in Chapter 5, we describe a modification of the method which can be used to price credit default swaps.

Background details and technical calculations are relegated to the appendices.

CHAPTER 2

European option pricing under Lévy models

2.1. Financial modelling under Lévy processes

We consider a model with a simplified market consisting of a riskless bank account B yielding a constant, continuously compounded interest rate r (known as the riskless or risk-free rate), so that its value at time t is given by $B_t = B_0 e^{rt}$, and a stock S with a constant, continuously compounded dividend yield q . In addition, our market includes a *derivative* or *contingent claim* security on the stock S , whose future payoff(s) depend on the future realizations of the value process of the stock, $\{S_t\}$. Typical examples of a contingent claim are European vanilla call and put options with expiry (or maturity) date T and strike price K . A call option gives the holder the right, but not the obligation, to buy the underlying stock at time T for price K . Hence, the holder stands to gain $(S_T - K)_+ = \max\{S_T - K, 0\}$ at expiry. This is known as the *terminal payoff* of the option. Similarly, a put option gives the holder the right to sell the underlying at time T for price K , and has terminal payoff $(K - S_T)_+$.

In order to develop a pricing approach, two important assumptions are usually made. First, one assumes that the market is *frictionless*, i.e., there are no transaction costs, unlimited borrowing and lending is allowed, and the rates for borrowing and lending, in the same currency, are the same. These assumptions are generally considered to be valid for large institutional investors. In addition, one assumes that the Efficient Market Hypothesis (EMH) holds, according to which all market agents are rational and have access to the same information¹.

¹This assumption can be relaxed (see [79, 76]).

2.1.1. The Equivalent martingale measure (EMM). It is well-known that, if the market is arbitrage-free², then all prices of contingent claims can be interpreted as expected values under a certain pricing measure \mathbb{Q} , equivalent to the historical measure \mathbb{P} , such that the discounted stock price process, with the re-invested dividends, is a martingale under \mathbb{Q} . \mathbb{Q} is known as the “equivalent martingale measure” (EMM) or the “risk-neutral measure” [48, 49, 50, 37, 80]. If the EMM exists and is unique, one says that the market is *complete*. Otherwise, if the EMM exists but is not unique, one says that the market is *incomplete*.

Whereas in the classic Black-Scholes-Merton model [10, 71] the market is complete, under a more general Lévy model, the market is incomplete and the EMM \mathbb{Q} is “chosen by the market” [8]. This means that the parameters of the underlying process under \mathbb{Q} can only be recovered by calibrating the pricing model to the traded prices of liquid derivative products, such as vanilla options [31].

We assume that $S_t = e^{X_t}$, where X is a Lévy process of exponential type³ (λ_-, λ_+) , where $\lambda_- \leq -1 \leq 0 \leq \lambda_+$ (see Definition A.7). In order \mathbb{Q} to be an EMM, we must have

$$\mathbb{E}^{\mathbb{Q}}[e^{-(r-q)t}S_t] = e^{-(r-q)t}\mathbb{E}^{\mathbb{Q}}[e^{X_t}] = e^{(-r+q+\psi^{\mathbb{Q}}(-i))t}S_0,$$

where $\psi^{\mathbb{Q}}$ denotes the characteristic exponent of X under \mathbb{Q} (cf. Appendix A.1). It follows that the EMM condition for \mathbb{Q} is

$$r - q + \psi^{\mathbb{Q}}(-i) = 0. \tag{1}$$

²I.e., if it is impossible to lock in a future nonnegative return with nonzero probability. More formally, if V_t denotes the value of a *self financing* portfolio at time t , then an arbitrage opportunity exists if $V_t = 0$, $\mathbb{P}(V_T \geq 0) = 1$, and $\mathbb{P}(V_T > 0) > 0$, for some $T > t$, where \mathbb{P} denotes the historical probability measure. For more details, including the definition of a self financing portfolio, see [8].

³For the purpose of this chapter, it suffices to know that the characteristic exponent $\psi(\xi)$ of such a process admits the analytic continuation into the strip $\text{Im } \xi \in (\lambda_-, \lambda_+)$.

Note that the reason why we take $\lambda_- \leq -1$ is that we require $\psi^{\mathbb{Q}}(\xi)$ to admit the analytic continuation into the closed strip $-1 \leq \text{Im } \xi \leq 0$. If this is not the case, then $\mathbb{E}[e^{X_t}] = \infty$ for all $t > 0$, i.e., the process $\{S_t\}$ cannot be priced; we exclude this situation from our consideration. From now on, for simplicity, it will be assumed that $\lambda_- < -1 < 0 < \lambda_+$. We will also usually write ψ instead of $\psi^{\mathbb{Q}}$ and \mathbb{E} instead of $\mathbb{E}^{\mathbb{Q}}$, with the understanding that, unless stated otherwise, all expectations are taken under \mathbb{Q} .

2.1.2. Model processes. The main classes of processes used in the study of financial markets enjoy the following property: there exist $\lambda_- < -1 < 0 < \lambda_+$ such that the underlying Lévy process X is of exponential type (λ_-, λ_+) . In fact, almost all Lévy processes used in financial modelling belong to the more restricted class of regular Lévy processes of exponential type (RLPEs, see Definition A.9), the only notable exception being the Variance Gamma model. RLPEs commonly used in option pricing include Brownian Motion, the Merton model [72], and the KoBoL model (cf. Example A.5) of order $\nu \in (0, 2)$, $\nu \neq 1$ [53, 17, 18], with characteristic exponent given by⁴

$$\psi(\xi) = -i\mu\xi + c\Gamma(-\nu)[\lambda_+^\nu - (\lambda_+ + i\xi)^\nu + (-\lambda_-)^\nu - (-\lambda_- - i\xi)^\nu], \quad (2)$$

where $c > 0$, $\lambda_- < -1 < 0 < \lambda_+$, $\mu \in \mathbb{R}$. They also include NIG (Normal Inverse Gaussian model [5]), hyperbolic processes [39], the double-exponential jump-diffusion model [62, 63, 54, 55, 56], its generalization constructed in [61] and labelled later hyper-exponential jump-diffusion model, and the majority of processes of the β -class [58]. Note that the parameter ν in (2) corresponds to the order of the process in the sense of Definition A.9. For the Variance Gamma process (VGP or VG model for

⁴For the expression of the KoBoL characteristic exponent of order $\nu = 1$, see [18, §3.1.2.2].

short) [69, 67, 66], we have

$$\psi(\xi) = -i\mu\xi + c \left[\ln \frac{\lambda_+ + i\xi}{\lambda_+} + \ln \frac{-\lambda_- - i\xi}{-\lambda_-} \right], \quad (3)$$

where $c > 0$ and $\lambda_- < -1 < 0 < \lambda_+$ (we use this non-standard parametrization of the VG model to make the analogy with KoBoL more transparent). The VG model can be naturally regarded as a process of order $\nu = 0$ (cf. Example A.5).

The most efficient conformal iFT methods developed in [19] require that $\psi(\xi)$ admit the analytic continuation into the complex plane with two cuts $i(-\infty, \lambda_-]$ and $i[\lambda_+, \infty)$ and satisfy certain conditions on growth as $\xi \rightarrow \infty$ in the complex plane with the cuts. These conditions are satisfied for the model classes of Lévy processes cited above. For a general definition of the class of strongly regular Lévy processes of exponential type, which enjoys these properties, see [12, 59]. In developing our pricing method for discretely monitored barrier options and CDS, in Chapters 4 and 5, respectively, we will consider a slightly different class of processes, for which the characteristic exponent $\psi(\xi)$ is of the form $\psi(\xi) = -i\mu\xi + \psi^0(\xi)$, for some $\mu \in \mathbb{R}$, so that $\psi^0(\xi)$ admits the analytic continuation into the complex plane with the cuts $i(-\infty, \lambda_-]$, $i[\lambda_+, \infty)$, $\lambda_- < -1 < 0 < \lambda_+$, and is such that, for $\rho \rightarrow \infty$, $\omega \in (\lambda_-, \lambda_+)$, and $\phi \in (-\pi/2, \pi/2)$,

$$\psi^0(i\omega + e^{i\phi}\rho) = d_+^0 e^{i\phi\nu} \rho^\nu (1 + O(\rho^{-1})), \quad (4)$$

$$\partial_\rho \operatorname{Re} \psi^0(i\omega + e^{i\phi}\rho) = \nu d_+^0 \cos(\phi\nu) \rho^{\nu-1} (1 + o(1)), \quad (5)$$

where $d_+^0 > 0$. For a KoBoL process of order $\nu > 0$, $d_+^0 = -c\Gamma(-\nu) (i^\nu + (-i)^\nu) = -2c\Gamma(-\nu) \cos(\pi\nu/2)$. We will refer to the class of such processes, together with VG, as model processes. We note that almost all Lévy processes used in finance belong to this class.

2.2. The iFT pricing method

Following [19], we outline the main details of the iFT pricing method for European options. The value function $V(\tau, X_t) := V(G; T; t, X_t)$ of a European option with payoff at maturity $G(X_T)$ and time to maturity $\tau = T - t$ is given by

$$V(\tau, x) = \mathbb{E}[e^{-r\tau} G(X_T) | X_t = x]. \quad (6)$$

In what follows, we assume that X is a model process of exponential type (λ_-, λ_+) , and the Fourier transform \widehat{G} of G satisfies the condition

$$|\widehat{G}(\xi)| = O(\xi^{-1}), \quad (7)$$

for $\xi \rightarrow \infty$ along any line $\text{Im } \xi = \omega$, with the exception of a finite number of omegas (this condition is satisfied for both vanilla and digital options, cf. Examples 2.1 and 2.2, respectively). We decompose the payoff G into the Fourier integral

$$G(x) = \frac{1}{2\pi} \int_{\text{Im } \xi = \omega} e^{ix\xi} \widehat{G}(\xi) d\xi, \quad (8)$$

where $\omega \in (\lambda_-, \lambda_+)$ is such that $e^{\omega x} G(x) \in L^1(\mathbb{R})$. Substituting this into (6), we obtain

$$\begin{aligned} V(\tau, x) &= \frac{e^{-r\tau}}{2\pi} \mathbb{E} \left[\int_{\text{Im } \xi = \omega} e^{iX_T \xi} \widehat{G}(\xi) d\xi \middle| X_t = x \right] \\ &= \frac{e^{-r\tau}}{2\pi} \int_{\text{Im } \xi = \omega} e^{ix\xi} \mathbb{E}[e^{iX_T \xi}] \widehat{G}(\xi) d\xi \\ &= \frac{e^{-r\tau}}{2\pi} \int_{\text{Im } \xi = \omega} e^{ix\xi - \tau\psi(\xi)} \widehat{G}(\xi) d\xi, \end{aligned} \quad (9)$$

where the standard properties of Lévy processes have been used (cf. Appendix A.1), and the application of Fubini's theorem is justified due to the regularity assumption (7) for G , together with the fact that, for a model process with $\nu > 0$, $e^{-\tau\psi(\xi)}$ decays

at infinity faster than $|\xi|^{-N}$, for any $N > 0$, while for VG it decays as $|\xi|^{-2c\tau}$, where $c > 0$, $\tau > 0$ (cf. (2) and (3), respectively).

Example 2.1 (Fourier transform of the vanilla option payoff). For a vanilla put option with strike K , the terminal payoff is given by $G(x) = (K - e^x)_+$. We have $G \notin L_1(\mathbb{R})$, but $e^{\omega x}G(x) \in L_1(\mathbb{R})$, for all $\omega > 0$. Hence, the Fourier transform of G , $\widehat{G}(\xi)$, is defined in the open upper half-plane $\{\xi \in \mathbb{C} \mid \text{Im } \xi > 0\}$, and is given there by

$$\begin{aligned} \widehat{G}(\xi) &= \mathcal{F}_{x \rightarrow \xi}((K - e^x)_+) = \int_{-\infty}^{\ln K} (Ke^{-i\xi x} - e^{(-i\xi+1)x})dx \\ &= -\frac{Ke^{-i\xi \ln K}}{i\xi} + \frac{Ke^{-i\xi \ln K}}{i\xi - 1} = -\frac{Ke^{-i\xi \ln K}}{(\xi + i)\xi}. \end{aligned} \quad (10)$$

Similarly, for a vanilla call option, with terminal payoff $G(x) = (e^x - K)_+$, the Fourier transform of G is defined in the open lower half-plane $\{\xi \in \mathbb{C} \mid \text{Im } \xi < -1\}$, and is also given there by (10).

Example 2.2 (Fourier transform of the digital option payoff). For a digital put option with strike K , the terminal payoff is given by $G(x) = \mathbb{1}_{(-\infty, \ln K]}(x)$. As in the vanilla put case, the Fourier transform of G , $\widehat{G}(\xi)$, is defined in the open upper half-plane $\{\xi \in \mathbb{C} \mid \text{Im } \xi > 0\}$. It is given there by

$$\widehat{G}(\xi) = \mathcal{F}_{x \rightarrow \xi}(\mathbb{1}_{(-\infty, \ln K]}(x)) = \int_{-\infty}^{\ln K} e^{-i\xi x} dx = \frac{e^{-i\xi \ln K}}{-i\xi}. \quad (11)$$

Similarly, for a digital call option, with terminal payoff $G(x) = \mathbb{1}_{[\ln K, \infty)}(x)$, the Fourier transform of G is defined in the open lower half-plane $\{\xi \in \mathbb{C} \mid \text{Im } \xi < 0\}$, and is given there by $\widehat{G}(\xi) = e^{-i\xi \ln K}/(i\xi)$.

Example 2.3 (Vanilla option price as a function of spot). Let S denote the current price of the underlying. If we redefine $x = \ln(S/K)$, in order to get rid of the oscillating factor in (10), then equation (9), for the case of a vanilla call or put

option, becomes

$$V(\tau, x) = -\frac{Ke^{-r\tau}}{2\pi} \int_{\text{Im}\xi=\omega} \frac{e^{ix\xi - \tau\psi(\xi)}}{\xi(\xi + i)} d\xi, \quad (12)$$

with $\omega \in (\lambda_-, -1)$ for the call and $\omega \in (0, \lambda_+)$ for the put option, respectively.

Example 2.4 (Vanilla option price as a function of strike). In practical calculations, it is sometimes more convenient to calculate the option price as a function of strike, since, at any one moment, only one spot price is observed, but several liquid options exist with different strikes and maturities. To this end, we set $x = \ln(K/S)$ and re-write formula (12) for the vanilla option as follows

$$V(\tau, x) = -\frac{Se^{-r\tau}}{2\pi} e^x \int_{\text{Im}\xi=\omega} \frac{e^{ix\xi - \tau\psi(\xi)}}{\xi(\xi + i)} d\xi. \quad (13)$$

2.2.1. The fast Fourier transform. In order to calculate the option price numerically using the ordinary (or flat) iFT method, one considers a truncated and discretized version of integral (9)

$$V(\tau, x) \approx e^{-r\tau} \frac{\zeta}{2\pi} \sum_{k=1}^M e^{ix\xi_k} e^{-\tau\psi(\xi_k)} \widehat{G}(\xi_k), \quad (14)$$

where, for some suitably large $\Lambda > 0$, we have $\boldsymbol{\xi} = (\xi_k)_{k=1}^M$, $\xi_k = -\Lambda + i\omega + (k-1)\zeta$, $k = 1, 2, \dots, M$, $\zeta = 2\Lambda/M$. In the case of vanilla call and put options, we obtain from (12)

$$V(\tau, x) \approx -\frac{K\zeta}{2\pi} \sum_{k=1}^M e^{ix\xi_k} f_k, \quad (15)$$

where

$$f_k = e^{-\tau(r+\psi(\xi_k))} / (\xi_k(\xi_k + i)). \quad (16)$$

The procedure for the case of the option price as a function of strike (cf. (13)) is similar. In practice, the calculation of (15) can be carried out using the well-known Fast Fourier Transform (FFT) algorithm [33]. If the price as a function of spot is

needed (i.e., if $x = \ln(S/K)$, K is fixed, and S varies), then the inverse FFT (iFFT) algorithm can be used, while for the price as a function of strike (i.e., if $x = \ln(K/S)$, S is fixed, and K varies), the FFT can be used.

2.2.1.1. *Ordinary and refined FFT.* Let f be a function on \mathbb{R} . We define the *discrete Fourier transform* of f as follows

$$(\mathcal{F}_{\text{disc}}f)(\xi) = \Delta \sum_{j=1}^M f(x_j) e^{-i\xi x_j}.$$

We note that $\mathcal{F}_{\text{disc}}f$ depends only on the array $(f(x_j))_{j=1}^M$ of values of f on the evenly spaced grid of points $\mathbf{x} = (x_j)_{j=1}^M$. Consider an evenly spaced grid $\boldsymbol{\xi} = (\xi_j)_{j=1}^M$ of points in \mathbb{C} such that $\xi_k = \xi_1 + (k-1)\zeta$, where $\zeta > 0$ is a fixed real number. Given a function g on \mathbb{C} , we define the *inverse discrete Fourier transform* of g as follows

$$(\mathcal{F}_{\text{disc}}^{-1}g)(\xi) = \frac{\zeta}{2\pi} \sum_{k=1}^M g(x_k) e^{ix\xi_k}.$$

In general $\mathcal{F}_{\text{disc}}$ and $\mathcal{F}_{\text{disc}}^{-1}$ need not be the inverse of each other. However, it is a well-known result that if the following condition, sometimes known as the uncertainty principle or the Nyquist relation, holds

$$\Delta\zeta = \frac{2\pi}{M}, \tag{17}$$

then, if f is a function whose domain of definition includes the grid $\mathbf{x} = (x_j)_{j=1}^M$, and $g(\xi) = (\mathcal{F}_{\text{disc}}f)(\xi)$, we have $f(x_j) = (\mathcal{F}_{\text{disc}}^{-1}g)(x_j)$, $j = 1, \dots, M$. In practice, there are many situations in which one has a function f defined on an evenly spaced grid $\mathbf{x} = (x_j)_{j=1}^M$ and wishes to calculate $\mathcal{F}_{\text{disc}}f$ on the evenly spaced grid $\boldsymbol{\xi} = (\xi_j)_{j=1}^{M_1}$ with different length M_1 and such that $\xi_k = \xi_1 + (k-1)\zeta$, and $\zeta > 0$ is fixed, however, condition (17) does not hold. A procedure which is sometimes used in these situations

is the “fractional FFT” method of Bailey and Swartztrauber [4], which results in an increase in the cost of the algorithm by a factor of 6. Fractional FFT does not rely on the uncertainty principle, however it requires both grids to be of equal length, i.e. $M = M_1$. Alternatively, a new FFT setup, introduced by M. Boyarchenko and Levendorskii in [14], can be used. This allows one to choose two positive integers M_2 and M_3 , which are used to stretch and refine the ξ grid, respectively. The total number of points in the ξ grid becomes $M_1 = MM_2M_3$. As noted in [14], one should still take M to be a power of 2, as in the ordinary FFT algorithm, but M_2 and M_3 can be arbitrary positive integers. This improved setup allows one to calculate the FFT of the function f on the grid $\xi' = (\xi_k)_{k=1}^{M_1}$, where $\xi_k = \xi_1 + (k-1)\zeta_1$, $k = 1, \dots, M_1$, and $\zeta_1 = \zeta/M_3$. We refer to this as the *refined FFT* method. Details of the flat iFT pricing algorithm, for both ordinary and refined FFT, can be found in Appendix B.

2.2.2. Reduction to an integral over the real half-line. Performing the change of variables $\xi = \eta + i\omega$ in (12), we obtain

$$V(\tau, x) = \frac{e^{-\omega x}}{2\pi} \int_{\mathbb{R}} e^{ix\eta - \tau(r + \psi_\omega(\eta))} \widehat{G}_\omega(\eta) d\eta, \quad (18)$$

where $\psi_\omega(\eta) = \psi(i\omega + \eta)$ and $\widehat{G}_\omega(\eta) = \widehat{G}(i\omega + \eta)$. As noted in [19], taking into account that, for real η, ω

- i. for a real valued function G , $\overline{\widehat{G}(i\omega + \eta)} = \widehat{G}(i\omega - \eta)$;
- ii. in particular, the characteristic function of a real-valued random variable, and hence the characteristic exponent ψ , enjoy the same property: $\overline{\mathbb{E}[e^{i(i\omega + \eta)X_t}]} = \mathbb{E}[e^{i(i\omega - \eta)X_t}]$, and $\overline{\psi(i\omega + \eta)} = \psi(i\omega - \eta)$,

we can write

$$\begin{aligned}
V(\tau, x) &= \frac{e^{-\omega x}}{2\pi} \left(\int_{-\infty}^0 + \int_0^{+\infty} \right) e^{ix\eta - \tau(r + \psi_\omega(\eta))} \widehat{G}_\omega(\eta) d\eta \\
&= \frac{e^{-\omega x}}{2\pi} \int_0^{+\infty} \left(e^{ix\eta - \tau(r + \psi_\omega(\eta))} \widehat{G}_\omega(\eta) + e^{-ix\eta - \tau(r + \psi_\omega(-\eta))} \widehat{G}_\omega(-\eta) \right) d\eta \\
&= \frac{e^{-\omega x}}{2\pi} \operatorname{Re} \int_0^{+\infty} e^{ix\eta - \tau(r + \psi_\omega(\eta))} \widehat{G}_\omega(\eta) d\eta.
\end{aligned} \tag{19}$$

Since (19) is the same integral (18) written in a slightly different form, the discretization and truncation errors will be the same in both cases. However, the number of terms in appropriate quadratures will be twice smaller when (19) is used, hence, the CPU time will be twice smaller as well.

2.2.3. Error control. There are two sources of error in the numerical realization of (18) or (19): discretization and truncation of the integral on the RHS. A detailed discussion of the discretization error for the flat iFT method, in a slightly more general context, can be found in Appendix O.1.1, together with recommendations for the choice of offset ω and mesh ζ . Estimates for the truncation error for flat iFT, for different classes of Lévy processes, can be found in [19]. We do not include them here, since they are not relevant for our purposes, except for the case of VG, for which we present a more accurate error bound (the details can be found in Appendix C.1).

2.3. Parabolic iFT method for European vanilla options

This method, introduced in [19], relies on deforming the contour of integration in (18) or (19) under a conformal map, such that the integrand decays faster along the deformed contour. Two versions of the method were introduced in *op. cit.*, one for put options with $x' = \ln(S_t/K) + \mu\tau \geq 0$ and one for call options with $x' \leq 0$. Although it is not strictly necessary to use both, due to the symmetry relations outlined in

Appendix D, we describe both cases in some detail, since the call version was used for the comparisons in [35], on which Chapter 3 is based, while the put version was used in [36], on which Chapter 4 is based.

As in [19], we refer to the situation in which $x' = x + \mu\tau = 0$ as the at-the-money (ATM) case⁵, for both call and put options. Similarly, we define a call (put) option to be out-of-the-money (OTM) if $x' < 0$ ($x' > 0$), and to be in-the-money (ITM) if it is neither ATM nor OTM. For the remainder of this chapter, we follow the exposition in [19].

2.3.1. ATM and OTM put case (KoBoL, $x' \geq 0$, $\nu \in (0, 2)$, $\nu \neq 1$). Recall that the price of the vanilla put option with strike K is given by (12), with $\omega \in (0, \lambda_+)$. We can deform the contour of integration in (12) under the conformal map χ_α^+ , defined on the half-plane $\text{Im } \xi < \lambda_+$ by

$$\chi_\alpha^+(\xi) = i\lambda_+ - i\lambda_+^{1-\alpha}(\lambda_+ + i\xi)^\alpha \quad (20)$$

for $\alpha \in [1, 2]$. If $\alpha \in (1, 2)$, then the image of the half-plane $\text{Im } \xi < \lambda_+$ is the obtuse angle

$$\{i\lambda_+ + z \mid z \neq 0, \arg z \notin [\pi/2 - \pi(1 - \alpha/2), \pi/2 + \pi(1 - \alpha/2)]\}.$$

For $\alpha = 2$, the image is the complex plane with the cut $i[\lambda_+, \infty)$. Figure 1 illustrates typical curves of the modified contour $\chi_\alpha^+(\xi)$ for different values of α .

⁵We note that this definition differs slightly from the various ones used by practitioners.

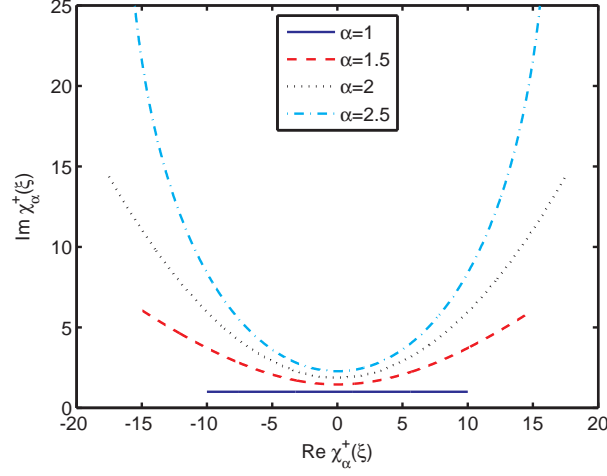


FIGURE 1. Typical curves of $\chi_\alpha^+(\xi) = i\lambda_+ - i\lambda_+^{1-\alpha}(\lambda_+ + i\xi)^\alpha$, $\xi = i\omega + \mathbb{R}$ ($\lambda_+ = 8$, $\omega = 1$).

As in [19], denote by $\mathcal{L}_{\omega; \chi_\alpha^+}$ the image of the line $\text{Im } \xi = \omega \in (0, \lambda_+)$ under χ_α^+ . Using Cauchy's theorem, one can deform the contour of integration in (12) and obtain

$$V(\tau, x) = -\frac{Ke^{-r\tau}}{2\pi} \int_{\mathcal{L}_{\omega; \chi_\alpha^+}} \frac{e^{ix'\xi - \tau\psi^0(\xi)}}{\xi(\xi + i)} d\xi, \quad (21)$$

where $\psi^0(\xi) = \psi(\xi) + i\mu\xi$. The justification of the contour deformation for KoBoL, VG, and NIG, can be found in [19]. We shall only focus on the KoBoL case with $\nu(0, 2)$, $\nu \neq 1$, since it is the only relevant one for our purposes. Changing the variable $\xi \mapsto \chi_\alpha^+(\xi)$ in (21), one obtains

$$V(\tau, x) = -\frac{Ke^{-r\tau}}{2\pi} \int_{\text{Im } \xi = \omega} \frac{e^{ix'\chi_\alpha^+(\xi) - \tau\psi^0(\chi_\alpha^+(\xi))}}{\chi_\alpha^+(\xi)(\chi_\alpha^+(\xi) + i)} \alpha \left(\frac{\lambda_+ + i\xi}{\lambda_+} \right)^{\alpha-1} d\xi. \quad (22)$$

Similarly to the case of (19) for flat iFT, one can reduce the integral on the RHS of (22) to the positive half-line, by considering that, if $\xi = i\omega + \eta$, where $\eta, \omega \in \mathbb{R}$, then $\overline{i\xi} = i(i\omega - \eta)$, hence $\overline{i\chi_\alpha^+(i\omega + \eta)} = i\chi_\alpha^+(i\omega - \eta)$, and $\overline{\psi^0(\chi_\alpha^+(i\omega + \eta))} = \psi^0(\chi_\alpha^+(i\omega - \eta))$.

One obtains

$$V(\tau, x) = -\frac{Ke^{-r\tau}}{\pi} \operatorname{Re} \int_{i\omega}^{i\omega+\infty} \frac{e^{ix'\chi_\alpha^+(\xi) - \tau\psi^0(\chi_\alpha^+(\xi))}}{\chi_\alpha^+(\xi)(\chi_\alpha^+(\xi) + i)} \alpha \left(\frac{\lambda_+ + i\xi}{\lambda_+} \right)^{\alpha-1} d\xi. \quad (23)$$

We call this variation of iFT conformal parabolic iFT method of order α , or Para(α) for short. Flat iFT can be regarded as Para(1). As noted in *op. cit.*, one can use the contour deformation $\mathcal{L}_{\omega; \chi_\alpha^+}$ for $\alpha \in [1, 4)$, rather than $\alpha \in [1, 2)$, with the understanding that, for $\alpha \in [2, 4)$, the contour belongs to an appropriate Riemann surface. For the ATM and OTM put case, which we consider, we have $x' \geq 0$. Hence, as $\eta = \operatorname{Re} \xi \rightarrow \pm\infty$

$$i\chi_\alpha^+(\xi) = -\lambda_+ + \frac{(\lambda_+ + i\xi)^\alpha}{\lambda_+^{\alpha-1}} = \lambda_+^{1-\alpha} \cdot (i\xi)^\alpha + o(\xi).$$

Therefore

$$\begin{aligned} \operatorname{Re}(ix'\chi_\alpha^+(\xi)) &= x'\lambda_+^{1-\alpha} \operatorname{Re}(e^{\pm\alpha\pi/2}) |\eta|^\alpha (1 + O(\eta^{-1})) \\ &= x'\lambda_+^{1-\alpha} \cos(\alpha\pi/2) |\eta|^\alpha (1 + O(\eta^{-1})). \end{aligned}$$

In order for this to tend to $-\infty$ for $\eta \rightarrow \pm\infty$, we must have $x' > 0$ (OTM case) and $\cos(\alpha\pi/2) < 0$, i.e. $\alpha \in (1, 3)$. For $\alpha \in [1, 4)$, and KoBoL with $\nu \in (0, 2)$, $\nu \neq 1$, we can write

$$\begin{aligned} \psi^0(\chi_\alpha^+(\xi)) &= c\Gamma(-\nu) [\lambda_+^\nu - \lambda_+^{\nu(1-\alpha)} (\lambda_+ + i\xi)^{\alpha\nu} + (-\lambda_-)^\nu \\ &\quad - (\lambda_+ - \lambda_- - \lambda_+^{1-\alpha} (\lambda_+ + i\xi)^\alpha)^\nu]. \end{aligned} \quad (24)$$

Since $\lambda_- < 0 < \omega < \lambda_+$, for any $\alpha \in [1, 4)$, the curve

$$\mathbb{R} \ni \eta \mapsto \lambda_+ - \lambda_- - \lambda_+^{1-\alpha} (\lambda_+ - \omega + i\eta)^\alpha$$

does not cross $(-\infty, 0]$, therefore the RHS of (24) is well-defined for $\alpha \in [1, 4)$. We have

$$(\lambda_+ + i\xi)^{\alpha\nu} = (\lambda_+ - \omega + i\eta)^{\alpha\nu} = (\pm i|\eta|)^{\alpha\nu}(1 + O(\eta^{-1})) = e^{\pm i\pi\alpha\nu/2}|\eta|^{\alpha\nu}(1 + O(\eta^{-1}))$$

as $\eta \rightarrow \pm\infty$ along $\text{Im } \xi = \omega$. Hence

$$\begin{aligned} \text{Re}[(\lambda_+ + i\xi)^{\alpha\nu}] &= \text{Re}(e^{\pm i\pi\alpha\nu/2}|\eta|^{\alpha\nu}(1 + O(\eta^{-1}))) \\ &= \cos(\alpha\pi\nu/2)|\eta|^{\alpha\nu}(1 + O(\eta^{-1})). \end{aligned}$$

Similarly, we have

$$\text{Re}[(\lambda_+ - \lambda_- - \lambda_+^{1-\alpha}(\lambda_+ + i\xi)^\alpha)^\nu] = \lambda_+^{\nu(1-\alpha)} \cos(\nu\pi(\alpha/2 - 1))|\eta|^{\alpha\nu}(1 + O(\eta^{-1})).$$

It follows that

$$\begin{aligned} -\text{Re}[\tau\psi^0(\chi_\alpha^+(\xi))] &= \tau c\Gamma(-\nu) \text{Re}[\cos(\alpha\nu\pi/2) + \cos(\nu\pi(\alpha/2 - 1))]| \eta|^{\alpha\nu}(1 + O(\eta^{-1})) \\ &= 2\tau c\Gamma(-\nu) \cos(\nu\pi/2) \cos(\nu\pi(1 - \alpha)/2) \eta^{\alpha\nu}|\eta|^{\alpha\nu}(1 + O(\eta^{-1})). \end{aligned}$$

For $\nu \in (0, 2)$ and $\nu \neq 1$, we have $\Gamma(-\nu) \cos(\nu\pi/2) < 0$. Hence, in order for $-\text{Re}[\tau\psi^0(\chi_\alpha^+(\xi))]$ to tend to $-\infty$ as $\eta \rightarrow \pm\infty$, we must have $\cos((1 - \alpha)\nu\pi/2) > 0$, i.e., $(1 - \alpha)\nu\pi/2 > -\pi/2$, for $\alpha \geq 1$. Therefore, we must have $\alpha \in [1, 1 + 1/\nu)$. If $\nu > 1$, this implies $\alpha < 2$. Hence, the real part of both terms in the exponential under the integral in (23) tends to $-\infty$ as $\eta \rightarrow \pm\infty$. If $\nu \in [0, 1)$ and $x' > 0$, then it is possible to have $\alpha \in (1 + 1/\nu, 3)$. Then, the real part of the first term tends to $-\infty$ as $|\eta|^\alpha$ and that of the second term tends to $+\infty$ as $|\eta|^{\alpha\nu}$. The real part of the

sum tends to $-\infty$, but the behaviour can be rather irregular. Hence, in these cases, it is recommended to take⁶ $\alpha < \alpha_0 = \min\{3, 1 + 1/\nu\}$ [19].

The following result is a consequence of the previous considerations.

Proposition 2.5 (Proposition 5.2(a) in [19]). *Let $\nu \in (0, 2)$, $\nu \neq 1$, and either $x' > 0$ and $\alpha \in [1, \min\{1 + 1/\nu, 3\})$, or $x' = 0$ and $\alpha \in [1, \min\{1 + 1/\nu, 4\})$. Then, as $\eta = \operatorname{Re} \xi \rightarrow \pm\infty$, the real part of the integrand in (22), including the factor outside the integral, admits an upper bound via*

$$\frac{K\lambda_+^{\alpha-1}}{2\pi e^{r\tau}} \alpha C(\eta) \exp[x' A(\eta)|\eta|^\alpha + B(\eta)\tau|\eta|^{\alpha\nu} - c\tau\Gamma(-\nu)(\lambda_+^\nu + (-\lambda_-)^\nu)] |\eta|^{-1-\alpha},$$

where $C(\eta) = (1 + O(\eta^{-1}))$, and

$$A(\eta) = \cos(\alpha\pi/2)\lambda_+^{1-\alpha}(1 + O(\eta^{-1})), \quad (25)$$

$$B(\eta) = 2c\Gamma(-\nu)\lambda_+^{(1-\alpha)\nu} \cos(\nu\pi/2) \cos(\nu\pi(\alpha - 1)/2)(1 + O(\eta^{-1})). \quad (26)$$

Remark 2.6. It follows from Proposition 2.5 that the integrand in (21) or (22) decays as $|\eta|^{-1-\alpha} e^{x' A(\infty)|\eta|^\alpha + B(\infty)\tau|\eta|^{\alpha\nu}}$, where $A(\infty), B(\infty) < 0$, as $|\eta| \rightarrow \infty$ along the line $\operatorname{Im} \xi = \omega \in (0, \lambda_+)$. This is generally a faster decay rate than the one for flat iFT, namely $|\xi|^{-2} \cdot e^{-\tau\kappa|\xi|^\nu}$, where $\kappa = -2c\Gamma(-\nu) \cos(\pi\nu/2)$.

2.3.2. ATM and OTM call case ($x' \leq 0$, VG). For the case of a call option, one again starts from (12), this time with $\omega = \operatorname{Im} \xi \in (-\lambda_-, -1)$. For $\alpha \in [1, 2]$, one considers the conformal map χ_α^- , defined on the half-plane $\operatorname{Im} \xi > \lambda_-$ by

$$\chi_\alpha^-(\xi) = i\lambda_- + i(-\lambda_- - 1)^{1-\alpha}(-\lambda_- - i\xi)^\alpha.$$

⁶As a rule of thumb, we recommend using $\alpha = \alpha_0 - 0.05$. The numerical examples in this thesis, unless stated otherwise, were calculated with this choice of α .

If $\alpha \in (1, 2)$, the image of the half-plane $\text{Im } \xi > \lambda_-$ is the obtuse angle

$$\{i\lambda_- + iz \mid z \neq 0, \arg z \notin [-\pi/2 - \pi(1 - \alpha/2), -\pi/2 + \pi(1 - \alpha/2)]\}.$$

For $\alpha = 2$, the image is the complex plane with the cut $i(-\infty, \lambda_-]$. Figure 2 illustrates typical curves of the modified contour $\chi_\alpha^-(\xi)$ for different values of α .

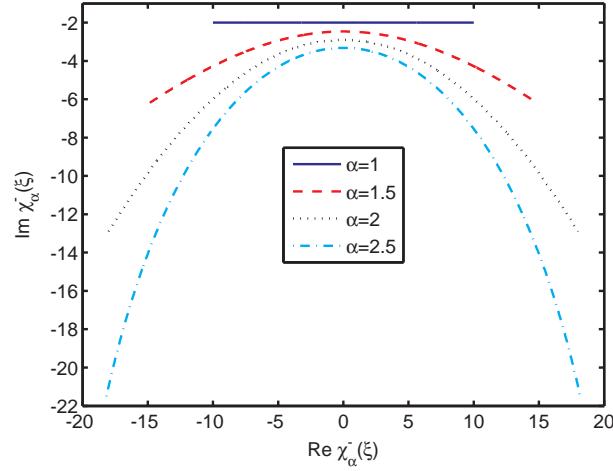


FIGURE 2. Typical curves of $\chi_\alpha^-(\xi) = i\lambda_- + i(-\lambda_- - 1)^{1-\alpha}(-\lambda_- - i\xi)^\alpha$, $\xi = i\omega + \mathbb{R}$ ($\lambda_- = -11$, $\omega = -2$).

The analogous pricing formula to (23) is given by

$$V(\tau, x) = -\frac{Ke^{-r\tau}}{\pi} \text{Re} \int_{i\omega}^{i\omega+\infty} \frac{e^{ix'\chi_\alpha^-(\xi) - \tau\psi^0(\chi_\alpha^-(\xi))}}{\chi_\alpha^-(\xi)(\chi_\alpha^-(\xi) + i)} \alpha \left(\frac{-\lambda_- - i\xi}{-\lambda_- - 1} \right)^{\alpha-1} d\xi. \quad (27)$$

As for the put option, one can use the contour transformation $\xi \mapsto \chi_\alpha^-(\xi)$ for the wider range $\alpha \in [1, 4)$, with the understanding that, for $\alpha \in [2, 4)$, the contour belongs to the appropriate Riemann surface. Then one has

$$\ln[-\lambda_- - i\chi_\alpha^-(\xi)] = (1 - \alpha) \ln(-\lambda_- - 1) + \alpha \ln(-\lambda_- - i\xi), \quad (28)$$

$$\ln[\lambda_+ + i\chi_\alpha^-(\xi)] = \ln(\lambda_+ - \lambda_- + (-\lambda_- - 1)^{1-\alpha}(-\lambda_- - i\xi)^\alpha). \quad (29)$$

Then, for $\alpha \in [1, 4)$, the integrand in (27) admits the analytic continuation into the strip $\text{Im } \xi \in (-\lambda_-, -1)$. From similar considerations to the ones in Section 2.3.1, it follows that, if the underlying follows a VG process, in order for the integrand to be of class L_1 on the line $\text{Im } \xi = \omega$, one must have $\alpha \in [1, 3)$ in the OTM case and $\alpha \in [1, 4)$ in the ATM case. It follows from (28) and (29) that the expression for $\psi^0(\chi_\alpha^-(\xi))$ for VG is given by, for $\alpha \in [1, 4)$

$$\begin{aligned} \psi^0(\chi_\alpha^-(\xi)) = c & [\alpha \ln(-\lambda_- - i\xi) - (\alpha - 1) \ln(-\lambda_- - 1) - \ln(-\lambda_- \lambda_+) \\ & + \ln(\lambda_+ - \lambda_- - (-\lambda_- - 1)^{1-\alpha} (-\lambda_- - i\xi)^\alpha)]. \end{aligned} \quad (30)$$

CHAPTER 3

Fast pricing of European options under VG

3.1. General remarks

The VG model, introduced to finance by Madan and Seneta in 1990 [69], was the first non-Gaussian Lévy model used in derivative pricing¹, and is still available on the Bloomberg system for the pricing and calibration of equity and index options² [27]. Although, the KoBoL model has become more popular in recent years, it should be recalled that VG corresponds to KoBoL with $\nu = 0$ (cf. Example A.5) and that, occasionally, one obtains VG as a best fit when the KoBoL model is calibrated to traded option prices, as is the case for the parameter set used in Section 3.4.5.3. As noted in [19], for processes of finite variation, all versions of iFT face the greatest difficulties in the ATM and near-ATM cases, particularly for short time to maturity τ and order ν close to zero. Under the VG model, it is possible to calculate the option price extremely accurately by using an alternative method, introduced in [35], based on an asymptotic expansion of the iFT integrand. The results calculated with this method can be used as a benchmark to investigate the performance of different versions of iFT. In addition, the method can be used in model fitting. When calibrating to the traded prices of vanilla options, especially those in the FX market, there is

¹The Lévy stable model was introduced to finance by Mandelbrot in 1963 [70]. However, in its general form it cannot be used for option pricing, since its exponential moments do not exist.

²The SKEW function on a Bloomberg terminal no longer allows the user to select VG as pricing model. However, the VG calculator is still available on the Bloomberg API.

usually at least one option with very short time to maturity which is close to ATM³. Moreover, these options are generally among the most liquid. During a calibration to market data, the optimization procedure may well come across regions of parameter space such that one of these options is either ATM or very close to ATM. Hence, the new method can be used to replace iFT during model fitting for VG.

We start with expression (19) for the price of a European option with terminal payoff G , which can be re-written as

$$V(\tau, x) = \frac{e^{-r\tau - \omega x'}}{\pi} \operatorname{Re} \int_0^\infty e^{ix'\eta} e^{-\tau\psi_\omega^0(\eta)} \widehat{G}_\omega(\eta) d\eta, \quad (31)$$

where $x' = x + \mu\tau$, $\widehat{G}_\omega(\eta) = \widehat{G}(\eta + i\omega)$, $\psi_\omega^0(\eta) = i\mu(\eta + i\omega) + \psi(\eta + i\omega)$, and $\omega \in (\lambda_-, -1)$ for the vanilla call option, $\omega \in (0, \lambda_+)$ for the vanilla put.

3.2. ATM case

For the rest of this chapter, unless stated otherwise, we will choose ω in (12) so that $\omega = (\lambda_+ + \lambda_-)/2$, and take $x = \ln(S/K)$. If $\omega > 0$ we price the put, and if $\omega < -1$ we price the call, applying put-call-parity if needed (we will consider the case $\omega \in [-1, 0]$ in Section 3.2.3). Putting $\sigma = (\lambda_+ - \lambda_-)/2$, we obtain $\pm\lambda_\pm \pm i\xi = \sigma \pm i\eta$, which can be used to simplify the expression of the characteristic exponent as follows

$$\psi_\omega^0(\eta) = -c \ln(-\lambda_- \lambda_+) + c \ln(\sigma^2 + \eta^2).$$

Hence

$$V(\tau, x) = -\frac{K e^{-r'\tau - \omega x'}}{2\pi} \int_{-\infty}^{+\infty} e^{ix'\eta} \frac{(\sigma^2 + \eta^2)^{-c\tau}}{(\eta + i\omega)(\eta + i\omega + i)} d\eta, \quad (32)$$

³The volatility surfaces available from various market data providers usually include quotes for options with maturity one day. In practice, options of even shorter maturity (e.g., 3-4 hours) are liquidly traded.

where $r' = r - c \ln(-\lambda_- \lambda_+)$. We note that, using this parametrization, it is possible to derive an upper bound for the truncation error of the VG option price. The details can be found in Appendix C.1. Recall that we refer to the situation in which $x' = 0$ as the ATM case, for both call and put options. Similarly, we define a call (put) option to be out-of-the-money, or OTM, if $x' < 0$ ($x' > 0$). If we set

$$I(x'; \sigma, \omega) = \int_{-\infty}^{+\infty} e^{ix'\eta} \frac{(\sigma^2 + \eta^2)^{-c\tau}}{(\eta + i\omega)(\eta + i\omega + i)} d\eta, \quad (33)$$

then we can write

$$I(0; \sigma, \omega) = \Phi(\sigma, \omega) - \Phi(\sigma, \omega + 1), \quad (34)$$

where

$$\Phi(\sigma, \omega) = -i \int_{-\infty}^{+\infty} \frac{(\sigma^2 + \eta^2)^{-c\tau}}{\eta + i\omega} d\eta. \quad (35)$$

Reducing this integral to \mathbb{R}_+ , we obtain

$$\Phi(\sigma, \omega) = 2\omega \int_0^{\infty} \frac{(\sigma^2 + \eta^2)^{-c\tau}}{\omega^2 + \eta^2} d\eta. \quad (36)$$

Hence, if we know how to calculate $\Phi(\sigma, \omega)$, we can obtain the vanilla option price from (32), (33) and (34). We start with the following result.

Proposition 3.1. *For $\eta > \sigma$, the integrand in the expression (36) for $\Phi(\sigma, \omega)$ admits the following series expansion*

$$(\sigma^2 + \eta^2)^{-c\tau} (\omega^2 + \eta^2)^{-1} = \eta^{-2-2c\tau} \sum_{n=0}^{\infty} c_n(\sigma, \omega, c\tau) \eta^{-2n}, \quad (37)$$

where the coefficients $c_n(\sigma, \omega, c\tau)$ can be calculated recursively⁴, by setting $a_0(\sigma, c\tau) = c_0(\sigma, \omega, c\tau) = 1$, and, in a cycle w.r.t. $n = 1, 2, \dots$

$$c_n(\sigma, \omega, c\tau) = -\omega^2 c_{n-1}(\sigma, \omega, c\tau) + a_n(\sigma, c\tau), \quad (38)$$

$$a_n(\sigma, c\tau) = -n^{-1}(c\tau + 1 - n)\sigma^2 a_{n-1}(\sigma, c\tau). \quad (39)$$

PROOF. Follows directly from the binomial theorem. The coefficients $c_n(\sigma, \omega, c\tau)$ are given by

$$c_n(\sigma, \omega, c\tau) = \sum_{j=0}^n a_j(\sigma, c\tau) b_{n-j}(\omega), \quad (40)$$

where in turn

$$a_j(\sigma, c\tau) = (-1)^j \frac{c\tau(c\tau + 1) \dots (c\tau + j - 1)}{j!} \sigma^{2j}, \quad (41)$$

and $b_\ell(\omega) = (-1)^\ell \omega^{2\ell}$. Then (39) follows from (41), and (38) follows from the following considerations. Recall that

$$\begin{aligned} c_n(\sigma, \omega, c\tau) &= \sum_{j=0}^n a_j(\sigma, c\tau) \omega^{2(n-j)} (-1)^{n-j}, \\ c_{n-1}(\sigma, \omega, c\tau) &= \sum_{j=0}^{n-1} a_j(\sigma, c\tau) \omega^{2(n-1-j)} (-1)^{n-1-j}. \end{aligned}$$

Therefore

$$\begin{aligned} \omega^2 c_{n-1}(\sigma, \omega, c\tau) &= \sum_{j=0}^{n-1} a_j(\sigma, c\tau) \omega^{2(n-j)} (-1)^{n-1-j} \\ &= -c_n(\sigma, \omega, c\tau) + a_n(\sigma, c\tau). \end{aligned}$$

□

⁴Alternatively, a convolution may be used. However, as shown in Appendix E.1, the choice of method makes little difference to the overall CPU time taken for the calculation of the price.

For $\Lambda > 0$, we can break the integral $\Phi(\sigma, \omega)$ into two pieces: $\Phi(\sigma, \omega) = \Phi_1(\sigma, \omega; \Lambda) + \Phi_2(\sigma, \omega; \Lambda)$, where

$$\Phi_1(\sigma, \omega; \Lambda) = 2\omega \int_0^\Lambda \frac{(\sigma^2 + \eta^2)^{-c\tau}}{\omega^2 + \eta^2} d\eta, \quad (42)$$

$$\Phi_2(\sigma, \omega; \Lambda) = 2\omega \int_\Lambda^\infty \frac{(\sigma^2 + \eta^2)^{-c\tau}}{\omega^2 + \eta^2} d\eta. \quad (43)$$

For $\Lambda > \sigma$, $\Phi_2(\sigma, \omega; \Lambda)$ can be calculated using the expansion (37), while $\Phi_1(\sigma, \omega; \Lambda)$, being the integral of a smooth function over a finite interval, can be computed very efficiently using one of several numerical integration techniques. We will examine each of these tasks in detail.

3.2.1. Calculation of $\Phi_2(\sigma, \omega; \Lambda)$. The next result follows directly from Proposition 3.1.

Proposition 3.2. *The value of $\Phi_2(\sigma, \omega; \Lambda)$, for $\Lambda > \sigma$, is given by*

$$\begin{aligned} \Phi_2(\sigma, \omega; \Lambda) &= 2\omega \sum_{n=0}^{\infty} c_n(\sigma, \omega, c\tau) \int_\Lambda^\infty \eta^{-2-2c\tau-2n} d\eta \\ &= 2\omega \sum_{n=0}^{\infty} c_n(\sigma, \omega, c\tau) \frac{\Lambda^{-1-2c\tau-n}}{1+2c\tau+n}. \end{aligned} \quad (44)$$

The next result can be used to determine the number of terms in the series (44) which ought to be included in order to reach a desired accuracy.

Proposition 3.3. *Denote by $\Phi_2^{(N)}(\sigma, \omega; \Lambda)$ the approximation to $\Phi_2(\sigma, \omega; \Lambda)$ obtained by discarding all terms from $n = N + 1$ onwards in the series expansion (44). Then the error of approximation of $\Phi_2(\sigma, \omega; \Lambda)$ by $\Phi_2^{(N)}(\sigma, \omega; \Lambda)$ admits the following bound*

$$|\Phi_2^{(N)}(\sigma, \omega; \Lambda) - \Phi_2(\sigma, \omega; \Lambda)| \leq 2|\omega|\varphi_N(\Lambda) \frac{\Lambda^{-3-2c\tau-2N}}{3+2c\tau+2N}, \quad (45)$$

where

$$\begin{aligned}
\varphi_N(\Lambda) &= |a_{N+1}(\sigma, c\tau)| \frac{\Lambda^{2N+2} - \omega^{2N+2}}{\Lambda^2 - \omega^2} + \omega^{2N+2} \sum_{n=0}^N |a_n(\sigma, c\tau)| \Lambda^{-2n} \\
&\quad + |a_{N+1}(\sigma, c\tau)| \frac{\omega^{2N+2}}{\Lambda^{2N+2}} + \sum_{n=0}^{N-1} |c_{n+N+1}(\sigma, \omega, c\tau)| \Lambda^{-2n}.
\end{aligned} \tag{46}$$

PROOF. From (44), we have

$$\Phi_2(\sigma, \omega; \Lambda) = 2\omega \int_{\Lambda}^{\infty} \eta^{-2-2c\tau} \left(\sum_{n=0}^{\infty} c_n(\sigma, \omega, c\tau) \eta^{-2n} \right) d\eta.$$

Consider the series $\sum_{n=0}^{\infty} c_n(\sigma, \omega, c\tau) \eta^{-2n}$. We need an estimate for its remainder, after discarding all terms from $n = N + 1$ onwards. Recall that, for $x \in (0, 1)$, $z \in \mathbb{R}$, we have

$$f(1+x) := (1+x)^z = \sum_{n=0}^{\infty} \frac{x^n}{n!} f^{(n)}(1).$$

The remainder is then given by Lagrange's formula

$$R_N^{(f)} := \sum_{n=N+1}^{\infty} \frac{x^n}{n!} f^{(n)}(1) = \frac{x^{N+1}}{(N+1)!} f^{(N+1)}(1 + \theta x),$$

for some $\theta \in (0, 1)$. We obtain

$$\begin{aligned}
R_N^{(f)} &= \frac{x^{N+1}}{(N+1)!} z(z-1) \dots (z-N) (1 + \theta x)^{z-N-1} \\
&= x^{N+1} \binom{z}{N+1} (1 + \theta x)^{z-N-1},
\end{aligned}$$

where $\binom{a}{k}$ denotes the generalized binomial coefficient

$$\binom{a}{k} = \frac{a(a-1) \dots (a-k+1)}{k(k-1) \dots 1},$$

for $a \in \mathbb{R}$, $k \in \mathbb{N}$. If $z < N + 1$, then

$$R_N^{(f)} \leq \left| \binom{z}{N+1} \right| x^{N+1}. \quad (47)$$

Take two (absolutely convergent) series $A = \sum_{n=0}^{\infty} A_n$ and $B = \sum_{n=0}^{\infty} B_n$. Define the product series $C = AB = \sum_{n=0}^{\infty} C_n$, where $C_n = \sum_{j=0}^n A_j B_{n-j}$. Denote by $R_N^{(a)}$, $R_N^{(b)}$, $R_N^{(c)}$, the remainders of A , B , C , respectively. Then the remainder of the product series $C = AB = \sum_{n=0}^{\infty} C_n$ is given by

$$R_N^{(c)} = \sum_{n=N+1}^{\infty} C_n = R_N^{(a)} \sum_{n=0}^N B_n + R_N^{(b)} \sum_{n=0}^N A_n + R_N^{(a)} R_N^{(b)} + \sum_{n=N+1}^{2N} C'_n,$$

where

$$C'_n = \sum_{j=n-N}^N A_j B_{n-j}. \quad (48)$$

Hence the following bound holds

$$|R_N^{(c)}| \leq |R_N^{(a)}| \sum_{n=0}^N |B_n| + |R_N^{(b)}| \sum_{n=0}^N |A_n| + |R_N^{(a)} R_N^{(b)}| + \sum_{n=N+1}^{2N} |C'_n|. \quad (49)$$

Note that, if we identify A and B with the series $\sum_{j=0}^{\infty} a_j(\sigma, c\tau)\eta^{-2j}$ and $\sum_{\ell=0}^{\infty} b_\ell(\omega)\eta^{-2\ell}$, respectively, then, in the last term on the RHS of (49), C'_n can be replaced by C_n , since all terms in the sum (40) for the coefficient $c_n(\sigma, \omega, c\tau)$, for a given n , have the same sign.

Consider the series $\sum_{n=0}^{\infty} c_n(\sigma, \omega, c\tau)\eta^{-2n}$. Denote by $\varphi(\eta)$ the integrand in (43), and write $\varphi(\eta) = \eta^{-2-2c\tau}\varphi_1(\eta)\varphi_2(\eta)$, where $\varphi_1(\eta) = (1 + \sigma^2/\eta^2)^{-c\tau}$ and $\varphi_2(\eta) = (1 + \omega^2/\eta^2)^{-1}$. For $\eta \geq \Lambda > \sigma$, we have $\varphi_1(\eta) = \sum_{n=0}^{\infty} a_n(\sigma, c\tau)\eta^{-2n}$, $\varphi_2(\eta) = \sum_{n=0}^{\infty} b_n(\omega)\eta^{-2n}$. Denote by $R_N^{(\varphi_1)}(\eta)$ and $R_N^{(\varphi_2)}(\eta)$ the remainders of the series for $\varphi_1(\eta)$ and $\varphi_2(\eta)$, respectively. From (47), with $x = \sigma^2\eta^{-2}$ and $x = \omega^2\eta^{-2}$, respectively,

we obtain

$$|R_N^{(\varphi_1)}(\eta)| \leq \left| \binom{-c\tau}{N+1} \right| \frac{\sigma^{2N+2}}{\eta^{2N+2}} = \frac{|a_{N+1}(\sigma, c\tau)|}{\eta^{2N+2}}, \quad (50)$$

$$|R_N^{(\varphi_2)}(\eta)| \leq \frac{\omega^{2N+2}}{\eta^{2N+2}}. \quad (51)$$

If we denote by $R_N^{(\varphi)}(\eta)$ the remainder of the series for $\varphi(\eta)$, we obtain from (49), (50), (51)

$$\begin{aligned} |R_N^{(\varphi)}(\eta)| &\leq \eta^{-4-2c\tau-2N} \left[|a_{N+1}(\sigma, c\tau)| \left(\sum_{n=0}^N \frac{\omega^{2n}}{\eta^{2n}} \right) + \omega^{2N+2} \left(\sum_{n=0}^N |a_n(\sigma, c\tau)| \eta^{-2n} \right) \right. \\ &\quad \left. + |a_{N+1}(\sigma, c\tau)| \frac{\omega^{2N+2}}{\eta^{2N+2}} + \sum_{n=N+1}^{2N} |c_n(\sigma, \omega, c\tau)| \eta^{-2n+2N+2} \right] \\ &= \eta^{-4-2c\tau-2N} \left[|a_{N+1}(\sigma, c\tau)| \eta^{-2N} \frac{\eta^{2N+2} - \omega^{2N+2}}{\eta^2 - \omega^2} + \omega^{2N+2} \left(\sum_{n=0}^N |a_n(\sigma, c\tau)| \eta^{-2n} \right) \right. \\ &\quad \left. + |a_{N+1}(\sigma, c\tau)| \frac{\omega^{2N+2}}{\eta^{2N+2}} + \sum_{n=0}^{N-1} |c_{n+N+1}(\sigma, \omega, c\tau)| \eta^{-2n} \right]. \end{aligned} \quad (52)$$

The result follows from (52), together with the fact that $\eta \geq \Lambda$. \square

From Proposition 3.3 it is clear that, if ϵ is the tolerance level for the absolute error $|\Phi_2^{(N)}(\sigma, \omega; \Lambda) - \Phi_2(\sigma, \omega; \Lambda)|$, the smallest value of N we can take can be found from

$$\frac{\varphi_N(\Lambda)}{(3 + c\tau + 2N)\Lambda^{3+c\tau+2N}} \leq \frac{\epsilon}{2|\omega|}. \quad (53)$$

The following iterative procedure can be used to find the smallest value of N , given the error tolerance ϵ : in a cycle w.r.t. $N = 1, 2, \dots$, calculate the LHS of (53), and stop as soon as its value drops below that of the RHS.

3.2.2. Calculation of $\Phi_1(\sigma, \omega; \Lambda)$. As mentioned earlier, $\Phi_1(\sigma, \omega; \Lambda)$ can be computed to a very high degree of accuracy using one of several numerical integration techniques. In a practical implementation, one would usually calculate an integral such as $\Phi_1(\sigma, \omega; \Lambda)$ by an adaptive quadrature scheme, i.e. one in which the integration grid is successively refined until certain convergence criteria are met, with the aim that the absolute error should lie under a tolerance level ϵ [75, §4.7]. In our numerical examples in Appendix E, we include results calculated with the adaptive Simpson's rule⁵ developed in [46], the adaptive Gauss-Lobatto rule⁶ of *op. cit.*, the adaptive Clenshaw-Curtis quadrature, implemented in MATLAB according to the algorithm in [74], and the vectorized Gauss-Kronrod quadrature method⁷ developed in [78]. Overall, the best results were obtained by Clenshaw-Curtis integration and vectorized Gauss-Kronrod quadrature.

3.2.3. Case $\omega \in [-1, 0]$. In this section, we will use $V(\tau, x; \omega)$ to denote the RHS of (12) for a specific choice of ω .

3.2.3.1. *Case $\omega \in (-1, 0)$.* Define $V_c(\tau, x)$ and $V_p(\tau, x)$ to be the vanilla call and put prices, respectively, and set $V_{(-1,0)}(\tau, x) = V(\tau, x; \omega)$ for $\omega \in (-1, 0)$. Then, using a similar procedure to that in [18, §4.2.2] to give a proof of the well-known vanilla put-call parity relationship

$$V_c(\tau, x) - V_p(\tau, x) = e^{-q\tau} K e^x - e^{-r\tau} K, \quad (54)$$

we can express the call price in terms of $V_{(-1,0)}(\tau, x)$.

⁵Available in MATLAB as the function `quad`.

⁶Available in MATLAB as the function `quadl`.

⁷Available in MATLAB as the function `quadgk`.

Proposition 3.4. *The following relationship holds between $V_c(\tau, x)$ and $V_{(-1,0)}(\tau, x)$*

$$V_c(\tau, x) - V_{(-1,0)}(\tau, x) = e^{-q\tau} K e^x.$$

PROOF. We have

$$V_c(\tau, x) - V_{(-1,0)}(\tau, x) = \left(\int_{\text{Im } \xi = \omega_-} - \int_{\text{Im } \xi = \sigma} \right) \frac{-K e^{-r\tau} e^{ix\xi - \tau\psi(\xi)}}{2\pi \xi(\xi + i)} d\xi,$$

where $\omega_- < -1$, $\sigma \in (-1, 0)$. The integrand has only one singularity in the strip $\text{Im } \xi \in [\omega_-, \sigma]$, a simple pole at $\xi = -i$. From this, the result easily follows. \square

3.2.3.2. *Case $\omega \in \{-1, 0\}$.* Define $V_{-1}(\tau, x) = V(\tau, x; -1)$ and $V_0(\tau, x) = V(\tau, x; 0)$, with the corresponding integrals in (12) defined in the sense of Cauchy's principal value. The next two propositions show how to express the call price in terms of $V_{-1}(\tau, x)$ and $V_0(\tau, x)$.

Proposition 3.5. *The following relationship holds between $V_c(\tau, x)$ and $V_{-1}(\tau, x)$*

$$V_c(\tau, x) - V_{-1}(\tau, x) = \frac{1}{2} e^{-q\tau} K e^x.$$

PROOF. We have

$$V_c(\tau, x) - V_{-1}(\tau, x) = \left(\int_{\text{Im } \xi = \omega_-} - P \int_{\text{Im } \xi = -i} \right) \frac{-K e^{-r\tau} e^{ix\xi - \tau\psi(\xi)}}{2\pi \xi(\xi + i)} d\xi,$$

where P denotes the Cauchy principal value of the integral. Compared to the situation in Proposition 3.4, we now have only half the contribution from the simple pole $\xi = -i$. \square

Proposition 3.6. *The following relationship holds between $V_c(\tau, x)$ and $V_0(\tau, x)$*

$$V_c(\tau, x) - V_0(\tau, x) = e^{-q\tau} K e^x - \frac{1}{2} e^{-r\tau} K.$$

PROOF. We have

$$V_c(\tau, x) - V_0(\tau, x) = \left(\int_{\text{Im } \xi = \omega_-} -P \int_{\mathbb{R}} \right) \frac{-K e^{-r\tau} e^{ix\xi - \tau\psi(\xi)}}{2\pi \xi(\xi + i)} d\xi,$$

Compared to the situation with put-call-parity, we now have only half the contribution from the simple pole $\xi = 0$, but the full contribution from the simple pole $\xi = -i$. \square

Finally, we note that, at ATM, we have

$$\begin{aligned} V_{-1}(\tau, -\mu\tau) &= -\frac{K e^{-r'\tau}}{2\pi} \Phi(\sigma, -1), \\ V_0(\tau, -\mu\tau) &= \frac{K e^{-r'\tau}}{2\pi} \Phi(\sigma, 1). \end{aligned}$$

3.3. Non-ATM case

In practice, interpolation near ATM is known to be very inaccurate, especially for short times to maturity. Since near-ATM options tend to be among the most liquid, it is important for model fitting purposes to calculate their prices accurately. In this section, we outline a similar method to that of Section 3.2, but valid for $x' \neq 0$. As we will see, this can be a useful alternative to iFT for the case in which x' is close to, but not quite zero, when iFT can take a long time to produce accurate results [19]. As in Section 3.2, we consider the vanilla option case when developing the algorithm. For the case of digitals, see Appendix F.

Taking (31) into account, the vanilla option price is given by

$$V(\tau, x) = -\frac{K}{\pi} e^{-r'\tau - \omega x'} \text{Re } I^+(x'; \sigma, \omega), \quad (55)$$

where

$$I^+(x'; \sigma, \omega) = \int_0^\infty e^{ix'\eta} \frac{(\sigma^2 + \eta^2)^{-c\tau}}{(\eta + i\omega)(\eta + i\omega + i)} d\eta, \quad (56)$$

for $x' \neq 0$. In a similar way to (34), we can write

$$I^+(x; \sigma, \omega) = \Psi(x; \sigma, \omega) - \Psi(x; \sigma, \omega + 1),$$

where

$$\Psi(x; \sigma, \omega) = -i \int_0^\infty e^{ix\eta} \frac{(\sigma^2 + \eta^2)^{-c\tau}}{\eta + i\omega} d\eta. \quad (57)$$

For $\Lambda > 0$, we set

$$\Psi_1(x; \sigma, \omega; \Lambda) = -i \int_0^\Lambda e^{ix\eta} \frac{(\sigma^2 + \eta^2)^{-c\tau}}{\eta + i\omega} d\eta, \quad (58)$$

$$\Psi_2(x; \sigma, \omega; \Lambda) = -i \int_\Lambda^\infty e^{ix\eta} \frac{(\sigma^2 + \eta^2)^{-c\tau}}{\eta + i\omega} d\eta, \quad (59)$$

so that $\Psi(x; \sigma, \omega) = \Psi_1(x; \sigma, \omega; \Lambda) + \Psi_2(x; \sigma, \omega; \Lambda)$. As in the case of $\Phi_1(\sigma, \omega)$, $\Psi_1(x; \sigma, \omega; \Lambda)$ can be calculated extremely accurately using one of several numerical integration techniques.

3.3.1. Calculation of $\Psi_2(x; \sigma, \omega; \Lambda)$. The following result is the equivalent of Proposition 3.2 for the non-ATM case.

Proposition 3.7. *For $x \neq 0$ and $\Lambda > \sigma$ we have*

$$\Psi_2(x; \sigma, \omega; \Lambda) = -i \sum_{n=0}^{\infty} c_n(\sigma, \omega, c\tau) (-ix)^{2c\tau+n} \Gamma(-2c\tau - n, -ix\Lambda), \quad (60)$$

where $\Gamma(\cdot, \cdot)$ denotes the principal branch of the upper incomplete gamma function, defined by

$$\Gamma(s, x) = \int_x^\infty e^{-t} t^{s-1} dt,$$

where $\text{Re } s > 0$, for integration paths which do not include the origin or cross the negative real axis (cf. [73, §8.2]). The coefficients $c_n(\sigma, \omega, c\tau)$ can be calculated by setting $a_0(\sigma, c\tau) = c_0(\sigma, \omega, c\tau) = 1$, $a_n(\sigma, c\tau) = 0$ for n odd, and using the following

recurrence relations

$$c_n(\sigma, \omega, c\tau) = a_n(\sigma, c\tau) - i\omega c_{n-1}(\sigma, c\tau), \quad (61)$$

$$a_n(\sigma, c\tau) = -\frac{2\sigma^2}{n} \left(c + \frac{n}{2} - 1 \right) a_{n-2}(\sigma, c\tau). \quad (62)$$

PROOF. For $|\eta| \geq \Lambda > \sigma$, we can write⁸

$$\begin{aligned} \frac{(\sigma^2 + \eta^2)^{-c\tau}}{\eta + i\omega} &= \eta^{-1-2c\tau} \left(1 + \frac{\sigma^2}{\eta^2} \right)^{-c\tau} \left(1 + \frac{i\omega}{\eta} \right)^{-1} \\ &= \eta^{-1-2c\tau} \left(\sum_{j=0}^{\infty} \alpha_j(\sigma, c\tau) \eta^{-2j} \right) \left(\sum_{k=0}^{\infty} b_k(\omega) \eta^{-k} \right) \\ &= \eta^{-1-2c\tau} \left(\sum_{j=0}^{\infty} a_j(\sigma, c\tau) \eta^{-j} \right) \left(\sum_{k=0}^{\infty} b_k(\omega) \eta^{-k} \right) \\ &= \eta^{-1-2c\tau} \sum_{n=0}^{\infty} c_n(\sigma, \omega, c\tau) \eta^{-n}, \end{aligned} \quad (63)$$

where

$$\alpha_j(\sigma, c\tau) = (-1)^j \frac{c\tau(c\tau + 1) \dots (c\tau + j - 1)}{j!} \sigma^{2j}, \quad (64)$$

$$a_j(\sigma, c\tau) = (-1)^{j/2} \frac{c\tau(c\tau + 1) \dots (c\tau + j/2 - 1)}{(j/2)!} \sigma^j \frac{(-1)^j + 1}{2}, \quad (65)$$

$$b_k(\omega) = (-i\omega)^k,$$

$$c_n(\sigma, \omega, c\tau) = \sum_{j=0}^n a_j(\sigma, c\tau) b_{n-j}(\omega). \quad (66)$$

Recurrence relations (62)-(61) follow from (65)-(66). Therefore, for $\Lambda > \sigma$, we obtain

$$\Psi_2(x; \sigma, \omega; \Lambda) = -i \sum_{n=0}^{\infty} c_n(\sigma, \omega, c\tau) \int_{\Lambda}^{\infty} e^{ix\eta} \eta^{-1-2c\tau-n} d\eta.$$

⁸With a slight abuse of notation, we re-use some of the symbols from Section 3.2 for the series expansion coefficients.

If we set

$$\mathcal{I}(x, z; \Lambda) = \int_{\Lambda}^{\infty} e^{ix\eta} \eta^{-1-z} d\eta,$$

for $z > 0$, then we can write

$$\Psi_2(x; \sigma, \omega; \Lambda) = -i \sum_{n=0}^{\infty} c_n(\sigma, \omega, c\tau) \mathcal{I}(x, 2c\tau + n; \Lambda).$$

Let us now calculate the value of the integral $\mathcal{I}(x, z; \Lambda)$. Put $t = -ix\eta$. For $x > 0$, we have

$$\mathcal{I}(x, z; \Lambda) = \int_{-ix\Lambda}^{-i\infty} e^{-t} (ix^{-1}t)^{-1-z} ix^{-1} dt$$

It follows that

$$\mathcal{I}(x, z; \Lambda) = (-ix)^z \int_{-ix\Lambda}^{-i\infty} e^{-t} t^{-1-z} dt = (-ix)^z \Gamma(-z, -ix\Lambda), \quad x > 0. \quad (67)$$

In a similar way, one obtains

$$\mathcal{I}(x, z; \Lambda) = (-ix)^z \int_{-ix\Lambda}^{i\infty} e^{-t} t^{-1-z} dt = (-ix)^z \Gamma(-z, -ix\Lambda), \quad x < 0.$$

Hence in both cases

$$\mathcal{I}(x, z; \Lambda) = (-ix)^z \Gamma(-z, -ix\Lambda), \quad x \neq 0. \quad (68)$$

□

3.3.1.1. Recommendations for the computation of the incomplete gamma function.

The value of the incomplete gamma function $\Gamma(s, y)$ can be calculated very efficiently using the following series expansion [1, §6.5.29], which converges for $s \notin \mathbb{Z}_-$

$$\Gamma(s, y) = \Gamma(s) \left(1 - e^{-y} y^s \sum_{n=0}^{\infty} \frac{y^n}{\Gamma(s + j + 1)} \right). \quad (69)$$

This converges very fast if s is not very close to a negative integer. All the numerical examples in this chapter were calculated using the expansion (69). For the case in which $c\tau$ is very close to an integer, other techniques, such as Legendre's continued fraction, can be used [83, 85].

3.3.1.2. *Error bounds for the remainder of the series expansion (63).* The following result is analogous to Proposition 3.3 for the ATM case, and can be used to choose the minimum number of terms N to include in the expansion (63) for a given error tolerance. For the sake of brevity, in the remainder of this section, we will drop the functional dependencies of the series coefficients, writing only a_n , b_n , c_n , instead of $a_n(\sigma, c\tau)$, $b_n(\omega)$, $c_n(\sigma, \omega, c\tau)$, respectively.

Proposition 3.8. *Denote by $\Psi_2^{(N)}(x; \sigma, \omega; \Lambda)$ the approximation to $\Psi_2(x; \sigma, \omega; \Lambda)$ obtained by discarding all terms from $n = N + 1$ onwards in the expansion (63). Then the error of approximation of $\Psi_2(x; \sigma, \omega; \Lambda)$ by $\Psi_2^{(N)}(x; \sigma, \omega; \Lambda)$ admits the following bound*

$$|\Psi_2^{(N)}(x; \sigma, \omega; \Lambda) - \Psi_2(x; \sigma, \omega; \Lambda)| \leq \psi_N(\Lambda) \frac{\Lambda^{-1-2c\tau-N}}{1 + 2c\tau + N}, \quad (70)$$

where

$$\begin{aligned} \psi_N(\Lambda) = & \frac{|a_{N'+2}|}{\Lambda^N} \frac{\Lambda^{N+1} - |\omega|^{N+1}}{\Lambda - |\omega|} + |\omega|^{N+1} \sum_{n=0}^N |a_n| \Lambda^{-n} \\ & + \frac{|a_{N'+2}| |\omega|^{N+1}}{\Lambda^{N+1}} + \sum_{n=0}^{N-1} |c_{n+N+1}| \Lambda^{-n}, \end{aligned} \quad (71)$$

and $N' = N - (1 + (-1)^{N+1})/2$.

PROOF. We need an estimate for the remainder of the series $\sum_{n=0}^{\infty} c_n \eta^{-n}$. Recall that $c_n = \sum_{j=0}^n a_j b_{n-j}$, where

$$a_j = (-1)^{j/2} \frac{c\tau(c\tau + 1) \dots (c\tau + j/2 - 1)}{(j/2)!} \delta_j \sigma^j,$$

and $b_k = (-i\omega)^k$, $\delta_n = (1 + (-1)^n)/2$. We can use (49), in which, again, the C'_n coefficients can be replaced by the C_n , due to the fact that all the terms in the sum (66) for the coefficient c_n , for a given n , have the same sign. Then, if we define the remainders $R_N^{(a)}(\eta) = \sum_{n=N+1}^{\infty} a_n \eta^{-n}$ and $R_N^{(b)}(\eta) = \sum_{n=N+1}^{\infty} b_n \eta^{-n}$, we have

$$R_N^{(a)}(\eta) \leq \max\{|a_{N+1}|, |a_{N+2}|\} \eta^{-N-1},$$

and

$$R_N^{(b)}(\eta) \leq |\omega|^{N+1} \eta^{-N-1}.$$

Assume for the moment that N is odd. Then, from (49) and the previous considerations, we have

$$\begin{aligned} \left| \sum_{n=N+1}^{\infty} c_n \eta^{-n} \right| &\leq \frac{|a_{N+1}|}{\eta^{N+1}} \left(\sum_{n=0}^N |\omega|^n \eta^{-n} \right) + \frac{|\omega|^{N+1}}{\eta^{N+1}} \left(\sum_{n=0}^N |a_n| \eta^{-n} \right) + \frac{|\omega^{N+1} a_{N+1}|}{\eta^{2N+2}} \\ &\quad + \sum_{n=N+1}^{2N} |c_n| \eta^{-n} \\ &= \eta^{-N-1} \left[|a_{N+1}| \frac{1 - |\omega/\eta|^{N+1}}{1 - |\omega/\eta|} + |\omega|^{N+1} \left(\sum_{n=0}^N |a_n| \eta^{-n} \right) + \frac{|\omega^{N+1} a_{N+1}|}{\eta^{N+1}} \right. \\ &\quad \left. + \sum_{n=N+1}^{2N} |c_n| \eta^{-n+N+1} \right]. \end{aligned}$$

Since $\eta > \Lambda$, we obtain

$$\begin{aligned} \left| \sum_{n=N+1}^{\infty} c_n \eta^{-n} \right| &\leq \Lambda^{-N-1} \left[\frac{|a_{N+1}|}{\Lambda^N} \frac{\Lambda^{N+1} - |\omega|^{N+1}}{\Lambda - |\omega|} + |\omega|^{N+1} \left(\sum_{n=0}^N |a_n| \Lambda^{-n} \right) + \frac{|\omega^{N+1} a_{N+1}|}{\Lambda^{N+1}} \right. \\ &\quad \left. + \sum_{n=0}^{N-1} |c_{n+N+1}| \Lambda^{-n} \right]. \end{aligned} \tag{72}$$

The above bound still holds in the case when n is even, if a_{N+1} is replaced by a_{N+2} . From this, (70) and (71) follow. \square

3.3.2. Case $\omega \in [-1, 0]$. For $\omega \in (-1, 0)$, the same results of Section 3.2.3.1 apply. If, on the other hand, either $\omega = -1$ or $\omega = 0$, then we can define

$$\Psi_1(x; \sigma, 0; \Lambda) = -\frac{i}{2} P \int_{-\Lambda}^{\Lambda} e^{ix\eta} \frac{(\sigma^2 + \eta^2)^{-c\tau}}{\eta} d\eta.$$

This can be re-written as

$$\Psi_1(x; \sigma, 0; \Lambda) = \frac{\pi i}{2} \mathcal{H}\psi(0), \quad (73)$$

where

$$\psi(\eta) = e^{ix\eta} (\sigma^2 + \eta^2)^{-c\tau} \mathbb{1}_{[-\Lambda, \Lambda]}(\eta), \quad (74)$$

and \mathcal{H} denotes the Hilbert transform, defined by

$$\mathcal{H}\psi(\xi) = \frac{1}{\pi} P \int_{-\infty}^{+\infty} \frac{\psi(\eta)}{\xi - \eta} d\eta.$$

As noted in [45], the Hilbert transform can be calculated very efficiently by using an approximation based on Whittaker's cardinal series (sinc expansion), which relies on the FFT realization of Toeplitz matrix-vector multiplication. The details of the algorithm can be found in Appendix P.2.4, and a discussion of the discretization error bound for the calculation of $\Psi_1(x; \sigma, 0; \Lambda)$ can be found in Appendix G.

3.4. Algorithms and numerical results

3.4.1. ATM case. From the results in Section 3.2, the following procedure can be used to calculate the ATM price of a vanilla option under the VG model. For the modifications needed in the case of the ATM vanilla delta and the digital price, see Appendix F.

1. Fix a value of Λ . As noted earlier, this choice is largely irrelevant to the accuracy which can be achieved by the algorithm. The only requirement is that $\Lambda > \sigma$. As a rule of thumb, for a fast implementation, we recommend the choice $\Lambda = 1.5\sigma$, since it is neither so small that it would force one to include several additional terms in the asymptotic expansion of $\Phi_2(\sigma, \omega; \Lambda)$, nor so large as to significantly slow down the calculation of $\Phi_1(\sigma, \omega; \Lambda)$.
2. Fix the value of the error tolerance ϵ for the option price, broken down as $\epsilon = \epsilon_1 + \epsilon_2$, where ϵ_1 is used for the calculation involving $\Phi_1(\sigma, \omega; \Lambda)$ and ϵ_2 for that involving $\Phi_2(\sigma, \omega; \Lambda)$. One may set $\epsilon_1 = \epsilon_2 = \epsilon/2$; however, as will be seen in Section 3.4.2, such a choice may not give the best performance, and in practice it is usually safe to set ϵ_1 about four orders of magnitude larger than ϵ , and ϵ_2 about one order of magnitude larger than ϵ . Set $\epsilon'_1 = \epsilon_1 2\pi K^{-1} e^{r'\tau + \omega x'}$, and $\epsilon'_2 = \epsilon_2 2\pi K^{-1} e^{r'\tau + \omega x'}$.
3. Calculate $\Phi_1(\sigma, \omega; \Lambda)$ and $\Phi_1(\sigma, \omega + 1; \Lambda)$ (cf. definition (42)), e.g. by using one of the numerical integration methods discussed in Section 3.2.2, with error tolerance $\epsilon'_1/2$.
4. Calculate $\Phi_2(\sigma, \omega; \Lambda)$ and $\Phi_2(\sigma, \omega + 1; \Lambda)$ (cf. definition (43)) with the method of Section 3.2.1, i.e., using the asymptotic expansion (44) with N terms, where N can be determined from Proposition 3.3. Use error tolerance $\epsilon'_2/2$.
5. Calculate the price by using (32)-(34) and (42)-(43), applying put-call-parity and/or one of Propositions 3.4-3.6, if needed.

We refer to the algorithm outlined above as the ATMVG method.

3.4.2. Numerical results.

3.4.2.1. *Choice of Λ .* First, we look at the behaviour of the ATMVG price for varying truncation parameter Λ . As pointed out in Section 3.4.1, the choice of Λ is

largely irrelevant to the accuracy of the algorithm, but should affect the overall CPU time taken for the calculation. We check this by comparing the CPU times⁹ for a range of Λ . Throughout this section, we will consider the case of an ATM call option with $K = 1$, $\tau = 0.004$ (approximately equal to one trading day), $r = 0.03$, $q = 0$, under process parameters¹⁰ $\lambda_- = -12$, $\lambda_+ = 8$, and $m_2 = 0.16$. We use the adaptive Gauss-Lobatto rule, implemented in MATLAB as the function `quadl`, for the calculation of $\Phi_1(\sigma, \omega; \Lambda)$. As we will see, other methods can be faster, but we found that adaptive Gauss-Lobatto quadrature could more easily cope with large ranges of integration and low error tolerances. Therefore, all the plots of CPU times in the remainder of this section should be used only to judge the *relative* performance of the algorithm for different choices of truncation parameter and error tolerances (the comparison of CPU times for other integration methods can be found in Appendix E.1). We take error tolerances $\epsilon_1 = \epsilon_2 = 10^{-16}$, include twice as many terms in the series (44) as necessary, and refer to the price calculated in this way as our “benchmark”. For a given choice of Λ we denote it by $V_{\text{bm}}(\Lambda)$. In Figure 1 we plot the CPU time taken by the calculation of $V_{\text{bm}}(\Lambda)$, where Λ varies between 11 and 100. As can be seen from the picture, the CPU times range between 13.35 ms for $\Lambda = 15$ and 24.6 ms for $\Lambda = 100$. We conclude that the choice of Λ does not greatly affect the overall CPU time, and from now on simply set $\Lambda = 1.5\sigma$ (which, in this case, produces the smallest CPU time).

⁹The calculations were carried out in MATLAB 7.9.0, on a PC with Intel Core 2 Duo, CPU P8400, 2.26 GHz and 3 GB RAM, running Windows XP Professional.

¹⁰ m_2 denotes the instantaneous second moment, which in the VG model determines c via $c = m_2(\lambda_-^{-2} + \lambda_+^{-2})^{-1}$.

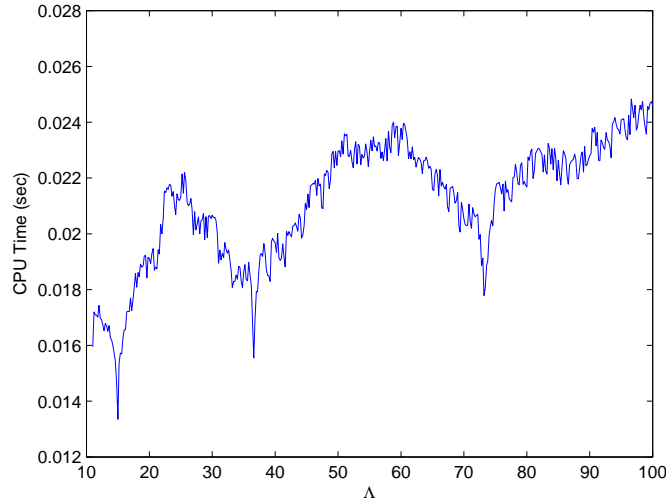


FIGURE 1. CPU times for varying Λ , for an ATM vanilla call option with $K = 1$, $\lambda_- = -12$, $\lambda_+ = 8$, $m_2 = 0.16$, $r = 0.03$, $q = 0$, $\tau = 0.004$, for $\epsilon_1 = \epsilon_2 = 10^{-16}$.

3.4.2.2. *Choice of ϵ_1 and ϵ_2 .* We consider the effect of the error tolerance on the calculation of $\Phi_1(\sigma, \omega; \Lambda)$ and $\Phi_2(\sigma, \omega; \Lambda)$. In Figure 2 we plot the absolute difference in the ATMVG price for varying ϵ_1 w.r.t. $\epsilon_1 = 10^{-16}$, while ϵ_2 is held fixed at 10^{-16} , and the corresponding CPU times. In Figure 3 we do the same for varying ϵ_2 , while ϵ_1 is held fixed at 10^{-16} . We note that

1. The price does not change at all between $\epsilon_1 = 10^{-16}$ and $\epsilon_1 \approx 2 \cdot 10^{-11}$. Even for larger values of ϵ_1 , the error is still several orders of magnitude smaller than ϵ_1 , and is of the order of 10^{-15} for $\epsilon_1 = 10^{-8}$. This remarkable accuracy is due to the high efficiency of adaptive quadrature methods for smooth integrands over small intervals.
2. The CPU time increases almost monotonically for decreasing ϵ_1 , from 4.54 ms for $\epsilon_1 = 10^{-8}$ to 48.77 ms for $\epsilon_1 = 10^{-16}$.

3. As ϵ_2 increases from 10^{-16} to 10^{-8} , the error increases more or less monotonically, staying about two orders of magnitude below ϵ_2 .
4. The CPU time is largely independent of ϵ_2 , reflecting the fact that the calculation of $\Phi_2(\sigma, \omega; \Lambda)$ is very fast compared to that of $\Phi_1(\sigma, \omega; \Lambda)$ (see Appendix E.1).

In light of these results, even if accuracy of the order of floating point error is desired for the benchmark, one might as well take ϵ_1 around 10^{-12} or even slightly larger, while ϵ_2 can be chosen in the range 10^{-16} – 10^{-15} .

3.4.2.3. Comparison with iFT. The absolute difference between the ATMVG benchmark and the price calculated by parabolic iFT, with $\alpha = 3.9$, using a very long and fine grid ($\zeta = 0.1$, $\Lambda = 100000$) is very small, at $2.56 \cdot 10^{-15}$. In Section 3.5 we include a more detailed comparison of the ATMVG prices with those obtained by flat and parabolic iFT. The results confirm the analysis of [19], according to which parabolic iFT is the most efficient version of the method, both in terms of accuracy and CPU time.

3.4.3. Non-ATM case. From the results in Section 3.3, we can obtain a procedure to calculate the non-ATM price or delta of a vanilla option, or the non-ATM price of a digital option. We outline the algorithm for vanilla prices. For the modifications needed in the case of the ATM vanilla delta and digital price, see Appendix F.

1. Fix a value of Λ . As will be seen in Section 3.4.5.1, the value of Λ is largely irrelevant to the accuracy of the results. For a fast implementation, we recommend taking Λ in the range 4σ – 5σ .
2. Fix the value of the error tolerances ϵ_1 and ϵ_2 , corresponding to the calculations involving $\Psi_1(x'; \sigma, \omega; \Lambda)$ and $\Psi_2(x'; \sigma, \omega; \Lambda)$, respectively. As in the ATM case, we

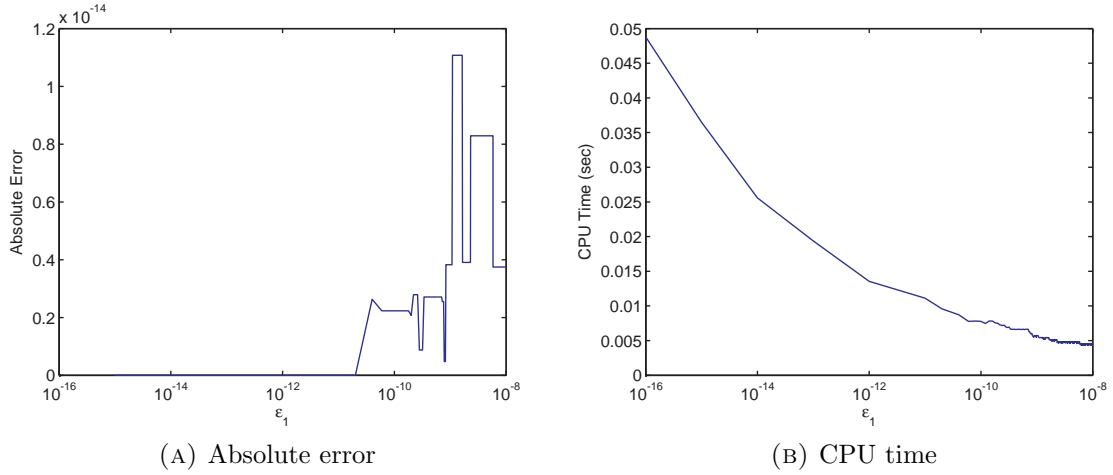


FIGURE 2. Absolute errors in the ATMVG price, and corresponding CPU times, for varying error tolerance level ϵ_1 w.r.t. $\epsilon = 10^{-16}$, for an ATM vanilla call option with $K = 1$, $\lambda_- = -12$, $\lambda_+ = 8$, $m_2 = 0.16$, $r = 0.03$, $q = 0$, $\tau = 0.004$, for $\Lambda = 1.5\sigma$.

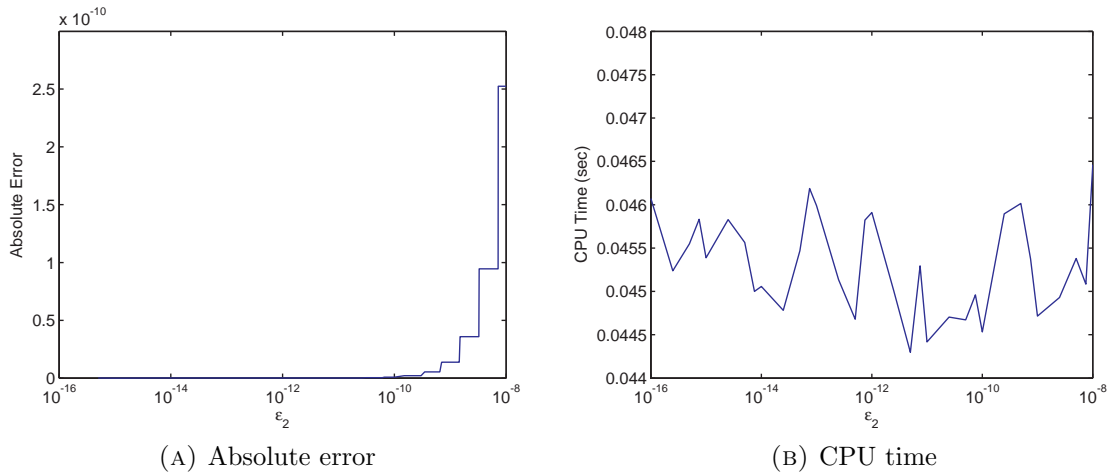


FIGURE 3. Absolute errors in the ATMVG price, and corresponding CPU times, for varying error tolerance level ϵ_2 w.r.t. $\epsilon = 10^{-16}$, for an ATM vanilla call option with $K = 1$, $\lambda_- = -12$, $\lambda_+ = 8$, $m_2 = 0.16$, $r = 0.03$, $q = 0$, $\tau = 0.004$, for $\Lambda = 1.5\sigma$.

write $\epsilon = \epsilon_1 + \epsilon_2$, where ϵ is the absolute error tolerance for the option price. However, as we will see in Section 3.4.5.2, it is usually safe to choose ϵ_1 five or six

orders of magnitude larger than ϵ , and ϵ_2 one or two orders of magnitude larger than ϵ . Set $\epsilon'_1 = \epsilon_1 \pi K^{-1} e^{r'\tau + \omega x'}$, and $\epsilon'_2 = \epsilon_2 \pi K^{-1} e^{r'\tau + \omega x'}$.

3. Calculate $\Psi_1(x'; \sigma, \omega; \Lambda)$ and $\Psi_1(x'; \sigma, \omega + 1; \Lambda)$ (cf. definition (58)), e.g. by using one of the numerical integration methods mentioned in Section 3.2.2, with error tolerance $\epsilon'_1/2$.
4. Calculate $\Psi_2(x'; \sigma, \omega; \Lambda)$ and $\Psi_2(x'; \sigma, \omega + 1; \Lambda)$ (cf. definition (59)) by using Proposition 3.7, i.e., using the asymptotic expansion (44) with N terms, where N can be determined from Proposition 3.8. Use error tolerance $\epsilon'_2/2$.
5. Calculate the price by using (55)-(59), applying put-call-parity, one of Propositions 3.4-3.6, or the method in Section 3.3.2, if needed.

We will refer to the algorithm outlined above as the FastVG method.

3.4.4. Digitals and deltas. The algorithm can be modified to price digital options, or to calculate the delta of a vanilla option, with $x' \neq 0$. The details can be found in Appendix F. In either of these cases, we expect the CPU time to be approximately halved compared to the case of the vanilla option price, since one only needs to calculate the value of one improper integral, rather than two.

3.4.5. Numerical results (non-ATM case).

3.4.5.1. *Choice of Λ .* As in the ATM case, the method has an almost free parameter, Λ . In Figure 4 (cf. Figure 1 for the ATMVG case) we plot the CPU times for the calculation of the benchmark¹¹ FastVG price of an OTM call option with $x' = -10^{-6}$, for varying Λ , under the same process parameters used in Section 3.4.2. This comparison corresponds to that of Figure 1 for the ATM case, and shows that, although

¹¹See Section 3.4.2 for the definition of the benchmark.

the CPU time increases more or less monotonically, it is not greatly affected by the choice of Λ . In what follows we will take¹² $\Lambda = 4.5\sigma$.

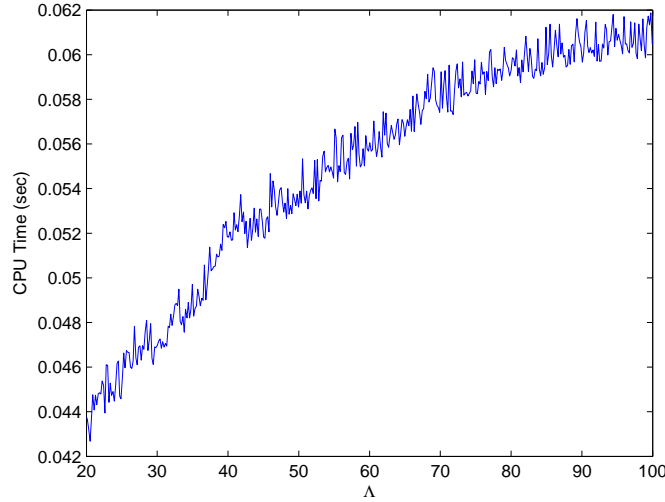


FIGURE 4. CPU times for varying Λ , for an OTM vanilla call option with $x' = -10^{-6}$, $K = 1$, $\lambda_- = -11$, $\lambda_+ = 8$, $m_2 = 0.16$, $r = 0.03$, $q = 0$, $\tau = 0.004$, for $\epsilon_1 = \epsilon_2 = 10^{-16}$.

3.4.5.2. *Choice of ϵ_1 and ϵ_2 .* Figures 5-6 show the effect of varying the error tolerances ϵ_1 and ϵ_2 used in the calculation of $\Psi_1(x'; \sigma, \omega; \Lambda)$ and $\Psi_2(x'; \sigma, \omega; \Lambda)$, respectively, on both price accuracy and CPU time (in seconds, cf. Figures 2-3 for the ATMVG case). As in Section 3.4.5.1, we take an OTM call option with $x' = -10^{-6}$. We note that, similarly to the ATMVG case

1. The price does not change between $\epsilon_1 = 10^{-16}$ and $\epsilon_1 \approx 2 \cdot 10^{-11}$, and the absolute difference w.r.t. $\epsilon_1 = 10^{-16}$ is still well below floating point accuracy up to $\epsilon_1 \approx 2.5 \cdot 10^{-10}$.

¹²As shown in Figure 4, smaller values of Λ , such as 2σ or 3σ , result in slightly faster calculation times. However, we observed that choosing too small a value of Λ (such as 1.5σ) can occasionally result in difficulties when evaluating the incomplete gamma function for the calculation of Ψ_2 . To be on the safe side, as a rule of thumb, we recommend taking a slightly larger value of Λ , in the range 4σ - 5σ .

2. The CPU time increases almost monotonically for decreasing ϵ_1 .
3. The absolute error increases approximately monotonically for increasing ϵ_2 , staying about two orders of magnitude below ϵ_2 , and the CPU time is largely independent of ϵ_2 .

We conclude that, even if accuracy of the order of floating point precision is needed, one might as well take ϵ_1 in the range 10^{-11} – 10^{-7} and ϵ_2 in the range 10^{-15} – 10^{-14} .

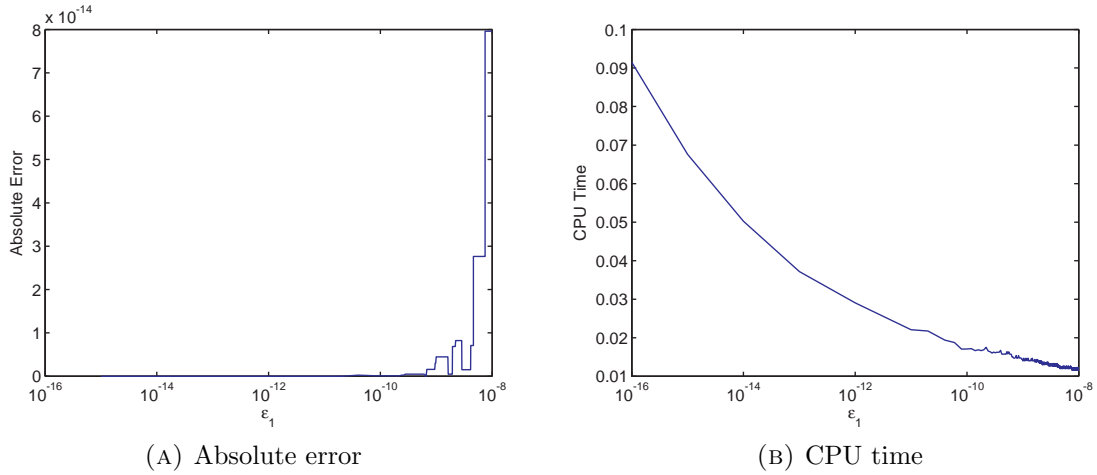


FIGURE 5. Absolute errors in the FastVG price, and corresponding CPU times (in seconds), for varying error tolerance level ϵ_1 w.r.t. $\epsilon = 10^{-16}$, for an OTM vanilla call option with $x' = -10^{-6}$, $K = 1$, $\lambda_- = -11$, $\lambda_+ = 8$, $m_2 = 0.16$, $r = 0.03$, $q = 0$, $\tau = 0.004$, for $\Lambda = 4.5\sigma$.

3.4.5.3. Comparison of CPU times. For comparisons of the performances obtained using different numerical integration methods, see Appendix E.2. In Figure 7 we plot the CPU times taken to price an OTM call option with the FastVG method, for a wide range of x' from $x' = -0.01$ to $x' = -10^{-10}$. It can be seen that the CPU time is almost independent of x' . This indicates that the conclusions from the previous examples, for $x' = -10^{-6}$, should also hold for other values of x' .

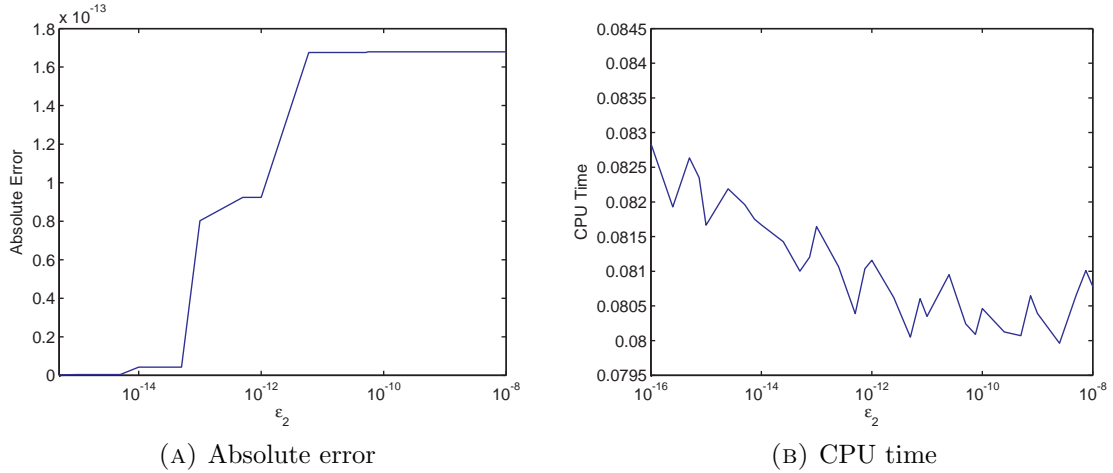


FIGURE 6. Absolute errors in the ATMVG price, and corresponding CPU times (in seconds), for varying error tolerance level ϵ_2 w.r.t. $\epsilon = 10^{-16}$, for an OTM vanilla call option with $x' = -10^{-6}$, $K = 1$, $\lambda_- = -11$, $\lambda_+ = 8$, $m_2 = 0.16$, $r = 0.03$, $q = 0$, $\tau = 0.004$, for $\Lambda = 4.5\sigma$.

In Figure 8, we show the CPU times taken by parabolic iFT with $\alpha = 2.9$ (solid line) versus those of FastVG using Clenshaw-Curtis integration, with $\epsilon_1 = 10^{-7}$, $\epsilon_2 = 10^{-15}$ (dashed line), for better than 1% accuracy (left panel) and better than 0.1% accuracy (right panel). The following parameter set¹³ was used: $\lambda_- = -31.6586$, $\lambda_+ = 14.9279$, $m_2 = 0.0232$. In both cases, we take a vanilla option with $K = 1$, $r = 0.03$, $q = 0$, and maturity $\tau = 0.004$ (approximately one day). Our results show that, for vanilla option prices, FastVG is faster than parabolic iFT for short maturities and options close to ATM, or for small error tolerances. As noted in Section 3.1, such short distances from the ATM point $x' = 0$ may naturally occur during a model calibration.

¹³Calibrated by the author to the volatility surface of AUDUSD options as of 12 March 2010.

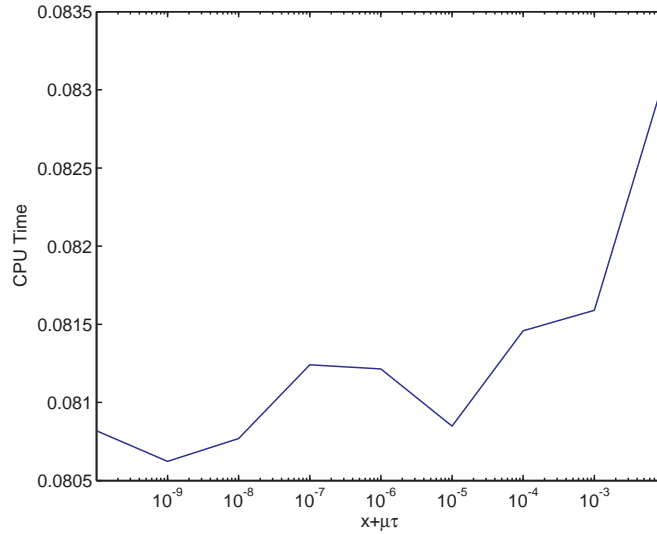
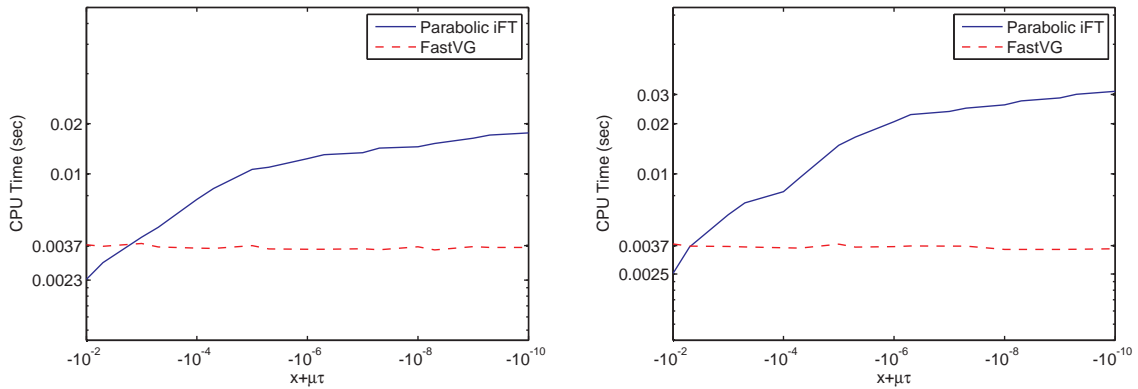


FIGURE 7. CPU times (in seconds) taken for the calculation of the FastVG price for an OTM vanilla call option with $K = 1$, $\lambda_- = -11$, $\lambda_+ = 8$, $m_2 = 0.16$, $r = 0.03$, $q = 0$, $\tau = 0.004$, for $\Lambda = 4.5\sigma$, for varying $x' = x + \mu\tau$, using Gauss-Lobatto quadrature.



(A) Better than 1% accuracy

(B) Better than 0.1% accuracy

FIGURE 8. Logarithmic plots of CPU times with parabolic iFT (with $\alpha = 2.9$) and FastVG, with Clenshaw-Curtis integration, for the price of a vanilla call option with $K = 1$, $\lambda_- = -31.6586$, $\lambda_+ = 14.9279$, $m_2 = 0.0232$, $r = 0.03$, $q = 0$, $\tau = 0.004$, for varying $x' = x + \mu\tau$, with different accuracy levels. The VG parameters were calibrated to the volatility surface of AUDUSD options as of 12 March 2010.

3.4.5.4. *CPU times for digitals.* In Figure 9 we show the CPU times taken by parabolic iFT with $\alpha = 2.9$ (solid line) versus those of FastVG with Clenshaw-Curtis integration, $\epsilon_1 = 10^{-7}$, $\epsilon_2 = 10^{-15}$ (dashed line), for better than 1% accuracy (left panel) and better than 0.1% accuracy (right panel), and time to maturity $\tau = 0.004$. In both cases, we take a digital call option with $K = 1$, $r = 0.03$, $q = 0$, and the same process parameters used in Section 3.4.5.3, namely $\lambda_- = -31.6586$, $\lambda_+ = 14.9279$, $m_2 = 0.0232$. In general, FastVG outperforms parabolic iFT for maturities up to about two weeks, except for deep OTM options.

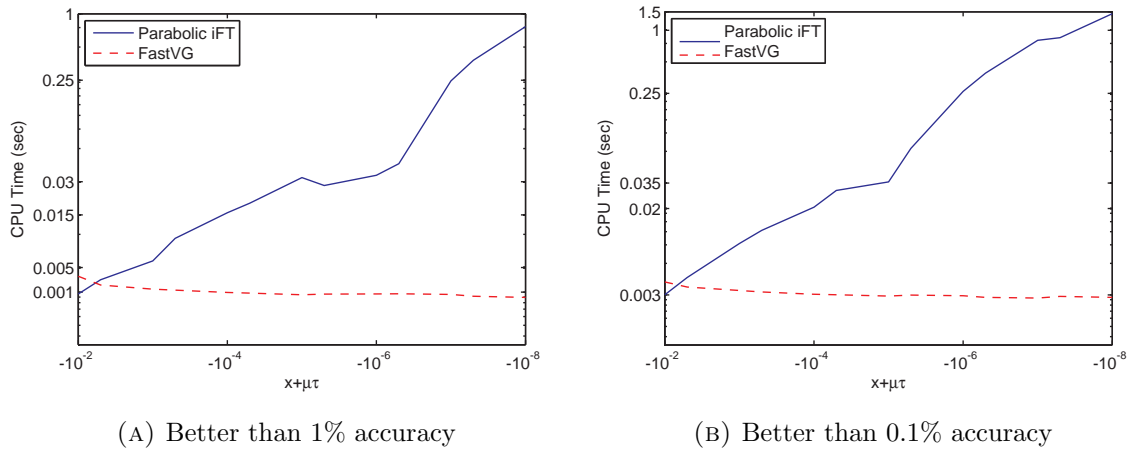


FIGURE 9. Logarithmic plots of CPU times with parabolic iFT (with $\alpha = 3$) and FastVG, with Clenshaw-Curtis integration, for the price of a digital call option with $K = 1$, $\lambda_- = -31.6586$, $\lambda_+ = 14.9279$, $m_2 = 0.0232$, $r = 0.03$, $q = 0$, $\tau = 1/26$, for varying $x' = x + \mu\tau$, with different accuracy levels.

3.5. Analysis of relative performance of flat and parabolic iFT

3.5.1. Flat iFT. Flat iFT consists in the computation of a truncated and discretized version of the integral on the RHS of (12) over a uniform grid (cf. Section 2.2). It was shown in [19] that flat iFT and its common variants are less efficient

than the new versions introduced in *op. cit.*, especially parabolic iFT. Flat iFT is, however, still widely used by practitioners.

Throughout this section, when comparing our results with those obtained by iFT, unless stated otherwise, we will use for the latter a grid $x_j = -\mu\tau - j\Delta$, $j = 0, \dots, M$, with $\Delta = 0.02$, $M = 12$, and $x_M = -\mu\tau$. We fix our initial error tolerance at $\epsilon = 10^{-7}$ and, using the error bound in Appendix C.1, choose the smallest $\Lambda = \Lambda_0$ such that the truncation error is smaller than $\epsilon/2$. Then, using this Λ_0 , we take an initial mesh $\zeta \gg 1$ in the dual space, calculate the option price, and progressively decrease ζ by a constant factor between 1 and 2, until the difference between two successive evaluations lies below $\epsilon/2$. The justification for this procedure lies in the fact that, as shown in [19] (cf. Appendix O.1.1), the error in the discretized version of (12), without truncation, decays as $C \exp[-2\pi d(\omega)/\zeta]$, where C is a constant and $d(\omega)$ is the minimum distance between the line $\text{Im } \xi = \omega$ and the boundary of the strip of analyticity of the integrand in (12). Therefore, by decreasing ζ in a loop by a factor of 1.5 each time, say, we can expect to reach very quickly a point where the discretization error is negligible. Figure 10 shows a logarithmic plot of the absolute pricing error w.r.t. the ATMVG price (solid line) as a function of ζ , when Λ is held fixed at a value chosen to ensure that the truncation error is smaller than $5 \cdot 10^{-10}$ ($\Lambda \approx 2.441 \cdot 10^8$). The solid line in Figure 10 is therefore a good approximation to the discretization error. The dashed line is just $C \exp[-2\pi d(\omega)/\zeta]$, where the constant C is chosen so that the theoretical estimate coincides with the actual error for $\zeta = 2$. The two curves closely follow each other as the mesh is reduced from $\zeta = 2$ down to about $\zeta = 0.6$. For lower values of ζ the curves diverge, since the theoretical discretization error for such values of ζ is smaller than residual numerical errors, which are mostly due to truncation.

Figure 11 shows the truncation error and CPU time as functions of Λ . We note that very large grids are needed for good accuracies, e.g. for a relative pricing error smaller than 1% one needs over 10,000 points, and 60 ms of CPU time. For relative errors smaller than 0.01%, over 120,000 points are needed, and 0.47 seconds of CPU time.

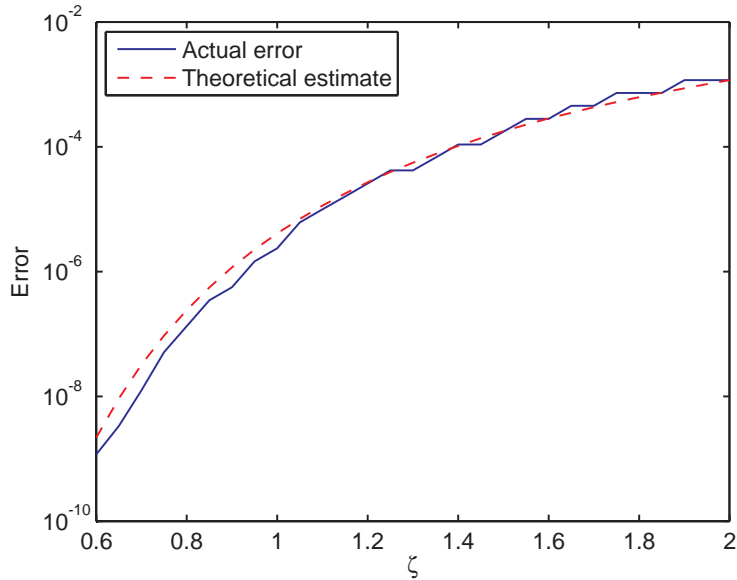


FIGURE 10. Discretization error under flat iFT for an ATM vanilla call option with $K = 1$, $\lambda_- = -11$, $\lambda_+ = 8$, $m_2 = 0.16$, $r = 0.03$, $q = 0$, $\tau = 0.004$, for varying ζ .

3.5.2. Parabolic iFT. A theoretical bound for the ATM truncation error in the VG case can be derived (the details can be found in Appendix C.2), and the same procedure as for flat iFT can be followed in order to separate the discretization and truncation errors. Figure 12 shows the absolute truncation error and the CPU time for the price of an ATM vanilla call option calculated using parabolic iFT with $\alpha = 3.9$. The comparison shows that parabolic iFT is several orders of magnitude faster and more accurate than flat iFT, needing only 880 points, and 4 ms of CPU

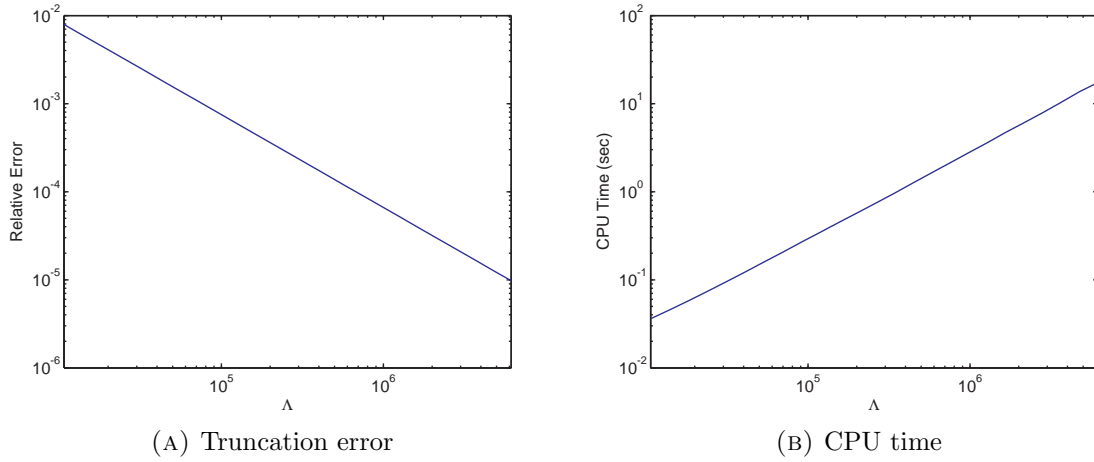


FIGURE 11. Truncation error (logarithmic plot) and CPU time (logarithmic plot) under flat iFT for an ATM vanilla call option with $K = 1$, $\lambda_- = -11$, $\lambda_+ = 8$, $m_2 = 0.16$, $r = 0.03$, $q = 0$, $\tau = 0.004$, for varying Λ .

time, for relative errors smaller than 1%, and 9535 points, and 34.6 ms of CPU time, for relative errors smaller than 0.01%. Increasing Λ further, one can achieve absolute and relative errors of the order of 10^{-10} to 10^{-9} . Of course, this gain in accuracy for increasing Λ comes at the cost of additional CPU time: already for errors of the order of 10^{-9} to 10^{-8} , the calculation can take 0.10–0.60 seconds, whereas, as we saw in Section 3.4.2, ATMVG is much faster.

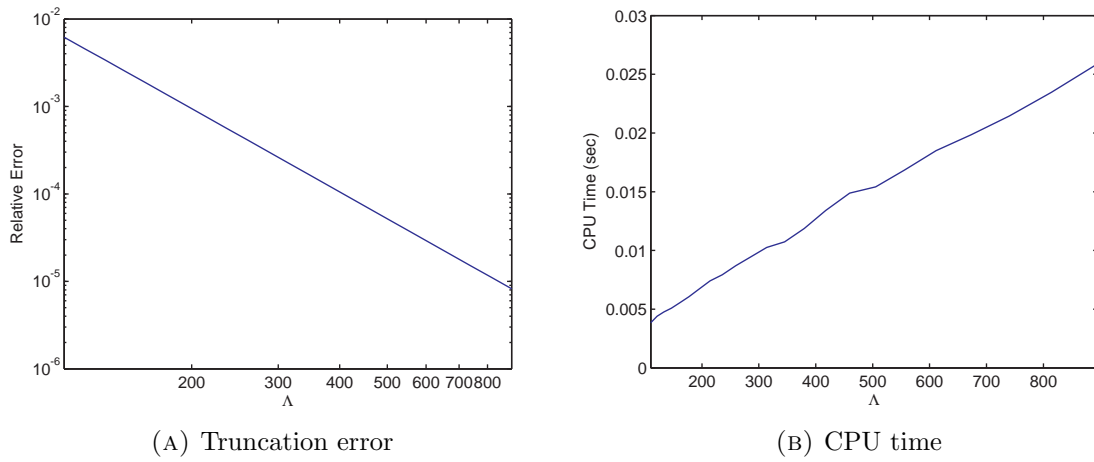


FIGURE 12. Truncation error (logarithmic plot) and CPU time under parabolic iFT, with $\alpha = 3$, for an ATM vanilla call option with $K = 1$, $\lambda_- = -11$, $\lambda_+ = 8$, $m_2 = 0.16$, $r = 0.03$, $q = 0$, $\tau = 0.004$, for varying Λ .

CHAPTER 4

Pricing discretely monitored barrier options under Lévy processes

4.1. General remarks

As noted in the Introduction, the backward induction approach, first used by Eydeland in [41], reduces the problem of pricing a discretely monitored barrier option to that of pricing a sequence of European options. Both the HT method [45] and the COS method [44] are efficient, provided the parameters of the numerical schemes are chosen optimally or close to optimally (given the desired error tolerance). However, if the choice is insufficiently accurate, sizable errors may result; for options of several years' maturity, the numerical scheme may blow up due to error accumulation. The error control is non-trivial because of several interacting sources of errors. In general, one should expect that, in order to control n sources of errors, a numerical scheme should be specified in terms of $m \geq n$ parameters. Both in [45] and [44], $m < n$, and, although the prescriptions for the choice of the parameters are fairly ingenious and work well in many cases, in other cases, the quality of the prescriptions is not good enough.

We describe a new version of backward induction, introduced in [36], which allows us to separate the sources of errors and control each of them efficiently. Our method consists of the following main blocks: (i) truncation of the state space; (ii) piece-wise polynomial approximation of the payoff G_s at each step of backward induction; (iii) pricing options with the modified payoff using the Fourier transform technique. In

the exponential Lévy models that we consider, the error of (i) decays exponentially, and can be efficiently controlled independently of other sources of errors. Modulo certain reservations in the case of the Variance Gamma model and the KoBoL model of order close to 0, the errors of (iii) also decay exponentially or even faster, and can be controlled relatively easily. We choose the corresponding parameters of the numerical scheme so that the contributions of errors of blocks (i) and (iii) are much smaller than the desired error tolerance. The resulting scheme behaves as if the interpolation error were the only source of errors. Figure 1 below shows the absolute error due to piece-wise quadratic interpolation versus the third power of the interpolation mesh Δ , for a down-and-out put option, with two parameter sets used in the literature (cf. Lemma 4.4 and Section 4.4).

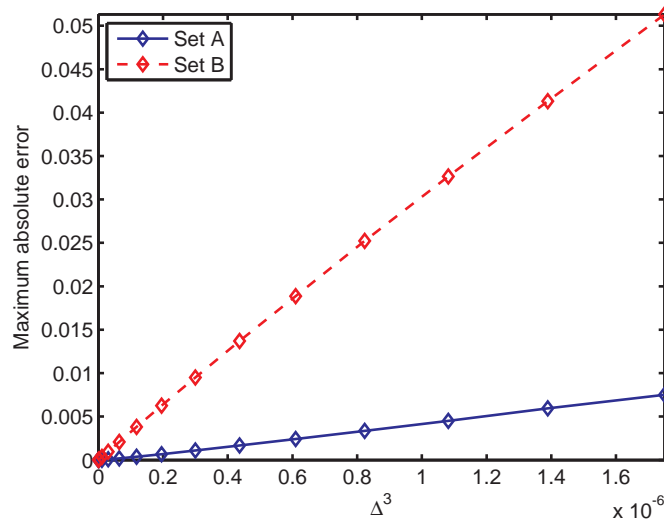


FIGURE 1. Maximum absolute error in the interval $1.01 \cdot H \leq S \leq K$ versus Δ^3 , where Δ is the interpolation mesh in $\log-S$ space, for a down-and-out put option with strike $K = 100$, barrier $H = 80$ and time to maturity $T = 0.25$, for parameter set A, used in [19], and parameter set B, used in [45] and [44]. The interval shown corresponds approximately to Δ lying between $2.23 \cdot 10^{-4}$ and 0.012 (see Section 4.4 for more details).

The scheme that we realize is stable but involves a certain overkill which results in an additional computational cost. However, due to the fast decay of errors, the CPU time increases by a factor of 2-3 only. The gain is that we can essentially guarantee the desired error tolerance, whereas the simplified prescriptions in [45] and [44] may result in sizable errors, and good results can be achieved only by trial and error, playing with the parameters of the scheme. Note that, in some cases, our method is much faster than the HT method (cf. Tables 1 and 3), and the ad hoc procedure for the choice of parameters given in [44] can result in very large errors for COS.

4.2. General scheme for pricing down-and-out put options

4.2.1. Reduction to pricing European options. We consider the down-and-out (DO) barrier put option¹ with barrier $H = e^h$, strike $K > H$, and monitoring dates $(0 =)t_0 < t_1 < \dots < t_N (= T)$. Let $V_s(x)$ denote the option price at time $t = t_s$ and $X_{t_s} = x$, $s = 0, 1, \dots, N$. Then $V_N(x) = (K - e^x)_+ \mathbb{1}_{(h, \infty)}(x)$. For $s = N - 1, N - 2, \dots, 0$, we set

$$V_s(x) = 0, \quad x \leq h, \quad (75)$$

and calculate

$$V_s(x) = e^{-r\bar{\Delta}_s} \int_{\mathbb{R}} p_{\bar{\Delta}_s}(y) V_{s+1}(x+y) dy, \quad x > h, \quad (76)$$

where $\bar{\Delta}_s = t_{s+1} - t_s$, and $p_{\bar{\Delta}_s}$ is the transition probability density of $X_{\bar{\Delta}_s}$. The option price at time $t \in (t_s, t_{s+1})$ can be calculated as the price of a European option with payoff $V_{s+1}(X_{t_{s+1}})$ and maturity t_{s+1} :

$$V(t, x) = e^{-r(t_{s+1}-t)} \int_{\mathbb{R}} p_{t_{s+1}-t}(y) V_{s+1}(x+y) dy, \quad x \in \mathbb{R}. \quad (77)$$

¹This is one of the most liquid contracts in the market. For the generalization of the method to other option types, see Appendix K.

For simplicity, we assume that the monitoring dates are equally spaced so that $\bar{\Delta}_s = \bar{\Delta} := T/N$.

Step I. The Fourier Transform of the terminal payoff $G(x) := V_N(x)$,

$$\widehat{G}(\xi) = -\frac{K}{\xi(\xi+i)}e^{-i\xi \ln K} + \left(\frac{K}{i\xi} + \frac{e^h}{1-i\xi}\right)e^{-ih\xi}, \quad (78)$$

is an analytic function in the complex plane, which decays at infinity as $|\xi|^{-1}$ as $\xi \rightarrow \infty$ in any strip of finite width around the real axis². Therefore, we can take any $\omega \in (\lambda_-, \lambda_+)$ and calculate $V_{N-1}(x)$, $x > h$, as follows (cf. Section 2.2)

$$V_{N-1}(x) = \frac{e^{-r\bar{\Delta}}}{2\pi} \int_{\text{Im } \xi = \omega} e^{i(x+\mu\bar{\Delta})\xi - \bar{\Delta}\psi^0(\xi)} \widehat{G}(\xi) d\xi. \quad (79)$$

In Appendix O, we describe the general procedure for the calculation of the RHS of (79) with both flat and parabolic iFT [19]. Other methods include the European option versions of the CONV [65] and COS [43] methods³. The parabolic iFT method is generally faster than flat iFT, since it allows one to use a far smaller number of points in the dual space in the discretized and truncated version of (79) (cf. Section 3.5, [19, 35]).

For practical computations, it is convenient to write the RHS of (79) as follows

$$\begin{aligned} V_{N-1}(x) = & -\frac{Ke^{-r\bar{\Delta}}}{2\pi} \int_{\text{Im } \xi = \omega} \frac{e^{i(x+\mu\bar{\Delta}-\ln K)\xi - \bar{\Delta}\psi^0(\xi)}}{\xi(\xi+i)} d\xi \\ & + \frac{e^{-r\bar{\Delta}}}{2\pi} \int_{\text{Im } \xi = \omega} e^{i(x+\mu\bar{\Delta}-h)\xi - \bar{\Delta}\psi^0(\xi)} \left(\frac{K}{i\xi} + \frac{e^h}{1-i\xi}\right) d\xi, \quad x > h, \end{aligned} \quad (80)$$

where we take $\omega \in (0, \lambda_+)$. Note that the first integral in (80) gives the price of a vanilla put option with strike K , and the second integral can be regarded as a correction due to the knock-out barrier.

²The singularities at $\xi = 0$ and $\xi = -i$ are removable.

³For a comprehensive review and analysis of performances, see [19].

Step II. For $s = N - 1, N - 2, \dots, 0$, the Fourier transform \widehat{V}_s does not have a sufficiently simple form, therefore, we will approximate V_s by a piece-wise polynomial \mathcal{V}_s , so that the Fourier transform $\widehat{\mathcal{V}}_s$ can be calculated explicitly. We choose a grid that contains h , and starts with h : $(h =)x_1 < x_2 < \dots < x_M$, because all $V_s(x)$ vanish below h . Next, the discretization error will be large unless we use $V_{s+1}(h + 0)$ instead of $V_{s+1}(h)(= 0)$ in the calculation of $V_s(x_j)$, $j = 1, 2, \dots, M$ at steps $s = N - 1, N - 2, \dots, 1$ of the backward induction procedure. Equivalently, we set $V_N(x) = (K - e^x)_+ \mathbb{1}_{[h, \infty)}(x)$, and, for $s = N - 1, N - 2, \dots, 1$, set

$$V_s(x) = 0, \quad x < h, \quad (81)$$

and calculate

$$V_s(x) = e^{-r\bar{\Delta}} \int_{\mathbb{R}} p_{\bar{\Delta}}(y) V_{s+1}(x + y) dy, \quad x \geq h. \quad (82)$$

Of course, this is only a useful computational trick. The option price at $x = h$ is zero at each monitoring date. For a numerical realization of (82) using the iFT method, it is necessary to approximate V_s by a function, whose Fourier transform can be calculated explicitly. We will use piece-wise polynomial approximations. The choice of the order of approximation generally depends on the smoothness of V_s . It turns out (cf. Section 4.2.3) that the main difficulties occur when ν and $\bar{\Delta}$ are both small⁴.

4.2.2. Greeks. The approach described above for the calculation of the price can be modified for the calculation of the option's delta and gamma. Since the underlying spot price S_0 at time t_0 equals e^x , the chain rule gives the following expressions for

⁴Naturally, which values of ν and $\bar{\Delta}$ qualify as small will generally depend on the process parameters. Our tests showed that, for steepness parameters and values of m_2 which typically arise from calibrations to market data, $\nu \in [0, 0.3]$ can be considered small, for the daily monitoring case.

the delta and gamma, respectively

$$\frac{\partial V}{\partial S_0} = e^{-x} \frac{\partial V}{\partial x}, \quad (83)$$

$$\frac{\partial^2 V}{\partial S_0^2} = e^{-x} \frac{\partial}{\partial x} \left(e^{-x} \frac{\partial V}{\partial x} \right) = e^{-2x} \left(\frac{\partial^2 V}{\partial x^2} - \frac{\partial V}{\partial x} \right). \quad (84)$$

For model processes of order $\nu > 0$, by differentiating n times under the integral sign of the iFT integral for $V_0(x)$, one obtains the following explicit expression for $V_0^{(n)}(x) := \partial_x^n V_0(x)$

$$V_0^{(n)}(x) = \frac{e^{-r\bar{\Delta}}}{2\pi} \int_{\text{Im } \xi = \omega} e^{i(x+\mu\bar{\Delta})\xi - \bar{\Delta}\psi^0(\xi)} (i\xi)^n \widehat{V}_1(\xi) d\xi. \quad (85)$$

The delta and gamma can be calculated as follows: at the last step of backward induction, one performs two additional convolutions to calculate approximations to $V_0'(x)$ and $V_0''(x)$, and then uses (83) and (84).

4.2.3. Regularity of the option price and sensitivities. Assume that X is a model process of order $\nu > 0$ (or, more generally, an RLPE; cf. Appendix A.2, [18, Ch. 3]), and let, as in the rest of this thesis, $\psi^0(\xi)$ denote the characteristic exponent without the term $-i\mu\xi$: $\psi(\xi) = -i\mu\xi + \psi^0(\xi)$. Then, for any $\tau > 0$, the integrand in

$$p_\tau(x) = \frac{1}{2\pi} \int_{\mathbb{R}} e^{-i\xi(x-\mu\tau) - \tau\psi^0(\xi)} d\xi \quad (86)$$

decays faster than any power of $|\xi|$ at infinity. Therefore, all the derivatives of the integrand w.r.t. x are continuous. Since X is an RLPE, the derivatives decay exponentially at infinity. Writing (82) in the form

$$V_s(x) = e^{-r\bar{\Delta}} \int_{\mathbb{R}} p_{\bar{\Delta}}(y-x) V_{s+1}(y) dy, \quad x \geq h, \quad (87)$$

and differentiating w.r.t. x under the integral sign, we obtain that $V_s \in C^\infty([h, \infty))$. Hence, formally, interpolation methods of arbitrary order are applicable. However, if $\bar{\Delta}$ and ν are both small, then $\exp[-\bar{\Delta}\psi^0(\xi)]$ decays slowly as $\xi \rightarrow \infty$, and, therefore, in the vicinity of $x = \mu\tau$, $p_\tau(x)$ is rather large, and the derivatives of $p_\tau(x)$ are very large indeed. Since V_N is discontinuous at $x = h$, we conclude from (82) that the derivatives of $V_s(x)$ are large at $x = h - (N - s)\mu\bar{\Delta}$. Of course, if $\mu > 0$, then $h - (N - s)\mu\bar{\Delta} < h$, and, therefore, this remark is irrelevant.

4.2.4. Piece-wise polynomial approximations. For a numerical realization, one discretizes and truncates the state space, choosing an appropriate grid⁵. To minimize the discretization error, a grid should ideally be chosen so that both h and $\ln K - \mu\bar{\Delta}$ are among its points.

We want to calculate $V_s(x)$ at points of a grid $\mathbf{x} = (x_j)_{j=1}^M$ given values v_j^{s+1} of $V_{s+1}(x)$ at points of the same grid. Consider the piece-wise polynomial interpolation⁶ of degree m of the function $V_s(x)$, $s = N - 1, N - 2, \dots, 1$, on the grid $\mathbf{x} = (x_j)_{j=1}^M$

$$V_s(x) \approx \mathcal{V}_s(x) = \sum_{j=1}^{M-1} \sum_{\ell=0}^m f_{j,\ell}^{m,s} \left(\frac{x - x_j}{x_{j+1} - x_j} \right)^\ell \mathbb{1}_{[x_j, x_{j+1})}(x). \quad (88)$$

(In general formulas below, $f_{j,\ell}^{m,s}$ with $\ell > m$ may appear; then $f_{j,\ell}^{m,s} = 0$). In Appendix M.1, we prove

Lemma 4.1. *The Fourier transform of $\mathcal{V}_s(x)$ is given by*

$$\widehat{\mathcal{V}}_s(\xi) = \sum_{\ell=0}^m \Delta^{-\ell} \sum_{j=1}^M \mathcal{W}_{j,\ell}^{m,s} e^{-ix_j\xi} (-i\xi)^{-\ell-1}, \quad (89)$$

⁵An alternative is to take the Fourier transform and do calculations in the dual space; then the dual space is discretized as well (cf. Appendix P).

⁶Hermite spline interpolation tends to perform less well than piece-wise quadratic or cubic interpolation.

where

$$\mathcal{W}_{1,0}^{m,s} = -f_{1,0}^{m,s}, \quad \mathcal{W}_{1,1}^{m,s} = f_{1,1}^{m,s}, \quad \mathcal{W}_{1,2}^{m,s} = -2f_{1,2}^{m,s}, \quad \mathcal{W}_{1,3}^{m,s} = 6f_{1,3}^{m,s}, \quad (90)$$

$$\mathcal{W}_{j,0}^{m,s} = 0, \quad j = 2, 3, \dots, M,$$

$$\mathcal{W}_{M,1}^{m,s} = -f_{M-1,1}^{m,s} - 2f_{M-1,2}^{m,s} - 3f_{M-1,3}^{m,s},$$

$$\mathcal{W}_{M,2}^{m,s} = 2f_{M-1,2}^{m,s} + 6f_{M-1,3}^{m,s}, \quad \mathcal{W}_{M,3}^{m,s} = -6f_{M-1,3}^{m,s},$$

and, for $j = 2, 3, \dots, M - 1$,

$$\mathcal{W}_{j,1}^{m,s} = f_{j,1}^{m,s} - f_{j-1,1}^{m,s} - 2f_{j-1,2}^{m,s} - 3f_{j-1,3}^{m,s}, \quad (91)$$

$$\mathcal{W}_{j,2}^{m,s} = 2f_{j-1,2}^{m,s} - 2f_{j,2}^{m,s} + 6f_{j-1,3}^{m,s},$$

$$\mathcal{W}_{j,3}^{m,s} = -6f_{j-1,3}^{m,s} + 6f_{j,3}^{m,s}.$$

Remark 4.2 (Notation conventions). The index denoting the time step is usually placed at the bottom, unless we need to denote the j -th element of an array, or the (j, k) element of a matrix, in which case the time step index will move to the top (e.g., $v_s(x_j)$ versus v_j^s , for $s = 1, 2, \dots, N - 1$ and $j = 1, 2, \dots, M$). Occasionally, in order to avoid ambiguity, we will denote a vector by using boldface letters (e.g., to distinguish the grid \mathbf{x} from the point $x = \ln S_0$). For ease of notation, from now on we will drop the superscript m in $\mathcal{W}_{j,\ell}^{m,s}$ and $f_{j,\ell}^{m,s}$, writing $\mathcal{W}_{j,\ell}^s$ and $f_{j,\ell}^s$, respectively.

Since, as will be shown in Section 4.4, the version with $m = 2$ is usually the most efficient one, this is the only case on which we will focus in the rest of this chapter and in the following one. A description of the procedures for piece-wise linear and cubic interpolation can be found in Appendix I. On $[x_{M-1}, x_M]$, we approximate $V_s(x)$ as

$$V_s(x) \approx \frac{(x - x_M)^2}{(x_{M-1} - x_M)^2} f_{M-1,2}^{2,s}, \quad (92)$$

on $[x_j, x_{j+1}]$, $j = 2, 3, \dots, M - 1$, as a quadratic polynomial $\mathcal{V}_{(j)}^s$ satisfying

$$\mathcal{V}_{(j)}^s(x_{j-1}) = v_{j-1}^s, \quad \mathcal{V}_{(j)}^s(x_j) = v_j^s, \quad \mathcal{V}_{(j)}^s(x_{j+1}) = v_{j+1}^s, \quad (93)$$

and, on $[x_1, x_2]$, as a quadratic polynomial satisfying

$$\mathcal{V}_{(1)}^s(x_1) = v_1^s, \quad \mathcal{V}_{(1)}^s(x_2) = v_2^s, \quad \mathcal{V}_{(1)}^s(x_3) = v_3^s. \quad (94)$$

In the case of an equally spaced grid, we find

$$f_{1,0}^s = v_1^s, \quad f_{1,1}^s = 2v_2^s - (3v_1^s + v_3^s)/2, \quad f_{1,2}^s = -v_2^s + (v_1^s + v_3^s)/2, \quad (95)$$

for $j = 2, 3, \dots, M - 2$,

$$f_{j,1}^s = (v_{j+1}^s - v_{j-1}^s)/2, \quad f_{j,2}^s = (v_{j+1}^s + v_{j-1}^s)/2 - v_j^s, \quad (96)$$

and, finally,

$$f_{M-1,0}^s = v_{M-1}^s, \quad f_{M-1,1}^s = -2v_{M-1}^s, \quad f_{M-1,2}^s = v_{M-1}^s. \quad (97)$$

It follows that, for piece-wise quadratic interpolation, we have

$$\mathcal{W}_{1,0}^s = -v_1^s, \quad (98)$$

$$\mathcal{W}_{1,1}^s = 2v_2^s - (3v_1^s + v_3^s)/2, \quad (99)$$

$$\mathcal{W}_{1,2}^s = 2v_j^s - v_{j+1}^s - v_{j-1}^s, \quad (100)$$

$$\mathcal{W}_{M,1}^s = 0, \quad (101)$$

$$\mathcal{W}_{M,2}^s = 2v_{M-1}^s, \quad (102)$$

and, for $j = 2, 3, \dots, M - 1$

$$\mathcal{W}_{j,1}^s = \frac{1}{2}(v_{j+1} - 3v_j + 3v_{j-1} - v_{j-2}), \quad (103)$$

$$\mathcal{W}_{j,2}^s = 2\mathcal{W}_{j,1}^s. \quad (104)$$

4.2.5. Calculation of (approximations to) $V_s(x_k)$ using the inverse Fourier transform. Assuming that the coefficients $f_{j,\ell}^{s+1}$ of approximation (88) with $s + 1$ instead of s are known, and the Fourier transform $\widehat{\mathcal{V}}_{s+1}(\xi)$ has been calculated, we find approximations to $V_s(x_k)$ by replacing V_{s+1} on the RHS of (82) with \mathcal{V}_{s+1} and applying the iFT method:

$$\begin{aligned} V_s(x_k) &\approx \frac{e^{-r\bar{\Delta}}}{2\pi} \int_{\text{Im } \xi = \omega} e^{i(x_k + \mu\bar{\Delta})\xi - \bar{\Delta}\psi^0(\xi)} \widehat{\mathcal{V}}_{s+1}(\xi) d\xi \\ &= \sum_{j=1}^M \sum_{\ell=0}^m \Delta^{-\ell} \mathcal{W}_{j,\ell}^{s+1}(f^{s+1}) \frac{e^{-r\bar{\Delta}}}{2\pi} \int_{\text{Im } \xi = \omega} \frac{e^{i(x_k - x_j + \mu\bar{\Delta})\xi - \bar{\Delta}\psi^0(\xi)}}{(-i\xi)^{\ell+1}} d\xi. \end{aligned} \quad (105)$$

Introduce the notation

$$I(\omega; n, \ell) = \frac{e^{-r\bar{\Delta}}}{2\pi} \int_{\text{Im } \xi = \omega} e^{i(n\Delta + \mu\bar{\Delta})\xi - \bar{\Delta}\psi^0(\xi)} (-i\xi)^{-\ell-1} d\xi. \quad (106)$$

We can re-write (105) as

$$V_s(x_k) = \sum_{j=1}^M \sum_{\ell=0}^m \Delta^{-\ell} \mathcal{W}_{j,\ell}^{s+1}(f^{s+1}) I(\omega; k - j, \ell). \quad (107)$$

We will use $\omega \in (0, \lambda_+)$. In what follows, we will sometimes write $I_\ell(n\Delta)$ instead of $I(\omega, n, \ell)$, in which case it will be understood that $\omega \in (0, \lambda_+)$. $I(\omega; n, \ell)$ is the time-0 price of a put-like option⁷ with the payoff $G(X_{\bar{\Delta}}) = (\ell!)^{-1}(-X_{\bar{\Delta}})_+^\ell$ at maturity date $\bar{\Delta}$; the spot is $X_0 = n\Delta$ (then it can be verified that $\widehat{G}(\xi) = (-i\xi)^{-\ell-1}$, $\text{Im } \xi > 0$).

⁷A put-like (call-like) option is a European option whose terminal payoff $G(x)$ vanishes above (below) a certain point.

Therefore, each $I(\omega; n, \ell)$ can be evaluated using any version of the iFT method, such as the new ones introduced in [19]. Of these, parabolic iFT has been shown to be the most efficient (cf. Chapter 3, [19, 35]). Details of the algorithm for both standard and parabolic iFT can be found in Appendices B and O. Parabolic iFT is applicable in the ATM ($n\Delta + \mu\bar{\Delta} = 0$) and OTM case. Put-like options are OTM iff $n\Delta + \mu\bar{\Delta} > 0$; if $n\Delta + \mu\bar{\Delta} < 0$, then we push the line of integration in (106) to $\text{Im } \xi = \omega' \in (\lambda_-, 0)$, and reduce to calculation of $I(\omega'; n, \ell)$, which is the price of an OTM call-like option. Using the residue theorem and the notation $z = i\xi$, we obtain

$$I(\omega; n, \ell) = I(\omega'; n, \ell) + \frac{(-1)^\ell}{\ell!} e^{-r\bar{\Delta}} \left(\frac{d^\ell}{dz^\ell} e^{z(n\Delta + \mu\bar{\Delta}) - \bar{\Delta}\psi^0(-iz)} \right) \Big|_{z=0}. \quad (108)$$

The $\mathcal{W}_{j,\ell}^{s+1}(f_{s+1})$ are linear functions of the entries of the matrix $f_{s+1} = [f_{j,\ell}^{s+1}]$, therefore, approximations to $V_s(x_k)$ are linear functions of the same entries. In turn, $f_{j,\ell}^{s+1}$ will be expressed as linear functions of $V_{s+1}(x_n)$, $n = 1, 2, \dots, M$. After the $I(\omega, n, \ell)$ are calculated for $n = -M + 1, -M + 2, \dots, M - 1$, the sum $\sum_{j=1}^M$ in (107) can be calculated using the fast convolution algorithm (see Appendix L, [14]). The pricing algorithm, for the case of piece-wise quadratic interpolation, can be found in Appendix H, and the modifications for the cases of piece-wise linear and cubic interpolation can be found in Appendix I.

4.3. Error estimates

The method has several sources of errors. We will examine each one in detail.

4.3.1. Truncation in the state space. The choice of a grid implies the absolute truncation of the state space above $x_M (> \ln K)$. In Appendix M.2, we will prove the following

Lemma 4.3. For any $\omega_- \in (\lambda_-, 0)$ and $\omega_+ \in (0, \lambda_+)$, the truncation error in the state space, for the time-0 option price at $X_0 = x$, admits an upper bound via

$$(K - H)e^{-(r+\psi(i\omega_+))T} \cdot e^{-\omega_+(x_M - \ln K) + \omega_-(x_M - x)} \sup_{\tau \in [0, T]} e^{-\tau(\psi(i\omega_-) - \psi(i\omega_+))}. \quad (109)$$

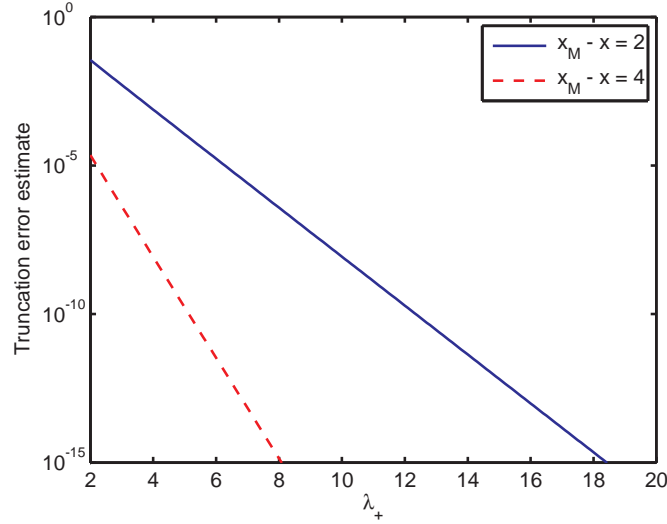


FIGURE 2. Logarithmic plot of the error estimate given by (109) for a DO put option with $K = 100$, $H = 80$, $T - t = 1$, under KoBoL with $\lambda_- = -2$, $m_2 = 0.16$, $\nu = 1.2$, for $e^x = 90$ and varying λ_+ .

It follows that, if at least one of the steepness parameters λ_- , λ_+ is large in absolute value, then a moderate $x_M - x$ should suffice to satisfy a very small error tolerance. Figure 2 shows the error estimate given by (109) for a DO put option with strike $K = 100$, barrier $H = 80$, time to maturity one year, and underlying spot $S_0 = e^x = 90$ under KoBoL, as a function of λ_+ , for $x_M - x = 2$ and $x_M - x = 4$, with $\lambda_- = -2$, second moment $m_2 = 0.16$, $\nu = 1.2$, $r = 0.03$, $q = 0$. It can be seen that, unless both steepness parameters are very small in absolute value, even the choice $x_M - x = 2$ produces very small errors. Moreover, as can easily be verified,

the magnitude of the error is largely independent of the second moment⁸ m_2 , ν and $T - t$. An additional attractive feature of this bound is that it is independent of the number N of monitoring dates. The remaining errors must be estimated for each step of backward induction. Equivalently, given a desired error tolerance ϵ for each type of error, one must try to achieve an error less than $\epsilon/(N - 1)$ at each step.

4.3.1.1. *Prescription.* From Lemma 4.3, the following procedure can be used to determine an appropriate value of $x_M - x$ in order to satisfy a given error tolerance ϵ : we minimize

$$x_M = \frac{-(r + \psi(i\omega_+))T + \omega_+ \ln K - \omega_- x + T(\psi(i\omega_+) - \psi(i\omega_-))_+ - \ln \frac{\epsilon}{K - H}}{\omega_+ - \omega_-}$$

over $\omega_- \in (\lambda_-, 0)$, $\omega_+ \in (0, \lambda_+)$, e.g., by using an optimization method such as conjugate gradient or Nelder-Mead⁹.

4.3.2. Interpolation error (discretization error in the state space). We consider the case of piece-wise quadratic interpolation, which, as will be shown in Section 4.4, is the most efficient one. Similar estimates for other interpolation methods can easily be derived. At each step, we estimate the error in L_∞ -norm. Since (an approximation to) the option price at date t_s and $X_{t_s} > h$ is a (discounted) expectation of the price at date t_{s+1} , we estimate the interpolation error in the same norm. Recall that the error of piece-wise polynomial interpolation of order m of a function $f \in C^{m+1}([0, \infty))$ over a uniform grid of mesh Δ admits the upper bound

$$\|f_\Delta - f\|_{L_\infty} = C_{m+1} \|f^{(m+1)}\|_{L_\infty} \Delta^{m+1}, \quad (110)$$

⁸For VG or KoBoL of order $\nu \neq 1$, m_2 determines the intensity c via $m_2 = c\Gamma(2-\nu)[(-\lambda_-)^{\nu-2} + \lambda_+^{\nu-2}]$ [18].

⁹The latter is implemented in MATLAB as the function `fminsearch`. Of course, this method should be used together with an appropriate change of variables, in order to transform the constrained optimization problem into an unconstrained one.

where $C_2 = 1/8$, $C_3 = 1/6$, $C_4 = 1/24$. Let $p_{\bar{\Delta}}$ denote the transition probability density. In Appendix M.3, we prove

Lemma 4.4. *Let X be a Lévy process whose transition density $p_{\bar{\Delta}}$ satisfies $p_{\bar{\Delta}} \in C^3(\mathbb{R})$ and its derivatives are such that $p_{\bar{\Delta}}^{(s)} \in L_1(\mathbb{R})$, $s = 1, 2, 3$, then the total error in the time-0 option price due to piece-wise quadratic interpolation admits the following approximate bound*

$$\mathcal{E}_{\text{int.tot.}} \leq \frac{e^{-rT}}{6} \Delta^3 (N-1)(K-H) \|p_{\bar{\Delta}}'''\|_{L_1}. \quad (111)$$

Remark 4.5. Lemma 4.4 applies to model processes of order $\nu > 0$, or, more generally, to RLPEs (cf. Theorem A.10, Appendix M.3).

In order to apply (111), we can use

Proposition 4.6. *Let X be a model process of order $\nu > 0$. Then, for $n = 1, 2, 3$, or 4, the following approximate bound holds*

$$\|p_{\bar{\Delta}}^{(n)}\|_{L_1} \leq \rho_n, \quad (112)$$

where

$$\rho_n = \frac{2\Gamma(n/\nu)}{(d_+^0)^{n/\nu} \pi \nu D(n)} \bar{\Delta}^{-n/\nu}, \quad (113)$$

and

$$D(n) = \sup_{\phi \in (0, \min\{\frac{\pi}{2}, \frac{\pi}{2\nu}\})} (\cos(\phi\nu))^{n/\nu} \cos(\phi - \pi/2). \quad (114)$$

The proof can be found in Appendix M.4.

4.3.2.1. *Prescription for a choice of Δ in the case of piece-wise quadratic interpolation.* Given an error tolerance $\epsilon > 0$, calculate ρ_3 using (113) and (114), and

set

$$\Delta = \left(\frac{e^{-rT}}{6\epsilon} (N-1)(K-H)\rho_3 \right)^{-\frac{1}{3}}. \quad (115)$$

4.3.3. Impact of errors of parabolic iFT. The parabolic iFT method, which we apply to calculate (approximations to) $v_{N-1}(x)$ and $I_\ell(x)$, $\ell = 0, 1, \dots, m$, is based on an appropriate conformal change of variables and the simplified trapezoid rule applied to the resulting integral over a horizontal line in the complex plane (cf. Section 2.3 and Appendix O.2). The simplified trapezoid rule has two sources of errors: the discretization error and the truncation error. In [19, 35], explicit upper bounds were derived for both types of error (see Appendix O.2.3 for a review). Denote the sum of the bounds for either type of error in the calculation of $v_{N-1}(x)$ and $I_\ell(x)$ by $\mathcal{E}_{v_{N-1}}(x)$ and $\mathcal{E}_{I_\ell}(x)$, respectively, and note that, as can be seen from the explicit formulas in Appendix O.2.3, upper bounds for the L_1 -norms of $\mathcal{E}_{v_{N-1}}$ and \mathcal{E}_{I_ℓ} can be derived. This explains why the following lemma for the absolute error $Err_{v_0}(x_k)$ can be applied to derive explicit recommendations for the choice of parameters of parabolic iFT. The proof can be found in Appendix M.5.

Lemma 4.7. *Let X be a model process. Assume that ν and $\bar{\Delta}$ are not both small, and the mesh Δ is chosen so that the interpolation error of piece-wise quadratic interpolation is small. Then the following approximate bound holds*

$$\begin{aligned} Err_{v_0}(x_k) \leq e^{-rT} & \left[|\mathcal{E}_{v_{N-1}}(h)| + (N-1)(K-H)(\|\mathcal{E}_{I_0}\|_{L_\infty} \right. \\ & \left. + \left(\|p''_{\Delta}\|_{L_1} + 3\Delta \|p'''_{\Delta}\|_{L_1} \right) \|\mathcal{E}_{I_1}\|_{L_1} + 2 \left(\Delta^{-1} \|p''_{\Delta}\|_{L_1} + 3 \|p'''_{\Delta}\|_{L_1} \right) \|\mathcal{E}_{I_2}\|_{L_1} \right]. \end{aligned} \quad (116)$$

4.3.3.1. *Prescription for the choice of parabolic iFT settings.* Let ϵ_{ds} be the tolerance for all errors due to approximations in the dual space¹⁰. We use parabolic iFT to calculate $v_{N-1}^{\text{put}}(\mathbf{x})$, $v_{N-1}^{\text{barr}}(\mathbf{x})$, $I_0(\mathbf{y})$, $I_1(\mathbf{z})$, and $I_2(\mathbf{z})$, where \mathbf{y} is the grid $n\Delta$, $n = 0, 1, \dots, M-1$, and \mathbf{z} is the grid $m\Delta$, $m = -M+1, -M+2, \dots, M-1$. In each case, we can use the procedure described in Appendix O.3, which requires the specification of a grid \mathbf{x}' , as well as the truncation parameters Λ_{\pm} and the pairs $(\omega_{\pm}, \zeta_{\pm})$ (where the plus and minus signs refer to the subgrids $\mathbf{x}' \geq 0$ and $\mathbf{x}' < 0$, respectively). This can be done as follows. Again, we consider the case of piece-wise quadratic interpolation, and assume that the conditions of Lemma 4.7 hold.

1. For the calculation of $v_{N-1}^{\text{put}}(\mathbf{x})$, set $\mathbf{x}' = \mathbf{x} + \mu\Delta - \ln K$, then apply the procedure in Appendix O.3.1.1 with grid \mathbf{x}' , error tolerance $\epsilon = e^{rT}\epsilon_{\text{ds}}/16$, and $x'_0 = h + \mu\bar{\Delta} - \ln K$ to break the grid \mathbf{x}' into the subgrids \mathbf{x}'_{\pm} and calculate the error tolerances ϵ_{\pm} , as well as the values x'_{\pm} . Then use these values to obtain: Λ_{\pm} , by using Proposition O.4, and $(\omega_{\pm}, \zeta_{\pm})$, by using the procedure in Appendix O.2.2, applying the symmetry of Appendix D in the minus cases.
2. For the calculation of $v_{N-1}^{\text{barr}}(\mathbf{x})$, set $\mathbf{x}' = \mathbf{x} + \mu\Delta - h$, $\epsilon = e^{rT}\epsilon_{\text{ds}}/16$, $x'_0 = h + \mu\bar{\Delta} - \ln K$, and proceed in the same manner as in step 1.
3. For the calculation of $I_0(\mathbf{y})$, set $\mathbf{x}' = \mathbf{y} + \mu\Delta$, $\epsilon = e^{rT}\epsilon_{\text{ds}}/[8(N-1)(K-H)]$, and proceed in the same manner as in step 1.
4. For the calculation of $I_1(\mathbf{z})$, set $\mathbf{x}' = \mathbf{z} + \mu\Delta$, then apply the procedure in Appendix O.3.1.1 with grid \mathbf{x}' , and error tolerance

$$\epsilon = \frac{\epsilon_{\text{ds}}}{8(N-1)(K-H)(\rho_2 + 3\Delta\rho_3)},$$

¹⁰Since in this section we focus only on one source of error (discretization or truncation) at a time, we will need to take an overall error tolerance of $\epsilon_{\text{ds}}/2$ rather than ϵ_{ds} when using the error bounds in Appendix O.

where ρ_n is an upper bound estimate for $\|p_{\bar{\Delta}}^{(n)}\|_{L_1}$, calculated using Proposition 4.6. Use the resulting error tolerances ϵ_{\pm} to calculate: Λ_{\pm} , using Proposition O.9, and the pair $(\omega_{\pm}, \zeta_{\pm})$, using Remark O.8 (applying the symmetry of Appendix D in the minus case).

5. For the calculation of $I_2(\mathbf{z})$, proceed in the same manner as in step 4, but with the following value of ϵ

$$\epsilon = \frac{\epsilon_{\text{ds}}}{16(N-1)(K-H)(\Delta^{-1}\rho_2 + 3\rho_3)}.$$

4.4. Comparison of relative performance of different methods

Consider a down-and-out put option with barrier $H = 80$, strike $K = 100$, monitoring interval $\bar{\Delta} = 1/252$ (approximately equal to one trading day) at time $t = 0$. We assume that the underlying asset follows an exponential KoBoL process under \mathbb{Q} , and compare the accuracy of the prices obtained with our method, for various times to maturity, against the HT and COS methods¹¹. We consider the following parameter sets:

- $\lambda_- = -8$, $\lambda_+ = 9$, $\nu = 1.2$, $m_2 = 0.16$, with $r = 0.03$ and $q = 0$ (used in [19]; henceforth referred to as set A);
- $\lambda_- = -60$, $\lambda_+ = 50$, $\nu = 0.7$, $c = 4$, with $r = 0.04$ and $q = 0.02$ (used in [45, 44]; henceforth referred to as set B).

The benchmarks were calculated using a combination of our method, with piecewise cubic interpolation, and HT. Specifically, for each set of parameters and maturity,

¹¹All calculations were carried out in MATLAB R2011b (win64), on a PC with Intel i5-2410M, 2.30 GHz with 4 GB RAM, running Windows 7 Professional (64 bit).

we used our method with mesh $\Delta_0 = (\ln K - h)/1000 \approx 2.23 \cdot 10^{-4}$, which was of the same order of magnitude as the value obtained using the prescription in Section 4.3 with error tolerance $\epsilon = 10^{-4}K$, for both parameter sets and all maturities involved¹². The accuracy of the settings was checked first, by halving the mesh in the state space and observing that the absolute changes in option price lay well below our tolerance and, second, by ensuring that the same price could be obtained with the HT method (which has very different sources of errors and numerical realization) for some suitably large M , up to a relative difference of less than 0.01%.

In Tables 1 and 2, we compare the accuracy of our method (for sets A and B, respectively), with piece-wise quadratic interpolation, versus HT and COS, at a point close to the barrier ($x = h + 50\Delta_0$, just over 1.1% of the barrier), and at the strike, for each parameter set, and times to maturity 0.25, 0.5, and 1 year¹³. In addition, in Tables 3 and 4, we show analogous results to those in Tables 1 and 2 for the set $\lambda_- = -28.5528$, $\lambda_+ = 10.2038$, $\nu = 0.9228$, $c = 3.6502$ (fitted to the traded prices of vanilla options on the Nikkei 225 index in [47]), and the set $\lambda_- = -32.95$, $\lambda_+ = 18.75$, $\nu = 0.5757$, $c = 6.51$ (fitted to the traded prices of vanilla options on Intel in [26]), respectively, in both cases with $r = 0.03$ and $q = 0$. The results for both sets are similar to those for set A.

In Figure 3 below, and Figures 1-3 in Appendix J, we plot the minimum CPU time taken by the different versions of our method, as well as by HT and COS, to achieve a relative error tolerance ranging between 0.1% and 1% in the region $\ln(1.02 \cdot H) \leq x \leq \ln K$, for times to maturity 0.25, 0.5, 1, and 2 years. Since

¹²The other settings were chosen to be (almost) as large (x_M, Λ) or small (ζ) as our computer could handle, and were much more “overkill” than the values given by the prescriptions in Section 4.3. Specifically, we used $x_M = h + 3$, and $\zeta = 0.1$, $\Lambda = 3000$ for all applications of parabolic iFT.

¹³For HT, we used a grid $y_j = h + (j - 1)\Delta$, $j = 1, 2, \dots, 12$, with $\Delta = 89 \cdot \Delta_0 \approx 0.00198$, for comparisons near the strike, and a similar grid $y'_j = h + (j - 1)\Delta'$, with $\Delta' = 50 \cdot \Delta_0 \approx 0.00112$, for comparisons near the barrier.

the descriptions in [45] and [44] do not include procedures for the choices of M and N in the HT and COS methods, respectively, for a given error tolerance¹⁴, we ran both HT¹⁵ and COS, gradually increasing M and N from 10 to 10^6 . For the different versions of our method, on the other hand, we started out by using a rather coarse grid with mesh $\Delta \approx 0.02$ and gradually refined it down to Δ_0 . In order to make a comparison with HT and COS, we used a grid \mathbf{y} in the state space ranging approximately between $\ln(1.02 \cdot H)$ and $\ln K$. More precisely, we set $y_j = h + (j-1)\Delta$, with $\Delta = 89 \cdot \Delta_0 \approx 0.00198$, and compared the performance of HT and COS w.r.t. the benchmarks for $(y_j)_{j=2}^{12}$. Since, by design, COS takes a single value of x rather than a grid, we ran it separately for each point (the benchmark prices over this grid can be found in Appendix N). For each choice of N , we stored the maximum relative error over j and the corresponding CPU time.

For COS, we note that the prescription in [44] for the choice of truncation interval (a, b) , given by (239)-(240) in Appendix Q.2, with $L = 8$, produces very large errors, especially for parameter set B used in *op. cit.*, as can be seen from Figure 4. This shows that for daily monitoring (which is by far the most common case in the market [6, 29]) COS can be unstable, especially for longer times to maturity, even if the recommendations for parameter choice in [44] are followed. We found that the choice $L = 25$ worked well for parameter set A, and $L = 40$ worked well for set B, for all maturities under consideration. However, as noted in [19], the choice of L , even for the European option case, is not straightforward, since this parameter controls different sources of errors at once.

¹⁴Recall that these parameters play a similar role to that of the mesh Δ in our method.

¹⁵For HT, we used the prescription in [45] for the choice of mesh ζ in the dual space (see (225) in Appendix P.2.5).

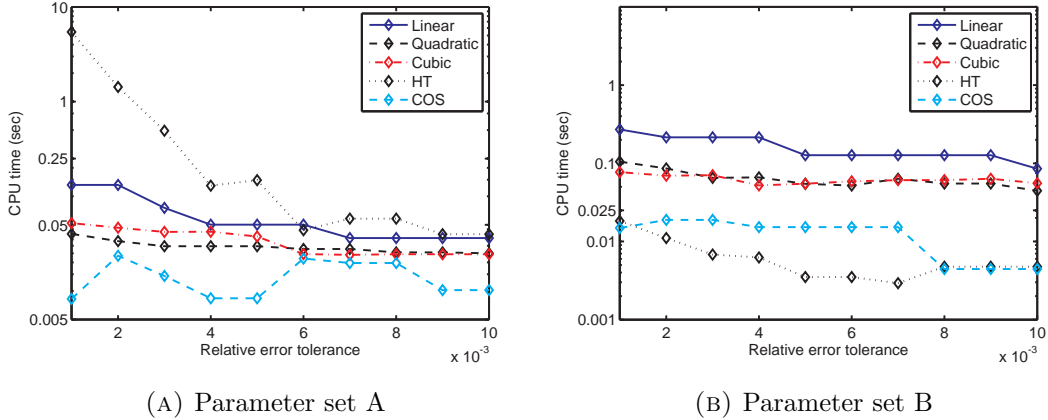


FIGURE 3. Logarithmic plots of CPU time versus relative error tolerance. Comparison of piece-wise linear (solid), quadratic (dashed) and cubic (dot-dashed) interpolation, as well as HT method (dotted) and COS method (dashed) to price a DO put option with $H = 80$, $K = 100$, $T = 0.25$, $\bar{\Delta} = 1/252$, over the interval $1.02 \cdot H \leq e^x \leq K$.

Our results show that

1. Our method performs much better than HT for parameter set A and for the example in Table 3, but, for set B, HT is about as fast as our method. This is due to the fact that, for smaller steepness parameters, one typically needs a smaller mesh ζ in the dual space (cf. Appendix O.2.2). Unless the steepness parameters are very large in magnitude, the prescription (225), given in [45], often requires a much larger number of points M than necessary in order to obtain a small enough value of ζ . Hence, if λ_+ and λ_- are not very large in magnitude (as is normally the case for calibrations to market data [26, 47, 52, 3]), this can result in much longer calculation times¹⁶.
2. With the prescriptions for L and (a, b) given in [44], COS produces large errors for sets A and B, especially for longer maturities; e.g., for set A and $T = 1, 2$, it

¹⁶Of course, one is free to ignore the recommendations in [45] for ζ . However, in that case the error estimates in *op. cit.* no longer apply.

results in relative errors larger than 20%. For set B, the situation is even worse. If an appropriate value of L is chosen somehow, then COS can outperform both our method and HT, especially for shorter maturity, at least when ν and $\bar{\Delta}$ are not both small. However, no universal prescription exists for the choice of L for a given error tolerance and set of process parameters.

3. For our method, quadratic and cubic interpolation perform much better than linear, except for larger error tolerances and very long maturities ($T = 1$ or 2).
4. For longer maturities, the performance gap between linear and quadratic/cubic interpolation is smaller. For error tolerances close to 1% and $T = 1$ or 2 , linear interpolation sometimes even outperforms quadratic and/or cubic.
5. The performance of quadratic and cubic interpolation is similar, although quadratic tends to run slightly faster, especially for longer maturities.

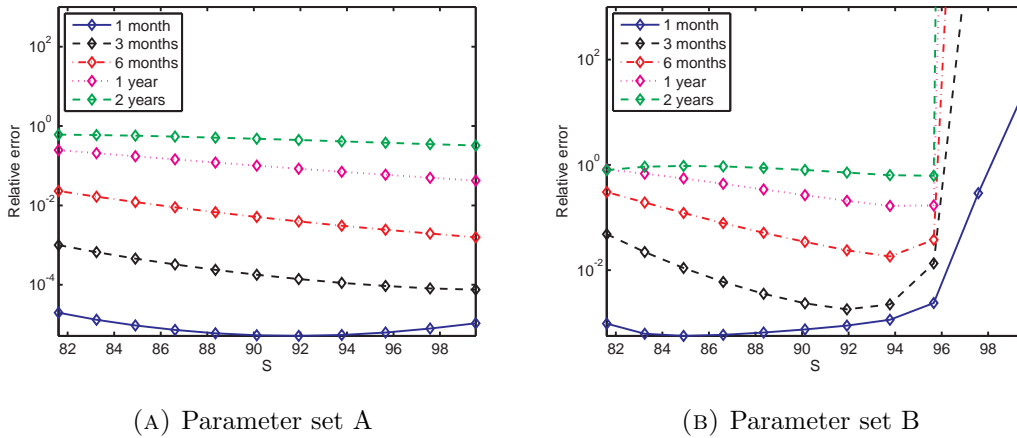


FIGURE 4. Logarithmic plots of relative errors of COS, with $N = 10^6$, for the price of a DO barrier put option with $H = 80$, $K = 100$, monitoring interval $\bar{\Delta} = 1/252$, for different times to maturity, under KoBoL, over the interval $1.02 \cdot H \leq e^x \leq K$, using the prescription $L = 8$, given in [44].

We also note that, on average, about 70–80% of the overall CPU time with our method is taken up by the parabolic iFT calculations before the backward induction loop (most of the remaining time is used by the fast convolution inside the loop). We therefore expect the performance of the algorithm to greatly improve with parallelization. Finally, we note that, as expected, for increasingly smaller monitoring interval $\bar{\Delta}$, the price calculated with our method can be seen to converge to that of a continuously monitored barrier option. In Figure 5 we compare the prices of a DO barrier put option with approximately monthly, weekly, daily and hourly monitoring, calculated using our method (with the benchmark settings) with those of a continuously monitored barrier option, calculated using the method of [13].

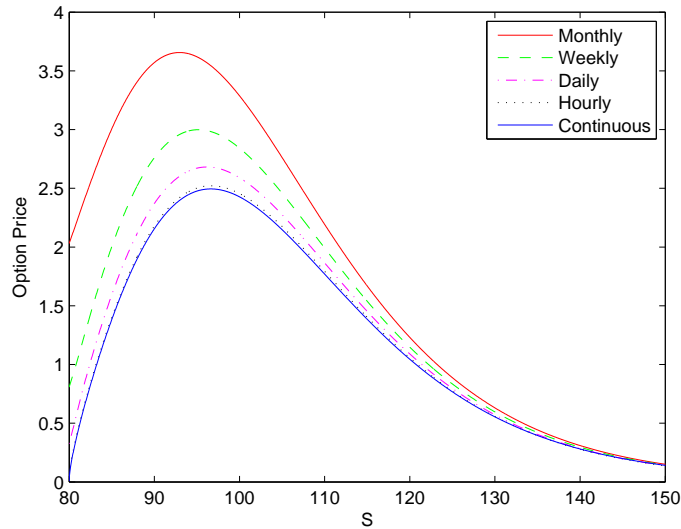


FIGURE 5. Price of a DO barrier put option with $H = 80$, $K = 100$ and $T = 0.25$, for monthly ($\bar{\Delta} = 1/12$), weekly ($\bar{\Delta} = 1/52$), daily ($\bar{\Delta} = 1/252$), hourly ($\bar{\Delta} = 1/6048$), and continuous monitoring, under KoBoL parameters $\lambda_- = -8$, $\lambda_+ = 9$, $\nu = 1.2$, $m_2 = 0.16$, with $r = 0.03$ and $q = 0$.

TABLE 1

	S	Price	ϵ_{abs}	ϵ_{rel}	Time	Δ	M	ζ	L	N
$T = 0.25$										
Benchmark	80.89757	0.58657346			184.8	0.000223				
Quadratic	80.89757	0.58657684	$3.38 \cdot 10^{-6}$	$1.00 \cdot 10^{-5}$	0.026	0.005579				
HT	80.89757	0.57137568	$1.52 \cdot 10^{-2}$	$2.59 \cdot 10^{-2}$	0.031		1000	1.13742		
HT	80.89757	0.59306974	$6.50 \cdot 10^{-3}$	$1.11 \cdot 10^{-2}$	0.14		5000	0.47278		
HT	80.89757	0.58113611	$5.44 \cdot 10^{-3}$	$9.27 \cdot 10^{-3}$	0.281		8000	0.36587		
HT	80.89757	0.58383383	$2.74 \cdot 10^{-3}$	$4.67 \cdot 10^{-3}$	1.794		50000	0.13465		
HT	80.89757	0.58850986	$1.94 \cdot 10^{-3}$	$3.30 \cdot 10^{-3}$	4.165		100000	0.09226		
HT	80.89757	0.58727466	$7.01 \cdot 10^{-4}$	$1.20 \cdot 10^{-3}$	34.057		1000000	0.02628		
COS	80.89757	0.58728375	$7.10 \cdot 10^{-4}$	$1.21 \cdot 10^{-3}$	0.012				8	300
Benchmark	100	2.59027151			184.8	0.000223				
Quadratic	100	2.5912833	$1.01 \cdot 10^{-3}$	$3.90 \cdot 10^{-4}$	0.026	0.005579				
HT	100	2.5895322	$7.39 \cdot 10^{-4}$	$2.90 \cdot 10^{-4}$	0.031		1000	1.13742		
COS	100	2.59042878	$1.57 \cdot 10^{-4}$	$6.00 \cdot 10^{-5}$	0.006				8	100
$T = 0.5$										
Benchmark	80.89757	0.22495341			185.23	0.000223				
Quadratic	80.89757	0.22496984	$1.64 \cdot 10^{-5}$	$7.00 \cdot 10^{-5}$	0.033	0.005579				
HT	80.89757	0.21911038	$5.84 \cdot 10^{-3}$	$2.60 \cdot 10^{-2}$	0.047		1000	1.13742		
HT	80.89757	0.22745049	$2.50 \cdot 10^{-3}$	$1.11 \cdot 10^{-2}$	0.281		5000	0.47278		
HT	80.89757	0.22390037	$1.05 \cdot 10^{-3}$	$4.68 \cdot 10^{-3}$	3.198		50000	0.13465		
HT	80.89757	0.2256977	$7.44 \cdot 10^{-4}$	$3.31 \cdot 10^{-3}$	8.128		100000	0.09226		
HT	80.89757	0.22522293	$2.70 \cdot 10^{-4}$	$1.20 \cdot 10^{-3}$	66.068		1000000	0.02628		
COS	80.89757	0.23097575	$6.02 \cdot 10^{-3}$	$2.68 \cdot 10^{-2}$	0.055				8	1000
COS	80.89757	0.22495453	$1.12 \cdot 10^{-6}$	$5.00 \cdot 10^{-6}$	0.054				15	1000
Benchmark	100	1.39574958			185.23	0.000223				
Quadratic	100	1.39624957	$5.00 \cdot 10^{-4}$	$3.60 \cdot 10^{-4}$	0.033	0.005579				
HT	100	1.39546539	$2.84 \cdot 10^{-4}$	$2.00 \cdot 10^{-4}$	0.062		1000	1.13742		
COS	100	1.39785172	$2.10 \cdot 10^{-3}$	$1.51 \cdot 10^{-3}$	0.056				8	1000
COS	100	1.39574989	$3.10 \cdot 10^{-7}$	$2.00 \cdot 10^{-7}$	0.055				15	1000
$T = 1$										
Benchmark	80.89757	0.08130903			187.25					
Quadratic	80.89757	0.08129447	$1.46 \cdot 10^{-5}$	$1.80 \cdot 10^{-4}$	0.051	0.005579				
HT	80.89757	0.08221303	$9.04 \cdot 10^{-4}$	$1.11 \cdot 10^{-2}$	0.468		5000	0.47278		
HT	80.89757	0.08092782	$3.81 \cdot 10^{-4}$	$4.69 \cdot 10^{-3}$	6.801		50000	0.13465		
HT	80.89757	0.0814066	$9.76 \cdot 10^{-5}$	$1.20 \cdot 10^{-3}$	130.7		1000000	0.02628		
COS	80.89757	0.10289052	$2.16 \cdot 10^{-2}$	$2.65 \cdot 10^{-1}$	0.108				8	1000
COS	80.89757	0.0813639	$5.49 \cdot 10^{-5}$	$6.70 \cdot 10^{-4}$	0.107				15	1000
Benchmark	100	0.60133743			187.25	0.000223				
Quadratic	100	0.60118634	$1.51 \cdot 10^{-4}$	$2.50 \cdot 10^{-4}$	0.051	0.005579				
HT	100	0.60123454	$1.03 \cdot 10^{-4}$	$1.70 \cdot 10^{-4}$	0.109		1000	1.13742		
COS	100	0.62570898	$2.44 \cdot 10^{-2}$	$4.05 \cdot 10^{-2}$	0.107				8	1000
COS	100	0.60136022	$2.28 \cdot 10^{-5}$	$4.00 \cdot 10^{-5}$	0.106				15	1000

Comparison of prices for a DO put option with barrier $e^h = 80$ and strike $K = 100$, for $x = h + 50\Delta_0$ and $x = \ln K$, where $\Delta_0 = (\ln K - h)/1000 \approx 2.23 \cdot 10^{-4}$. Time: CPU time (seconds).

For HT, we used the Feng-Linetsky [45] prescription for ζ (cf. (225)).

Parameters of KoBoL: $\lambda_- = -8$, $\lambda_+ = 9$, $\nu = 1.2$, second moment $m_2 = 0.16$ (hence, $c \approx 0.3796$), with riskless rate $r = 0.03$ and dividend rate $q = 0$ (parameter set A, used in [19]).

ϵ_{abs} and ϵ_{rel} denote absolute and relative errors, respectively. Benchmarks were calculated using cubic interpolation with state space mesh Δ_0 .

Settings for quadratic interpolation: $x_M = h + 1$, $\zeta = 1$, $\Lambda = 100$. Calculations were carried out with MATLAB R2011b (win64), on Intel i5-2410M, 2.30 GHz with 4 GB RAM, running Windows 7 Professional (64 bit).

TABLE 2

	S	Price	ϵ_{abs}	ϵ_{rel}	Time	Δ	M	ζ	L	N
$T = 0.25$										
Benchmark	80.89757	1.77132603			191.66	0.000223				
Quadratic	80.89757	1.77103311	$2.93 \cdot 10^{-4}$	$1.70 \cdot 10^{-4}$	0.041	0.002231				
HT	80.89757	1.76453336	$6.80 \cdot 10^{-2}$	$3.83 \cdot 10^{-3}$	0.047		1000	5.69475		
HT	80.89757	1.76962911	$1.70 \cdot 10^{-2}$	$9.60 \cdot 10^{-4}$	0.172		6000	2.72307		
COS	80.89757	1.89363042	$1.22 \cdot 10^{-1}$	$6.91 \cdot 10^{-2}$	0.029				8	1000
COS	80.89757	1.78247147	$1.11 \cdot 10^{-2}$	$6.29 \cdot 10^{-3}$	0.03				10	1000
COS	80.89757	1.7724825	$1.16 \cdot 10^{-3}$	$6.50 \cdot 10^{-4}$	0.03				15	1000
Benchmark	100	3.11359622			191.66	0.000223				
Quadratic	100	3.11373903	$1.43 \cdot 10^{-4}$	$5.00 \cdot 10^{-5}$	0.041	0.002231				
HT	100	3.11668802	$3.09 \cdot 10^{-3}$	$9.90 \cdot 10^{-4}$	0.062		2000	4.28076		
COS	100	$1.19 \cdot 10^{13}$	$1.19 \cdot 10^{13}$	$3.83 \cdot 10^{12}$	0.029				8	1000
COS	100	3.13122123	$1.76 \cdot 10^{-2}$	$5.66 \cdot 10^{-3}$	0.029				10	1000
COS	100	3.11697328	$3.38 \cdot 10^{-3}$	$1.08 \cdot 10^{-3}$	0.029				15	1000
$T = 0.5$										
Benchmark	80.89757	0.83350436			192.24	0.000223				
Quadratic	80.89757	0.8333734	$1.31 \cdot 10^{-4}$	$1.60 \cdot 10^{-4}$	0.1	0.002231				
HT	80.89757	0.83043581	$3.07 \cdot 10^{-3}$	$3.68 \cdot 10^{-3}$	0.14		1000	5.69475		
HT	80.89757	0.83282627	$6.78 \cdot 10^{-4}$	$8.10 \cdot 10^{-4}$	0.561		6000	2.72307		
COS	80.89757	1.14068967	$3.07 \cdot 10^{-1}$	$3.69 \cdot 10^{-1}$	0.057				8	1000
COS	80.89757	0.83416434	$6.60 \cdot 10^{-4}$	$7.90 \cdot 10^{-4}$	0.055				20	1000
Benchmark	100	2.89634078			192.24	0.000223				
Quadratic	100	2.89651621	$1.75 \cdot 10^{-4}$	$6.00 \cdot 10^{-5}$	0.1	0.002231				
HT	100	2.89897574	$2.63 \cdot 10^{-3}$	$9.10 \cdot 10^{-4}$	0.062		1000	4.28076		
COS	100	$5.66 \cdot 10^{29}$	$5.66 \cdot 10^{29}$	$1.96 \cdot 10^{29}$	0.055				8	1000
COS	100	2.89910955	$2.77 \cdot 10^{-3}$	$9.60 \cdot 10^{-4}$	0.055				20	1000
$T = 1$										
Benchmark	80.89757	0.34160881			193.74	0.000223				
Quadratic	80.89757	0.34153123	$7.76 \cdot 10^{-5}$	$2.30 \cdot 10^{-4}$	0.223	0.001116				
Quadratic	80.89757	0.34155933	$4.940 \cdot 10^{-5}$	$1.40 \cdot 10^{-4}$	0.061	0.002231				
HT	80.89757	0.34038686	$1.22 \cdot 10^{-3}$	$3.58 \cdot 10^{-3}$	0.094		1000	5.69475		
HT	80.89757	0.34136607	$2.42 \cdot 10^{-3}$	$7.10 \cdot 10^{-4}$	0.25		6000	2.72307		
COS	80.89757	0.63866249	$2.97 \cdot 10^{-1}$	$8.70 \cdot 10^{-1}$	0.031				8	200
COS	80.89757	0.356945	$1.53 \cdot 10^{-2}$	$4.49 \cdot 10^{-2}$	0.031				15	200
COS	80.89757	0.34221689	$6.08 \cdot 10^{-4}$	$1.78 \cdot 10^{-3}$	0.046				20	300
Benchmark	100	1.90919403			193.74	0.000223				
Quadratic	100	1.90929924	$1.05 \cdot 10^{-4}$	$6.00 \cdot 10^{-5}$	0.061	0.002231				
HT	100	1.91088427	$1.69 \cdot 10^{-3}$	$8.90 \cdot 10^{-4}$	0.031		1000	5.69475		
COS	100	$1.28 \cdot 10^{63}$	$1.28 \cdot 10^{63}$	$6.70 \cdot 10^{62}$	0.049				8	400
COS	100	1.91185873	$2.66 \cdot 10^{-3}$	$1.40 \cdot 10^{-3}$	0.032				15	200
COS	100	1.91047424	$1.28 \cdot 10^{-3}$	$6.70 \cdot 10^{-4}$	0.024				20	100

Comparison of prices for a DO put option with barrier $e^h = 80$ and strike $K = 100$, for $x = h + 50\Delta_0$ and $x = \ln K$, where $\Delta_0 = (\ln K - h)/1000 \approx 2.23 \cdot 10^{-4}$. Time: CPU time (seconds).

For HT, we used the Feng-Linetsky [45] prescription for ζ (cf. (225)).

Parameters of KoBoL: $\lambda_- = -60$, $\lambda_+ = 50$, $\nu = 0.7$, $c = 4$, with riskless rate $r = 0.03$ and dividend rate $q = 0$ (parameter set B, used in both [45] for HT and in [44] for COS).

ϵ_{abs} and ϵ_{rel} denote absolute and relative errors, respectively. Benchmarks were calculated using cubic interpolation with state space mesh Δ_0 .

Settings for quadratic interpolation: $x_M = h + 1$, $\zeta = 5$, $\Lambda = 200$. Calculations were carried out in MATLAB R2011b (win64), on a PC with Intel i5-2410M, 2.30 GHz with 4 GB RAM, running Windows 7 Professional (64 bit).

TABLE 3

	S	Price	ϵ_{abs}	ϵ_{rel}	Time	Δ	M	ζ	L	N
$T = 0.25$										
Benchmark	80.89757	0.26322875			182.37	0.000223				
Quadratic	80.89757	0.26326994	$4.10 \cdot 10^{-5}$	$1.56 \cdot 10^{-4}$	0.037	0.005579				
HT	80.89757	0.25409413	$9.14 \cdot 10^{-3}$	$3.47 \cdot 10^{-2}$	0.125		1000	1.04987		
HT	80.89757	0.26294396	$2.85 \cdot 10^{-4}$	$1.08 \cdot 10^{-3}$	33.951		1000000	0.03814		
COS	80.89757	0.26364695	$4.18 \cdot 10^{-4}$	$1.59 \cdot 10^{-3}$	0.072				8	3000
COS	80.89757	0.26323591	$7.00 \cdot 10^{-6}$	$2.72 \cdot 10^{-5}$	0.008				10	200
Benchmark	100	1.09016924			182.37	0.000223				
Quadratic	100	1.09034561	$1.76 \cdot 10^{-4}$	$1.62 \cdot 10^{-4}$	0.037	0.005579				
HT	100	1.08973156	$4.38 \cdot 10^{-4}$	$4.01 \cdot 10^{-4}$	0.016		1000	1.04987		
COS	100	1.09024719	$7.80 \cdot 10^{-5}$	$7.15 \cdot 10^{-5}$	0.007				8	100
COS	100	1.09017578	$7.00 \cdot 10^{-6}$	$6.00 \cdot 10^{-6}$	0.006				10	100
$T = 0.5$										
Benchmark	80.89757	0.09416167			183.14	0.000223				
Quadratic	80.89757	0.09417632	$1.50 \cdot 10^{-5}$	$1.56 \cdot 10^{-4}$	0.053	0.005579				
HT	80.89757	0.09090297	$3.26 \cdot 10^{-3}$	$3.46 \cdot 10^{-2}$	0.078		1000	1.04987		
HT	80.89757	0.09406005	$1.02 \cdot 10^{-4}$	$1.08 \cdot 10^{-3}$	66.151		1000000	0.03814		
COS	80.89757	0.10190078	$7.74 \cdot 10^{-3}$	$8.22 \cdot 10^{-2}$	0.139				8	3000
COS	80.89757	0.09507403	$9.12 \cdot 10^{-4}$	$9.69 \cdot 10^{-3}$	0.141				10	3000
COS	80.89757	0.09411302	$4.90 \cdot 10^{-5}$	$5.17 \cdot 10^{-4}$	0.012				15	100
Benchmark	100	0.47311846			183.14	0.000223				
Quadratic	100	0.47319172	$7.30 \cdot 10^{-5}$	$1.55 \cdot 10^{-4}$	0.053	0.005579				
HT	100	0.47296231	$1.56 \cdot 10^{-4}$	$3.30 \cdot 10^{-4}$	0.047		1000	1.04987		
COS	100	0.47803122	$4.91 \cdot 10^{-3}$	$1.04 \cdot 10^{-2}$	0.139				8	3000
COS	100	0.47350924	$3.91 \cdot 10^{-4}$	$8.26 \cdot 10^{-4}$	0.012				10	100
$T = 1$										
Benchmark	80.89757	0.032677			184.76	0.000223				
Quadratic	80.89757	0.03267633	$1.00 \cdot 10^{-6}$	$2.03 \cdot 10^{-5}$	0.085	0.005579				
HT	80.89757	0.0315477	$1.13 \cdot 10^{-3}$	$3.46 \cdot 10^{-2}$	0.156		1000	1.04987		
HT	80.89757	0.03264177	$3.50 \cdot 10^{-5}$	$1.08 \cdot 10^{-3}$	131.19		1000000	0.03814		
COS	80.89757	0.04709172	$1.44 \cdot 10^{-2}$	$4.41 \cdot 10^{-1}$	0.274				8	3000
COS	80.89757	0.03908499	$6.41 \cdot 10^{-3}$	$1.96 \cdot 10^{-1}$	0.272				10	3000
COS	80.89757	0.03284474	$1.68 \cdot 10^{-4}$	$5.13 \cdot 10^{-3}$	0.274				15	3000
COS	80.89757	0.03267762	$1.00 \cdot 10^{-6}$	$1.92 \cdot 10^{-5}$	0.046				20	300
Benchmark	100	0.18159309			184.76	0.000223				
Quadratic	100	0.18155885	$3.40 \cdot 10^{-5}$	$1.89 \cdot 10^{-4}$	0.085	0.005579				
HT	100	0.18153898	$5.40 \cdot 10^{-5}$	$2.98 \cdot 10^{-4}$	0.094		1000	1.04987		
COS	100	0.21293813	$3.13 \cdot 10^{-2}$	$1.73 \cdot 10^{-1}$	0.275				8	3000
COS	100	0.19093063	$9.34 \cdot 10^{-3}$	$5.14 \cdot 10^{-2}$	0.273				10	3000

Comparison of prices for a DO put option with barrier $e^h = 80$ and strike $K = 100$, for $x = h + 50\Delta_0$ and $x = \ln K$, where $\Delta_0 = (\ln K - h)/1000 \approx 2.23 \cdot 10^{-4}$. Time: CPU time (seconds).

For HT, we used the Feng-Linetsky [45] prescription for ζ (cf. (225)).

Parameters of KoBoL: $\lambda_- = -28.5528$, $\lambda_+ = 10.2038$, $\nu = 0.9228$, $c = 3.6502$ with riskless rate $r = 0.03$ and dividend rate $q = 0$ (calibrated to European options on the Nikkei 225 index in [47]).

ϵ_{abs} and ϵ_{rel} denote absolute and relative errors, respectively. Benchmarks were calculated using cubic interpolation with state space mesh Δ_0 .

Settings for quadratic interpolation: $x_M = h + 2$, $\zeta = 1$, $\Lambda = 100$. Calculations were carried out in MATLAB R2011b (win64), on a PC with Intel i5-2410M, 2.30 GHz with 4 GB RAM, running Windows 7 Professional (64 bit).

TABLE 4

	S	Price	ϵ_{abs}	ϵ_{rel}	Time	Δ	M	ζ	L	N
$T = 0.25$										
Benchmark	80.89757	0.83086523			485.21	0.000223				
Quadratic	80.89757	0.83092984	$6.46 \cdot 10^{-5}$	$7.78 \cdot 10^{-5}$	0.042	0.002231				
Quadratic	80.89757	0.83177595	$9.11 \cdot 10^{-4}$	$1.10 \cdot 10^{-3}$	0.019	0.005579				
HT	80.89757	0.83790481	$7.04 \cdot 10^{-3}$	$8.47 \cdot 10^{-3}$	0.031		1000	4.04752		
HT	80.89757	0.83167846	$8.13 \cdot 10^{-4}$	$9.79 \cdot 10^{-4}$	0.789		30000	1.16817		
COS	80.89757	0.83207781	$1.21 \cdot 10^{-3}$	$1.46 \cdot 10^{-3}$	0.053				8	2000
COS	80.89757	0.83083116	$3.41 \cdot 10^{-5}$	$4.10 \cdot 10^{-5}$	0.011				10	300
Benchmark	100	2.50677158			485.21	0.000223				
Quadratic	100	2.50684785	$7.63 \cdot 10^{-5}$	$3.04 \cdot 10^{-5}$	0.042	0.002231				
Quadratic	100	2.50814994	$1.38 \cdot 10^{-3}$	$5.50 \cdot 10^{-4}$	0.019	0.005579				
HT	100	2.50700086	$2.29 \cdot 10^{-4}$	$9.15 \cdot 10^{-5}$	0.062		2000	3.14199		
COS	100	2.50683739	$6.58 \cdot 10^{-5}$	$2.63 \cdot 10^{-5}$	0.006				8	100
COS	100	2.50663377	$1.38 \cdot 10^{-4}$	$5.50 \cdot 10^{-5}$	0.006				10	100
$T = 0.5$										
Benchmark	80.89757	0.32091967			487.7	0.000223				
Quadratic	80.89757	0.32094552	$2.59 \cdot 10^{-5}$	$8.06 \cdot 10^{-5}$	0.064	0.002231				
Quadratic	80.89757	0.32128764	$3.68 \cdot 10^{-4}$	$1.15 \cdot 10^{-3}$	0.028	0.005579				
HT	80.89757	0.32362993	$2.71 \cdot 10^{-3}$	$8.45 \cdot 10^{-3}$	0.062		1000	4.04752		
HT	80.89757	0.32123278	$3.13 \cdot 10^{-4}$	$9.76 \cdot 10^{-4}$	1.552		30000	1.16817		
COS	80.89757	0.34100488	$2.01 \cdot 10^{-2}$	$6.26 \cdot 10^{-2}$	0.043				8	700
COS	80.89757	0.32301646	$2.10 \cdot 10^{-3}$	$6.53 \cdot 10^{-3}$	0.035				10	600
COS	80.89757	0.32090339	$1.63 \cdot 10^{-5}$	$5.07 \cdot 10^{-5}$	0.025				15	400
Benchmark	100	1.46997127			487.7	0.000223				
Quadratic	100	1.47002451	$5.32 \cdot 10^{-5}$	$3.62 \cdot 10^{-5}$	0.064	0.002231				
Quadratic	100	1.47089699	$9.26 \cdot 10^{-4}$	$6.30 \cdot 10^{-4}$	0.028	0.005579				
HT	100	1.47005962	$8.84 \cdot 10^{-5}$	$6.01 \cdot 10^{-5}$	0.140		2000	3.14199		
COS	100	1.47390845	$3.94 \cdot 10^{-3}$	$2.68 \cdot 10^{-3}$	0.022				8	300
COS	100	1.47003247	$6.12 \cdot 10^{-5}$	$4.16 \cdot 10^{-5}$	0.013				10	100
$T = 1$										
Benchmark	80.89757	0.11677253			492.42	0.000223				
Quadratic	80.89757	0.11678081	$8.29 \cdot 10^{-6}$	$7.10 \cdot 10^{-5}$	0.105	0.002231				
Quadratic	80.89757	0.11690746	$1.35 \cdot 10^{-4}$	$1.16 \cdot 10^{-3}$	0.044	0.005579				
HT	80.89757	0.1176323	$8.60 \cdot 10^{-4}$	$7.36 \cdot 10^{-3}$	0.094		1000	4.04752		
HT	80.89757	0.11688626	$1.14 \cdot 10^{-4}$	$9.74 \cdot 10^{-4}$	3.34		30000	1.16817		
COS	80.89757	0.16822278	$5.15 \cdot 10^{-2}$	$4.41 \cdot 10^{-1}$	0.023				8	100
COS	80.89757	0.11710773	$3.35 \cdot 10^{-4}$	$2.87 \cdot 10^{-3}$	0.069				15	600
COS	80.89757	0.11678388	$1.14 \cdot 10^{-5}$	$9.72 \cdot 10^{-5}$	0.064				20	500
Benchmark	100	0.67934308			492.42	0.000223				
Quadratic	100	0.67933135	$1.17 \cdot 10^{-5}$	$1.73 \cdot 10^{-5}$	0.105	0.002231				
Quadratic	100	0.67974327	$4.00 \cdot 10^{-4}$	$5.89 \cdot 10^{-4}$	0.044	0.005579				
HT	100	0.67937213	$2.90 \cdot 10^{-5}$	$4.28 \cdot 10^{-5}$	0.218		2000	3.14199		
COS	100	0.72867580	$4.93 \cdot 10^{-2}$	$7.26 \cdot 10^{-2}$	0.023				8	100
COS	100	0.67942229	$7.92 \cdot 10^{-5}$	$1.17 \cdot 10^{-4}$	0.083				15	700

Comparison of prices for a DO put option with barrier $e^h = 80$ and strike $K = 100$, for $x = h + 50\Delta_0$ and $x = \ln K$, where $\Delta_0 = (\ln K - h)/1000 \approx 2.23 \cdot 10^{-4}$. Time: CPU time (seconds).

For HT, we used the Feng-Linetsky [45] prescription for ζ (cf. (225)).

Parameters of KoBoL: $\lambda_- = -32.95$, $\lambda_+ = 18.75$, $\nu = 0.5757$, $c = 6.51$ with riskless rate $r = 0.03$ and dividend rate $q = 0$ (KoBoL parameters as calibrated to European options on Intel in [26], with diffusion coefficient set to zero). ϵ_{abs} and ϵ_{rel} denote absolute and relative errors, respectively. Benchmarks were calculated using cubic interpolation with state space mesh Δ_0 .

Settings for quadratic interpolation: $x_M = h + 1$, $\zeta = 1$, $\Lambda = 300$. Calculations were carried out in MATLAB R2011b (win64), on a PC with Intel i5-2410M, 2.30 GHz with 4 GB RAM, running Windows 7 Professional (64 bit).

CHAPTER 5

Pricing credit default swaps under Lévy processes

5.1. General remarks

The credit default swap (CDS), a basic building block of the credit derivative market, is a contract to buy or sell protection against the default of a reference entity (usually, a bond issuer). One party (protection buyer) makes a periodic payment, known as the CDS *spread* or *premium*, until either the contract matures or the reference entity defaults, whichever happens sooner. If default occurs before maturity, then the other party (protection seller) compensates the protection buyer for any losses incurred. The maturity of a typical CDS contract is around five years, although in some cases it can be considerably longer, especially for a sovereign CDS. Clearly, the *par* or *fair* spread, defined as the spread which makes the CDS price zero at inception, depends on the probability of default of the underlying entity under the risk-neutral measure \mathbb{Q} . In the approach pioneered by Black and Cox in 1976, the asset value of the firm under \mathbb{Q} is modeled as Geometric Brownian Motion, with default occurring when it reaches a pre-determined barrier level [9]. In recent years, alternative models have been proposed in which the underlying follows a more general exponential Lévy process. In [23], a partial integro-differential equation approach was used to price CDS contracts under VG. In [68], a simplified approach involving the Wiener-Hopf factorization for one-sided Lévy processes was used for spectrally negative versions of VG, NIG, and KoBoL. Finally, in [42], an extension of the COS method was used, for both KoBoL and a mixture of NIG and Brownian Motion. Note that there exists

effectively no secondary market for CDS contracts, hence, in the front office, “pricing” a CDS means calculating its par spread. In risk management, however, one typically needs to calculate the actual CDS price, with the spread provided as an input. We will consider both cases.

5.1.1. Discrete time model for CDS. We model the value of the underlying asset, under \mathbb{Q} , by a stochastic process $S = \{S_t\}$, such that $S_t = S_0 e^{Y_t}$, where $Y = \{Y_t\}$ is a Lévy process under \mathbb{Q} , and $S_0 > 0$. As in the Black-Cox model, we assume that default occurs as soon as S_t reaches or falls below a time-dependent barrier level $H(t) = e^{\alpha t + \beta}$, such that $e^\beta < S_0$. Note that, since Y_t is unobservable, we can consider the process $X_t = Y_t - \alpha t$ instead, which reduces calculations to the case of a flat boundary, with default occurring when X_t reaches or crosses the barrier $h = \beta - \ln S_0$. If the underlying process reaches or crosses the barrier, then the continuous stream of premium payments from protection buyer to seller terminates, and the seller compensates the buyer for any losses incurred from default, i.e. $(1 - R)$ times the underlying notional¹.

Under these assumptions, the time-0 price of a CDS with maturity T , unit notional, and constant, continuously compounded spread $c > 0$, from the point of view of the protection seller, is given by

$$\begin{aligned} V_{CDS}(T) &= c \int_0^T e^{-r\tau} P(\tau) d\tau - (1 - R) \int_0^T e^{-r\tau} dP_{def}(\tau) \\ &= c \int_0^T e^{-r\tau} P(\tau) d\tau + (1 - R) \int_0^T e^{-r\tau} dP(\tau), \end{aligned} \quad (117)$$

¹Although common in the mathematical finance literature (see, e.g., [23, 68, 42]) these simplifying assumptions describe an idealized form of CDS, which differs from actual traded contracts. In reality, the premium is paid periodically in arrears, and the compensation payment from the protection seller in case of default is settled at the following premium payment date, rather than at default. We will ignore such complications for the purpose of this thesis.

where $P(\tau)$ is the probability of survival of the underlying up to time τ , i.e. the probability that default time is larger than τ , and $P_{def}(\tau) = 1 - P(\tau)$ is the probability that default time lies in $(0, \tau]$ (both probabilities are under \mathbb{Q}). Note that the first term on the RHS of (118) gives the time-0 price of a defaultable bond with constant, continuously compounded coupon c , and maturity T . Integrating by parts in the second integral on the RHS of (117), we obtain (cf. [23])

$$V_{CDS}(T) = [c + (1 - R)r] \int_0^T e^{-r\tau} P(\tau) d\tau - (1 - R)(1 - e^{-rT} P(T)). \quad (118)$$

The par CDS spread is defined as the premium c which makes the price zero. It is therefore given by

$$c(T) = (1 - R) \left(\frac{1 - e^{-rT} P(T)}{\int_0^T e^{-r\tau} P(\tau) d\tau} - r \right). \quad (119)$$

As in [23, 68, 42], we approximate the continuous time model by a discrete time model with time step $\bar{\Delta}$. With the assumption of discrete monitoring, the survival probability $P(\tau)$, for $\tau \in [t_s, t_{s+1})$, is

$$P(\tau) = \mathbb{E} \left[\mathbb{1}_{(h, \infty)}(X_{\bar{\Delta}}) \mathbb{1}_{(h, \infty)}(X_{2\bar{\Delta}}) \dots \mathbb{1}_{(h, \infty)}(X_{s\bar{\Delta}}) \mid X_0 = 0 \right]. \quad (120)$$

Under this assumption, $P(\tau)$ becomes a right-continuous step function. Therefore we have $\int_0^T e^{-r\tau} P(\tau) d\tau = r^{-1}(1 - e^{-r\bar{\Delta}}) \sum_{s=0}^{N-1} e^{-rs\bar{\Delta}} P(s\bar{\Delta})$. The expressions for the CDS price and par spread, for unit notional, become

$$V_{CDS}(T) = \left(\frac{c}{r} + 1 - R \right) (1 - e^{-r\bar{\Delta}}) \sum_{s=0}^{N-1} e^{-rs\bar{\Delta}} P_s - (1 - R)(1 - e^{-rT} P_N), \quad (121)$$

$$c(T) = r(1 - R) \left(\frac{1 - e^{-rT} P(T)}{(1 - e^{-r\bar{\Delta}}) \sum_{s=0}^{N-1} e^{-rs\bar{\Delta}} P(s\bar{\Delta})} - 1 \right), \quad (122)$$

respectively. Note that $P(\tau)$ is equal to $e^{r\tau}$ times the price of a (discretely monitored) DO “no touch” option with time to maturity τ and the terminal payoff of a European

digital call option, $G_{\text{dc}}(x) = \mathbb{1}_{(h, \infty)}(x)$, whose Fourier transform is given by $\widehat{G}_{\text{dc}}(\xi) = e^{-ih\xi}/(i\xi)$, for $\text{Im } \xi < 0$ (cf. Example 2.2). Hence, using a change of measure², we obtain $P(\bar{\Delta}) = e^{r\tau}V_{\text{dc}}(\bar{\Delta}, 0)$, where $V_{\text{dc}}(\tau, x)$ is the price of a European digital call option

$$V_{\text{dc}}(\tau, x) = \frac{e^{-r\tau + \gamma(x + \mu\tau - h)}}{2\pi} \int_{\text{Im } \xi = \omega} \frac{e^{i(x + \mu\tau - h)\xi - \tau\psi^0(\xi - i\gamma)}}{\gamma + i\xi} d\xi, \quad (123)$$

where $\gamma \in (0, -\lambda_-)$ and $\omega \in (\gamma + \lambda_-, \gamma)$. It follows from similar arguments to the ones in Section 4.2.3 that, for model processes of order $\nu > 0$, P is of class $C^\infty([0, \infty))$.

5.1.2. Backward induction algorithm for CDS. From the argument in the previous subsection, it follows that a modification of the backward induction procedure for barrier options can be used to price a CDS with maturity T , continuously compounded spread c , recovery rate R , and notional Ω , or calculate its par spread, under a discrete time model with time step $\bar{\Delta}$. We assume that the underlying follows the exponential of a model process of order $\nu > 0$, and that ν and $\bar{\Delta}$ are not both small. As in Chapter 4, we consider only the case of piece-wise quadratic interpolation.

5.1.2.1. Choice of parameters.

1. Choose an overall error tolerance ϵ .
2. Allocate, e.g., $\epsilon_{\text{int}} = 0.80 \cdot \epsilon$ for the interpolation error, and set $\epsilon_{\text{tr}} = \epsilon_{\text{ds}} = 0.10 \cdot \epsilon$ for the errors due to truncation in the state space and approximations in the dual space, respectively.

²The change of measure from \mathbb{Q} to \mathbb{Q}^γ is such that the corresponding likelihood process is given by $(d\mathbb{Q}^\gamma/d\mathbb{Q})_t = e^{\gamma X_t}$. For more details on the use of this technique in option pricing, see Appendix A.3.2.

3. Choose x_M so that $e^{\omega_- x_M} \sup_{\tau \in [0, T]} e^{-\tau \psi(i\omega_-)} \leq \epsilon_P^{\text{tr}}$, for any $\omega_- \in (\lambda_-, 0)$, where ϵ_P^{tr} is given by the RHS of (194) in Appendix M.6 with ϵ replaced by ϵ_{tr} (cf. Lemmas M.7 and M.8).
4. Calculate ρ_3 (cf. (113)).
5. Find the maximum value Δ_0 of the mesh Δ in the state space, according to $\Delta_0 = (\epsilon_P^{\text{int}} \rho_3)^{-1/3}$, where ϵ_P^{int} is given by the RHS of (193) in Appendix M.6, with ϵ replaced by ϵ_{int} .
6. Set up the grid \mathbf{x} as described in Appendix H.
7. Denote by ϵ_P^{ds} the RHS of (193) with ϵ replaced by ϵ_{ds} . Then
 - a. For the calculation of Π_{N-1} , use the same procedure in step 2 of the algorithm in Section 4.3.3.1, with ϵ now equal to $\epsilon_P^{\text{ds}}/8$.
 - b. For the calculations of I_0, I_1, I_2 , use the same procedure as in steps 3–5 of the algorithm in Section 4.3.3.1, with ϵ_{ds} replaced by ϵ_P^{ds} .

5.1.2.2. Algorithm.

1. Calculate an approximation to the integral

$$\Pi_{N-1}(x) = \mathbb{1}_{[h, \infty)}(x) \cdot \frac{e^{-\gamma x'}}{2\pi} \int_{\text{Im } \xi = \omega} e^{-ix'\xi - \bar{\Delta} \tilde{\psi}^0(\xi)} (-i\xi)^{-1} d\xi, \quad (124)$$

where $\omega \in (0, -\lambda_-)$ and $\tilde{\psi}^0(\xi) = \psi^0(-\xi)$ (cf. Appendix D), using parabolic iFT, on a uniform grid $\mathbf{x}' = (x_j + \mu\bar{\Delta} - h)_{j=1}^M$, where $x_j = h + (j-1)\Delta$.

2. In a cycle w.r.t. $s = N-2, N-3, \dots, 0$, calculate an approximation to

$$\Pi_s(x) = \mathbb{1}_{[h, \infty)}(x) \cdot \frac{e^{-\gamma x'}}{2\pi} \int_{\text{Im } \xi = \omega} e^{-ix'\xi - \bar{\Delta} \tilde{\psi}^0(\xi)} \widehat{\Pi}_{s+1}(\xi) d\xi,$$

on the grid \boldsymbol{x}' , using the method described in Appendix H for the calculation of $V_s(x)$, $s = N - 2, N - 3, \dots, 1$, in the barrier option case. At each step $s = N - 1, N - 2, \dots, 0$, store the values $P_{N-s} = \Pi_s(0)$.

3. Calculate the approximation to the CDS price or its par spread using (121) or (122), respectively.

5.2. Numerical results

For our numerical comparisons, we used the parameter set $\lambda_- = -11$, $\lambda_+ = 0.06$, $c = 0.038$, $\nu = 1.32$, with $r = 0.04$ and $q = 0$, which was calibrated to the CDS spreads for ABN Amro Bank for 2 February 2008 in [42]. As in *op. cit.*, we take $T = 1$, $h = \ln R$, and $R = 0.4$. In Table 2, we compare the par CDS spreads calculated for discretization time steps $\bar{\Delta} = 1/48$ and $\bar{\Delta} = 1/252$ using our method, again with quadratic interpolation, and with COS. In Figure 1, we compare the minimum CPU time (in seconds) taken by our method with that taken by COS. In the left panel, we used time step $\bar{\Delta} = 1/48$ (as in *op. cit.*), and in the right panel we used $\bar{\Delta} = 1/252$ (approximately equal to one trading day). The benchmarks for each choice of $\bar{\Delta}$ were calculated in the same way as for barrier options³. The relative error shown in Figure 1 is in terms of the CDS spread (our comparison is for illustrative purposes only, since in practical applications the relevant error would be the one in the price, which in turn depends on the underlying notional amount of the contract). For our method, we used $\zeta = 0.5$, $\Lambda = 400$, $x_M - h = 3$. For COS, again we found that the recommendations in [42] (cf. (239)-(240) in Appendix Q.2, with $L \in [7.5, 10]$) gave relative errors of over 10% for daily time steps. Empirically, we found that a larger value of L was needed, and set $L = 15$ for $\bar{\Delta} = 1/48$ and $L = 25$ for $\bar{\Delta} = 1/252$.

³For the calculation of the benchmarks, we used $\Delta = 0.0001$, $x_M = h + 5$, and $\zeta = 0.1$, $\Lambda = 3000$, for all applications of parabolic iFT.

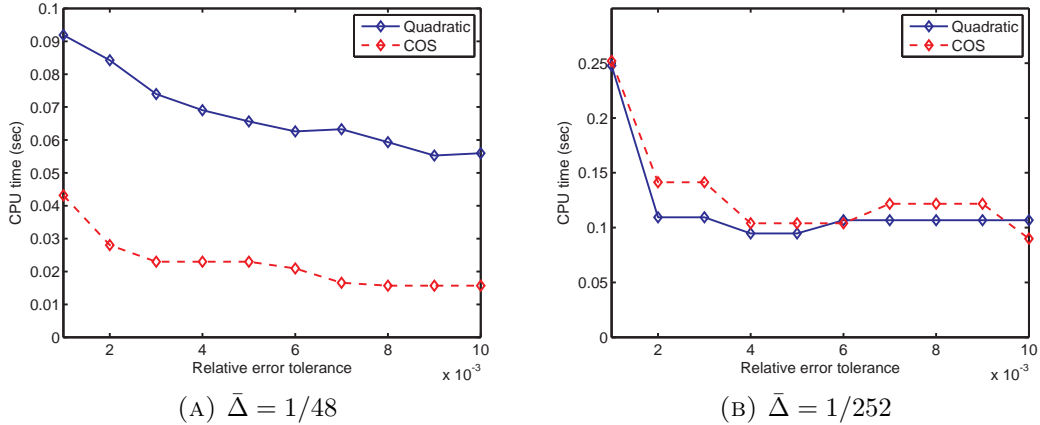


FIGURE 1. Plots of CPU time versus relative error tolerance. Comparison of our method with quadratic interpolation (solid) and COS method (dashed) to calculate the fair spread of a CDS with $T = 1$, $R = 0.4$, $h = \ln R$, under KoBoL with parameters $\lambda_- = -11$, $\lambda_+ = 0.06$, $c = 0.038$, $\nu = 1.32$ and risk free rate $r = 0.04$ (from [42]).

We note that, for daily time steps, the performance of our method and COS is similar, conditional on an appropriate choice of L for COS. For weekly monitoring, COS is slightly faster. However, it should be noted that weekly monitoring results in a relative difference in the CDS spread of over 1%, which in most practical applications would lead to a sizable error in the CDS price. This can also be seen from Table 1, where we list the relative errors in the calculation of the par spread benchmarks for monitoring intervals $\bar{\Delta} = 1/252$ (approximately once a day), $\bar{\Delta} = 1/52$ (approximately once a week), and $\bar{\Delta} = 1/48$ (as in [42]) versus $\bar{\Delta} = 1/6048$ (approximately once an hour).

TABLE 1. Relative errors of par CDS spreads calculated using our method with $\bar{\Delta} = 1/252$ (approx. daily monitoring), $\bar{\Delta} = 1/52$ (approx. weekly monitoring), and $\bar{\Delta} = 1/48$ (as in [42]) w.r.t. $\bar{\Delta} = 1/6048$ (approx. hourly monitoring) for a CDS with $T = 1$, $R = 0.4$, $h = \ln R$, under KoBoL with parameters $\lambda_- = -11$, $\lambda_+ = 0.06$, $c = 0.038$, $\nu = 1.32$ and risk free rate $r = 0.04$ (from [42]).

	$\bar{\Delta} = 1/252$	$\bar{\Delta} = 1/52$	$\bar{\Delta} = 1/48$
$T = 1$	0.00459	0.01702	0.01807
$T = 2.5$	0.00475	0.01705	0.01809
$T = 5$	0.00162	0.00960	0.01055

One reason for the poorer performance of COS in the CDS case lies in the fact that for a CDS we need to compute the survival probability at each step of backward induction, which results in additional calculations for COS, but not for our method.

Apart from these differences, the same considerations as in Section 4.4 apply regarding the performance of our method versus COS, especially about COS being unstable if L is not chosen properly, and the difficulty in finding a universal prescription for the choice of this parameter.

TABLE 2

	Spread	ϵ_{abs}	ϵ_{rel}	Time	Δ	L	N
$\bar{\Delta} = 1/48$							
Benchmark	0.00898124			782.712	0.0001		
Quadratic	0.0089883	$7.06 \cdot 10^{-6}$	$7.86 \cdot 10^{-4}$	0.404	0.0035		
Quadratic	0.0090315	$5.03 \cdot 10^{-5}$	$5.60 \cdot 10^{-3}$	0.22	0.0065		
COS	0.00883013	$1.51 \cdot 10^{-4}$	$1.68 \cdot 10^{-2}$	0.049		8	1000
COS	0.0089339	$4.73 \cdot 10^{-5}$	$5.27 \cdot 10^{-3}$	0.046		10	1000
COS	0.00897318	$8.06 \cdot 10^{-6}$	$8.97 \cdot 10^{-4}$	0.03		15	600
$\bar{\Delta} = 1/252$							
Benchmark	0.00910459			901.341	0.0001		
Quadratic	0.0091136	$9.01 \cdot 10^{-6}$	$9.90 \cdot 10^{-4}$	2.628	0.0007		
Quadratic	0.00915516	$5.06 \cdot 10^{-5}$	$5.55 \cdot 10^{-3}$	0.465	0.0035		
COS	0.00807571	$1.03 \cdot 10^{-3}$	$1.13 \cdot 10^{-1}$	0.829		8	5000
COS	0.0089339	$1.71 \cdot 10^{-4}$	$1.87 \cdot 10^{-2}$	0.049		10	1000
COS	0.00905311	$5.15 \cdot 10^{-5}$	$5.65 \cdot 10^{-3}$	0.466		15	2000
COS	0.00909517	$9.43 \cdot 10^{-6}$	$1.04 \cdot 10^{-3}$	0.822		20	5000
COS	0.00910313	$1.47 \cdot 10^{-6}$	$1.60 \cdot 10^{-4}$	0.456		25	2000

Comparison of par spreads for a CDS with $T = 1$, $R = 0.4$, $h = \ln R$, for discretization time steps $\bar{\Delta} = 1/48$ and $\bar{\Delta} = 1/252$. Time: CPU time (seconds).

Parameters of KoBoL: $\lambda_- = -11$, $\lambda_+ = 0.06$, $\nu = 1.32$, $c = 0.038$, with riskless rate $r = 0.04$ and dividend rate $q = 0$ (calibrated by Fang et al. to CDS spreads for ABN Amro as of 2 February 2008 in [42]).

ϵ_{abs} and ϵ_{rel} denote absolute and relative errors, respectively. Benchmarks were calculated using cubic interpolation.

Settings for quadratic interpolation: $x_M = h + 3$, $\zeta = 0.5$, $\Lambda = 400$. Calculations were carried out in MATLAB R2011b (win64), on a PC with Intel i5-2410M, 2.30 GHz with 4 GB RAM, running Windows 7 Professional (64 bit).

CHAPTER 6

Conclusions

We introduced a new method (ATMVG) to calculate the price of ATM European options under the VG model, and showed that it is much faster and more accurate, for short times to maturity, than either standard iFT or the parabolic iFT method (introduced in [19]). Using the ATMVG price as a benchmark, we compared the ATM prices of short maturity vanilla options calculated with both flat and parabolic iFT. As expected from the analysis in [19], we found that parabolic iFT is much more efficient than flat iFT, and its errors w.r.t. ATMVG can be made as small as 10^{-14} or 10^{-15} . We also introduced the FastVG method to calculate the price or delta of a non-ATM European option, or the price of a digital option, under the VG model. Despite having to rely on numerical computation of the incomplete gamma function, this procedure is both very accurate and much faster, for short maturity and near-ATM options, than parabolic iFT, particularly for the calculation of the digital price and the vanilla delta. In these cases, FastVG can replace iFT for applications, such as model fitting and risk management, in which speed is an important concern. The same can be done with the ATMVG method for ATM options.

We introduced a new method to price discretely monitored barrier options and CDS using a backward induction procedure, based on approximation of the option price at each step by piece-wise polynomial interpolation, fast convolution (cf. Appendix L, [14]), and the parabolic iFT method for fast pricing of European options (introduced in [19]). An analysis of the errors incurred by approximations in both

state and dual spaces showed that the most important source of error is the interpolation, since the interpolation error decays polynomially, whereas all other errors decay exponentially, and are thus easier to control. Error bounds were derived, and a general prescription for the implementation of the method was outlined. Examination of numerical results for barrier options for the case in which the underlying follows an exponential KoBoL process showed that the version of the method involving piecewise quadratic interpolation is usually the most efficient one, in terms of relative error versus CPU time. While COS can sometimes be faster than our algorithm, its accuracy depends on the choice of truncation interval as well as the number of terms in the cosine expansion, and the prescriptions given in [44] and [42] can result in very large errors for daily monitoring, even for the KoBoL parameters used in [44, 42]. As shown in [19], an appropriate choice of truncation interval for COS and similar methods can sometimes be non-trivial. The HT method, while remarkably accurate for some choices of process parameters, can sometimes be considerably slower than ours, especially if the steepness parameters are not very large, which is normally the case for processes calibrated to market data [26, 47, 52, 3].

APPENDIX A

Lévy processes: general background and results

A.1. Main definitions

We recall some general results about Lévy processes. For an exposition of the general theory of Lévy processes and their applications to pricing derivative securities, we refer the reader to [7, 77, 2] and [18, 32, 82], respectively.

Definition A.1. Let $(\Omega, \mathcal{F}, \mathbb{P})$ be a probability space. An \mathbb{R}^n -valued stochastic process $X = \{X_t\}_{t \geq 0}$ on $(\Omega, \mathcal{F}, \mathbb{P})$ is called a *Lévy process* if it has the following properties

1. There exists a subset $N \subset \Omega$ such that $\mathbb{P}[N] = 0$ and, for every $\omega \in \Omega \setminus N$, the trajectory $t \mapsto X_t(\omega)$ is right-continuous with left limits for all $t > 0$.
2. For any integer $m \geq 1$, and any collection of times $0 \leq t_0 \leq t_1 \leq \dots \leq t_m$, the random variables $X_{t_0}, X_{t_1} - X_{t_0}, \dots, X_{t_m} - X_{t_{m-1}}$, are independent.
3. For any $s, t \geq 0$, the distribution of $X_{t+s} - X_t$ does not depend on t .

We recall that every Lévy process has a characteristic exponent, which is a continuous function $\psi : \mathbb{R}^n \rightarrow \mathbb{C}$ satisfying $\psi(0) = 0$ and

$$\mathbb{E}[e^{i\langle \xi, X_t \rangle}] = e^{-t\psi(\xi)} \quad \forall \xi \in \mathbb{R}^n, t \geq 0, \quad (125)$$

where $\langle \cdot, \cdot \rangle$ denotes the inner product in \mathbb{R}^n . Conversely, the law of a Lévy process is uniquely determined by its characteristic exponent [7, §I.1]. The following well-known result, known as the Lévy-Khintchine formula, gives the general form of the characteristic exponent for all Lévy processes.

Theorem A.2 (Lévy-Khintchine Formula, cf. Theorem 1 in [7]). *Let X be a Lévy process on \mathbb{R}^n . Then its characteristic exponent admits the following representation*

$$\psi(\xi) = \frac{1}{2} \langle A\xi, \xi \rangle - i \langle \mu, \xi \rangle - \int_{\mathbb{R}^n} (e^{i\langle x, \xi \rangle} - 1 - i \langle x, \xi \rangle \mathbb{1}_D(x)) F(dx), \quad (126)$$

where A is a symmetric nonnegative-definite $n \times n$ matrix, $\mu \in \mathbb{R}^n$, $D = \{x \mid \|x\| \leq 1\}$, with $\|\cdot\|$ denoting the Euclidean norm in \mathbb{R}^n , and F is a measure on \mathbb{R}^n satisfying

$$F(\{0\}) = 0, \quad \int_{\mathbb{R}^n} \min\{1, \|x\|^2\} F(dx) < \infty. \quad (127)$$

The representation (126) is unique. Conversely, if A is a symmetric nonnegative-definite $n \times n$ matrix, $\mu \in \mathbb{R}^n$, and F is a measure on \mathbb{R}^n satisfying (127), then there exists a Lévy process X defined by (125), together with (126) and (127).

Remark A.3. The measure F can be interpreted as follows: during a unit time interval, the expected number of jumps from 0 into a measurable set $U \subset \mathbb{R}^n \setminus \{0\}$ equals $F(U)$.

F is known as the *Lévy measure*, A as the gaussian covariance matrix, and we will sometimes refer to μ as the “drift”. (A, F, μ) is known as the characteristic triplet of X . If $F(D) = \infty$, X is said to have infinite activity.

Remark A.4. For a Lévy process on \mathbb{R} , it is customary to write σ^2 instead of A , where $\sigma \geq 0$ is known as the diffusion coefficient. We will follow this convention.

Example A.5. A KoBoL process (cf. Section 2.1.2) of order $\nu \in [0, 2)$ is a one-dimensional Lévy process with $A = 0$ and the Lévy measure of the form

$$F(dx) = c_+ x^{-\nu-1} e^{\lambda-x} \mathbb{1}_{\{x>0\}} dx + c_- |x|^{-\nu-1} e^{\lambda+|x|} \mathbb{1}_{\{x<0\}} dx, \quad (128)$$

where¹ $c_{\pm} > 0$ and $\lambda_- < 0 < \lambda_+$. This process was introduced in [17] and used in [18] under the name “KoBoL²”. In [32] it was termed a “tempered stable Lévy process”, since it can be obtained from the stable Lévy process, introduced to finance by Mandelbrot in 1963 [70], by tempering the Lévy measure with exponentially decaying factors, which ensure finiteness of all moments. The λ_{\pm} are known as *steepness parameters*. In general, a good fit to market data for vanilla options can be obtained with $c_{\pm} = c$ [26, 47]. In the rest of this thesis, we restrict our attention to this case, unless stated otherwise. The parameter c is known as the *intensity* of the process. Note that the case $\nu = 0$ corresponds to the VG model (cf. [18, §3.1.2]).

In the rest of this thesis, we only consider Lévy processes on \mathbb{R} . Recall that the total variation of a function $f : [a, b] \rightarrow \mathbb{R}$ is defined by

$$V(f) = \sup_P \sum_{i=1}^{N_P} |f(t_i) - f(t_{i-1})|,$$

where the limit is taken over the set of partitions

$$\mathcal{P} = \{P = \{t_0, t_1, \dots, t_{N_P}\} \mid 0 = t_0 < t_1 < \dots < t_{N_P} = b\}$$

of the interval $[a, b]$. A Lévy process X is said to be of finite variation if all its trajectories are functions of finite variation (almost surely). It can be shown [77, Definition 11.9, Theorem 21.9] that X is of finite variation if and only if its characteristic triplet (σ^2, F, γ) satisfies

$$\sigma = 0, \quad \int_{|x| \leq 1} |x| F(dx) < \infty.$$

¹When the KoBoL model is used for pricing, one must impose the additional condition $\lambda_- \leq -1$ (see Section 2.1.1).

²A version with $c_- = c_+$ was later used in [26] under the name “CGMY process”.

If X is of finite variation, then the Lévy-Khintchine formula (126) simplifies as follows

$$\psi(\xi) = -i\mu_0\xi - \int_{\mathbb{R}} (e^{i\xi x} - 1) F(dx),$$

where $\mu_0 = \mu - \int_{-1}^1 xF(dx)$ is known as the *drift* of X . If, on the other hand, X satisfies the condition $\int_{|x|\geq 1} |x|F(dx) < \infty$, while not necessarily being of finite variation, then use of the truncation function $\mathbb{1}_D$ in (126) becomes unnecessary and we can write

$$\psi(\xi) = \frac{1}{2}\sigma^2\xi^2 - i\mu_c\xi - \int_{\mathbb{R}} (e^{i\xi x} - 1 - ix\xi) F(dx),$$

where $\mu_c = \mu + \int_{|x|\geq 1} xF(dx)$ is known as the *center* of X [77, §11]. In this case, we have $\mathbb{E}[X_t] = \mu_c t$.

A.2. Regular Lévy processes of exponential type

Recall the following result.

Proposition A.6 (cf. Theorem 25.17 in [77]). *Let X be a Lévy process with characteristic triplet (σ^2, F, μ) . Let C_X be the set defined by*

$$C_X = \left\{ \alpha \in \mathbb{R} \mid \int_{|x|>1} e^{\alpha x} F(dx) < \infty \right\}. \quad (129)$$

Then, $\alpha \in C_X$ if and only if $\mathbb{E}[e^{\alpha X_t}] < \infty$ for every $t > 0$.

This motivates the following definition.

Definition A.7. Let X be a Lévy process with characteristic triplet (σ^2, F, μ) . Then X is a *Lévy process of exponential type* (λ_-, λ_+) , with $\lambda_- \in (-\infty, 0)$, $\lambda_+ \in (0, \infty)$, if the set C_X , defined by (129), contains the interval (λ_-, λ_+) .

Remark A.8. It follows from Proposition A.6 and Definition A.7 that, if X is a Lévy process of exponential type (λ_-, λ_+) , then its characteristic exponent $\psi(\xi)$ admits the analytic continuation into the strip $\text{Im } \xi \in (\lambda_-, \lambda_+)$.

Following Boyarchenko and Levendorskii [18, §3.2.2], we consider a special class of processes, that of *regular Lévy processes of exponential type* (RPLEs), which satisfy the following definition.

Definition A.9. Let $\lambda_- < 0 < \lambda_+$ and $\nu \in (0, 2]$. A Lévy process X is called a *regular Lévy process of exponential type* (λ_-, λ_+) and *order* ν if the following conditions are satisfied

1. the characteristic exponent of X admits the representation

$$\psi(\xi) = -i\mu\xi + \psi^0(\xi), \quad (130)$$

where $\mu \in \mathbb{R}$, ψ^0 is holomorphic in the strip $\text{Im } \xi \in (\lambda_-, \lambda_+)$, is continuous up to the boundary of the strip, and admits the representation

$$\psi^0(\xi) = c|\xi|^\nu + O(|\xi|^{\nu_1}), \quad (131)$$

for some constant $c > 0$, as $|\xi| \rightarrow \infty$ in the strip $\text{Im } \xi \in (\lambda_-, \lambda_+)$, for some $\nu_1 < \nu$;

2. there exist some $\nu_2 < \nu$ and some constant $C \in \mathbb{R}$ such that

$$|\partial_\xi \psi^0(\xi)| \leq C(1 + |\xi|)^{\nu_2}, \quad \text{Im } \xi \in [\lambda_-, \lambda_+]. \quad (132)$$

Most processes commonly used in finance are RLPEs, the most prominent exception being Variance Gamma (cf. Section 2.1.2). We recall the following result from [18].

Theorem A.10 (Theorem 3.1 in [18]). *For any $\tau > 0$, the probability density p_τ of a RLPE X is infinitely smooth and decays exponentially at infinity, together with all of its derivatives.*

PROOF. (Adapted from [18]). Let X be of exponential type (λ_-, λ_+) . Take $\omega \in (\lambda_-, \lambda_+)$. From the definition of the characteristic exponent, it follows that the transition probability density function is given by

$$p_\tau(x) = \frac{1}{2\pi} \int_{\mathbb{R}} e^{-ix\xi - \tau\psi(\xi)} d\xi. \quad (133)$$

If $\omega \in (\lambda_-, \lambda_+)$, we can write

$$\begin{aligned} p_\tau(x) &= \frac{e^{\omega x}}{2\pi} \int_{\mathbb{R}} e^{-ix(\xi - i\omega) - \tau\psi(\xi)} d\xi \\ &= \frac{e^{\omega x}}{2\pi} \int_{\text{Im } \xi = -\omega} e^{-ix\xi - \tau\psi(\xi + i\omega)} d\xi \\ &= \frac{e^{\omega x}}{2\pi} \int_{\mathbb{R}} e^{-ix\xi - \tau\psi(\xi + i\omega)} d\xi, \end{aligned} \quad (134)$$

where the shift of the line of integration in the last equality is justified by Cauchy's theorem. The integral in (134) converges absolutely and uniformly in x , even after differentiating w.r.t. x under the integral sign any number of times. \square

A.3. Measure changes for Lévy processes

A.3.1. General results. We quote the following result from [77].

Theorem A.11 (Theorem 33.1 in [77]). *Let (X_t, \mathbb{P}) and (X_t, \mathbb{P}') be Lévy processes on \mathbb{R} , with characteristic triplets (σ^2, F, μ) and (σ'^2, F', μ') , respectively. Then the measures $\mathbb{P}|_{\mathcal{F}_t}$ and $\mathbb{P}'|_{\mathcal{F}_t}$ are equivalent for all $t \in [0, \infty)$ if and only if*

$$(1) \quad \sigma = \sigma',$$

(2) F and F' are equivalent measures and

$$\int_{-\infty}^{\infty} \left(\left(\frac{dF'}{dF} \right)^{\frac{1}{2}} - 1 \right)^2 F(dx) < \infty, \quad (135)$$

where dF'/dF denotes the Radon-Nikodym derivative.

(3) If $\sigma = 0$, then

$$\mu' = \mu + \int_{-1}^1 x(F' - F)(dx). \quad (136)$$

As a consequence, we can state the following

Corollary A.12 (See example 9.1 in [32]). *If (X_t, \mathbb{P}) is a general KoBoL process with order $\nu \in (0, 2)$, with $c_{\pm} > 0$ and steepness parameters $\lambda_{\pm} > 0$, then $\mathbb{P}' \sim \mathbb{P}$ if and only if (X_t, \mathbb{P}') is a KoBoL process with order $\nu' = \nu$ and intensities $c'_{\pm} = c_{\pm}$.*

PROOF. (Adapted from [32]). From the expression (128) for the Lévy measure of a KoBoL process, it follows that, if (135) is to be satisfied, then we must have

$$\int_0^{\infty} \left(x^{\frac{\nu-\nu'}{2}} e^{\frac{1}{2}(\lambda_+ - \lambda'_+)x} \sqrt{\frac{c'_+}{c_+}} - 1 \right)^2 \frac{e^{-\lambda_+x}}{x^{1+\nu}} dx < \infty,$$

with an equivalent condition holding for the integral on the negative half-line. By expanding the exponential inside the brackets as a Taylor series, it can be seen that, if $\nu' \neq \nu$, or if $\nu' = \nu$ and $c'_+ \neq c_+$, then the integrand behaves like $x^{-1-\nu}$ for $x \rightarrow 0$, and is therefore divergent. If, on the other hand, $\nu' = \nu$ and $c'_+ = c_+$, then the integrand behaves like $x^{1-\nu}$, which is integrable, since $\nu < 2$. By considering the integral corresponding to the negative half-line, one similarly obtains the condition $c'_- = c_-$. \square

A.3.2. Measure changes and European option pricing. We start with the following

Proposition A.13. *Let X be a Lévy process on \mathbb{R} under \mathbb{Q} such that its characteristic exponent under \mathbb{Q} , $\psi(\xi)$, admits the analytic continuation into the domain $\mathbb{R} + iU$, where $U \subset \mathbb{R}$ is an open interval containing the origin. Then, for any $\gamma \in -U$, under the measure change with likelihood process*

$$(d\mathbb{Q}^\gamma/d\mathbb{Q})_t = e^{\gamma X_t}, \quad (137)$$

X becomes a \mathbb{Q}^γ -Lévy process with characteristic exponent $\psi^\gamma(\xi) = \psi(\xi - i\gamma)$.

PROOF. We have

$$\mathbb{E}^{\mathbb{Q}^\gamma}[e^{i\xi X_t}] = \mathbb{E}^{\mathbb{Q}}[e^{\gamma X_t} e^{i\xi X_t}] = \mathbb{E}^{\mathbb{Q}}[e^{i(\xi - i\gamma)X_t}] = e^{-t\psi(\xi - i\gamma)}.$$

□

Remark A.14. The measure change in (137) is similar to the Esscher transform, which has $(d\tilde{\mathbb{Q}}^\gamma/d\mathbb{Q})_t = e^{\gamma X_t + t\psi(-i\gamma)}$, for $\gamma \in -U$, and under which $\psi(\xi) \mapsto \tilde{\psi}^\gamma(\xi) := \psi(\xi - i\gamma) - \psi(-i\gamma)$. Note a Lévy process and its dual (cf. Appendix D) are related by an Esscher transform with $\gamma = 1$.

Recall that an operator of the form

$$Au(x) = a(x, D)u(x) = \frac{1}{2\pi} \int_{-\infty}^{+\infty} e^{ix\xi} a(x, \xi) \hat{u}(\xi) d\xi$$

is called a *pseudo-differential operator (PDO)* with the *symbol* a . If a does not depend on x , then A is called a PDO with constant symbol. Let $V(t, x)$ denote the price at time t of a European option, with maturity T and terminal payoff $G(X_T)$, on an underlying following the exponential Lévy process e^{X_t} , such that $X_t = x$. Then, if $\psi(\xi)$ is the characteristic exponent of X under the risk-neutral measure \mathbb{Q} , it can be

shown that $V(t, x)$ satisfies

$$\partial_t V(t, x) - (r + \psi(D))V(t, x) = 0, \quad t < T, \quad (138)$$

$$V(T, x) = G(x), \quad (139)$$

where $\psi(D)$ is the PDO with constant symbol $\psi(\xi)$ (for a formal derivation, see Chapters 1-2 of [18]). For some $\gamma \in -U$, define $V^\gamma(t, x) = e^{-\gamma x}V(t, x)$ and $G^\gamma(x) = e^{-\gamma x}G(x)$. Then, using the equality $e^{\gamma x}\psi(D)e^{-\gamma x} = \psi(D + i\gamma)$, we obtain from (138)-(139)

$$\partial_t V^\gamma(t, x) - (r + \psi^\gamma(D))V^\gamma(t, x) = 0, \quad t < T, \quad (140)$$

$$V^\gamma(T, x) = G^\gamma(x). \quad (141)$$

Hence, if we change the measure from \mathbb{Q} to \mathbb{Q}^γ using (137), we can price the original option by solving (140)-(141) instead of (138)-(139), then changing the measure back by setting $V(t, x) = e^{\gamma x}V^\gamma(t, x)$. For more details, see [18].

APPENDIX B

Algorithms for vanilla option pricing using flat iFT

Following [19], we include the algorithms for the calculation of the vanilla option price under flat iFT, for both ordinary and refined FFT. Recall that, for the vanilla call and put option, one should take $\omega \in (\lambda_-, -1)$ and $\omega \in (0, \lambda_+)$, respectively¹. As in Chapter 2, we denote by S the current (spot) price of the underlying.

B.1. Calculation of option price as function of strike using FFT

Suppose that, given S , we need to calculate call option prices for several strikes $K = K_\ell$, $\ell = 1, 2, \dots, n$, at time $\tau > 0$ to maturity. Then

1. Choose x_1 , $M = 2^m$ and $\Delta > 0$ such that for all ℓ , $x_1 \leq \ln(K_\ell/S) \leq x_1 + (M - 1)\Delta$, and construct the grid $\mathbf{x} = (x_j)_{j=1}^M$, where $x_j = x_1 + (j - 1)\Delta$. If possible, all $\ln(K_\ell/S)$ ought to be among the points of the grid; this allows one to avoid interpolation errors.
2. Set $\zeta = 2\pi/(M\Delta)$ so that the uncertainty principle (17) holds. Set $\Lambda = M\zeta/2(= \pi/\Delta)$, $\xi_1 = i\omega - \Lambda$, and construct the grid $\boldsymbol{\xi} = (\xi_k)_{k=1}^M$, where $\xi_k = \xi_1 + (k - 1)\zeta$.
3. Calculate the array $\mathbf{f} = (f_k)_{k=1}^M$, where the f_k are given by (16).
4. Calculate the array²

$$\mathbf{V} = -\frac{S\zeta}{2\pi} \exp((1 - i * \xi_1) * \mathbf{x}) .* \mathbf{fft}(\mathbf{f} .* \exp(-i * \zeta * x_1 * (0 : M - 1))).$$

The array \mathbf{V} consists of (approximations to) the option prices $V(\tau, x_j)$.

¹For the choice of offset ω and mesh ζ under flat iFT, see Appendix O.1.1.1.

²In this appendix, we will use a notation reminiscent of MATLAB syntax.

5. If some of the points $y_\ell := \ln(K_\ell/S)$ are not among the points of the grid \mathbf{x} , then an additional interpolation procedure must be used to calculate $V(\tau, y_\ell)$.

B.2. Calculation of option price as function of spot using iFFT

Suppose that, given K , we need to calculate call option prices for several $S = S_\ell, s = 1, 2, \dots, n$, at time $\tau > 0$ to maturity. Then

1. Choose x_1 , $M = 2^m$ and $\Delta > 0$ such that for all ℓ , $x_1 \leq \ln(S_\ell/K) \leq x_1 + (M - 1)\Delta$, and construct the grid $\mathbf{x} = (x_j)_{j=1}^M$, where $x_j = x_1 + (j - 1)\Delta$. If possible, all $\ln(S_\ell/K)$ ought to be among the points of the grid; this allows one to avoid interpolation errors.
2. Set $\zeta = 2\pi/(M\Delta)$ so that the uncertainty principle (17) holds. Set $\Lambda = M\zeta/2 (= \pi/\Delta)$, $\xi_1 = i\omega - \Lambda$, and construct the grid $\boldsymbol{\xi} = (\xi_k)_{k=1}^M$, where $\xi_k = \xi_1 + (k - 1)\zeta$.
3. Calculate the array $\mathbf{f} = (f_k)_{k=1}^M$, where the f_k are given by (16).
4. Calculate the array

$$\mathbf{V} = -(K/\Delta) * \exp(i * \xi_1 * \mathbf{x}) .* \text{ifft}(\mathbf{f} .* \exp(i * \zeta * x_1 * (0 : M - 1))).$$

The array \mathbf{V} consists of (approximations to) the option prices $V(\tau, x_j)$.

5. If some of the points $y_\ell := \ln(S_\ell/K)$ are not among the points of the grid \mathbf{x} , then an additional interpolation procedure must be used to calculate $V(\tau, y_\ell)$.

B.3. Calculation of option price as function of strike using refined FFT

If the characteristic exponent increases slowly at infinity and/or time to maturity is too small, then the truncation parameter $\Lambda = \pi/\Delta$ chosen above may be too small in the sense that the truncation error is too large. If we decrease Δ and keep the number M of points on the grids \mathbf{x} and $\boldsymbol{\xi}$ fixed, then, on the strength of the uncertainty principle, $\zeta = 2\pi/(M\Delta)$ will increase and the discretization error may

become too large; in addition, the interval $[x_1, x_M]$ may become too small and some of the points $\ln(K_\ell/S)$ of interest will be outside this interval.

Thus, it is useful to keep the same grid \mathbf{x} and a moderately small mesh ζ in the dual space but extend, and, if necessary, refine the grid in the dual space. The following approach (refined FFT method) was introduced by M. Boyarchenko and Levendorskiĭ in [14]. We take integers $M_2 \geq 2$, $M_3 \geq 1$, set $M_1 = MM_2M_3$, $\zeta_1 = \zeta/M_3$, and use $\Lambda = M_1\zeta/2$ as the truncation parameter and ζ_1 as the mesh of the grid on the line $\text{Im } \xi = \omega$ of M_1 points: $\xi_j = -\Lambda + i\omega + (j-1)\zeta$, $j = 1, 2, \dots, M_1 - 1$. We approximate the truncated integral using the simplified trapezoid rule.

$$V(\tau, x) \approx -\frac{S\zeta_1}{2\pi} e^x \sum_{k=1}^{M_1} e^{-ix\xi_k} f_k, \quad (142)$$

where $f_k = f(\xi_k)$, $f(\xi) = \exp[-(r + \psi)(\xi_k)]/((\xi_k + i)\xi_k)$. To apply the standard FFT, we need to divide the sum in (142) into M_2M_3 sums, each sum having M terms

$$V(\tau, x) \approx -\frac{S\zeta_1}{2\pi} e^x \sum_{j=1}^{M_2} \sum_{k=1}^{M_3} \sum_{\ell=1}^M e^{-ix\xi_\ell^{jk}} f_\ell^{jk}, \quad (143)$$

where $\xi_\ell^{jk} = i\omega - M_1\zeta_1/2 + (j-1)M\zeta + (k-1)\zeta_1 + (\ell-1)\zeta$, $f_\ell^{jk} = f(\xi_\ell^{jk})$, and apply to each interior sum the procedure described in Appendix B.1 with the grid $(\xi_\ell^{jk})_{\ell=1}^M$ instead of $\boldsymbol{\xi}$ and array $(f_\ell^{jk})_{\ell=1}^M$ instead of $(f_k)_{k=1}^M$: for $j = 1, 2, \dots, M_2$ and $k = 1, 2, \dots, M_3$, calculate

$$\mathbf{V}^{jk} = \exp((1 - i * \xi_1^{jk}) * \mathbf{x}) .* (\mathbf{f}^{jk} .* \exp(-i * \zeta * x_1 * (0 : M - 1))),$$

and then set

$$\mathbf{V} = -\frac{S\zeta_1}{2\pi} \sum_{j=1}^{M_2} \sum_{k=1}^{M_3} \mathbf{V}^{jk}.$$

B.4. Calculation of option price as function of spot using refined FFT

We modify the algorithm in Appendix B.2 in the same way as the algorithm in Appendix B.1 was modified in Appendix B.3: for $j = 1, 2, \dots, M_2$, we calculate

$$\mathbf{V}^{jk} = \exp(i * \xi_1^{jk} * \mathbf{x}) .* \text{ifft}(\mathbf{f}^{jk} .* \exp(i * \zeta * x_1 * (0 : M - 1))),$$

and then set

$$\mathbf{V} = -\frac{K}{M_3 \Delta} \sum_{j=1}^{M_2} \sum_{k=1}^{M_3} \mathbf{V}^{jk}.$$

APPENDIX C

Truncation error bounds for the VG option price

C.1. Flat iFT case

We truncate the integral on the RHS of (32) as follows

$$V(\tau, x; \Lambda) = -\frac{e^{-r'\tau - \omega x'}}{2\pi} \int_{-\Lambda}^{\Lambda} e^{ix'\eta} \frac{(\sigma^2 + \eta^2)^{-c\tau}}{(\eta + i\omega)(\eta + i\omega + i)} d\eta. \quad (144)$$

We refer to $V(\tau, x; \Lambda)$ as the truncated price and to $\text{Tr.Err.}(V; \tau, x; \Lambda) = |V(\tau, x; \Lambda) - V(\tau, x)|$ as the (absolute) truncation error. Recall that the hypergeometric function is defined by [1, §15]

$${}_2F_1(a, b; c; z) = \sum_0^{\infty} \frac{(a)_n (b)_n}{(c)_n} \frac{z^n}{n!},$$

for $c \notin \{0\} \cup \mathbb{Z}_-$ and $|z| < 1$, where $(\cdot)_n$, known as the Pochhammer symbol, is defined according to

$$(q)_n = \begin{cases} 1, & n = 0, \\ q(q+1) \dots (q+n-1), & n > 0. \end{cases}$$

A useful bound for the truncation error in (144) is given by the following result.

Proposition C.1. *If the underlying follows a VG process, $\text{Tr.Err.}(V; \tau, x; \Lambda)$ admits the following bound*

$$|\text{Tr.Err.}(V; \tau, x; \Lambda)| \leq C(\Lambda) \frac{e^{-r'\tau - \omega x'}}{\pi(1 + 2c\tau)} \Lambda^{-1-c\tau}, \quad (145)$$

where $C(\Lambda) = {}_2F_1\left(\frac{1}{2} + c\tau, 1 + c\tau; \frac{3}{2} + c\tau; -\frac{\omega^2}{\Lambda^2}\right)$.

PROOF. Putting $\alpha = \pi^{-1}e^{-r'\tau - \omega x'}$, we have

$$\begin{aligned} \text{Tr.Err.}(\tau, x; \Lambda) &= \left| \alpha \operatorname{Re} \int_{\Lambda}^{+\infty} \frac{e^{ix'\eta}(\sigma^2 + \eta^2)^{-c\tau}}{(\eta + i\omega)(\eta + i\omega + i)} d\eta \right| \leq \alpha \int_{\Lambda}^{+\infty} \left| \frac{e^{ix'\eta}(\sigma^2 + \eta^2)^{-c\tau}}{(\eta + i\omega)(\eta + i\omega + i)} \right| d\eta \\ &\leq \alpha \int_{\Lambda}^{+\infty} \frac{(\sigma^2 + \eta^2)^{-c\tau}}{|\eta + i\omega|^2} d\eta \leq \alpha \int_{\Lambda}^{+\infty} \frac{d\eta}{(\omega^2 + \eta^2)^{1+c\tau}}. \end{aligned}$$

Define

$$C(\Lambda) = \int_{\Lambda}^{+\infty} \frac{d\eta}{(\omega^2 + \eta^2)^{1+c\tau}} = \omega^{-1-2c\tau} \int_{\Lambda/\omega}^{+\infty} \frac{dx}{(1+x^2)^{1+c\tau}}.$$

Consider the integral

$$I(L) = \int_{L^{-1}}^{+\infty} \frac{dx}{(1+x^2)^{1+p}},$$

for $L > 0$, $p > 0$. Changing the variable $z = x^{-1}$, we obtain

$$I(L) = \int_0^L \frac{z^{2p} dx}{(1+z^2)^{1+p}}.$$

Recall that (cf. [1, §15.2.4]), for $|y| < 1$, $d \notin \{0, 1\} \cup \mathbb{Z}_-$, we have

$$y \frac{d}{dy} {}_2F_1(a, b; d; y) = (d-1)[{}_2F_1(a, b; d-1; y) - {}_2F_1(a, b; d; y)]. \quad (146)$$

Hence, for $p > 0$, we have

$$y \frac{d}{dy} {}_2F_1\left(\frac{1}{2} + p, 1 + p; \frac{3}{2} + p; y\right) = \left(\frac{1}{2} + p\right) \left[(1-y)^{-1-p} - {}_2F_1\left(\frac{1}{2} + p, 1 + p; \frac{3}{2} + p; y\right) \right], \quad (147)$$

where we have used the fact that [1, §15.1.8], for $b \notin \{0\} \cup \mathbb{Z}_-$

$${}_2F_1(a, b; b; y) = (1-y)^{-a}. \quad (148)$$

Substituting $y = -z^2$ in (147), we obtain

$$z \frac{d}{dz} {}_2F_1\left(\frac{1}{2} + p, 1 + p; \frac{3}{2} + p; -z^2\right) = (1+2p) \left[(1+z^2)^{-1-p} - {}_2F_1\left(\frac{1}{2} + p, 1 + p; \frac{3}{2} + p; -z^2\right) \right].$$

Multiplying both sides by z^{2p} , it can be seen that

$$\frac{z^{2p}}{(1+z^2)^{1+p}} = \frac{1}{1+2p} \left[z^{1+2p} {}_2F_1 \left(\frac{1}{2} + p, 1 + p; \frac{3}{2} + p; -z^2 \right) \right],$$

which gives

$$I(L) = \frac{L^{1+2p}}{1+2p} {}_2F_1 \left(\frac{1}{2} + p, 1 + p; \frac{3}{2} + p; -L^2 \right).$$

□

Remark C.2. This result is similar to Proposition 2.5 in [19], except that the value of $C(\Lambda)$ is now given explicitly.

Remark C.3. Since $C(\Lambda)$ tends to 1 very rapidly for $\Lambda \rightarrow \infty$, in a practical application one can safely set $C(\Lambda) = 1$ for large Λ .

C.2. Parabolic iFT (ATM case)

The following bound is the analogue of the one in Proposition C.1 for the ATM call case under parabolic iFT.

Proposition C.4. *If the underlying follows a VG process, then the ATM truncation error under the parabolic iFT procedure described in Section 2.3.2, with truncation parameter Λ , $\text{Tr.Err.}^{(p)}(V; \tau, -\mu\tau; \Lambda)$ (defined analogously to the error for the flat iFT case in Proposition C.1), admits the following approximate bound*

$$|\text{Tr.Err.}^{(p)}(V; \tau, -\mu\tau; \Lambda)| \leq C_1 \frac{\Lambda^{-\alpha(1+2c\tau)}}{\alpha(1+2c\tau)}, \quad (149)$$

where

$$C_1 = \frac{\alpha K}{\pi} (-\lambda_- \lambda_+)^{c\tau} (-\lambda_- - 1)^{(\alpha-1)(1+2c\tau)},$$

PROOF. Recall that the ATM call price under parabolic iFT, for a VG process, is given by (27) with $\alpha \in [1, 4)$, and $\psi^0(\chi_\alpha^-(\xi))$ given by (30). Put $\xi = \eta + i\omega$, where

$\eta \in \mathbb{R}$ and $\omega \in (\lambda_-, -1)$. In the ATM case $x' = 0$, so we need an upper bound for the quantity

$$\Phi_p^-(\xi) = \frac{\alpha K}{\pi(-\lambda_- - 1)^{\alpha-1}} \frac{e^{-\tau \operatorname{Re} \psi^0(\chi_\alpha^-(\xi))} |(-\lambda_- - i\xi)^{\alpha-1}|}{|i\chi_\alpha^-(\xi)(1 - \chi_\alpha^-(\xi))|}, \quad (150)$$

in the limit as $\eta \rightarrow \pm\infty$. We start by calculating the asymptotics of $\operatorname{Re} \psi^0(\chi_\alpha^-(\xi))$ as $\eta \rightarrow \pm\infty$. We have

$$\operatorname{Re} \ln(-\lambda_- - i\xi) = \ln |\eta| + \frac{(-\lambda_- + \omega)^2}{2\eta^2} + O(\eta^{-4}). \quad (151)$$

Consider the factor $\ln(\lambda_+ - \lambda_- - (-\lambda_- - 1)^{1-\alpha}(-\lambda_- - i\xi)^\alpha)$. Write

$$Y(\eta) = -(-\lambda_- - 1)^{1-\alpha}(-\lambda_- + \omega - i\eta)^\alpha.$$

As $\eta \rightarrow \pm\infty$, $|Y(\eta)| \rightarrow +\infty$. Hence $\ln(\lambda_+ - \lambda_- + Y(\eta)) = \ln(Y(\eta)) + O(\eta^{-\alpha})$. If $\alpha \in (2, 4)$, then

$$\begin{aligned} \operatorname{Re} \ln(\lambda_+ - \lambda_- + Y(\eta)) &= \ln(-(-\lambda_- - 1)^{1-\alpha}) + \alpha \operatorname{Re} \ln(-\lambda_- + \omega - i\eta) + O(\eta^{-\alpha}) \\ &= \ln(-(-\lambda_- - 1)^{1-\alpha}) + \alpha \ln |\eta| + \frac{\alpha(-\lambda_- + \omega)^2}{2\eta^2} + O(\eta^{-\alpha}). \end{aligned}$$

Hence

$$\begin{aligned} \operatorname{Re} \psi^0(\chi_\alpha^-(\xi)) &= c[-\ln(-\lambda_- \lambda_+) + 2(1 - \alpha) \ln(-\lambda_- - 1) + 2\alpha \ln |\eta| + \\ &\quad \alpha(-\lambda_- + \omega)^2 \eta^{-2} + O(\eta^{-\alpha})]. \end{aligned}$$

Therefore

$$\begin{aligned} e^{-\tau \operatorname{Re} \psi^0(\chi_\alpha^-(\xi))} &= \left(\frac{-\lambda_- \lambda_+}{(-\lambda_- - 1)^{2(1-\alpha)}} \right)^{c\tau} |\eta|^{-2c\tau\alpha} e^{-c\tau\alpha(-\lambda_- + \omega)^2 \eta^{-2}} (1 + O(\eta^{-\alpha})) \\ &\leq \left(\frac{-\lambda_- \lambda_+}{(-\lambda_- - 1)^{2(1-\alpha)}} \right)^{c\tau} |\eta|^{-2c\tau\alpha} (1 + O(\eta^{-\alpha})). \end{aligned} \quad (152)$$

Next, we need the asymptotics of

$$\begin{aligned}
|(-\lambda_- + \omega - i\eta)^{\alpha-1}| &= |\eta|^{\alpha-1} \left| 1 + (\alpha-1) \frac{-\lambda_- + \omega}{-i\eta} - \frac{(\alpha-1)(\alpha-2)(-\lambda_- + \omega)^2}{2\eta^2} + O(\eta^{-3}) \right| \\
&= |\eta|^{\alpha-1} \left[\left(1 - \frac{(\alpha-1)(\alpha-2)(-\lambda_- + \omega)^2}{2\eta^2} \right)^2 + \left((\alpha-1) \frac{\lambda_- + \omega}{\eta} \right)^2 + O(\eta^{-3}) \right] \\
&= |\eta|^{\alpha-1} \left(1 + \frac{(\alpha-1)(-\lambda_- + \omega)}{\eta^2} + O(\eta^{-3}) \right). \tag{153}
\end{aligned}$$

Next, we calculate

$$\begin{aligned}
- [i\chi_\alpha^-(\xi)(1 - i\chi_\alpha^-(\xi))]^{-1} &= -(-\lambda_- - 1)^{2(\alpha-1)}(-\lambda_- + \omega - i\eta)^{-2\alpha} + O(\eta^{-3\alpha}) \\
&= -(-\lambda_- - 1)^{2(\alpha-1)}(-i\eta)^{-2\alpha} + O(\eta^{-3\alpha}).
\end{aligned}$$

Hence

$$\left| [i\chi_\alpha^-(\xi)(1 - i\chi_\alpha^-(\xi))]^{-1} \right| = (-\lambda_- - 1)^{2(\alpha-1)} |\eta|^{-2\alpha} + O(\eta^{-3\alpha}). \tag{154}$$

Finally, using (150), (151), (152), (153), and (154), we obtain

$$\begin{aligned}
|\Phi_p^-(\xi)| &\leq \frac{\alpha K}{\pi} (-\lambda_- \lambda_+)^{c\tau} (-\lambda_- - 1)^{(\alpha-1)(1+2c\tau)} |\eta|^{-1-\alpha(1+2c\tau)} (1 + O(\eta^{-\alpha})) \\
&\quad + \frac{\alpha K}{\pi} (-\lambda_- \lambda_+)^{c\tau} (-\lambda_- - 1)^{(\alpha-1)(1+2c\tau)} (\alpha-1)(-\lambda_- + \omega) |\eta|^{-3-\alpha(1+2c\tau)} \\
&\quad \times (1 + O(\eta^{-\alpha})).
\end{aligned}$$

Hence, for $\eta \rightarrow +\infty$, we have

$$|\Phi_p^-(\xi)| = C(\eta) C_1 (1 + C_2 \eta^{-2}) \eta^{-1-\alpha(1+2c\tau)},$$

where $C(\eta) = 1 + O(\eta^{-\alpha})$, $C_2(\eta) = (\alpha - 1)(-\lambda_- + \omega)$. Since, for $\eta \rightarrow +\infty$, $C(\eta)$ will tend to 1 very rapidly, we can write, for large Λ

$$\begin{aligned} |\text{Tr.Err.}^{(p)}(V; \tau, -\mu\tau; \Lambda)| &\leq C_1 \int_{\Lambda}^{\infty} \eta^{-1-\alpha(1+2c\tau)} d\eta \\ &\quad + C_1 C_2 \int_{\Lambda}^{\infty} \eta^{-3-\alpha(1+2c\tau)} d\eta, \end{aligned} \tag{155}$$

which gives (149), since, for large enough Λ , the second integral in (155) can usually be neglected. \square

APPENDIX D

A put-call symmetry

Recall the following result [8]

Lemma D.1. *Let Z_t be a \mathbb{Q} -martingale. Then, the process Z_t^{-1} is a martingale under the dual measure $\tilde{\mathbb{Q}}$, such that the likelihood process (process of Radon-Nikodym derivatives) is given by $L_t := (d\tilde{\mathbb{Q}}/d\mathbb{Q})_t = Z_t$.*

PROOF. If $L_t = (d\tilde{\mathbb{Q}}/d\mathbb{Q})_t = Z_t$, then Y_t is a $\tilde{\mathbb{Q}}$ -martingale if and only if $L_t Y_t$ is a \mathbb{Q} -martingale. From this the result follows. \square

The discounted stock price (\mathbb{Q} -martingale) is $Z_t = e^{-rt} S_t$, hence $L_t = e^{-rt} e^{X_t}$. Also recall the following result on the change of measure for conditional expectations of processes

$$\mathbb{E}^{\mathbb{Q}}[L_t Y_t | \mathcal{F}_s] = L_s \mathbb{E}^{\tilde{\mathbb{Q}}}[Y_t | \mathcal{F}_s], \quad (156)$$

where $s < t$. Defining the *dual process* \tilde{X} by $\tilde{X}_t = -X_t$, we obtain the following

Corollary D.2. *The characteristic exponent of the dual process \tilde{X} is given by $\tilde{\psi}(\xi) = \psi(-\xi - i) - \psi(-i)$.*

PROOF.

$$\begin{aligned} e^{-t\tilde{\psi}(\xi)} &= \mathbb{E}^{\tilde{\mathbb{Q}}}[e^{i\xi\tilde{X}_t}] = \mathbb{E}^{\mathbb{Q}}[e^{-rt} e^{X_t} e^{-i\xi X_t}] = e^{-rt} \mathbb{E}^{\mathbb{Q}}[e^{i(-\xi-i)X_t}] \\ &= e^{-rt} e^{-t\psi(-\xi-i)} = e^{-t(\psi(-\xi-i) - \psi(-i))}, \end{aligned}$$

where the EMM condition (1) has been used. It can easily be seen that the risk-neutral “drift” of the dual process is the same as that of the original process, but with the opposite sign. \square

We can now prove the following results.

Proposition D.3. *The price of a European call option with maturity T , strike K , riskless rate r on an underlying asset following the exponential RLPE (or model process) e^{X_t} , with continuous dividend yield q and spot value S , equals the price of a European put option with maturity T , strike S , riskless rate q on an underlying asset with continuous dividend yield r and spot value K , following the exponential dual RLPE (or model process) $e^{\tilde{X}_t}$.*

PROOF. Change the variable $\xi \mapsto -\xi - i$ in (12), and substitute $r = \mu + q - \psi^0(-i)$ (which follows from the EMM condition (1)). Use Corollary D.2. \square

Proposition D.4. *The price of a European call option with maturity T , strike K , riskless rate r on an underlying asset following an exponential KoBoL (or VG) process e^{X_t} , with continuous dividend yield q and spot value S , equals the price of a European put option with maturity T , strike S , riskless rate r on an underlying with continuous dividend yield q and spot value K , following an exponential KoBoL (or VG) process $e^{X'_t}$, where X' is such that its “steepness parameters” λ_- and λ_+ are interchanged w.r.t. to those of X .*

PROOF. Change the variable $\xi \mapsto -\xi$ in (12). \square

Remark D.5. The last result is sometimes referred to as “foreign-domestic symmetry” in the FX option market [86].

APPENDIX E

Comparison of different quadrature methods

E.1. ATMVG case

We compare the ATMVG price calculated with $\Lambda = 1.5\sigma$, $\epsilon_1 = 10^{-12}$, $\epsilon_2 = 10^{-15}$, using each of the methods in Section 3.2.2, namely: adaptive Simpson's rule, Clenshaw-Curtis integration, the adaptive Gauss-Lobatto rule (used in several examples in Chapter 3), and vectorized Gauss-Kronrod quadrature. In Table 1 we list the absolute and relative differences of the ATMVG prices obtained with each of these methods w.r.t. the benchmark price calculated with the adaptive Gauss-Lobatto rule, and the CPU times taken by each. In addition, we list the corresponding results obtained using Integration Along Cut (IAC, cf. [18, 60]) and parabolic iFT¹. The absolute differences are very small indeed, ranging from $4.58 \cdot 10^{-15}$ for Gauss-Lobatto to $3.98 \cdot 10^{-16}$ for Clenshaw-Curtis and Gauss-Kronrod quadratures. CPU times range from 37.76 ms for Adaptive Simpson integration to 5.08 ms for Clenshaw-Curtis, and 1.84 ms for Gauss-Kronrod quadrature.

Finally, we note that the CPU time taken by the calculation of $\Phi_2(\sigma, \omega; \Lambda)$ in the above example is only 0.56 ms, which shows that most of the time is taken up by the calculation of $\Phi_1(\sigma, \omega; \Lambda)$.

¹Run with $\zeta = 0.125$, $\Lambda = 180000$, $\alpha = 3.9$ (cf. Section 3.5.2).

TABLE 1. Differences w.r.t. the benchmark and CPU times for ATMVG calculation of the price of an ATM call option with $K = 1$, $\lambda_- = -11$, $\lambda_+ = 8$, $m_2 = 0.16$, $r = 0.03$, $q = 0$, $\tau = 0.004$.

Method	Abs. Diff.	Rel. Diff.	CPU Time (sec.)
Adapt. Simpson	$3.43 \cdot 10^{-15}$	$1.40 \cdot 10^{-12}$	0.03776
Clenshaw Curtis	$3.98 \cdot 10^{-16}$	$1.62 \cdot 10^{-13}$	0.00486
Gauss-Kronrod	$3.98 \cdot 10^{-16}$	$1.62 \cdot 10^{-13}$	0.00148
Gauss-Lobatto	$4.58 \cdot 10^{-15}$	$1.87 \cdot 10^{-12}$	0.01373
parabolic iFT	$3.17 \cdot 10^{-14}$	$1.29 \cdot 10^{-11}$	12.223

E.2. FastVG case

We compare the FastVG price calculated with $\Lambda = 4.5\sigma$, $\epsilon_1 = 10^{-7}$, $\epsilon_2 = 10^{-15}$, using different quadrature methods for the calculation of $\Psi_1(x'; \sigma, \omega; \Lambda)$. In addition to the adaptive Gauss-Lobatto rule used in several examples in Chapter 3, we include the other adaptive schemes mentioned in Section 3.2.2: the adaptive Simpson's rule, Clenshaw-Curtis integration, and vectorized Gauss-Kronrod quadrature. We also include parabolic iFT (with $\alpha = 2.9$) and IAC in the comparison. The results, for an OTM vanilla call option with $x' = -10^{-6}$, are shown in Table 2. It can be seen that absolute and relative differences w.r.t. the benchmark (calculated with the adaptive Gauss-Lobatto rule) are very close to floating point accuracy for all integration methods, apart from the adaptive Simpson's rule. The price calculated with parabolic iFT is also extremely close to this benchmark, with an absolute difference of about $1.53 \cdot 10^{-16}$, while the absolute error of the IAC price is much larger ($1.73 \cdot 10^{-10}$). The most efficient FastVG implementations are the ones using Clenshaw-Curtis and Gauss-Kronrod integration, which both take 6.94 ms, whereas parabolic iFT takes 0.28 seconds of CPU time to obtain the same accuracy.

TABLE 2. Differences w.r.t. the benchmark and CPU times for FastVG calculation of the price of an OTM call option with $x' = -10^{-6}$, $K = 1$, $\lambda_- = -11$, $\lambda_+ = 8$, $m_2 = 0.16$, $r = 0.03$, $q = 0$, $\tau = 0.004$.

Method	Abs. Diff.	Rel. Diff.	CPU Time (sec.)
Adapt. Simpson	$6.94 \cdot 10^{-11}$	$2.83 \cdot 10^{-08}$	0.00674
Clenshaw Curtis	$4.38 \cdot 10^{-16}$	$1.79 \cdot 10^{-13}$	0.00694
Gauss-Kronrod	$1.99 \cdot 10^{-16}$	$8.14 \cdot 10^{-14}$	0.00694
Gauss-Lobatto	$7.57 \cdot 10^{-16}$	$3.36 \cdot 10^{-12}$	0.00742
Parabolic iFT	$1.53 \cdot 10^{-16}$	$6.80 \cdot 10^{-13}$	0.28169
IAC	$1.73 \cdot 10^{-10}$	$7.69 \cdot 10^{-7}$	0.00140

APPENDIX F

Deltas and digitals

Since $\partial_S = K^{-1}e^{-x}\partial_x$, the vanilla option delta $\Delta(\tau, x) = K^{-1}e^{-x}\partial_x V(\tau, x)$ is given by

$$\Delta(\tau, x; \omega) = \frac{e^{-r\tau-x}}{2\pi} \int_{\text{Im}\xi=\omega} \frac{e^{ix\xi-\tau\psi(\xi)}}{i\xi-1} d\xi, \quad (157)$$

where $\Delta(\tau, x; \omega)$ is equal to the vanilla call delta $\Delta_c(\tau, x)$ if $\omega < -1$ and to the vanilla put delta $\Delta_p(\tau, x)$ if $\omega > -1$. From (157) we obtain

$$\Delta(\tau, x; \omega) = \frac{e^{-r\tau-(\omega+1)x}}{2\pi} \int_{-\infty}^{\infty} \frac{e^{ix'\eta-\tau\psi_{\omega}^0(\eta)}}{i\eta-\omega-1} d\eta.$$

Hence, in the ATMVG case, we can write

$$\Delta(\tau, -\mu\tau; \omega) = \frac{e^{-r'\tau-x}}{2\pi} \Phi(\sigma, \omega+1), \quad (158)$$

where $\Phi(\sigma, \omega+1)$ is given by (36). For the FastVG case, we have

$$\Delta(\tau, x; \omega) = \frac{e^{-r'\tau-\omega x'-x}}{\pi} \text{Re} \Psi(x'; \sigma, \omega+1), \quad (159)$$

where $\Psi(x'; \sigma, \omega+1)$ is given by (57).

For $\omega = -1$ and $\omega > -1$, (158)-(159) give the values of $\Delta_{-1}(\tau, x)$ (defined in the same way as $V_{-1}(\tau, x)$ in Section 3.2.3) and $\Delta_p(\tau, x)$, respectively. In each case, the vanilla call delta is given by

$$\Delta_c(\tau, x) = \begin{cases} \Delta_{-1}(\tau, x) + \frac{1}{2}e^{-q\tau}, & \omega = -1, \\ \Delta_p(\tau, x) + e^{-q\tau}, & \omega > -1, \end{cases}$$

respectively. The payoff at maturity of a digital call or put option is given by $G(x) = \mathbb{1}_{[\ln K, \infty)}(x)$ and $G(x) = \mathbb{1}_{(-\infty, \ln K]}(x)$, respectively. Denote the price of the digital call by $V_{dc}(\tau, x)$ and that of the digital put by $V_{dp}(\tau, x)$. If, for $\omega \neq 0$, we define

$$V_d(\tau, x; \omega) = \frac{e^{-r\tau}}{2\pi} \int_{\text{Im} \xi = \omega} \frac{e^{ix\xi - \tau\psi(\xi)}}{i\xi} d\xi, \quad (160)$$

then $V_d(\tau, x; \omega) = V_{dc}(\tau, x)$ if $\omega < 0$ and $V_d(\tau, x; \omega) = -V_{dp}(\tau, x)$ if $\omega > 0$. In the ATMVG case, for $\omega \neq 0$, we can write

$$V_d(\tau, -\mu\tau; \omega) = \frac{e^{-r'\tau}}{2\pi} \Phi(\sigma, \omega), \quad (161)$$

and in the FastVG case we have

$$V_d(\tau, x; \omega) = \frac{e^{-r'\tau - \omega x'}}{\pi} \Psi(x'; \sigma, \omega). \quad (162)$$

The digital call and put prices are related by digital put-call parity: $V_{dc}(\tau, x) + V_{dp}(\tau, x) = e^{-r\tau}$. Regarding the case $\omega = 0$, using the same argument as in Section 3.2.3 it can be seen that $V_{dc}(\tau, x) + V_d(\tau, x; 0) = \frac{1}{2}e^{-r\tau}$, where $V_d(\tau, x; 0)$ is defined in terms of Cauchy's principal value. From this it follows, in particular, that for a symmetric VG process (i.e., one with $\lambda_+ = -\lambda_-$), the ATM price of a digital call or put option is always equal to $\frac{1}{2}e^{-r\tau}$. For $x' \neq 0$ and $\omega \in [-1, 0]$, the same method as in Section 3.3.2 can be applied.

APPENDIX G

Discretization error bound for $\Psi_1(x; \sigma, 0; \Lambda)$.

Due to the presence of the indicator function in the expression (74) for $\psi(\eta)$, we need not concern ourselves with a truncation error in the numerical realization of (73). The following result can be used to choose an appropriate value of the discretization mesh ζ in order to ensure that the error lies within a specified tolerance.

Proposition G.1. *Denote by $\tilde{\Psi}_1(x; \sigma, 0; \Lambda; \zeta)$ the approximation to $\Psi_1(x; \sigma, 0; \Lambda)$ calculated according to (73), and define the discretization error with mesh ζ as*

$$\text{Disc.Err.}(\Psi_1; x; \sigma, 0; \Lambda; \zeta) = |\tilde{\Psi}_1(x; \sigma, 0; \Lambda; \zeta) - \Psi_1(x; \sigma, 0; \Lambda)|.$$

Then, if $c\tau < 1$, the discretization error satisfies the following bounds¹

$$\text{Disc.Err.}(\Psi_1; x; \sigma, 0; \Lambda; \zeta) \leq \mu(\chi, \zeta)(e^{\sigma x} + e^{-\sigma x}) \frac{\pi(2\sigma)^{-c\tau} \Lambda^{1-c\tau} {}_2F_1\left(\frac{1-c\tau}{2}, \frac{c\tau}{2}, \frac{3-c\tau}{2}, -\frac{\Lambda^2}{4\sigma^2}\right)}{1-c\tau} \quad (163)$$

$$\leq \mu(\chi, \zeta)(e^{\sigma x} + e^{-\sigma x}) \frac{\pi(2\sigma)^{-c\tau} \Lambda^{1-c\tau}}{1-c\tau}, \quad (164)$$

where $\mu(\chi, \zeta) = e^{-2\pi\chi/\zeta}/(1 - e^{-2\pi\chi/\zeta})$.

PROOF. The discretization error in the numerical calculation of the Hilbert transform of a function f is bounded above by (cf. Appendix O.1.1, [81])

$$\frac{e^{-2\pi\chi/\zeta}}{1 - e^{-2\pi\chi/\zeta}} \|\psi\|_{H^1(\mathcal{D}_\chi)},$$

¹For options of a few days' maturity and typical parameter ranges, the condition $c\tau < 1$ is almost always satisfied.

where ζ is the interpolation mesh of the discretization grid, $\mathcal{D}_\chi := \{z \in \mathbb{C} : |\operatorname{Im} z| < \chi\}$, and $H^1(\mathcal{D}_\chi)$ denotes the Hardy space of functions f analytic in the strip \mathcal{D}_χ such that $\int_{-\chi}^\chi f(x + iy)dy \rightarrow 0$ as $x \rightarrow \pm\infty$, and the Hardy norm is finite

$$\|f\|_{H^1(\mathcal{D}_\chi)} := \lim_{y \rightarrow \chi^-} \left[\int_{\mathbb{R}} |f(x + iy)|dx + \int_{\mathbb{R}} |f(x - iy)|dx \right] < \infty.$$

In our case $\chi = \sigma$, and

$$\begin{aligned} \int_{\mathbb{R}} |\psi(\eta + i\omega)|d\eta &= \int_{-\Lambda}^{\Lambda} |e^{ix(\eta+i\omega)}(\sigma^2 + (\eta + i\omega)^2)^{-c\tau}|d\eta \leq e^{-\omega x} \int_{-\Lambda}^{\Lambda} \frac{d\eta}{|\sigma^2 + (\eta + i\omega)^2|^{c\tau}} \\ &= 2e^{-\omega x} \int_0^{\Lambda} \frac{d\eta}{|\sigma^2 + \eta^2 - \omega^2 + 2i\omega\eta|^{c\tau}} \\ &= 2e^{-\omega x} \int_0^{\Lambda} \frac{d\eta}{[(\sigma^2 - \omega^2 + \eta^2)^2 + 4\omega^2\eta^2]^{c\tau/2}}. \end{aligned}$$

Define

$$H(\omega, \sigma, \Lambda, c\tau) = \int_0^{\Lambda} \frac{d\eta}{[(\sigma^2 - \omega^2 + \eta^2)^2 + 4\omega^2\eta^2]^{c\tau/2}}. \quad (165)$$

Then the norm $\|\psi\|_{H^1(\mathcal{D}_\sigma)}$ admits the bound

$$\|\psi\|_{H^1(\mathcal{D}_\sigma)} \leq 2e^{\sigma x} H(-\sigma, \sigma, \Lambda, c\tau) + 2e^{-\sigma x} H(\sigma, \sigma, \Lambda, c\tau).$$

We have

$$H(\sigma, \sigma, \Lambda, c\tau) = H(-\sigma, \sigma, \Lambda, c\tau) = (2\sigma)^{1-2c\tau} \int_0^{\Lambda/2\sigma} \frac{z^{-c\tau}}{(1+z^2)^{c\tau/2}}.$$

Using (146) and (148), we obtain, for $|y| < 1$, $p < 1$,

$$y \frac{d}{dy} {}_2F_1 \left(\frac{1-p}{2}, \frac{p}{2}; \frac{3-p}{2}; y \right) = \frac{1-p}{2} \left[(1-y)^{-p/2} - {}_2F_1 \left(\frac{1-p}{2}, \frac{p}{2}; \frac{3-p}{2}; y \right) \right]. \quad (166)$$

The bound (163) then follows by substituting $y = -z^2$ and multiplying both sides of (166) by z^{-p} , as in the proof of Proposition C.1. The bound (164) can easily be

proved by discarding the η^4 term in the square brackets in the denominator on the RHS of (165). \square

APPENDIX H

Pricing algorithm for discretely monitored barrier options

In what follows, we will use the notation $v_j^s = V_s(x_j)$; to be more precise, these equalities are almost exact if $s = N - 1$ and $j < M$ (we cannot evaluate the inverse Fourier transform in (79) exactly). Also, we set $v_M^s = 0$, $s = N - 1, N - 2, \dots, 0$, and, for $s < N - 1$ and $j = 1, 2, \dots, M - 1$, evaluate $v_j^s \approx V_s(x_j)$ at each step of backward induction. We assume that $\bar{\Delta}$ and ν are not very small so that the second, third and fourth derivatives of the option price w.r.t. x are not large. This condition will be used at the first step of each algorithm, where an appropriate grid will be chosen.

1. Fix the overall absolute error tolerance ϵ .
2. Allocate, e.g., tolerance $\epsilon_{\text{int}} = 0.80 \cdot \epsilon$ for the interpolation error, then set $\epsilon_{\text{tr}} = \epsilon_{\text{ds}} = 0.10 \cdot \epsilon$, where ϵ_{tr} and ϵ_{ds} denote the errors due to truncation in the state space and to approximations in the dual space, respectively.
3. Using the procedure outlined in Section 4.3.1.1, find the minimum value of x_M , so that the total error due to truncation in the state space lies below the tolerance ϵ_{tr} . Call this x_M^0 .
4. Using the procedure outlined in Section 4.3.2.1, find the maximum value Δ_0 of the mesh in the state space so that the total interpolation error lies below the tolerance ϵ_{int} .
5. Create a uniform grid $\mathbf{x} = (x_j)_{j=1}^M$, $x_j = h + (j - 1)\Delta$, such that $\Delta \leq \Delta_0$, and $x_M \geq x_M^0$ and, ideally, $\ln K - \mu\bar{\Delta}$ lies on one of its nodes. E.g., set $M_0 =$

$\text{ceil}(\ln K - \mu\bar{\Delta} - h)/\Delta_0$, then set $\Delta = (\ln K - \mu\bar{\Delta} - h)/M_0$, and $M = \text{ceil}(x_M^0 - h)/\Delta$. Finally, set $x_j = h + (j - 1)\Delta$, $j = 1, 2, \dots, M$.

6. Calculate the price grid \mathbf{v}_{N-1} at step $s = N - 1$, as follows
 - a. Run parabolic iFT on the grid $\mathbf{x} + \mu\bar{\Delta} - \ln K$, using the procedure in Appendix O.3.2 with $\widehat{G}(\xi) = -K/(\xi(\xi + i))$, with the settings calculated using the procedure in Section 4.3.3.1 with error tolerance ϵ_{ds} . This calculates the price of a vanilla put option $\mathbf{v}_{N-1}^{\text{put}}$ over the grid \mathbf{x} with time to maturity $\bar{\Delta}$.
 - b. Run parabolic iFT on the grid $\mathbf{x} + \mu\bar{\Delta} - h$, using the procedure in Appendix O.3.2 with $\widehat{G}(\xi) = -K/\xi + e^h/(1 - i\xi)$, and the settings calculated using the procedure in Section 4.3.3.1 with error tolerance ϵ_{ds} . This calculates the “barrier correction” $\mathbf{v}_{N-1}^{\text{barr}}$ to the vanilla put price $\mathbf{v}_{N-1}^{\text{put}}$.
 - c. Set $\mathbf{v}_{N-1} = \mathbf{v}_{N-1}^{\text{put}} + \mathbf{v}_{N-1}^{\text{barr}}$.
 - d. Set $v_M^{N-1} = 0$.
7. Calculate arrays $\mathbf{I}_0 := [I(\omega; n, 0)]_{n=0,1,\dots,M-1}$ and $\mathbf{I}_\ell := [I(\omega; n, \ell)]_{n=1-M,1,\dots,M-1}$, for $\ell = 1, 2$, over the grids $\mathbf{y} = (0 : M - 1)\Delta + \mu\bar{\Delta}$ and $\mathbf{z} = (1 - M : M - 1)\Delta + \mu\bar{\Delta}$, respectively. Again, the algorithm of Appendix O.3.2 can be used, with the settings calculated using the procedure in Section 4.3.3.1 with error tolerance ϵ_{ds} .
8. calculate $\mathcal{W}_{j,\ell}^s$, $j = 1, \dots, M$, $\ell = 0, 1, 2$, using (90) and (91), together with (95)-(97).
9. In a cycle w.r.t. $s = N - 2, \dots, 0$
 - a. Calculate the array

$$v_k^s = \mathcal{W}_{1,0}^{s+1} I(\omega, k - 1, 0) + \sum_{\ell=1}^2 \Delta^{-\ell} \sum_{j=1}^M \mathcal{W}_{j,\ell}^{s+1} I(\omega, k - j, \ell), \quad k = 1, 2, \dots, M - 1$$

(the interior sum can be calculated for all k using the fast convolution algorithm;
cf. Appendix L);

- b. Set $v_M^s = 0$.
10. Set $v_1^0 = 0$.
11. The array \mathbf{v}_0 stores the approximations to the option prices $V(0, x_j)$, $j = 1, \dots, M$.

APPENDIX I

Other interpolation methods

In this Appendix, we give a description of the procedures for piece-wise linear and cubic interpolation of the option price at each step of backward induction.

I.1. Piece-wise linear interpolation

On $[x_j, x_{j+1}]$, $j = 1, 2, \dots, M - 1$, we approximate $V_s(x)$ as

$$V_s(x) \approx v_j^s + \frac{x - x_j}{x_{j+1} - x_j} (v_{j+1}^s - v_j^s). \quad (167)$$

Hence, we use (88) with $m = 2$ and $f_{j,0}^s = v_j^s$, $f_{j,1}^s = v_{j+1}^s - v_j^s$. Since $v_M^s = 0$ and the grid is equally spaced, equality (89) simplifies to

$$\widehat{\mathcal{V}}_s(\xi) = \mathcal{W}_{1,0}^s e^{-ix_1\xi} \frac{1}{-i\xi} + \sum_{j=1}^M \Delta^{-1} \mathcal{W}_{j,1}^s e^{-ix_j\xi} \frac{1}{(-i\xi)^2}, \quad (168)$$

where

$$\begin{aligned} \mathcal{W}_{1,0}^s &= -v_1^s, & \mathcal{W}_{1,1}^s &= v_2^s - v_1^s, & \mathcal{W}_{M,1}^s &= v_{M-1}^s, \\ \mathcal{W}_{j,1}^s &= v_{j+1}^s + v_{j-1}^s - 2v_j^s, & j &= 2, 3, \dots, M-1. \end{aligned} \quad (169)$$

I.2. Piece-wise cubic interpolation

Since very good approximations on $[x_{M-1}, x_M]$ and $[x_{M-2}, x_{M-1}]$ are not needed, we use the same quadratic approximations (92) and (96) with $j = M - 2$. Thus, we have

$$f_{M-1,0}^s = v_{M-1}^s, \quad f_{M-1,1}^s = -2v_{M-1}^s, \quad f_{M-1,2}^s = v_{M-1}^s, \quad f_{M-1,3}^s = 0, \quad (170)$$

and

$$f_{M-2,0}^s = v_{M-2}^s, \quad f_{M-2,1}^s = (v_{M-1}^s - v_{M-3}^s)/2, \quad (171)$$

$$f_{M-2,2}^s = (v_{M-1}^s + v_{M-3}^s)/2 - v_{M-2}^s, \quad f_{M-2,3}^s = 0.$$

On $[x_j, x_{j+1}]$, $j = 1, 2, \dots, M-3$, we approximate $V_s(x)$ as a cubic polynomial $\mathcal{V}_{(j)}^s$ satisfying

$$\mathcal{V}_{(j)}^s(x_j) = v_j^s, \quad \mathcal{V}_{(j)}^s(x_{j+1}) = v_{j+1}^s, \quad \mathcal{V}_{(j)}^s(x_{j+2}) = v_{j+2}^s, \quad \mathcal{V}_{(j)}^s(x_{j+3}) = v_{j+3}^s. \quad (172)$$

Therefore, for $j = 1, 2, \dots, M-3$,

$$f_{j,1}^s = -\frac{11}{6}v_j^s + 3v_{j+1}^s - \frac{3}{2}v_{j+2}^s + \frac{1}{3}v_{j+3}^s, \quad (173)$$

$$f_{j,2}^s = v_j^s - \frac{5}{2}v_{j+1}^s + 2v_{j+2}^s - \frac{1}{2}v_{j+3}^s,$$

$$f_{j,3}^s = -\frac{1}{6}v_j^s + \frac{1}{2}v_{j+1}^s - \frac{1}{2}v_{j+2}^s + \frac{1}{6}v_{j+3}^s.$$

APPENDIX J

Additional numerical results for Chapter 4

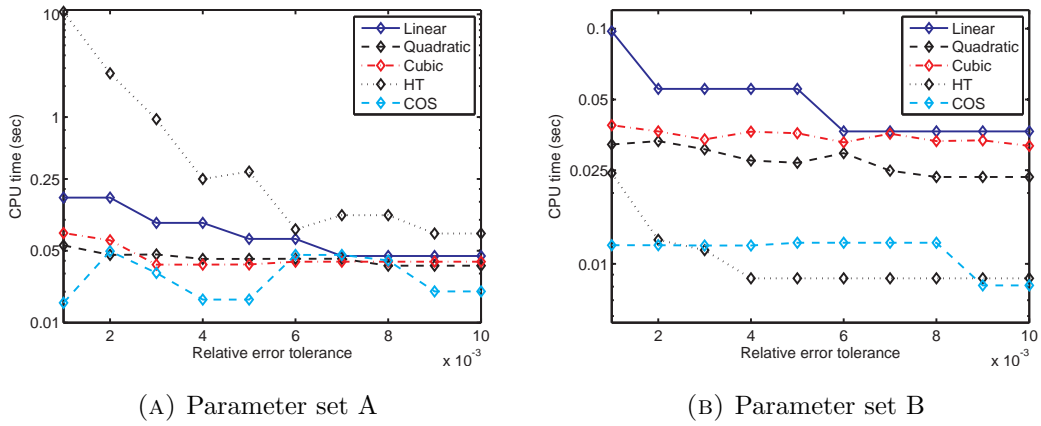


FIGURE 1. Logarithmic plots of CPU time versus relative error tolerance. Comparison of piece-wise linear (solid), quadratic (dashed) and cubic (dot-dashed) interpolation, as well as HT method (dotted) and COS method (dashed) to price a DO put option with $H = 80$, $K = 100$, $T = 0.5$, $\bar{\Delta} = 1/252$, over the interval $1.02 \cdot H \leq e^x \leq K$.

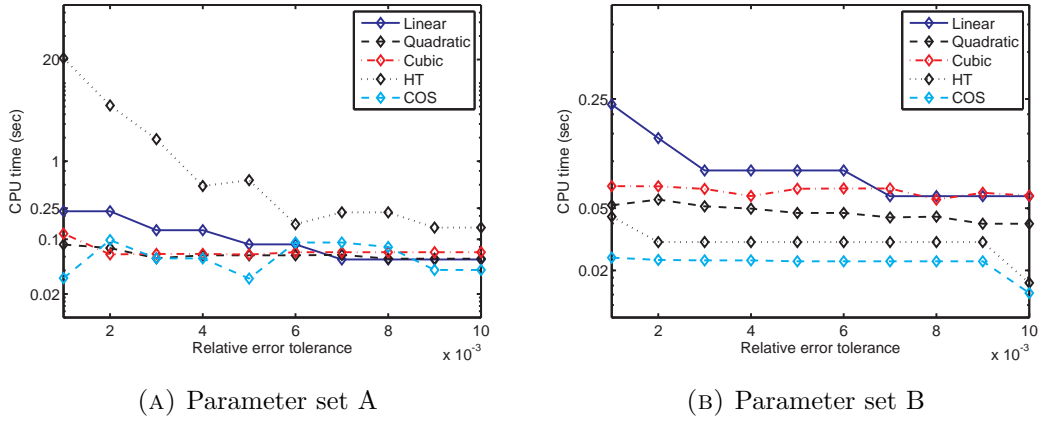


FIGURE 2. Logarithmic plots of CPU time versus relative error tolerance. Comparison of piece-wise linear (solid), quadratic (dashed) and cubic (dot-dashed) interpolation, as well as HT method (dotted) and COS method (dashed) to price a DO put option with $H = 80$, $K = 100$, $T = 1$, $\bar{\Delta} = 1/252$, over the interval $1.02 \cdot H \leq e^x \leq K$.

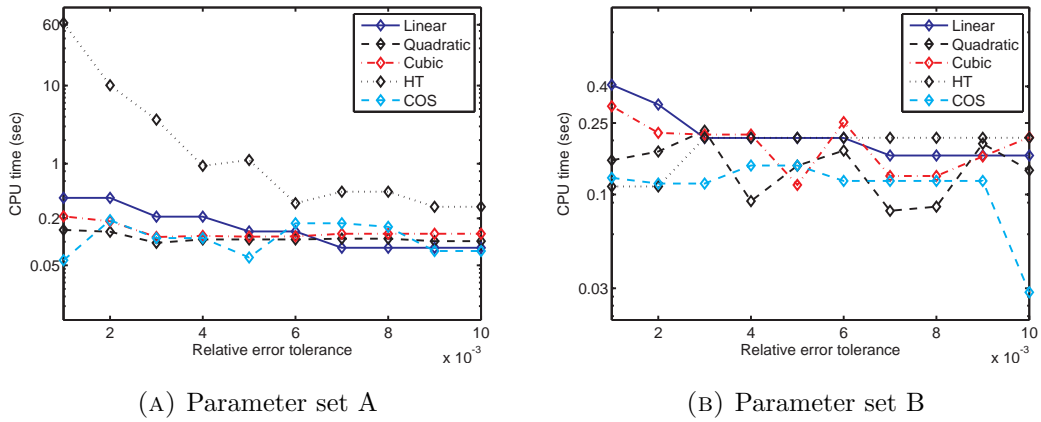


FIGURE 3. Logarithmic plots of CPU time versus relative error tolerance. Comparison of piece-wise linear (solid), quadratic (dashed) and cubic (dot-dashed) interpolation, as well as HT method (dotted) and COS method (dashed) to price a DO put option with $H = 80$, $K = 100$, $T = 2$, $\bar{\Delta} = 1/252$, over the interval $1.02 \cdot H \leq e^x \leq K$.

APPENDIX K

Other types of barrier options

K.1. Down-and-out call option

The algorithm is almost the same as in the case of the down-and-out put option. The most important difference is that the payoff $G(x) = (e^x - K)_+ \mathbb{1}_{(h, \infty)}(x)$, and hence the option price, increases exponentially as $x \rightarrow \infty$; hence, a straightforward truncation will lead to a sizable error. Therefore, in the very beginning, it is necessary to change the measure (cf. Section 5.1.1, Appendix A.3.2) and reduce calculations to the case of the option with payoff function $G_\gamma(x) = e^{-\gamma x} (e^x - K)_+ \mathbb{1}_{(h, \infty)}(x)$, where $\gamma \in (1, -\lambda_-)$.

K.2. Up-and-out put and call options

The results and algorithms for these options can be obtained by symmetry $x \mapsto -x$.

K.3. Down-and-in and up-and-in options

The prices of these options can be obtained by in-out parity (in+out = vanilla).

K.4. Options with rebate and first-touch digitals

Consider the down-and-out put with rebate. For simplicity, we consider the case of constant rebate R . The only difference with the case $R = 0$ is that, at each time step, the restriction of the option price to $[h, \infty)$ is the sum of the term, which we

already calculated, and the term

$$Re^{-r\bar{\Delta}} \int_{-\infty}^{h-x} p_{\bar{\Delta}}(y) dy,$$

which can be calculated using the iFT method for x at the points of the chosen grid.

K.5. Double barrier options

The calculations are almost the same as in the case of the down-and-out option without a rebate. The differences are:

1. a grid should ideally be chosen so that x_1 and x_M are the boundary points. However, unless the strike is chosen so that $(\ln K - \mu\bar{\Delta} - x_1)/(x_M - x_1)$ is rational, it is impossible to have a uniform grid with $x_1, \ln K - \mu\bar{\Delta}, x_M$ at the grid, and a non-uniform grid should be preferred;
2. an approximation on $[x_{M-1}, x_M]$ should be chosen in the same way as the approximation on $[x_1, x_M]$. In particular, at each step of the backward induction procedure, we calculate $V_s(x_M - 0)$ instead of $V(x_M)(= 0)$, and use $V_s(x_M - 0)$ as an input at the next step.

APPENDIX L

Fast convolution algorithm

In this appendix we describe the main details of the fast convolution algorithm, introduced to finance in [14]. We follow the exposition in *op. cit.*, which we reformulate in accordance with our system of notation. Recall that the convolution of two functions f and g , defined on \mathbb{R} , is given by

$$(f * g)(x) = \int_{-\infty}^{+\infty} f(x - y)g(y)dy,$$

assuming that the integral on the RHS converges. As in the case of the numerical realization of the (inverse) Fourier transform, one can truncate and discretize the integral on the RHS using the simplified trapezoid rule on an evenly spaced grid $\mathbf{x} = (x_j)_{j=1}^M$, $x_j = x_1 + (j - 1)\Delta$, with fixed mesh $\Delta > 0$. One obtains

$$(f * g)(x) \approx \Delta \sum_{j=1}^M f(x_j)g(x - x_j). \quad (174)$$

In order to calculate the RHS of (174) at all points of the grid \mathbf{x} , one needs to know the values of f at all points of \mathbf{x} , together with all the values of g at the points $k\Delta$, for $1 - M \leq k \leq M - 1$. Then, the following algorithm can be used¹

1. Take two arrays $\mathbf{f} = (f_j)_{j=1}^M$ and $\mathbf{g} = (g_k)_{k=1-M}^{M-1}$. We want to calculate the array $\mathbf{h} = (h_\ell)_{\ell=1}^M$, given by

$$h_\ell = \sum_{j=1}^M f_j g_{\ell-j}.$$

¹In this appendix, we use a notation reminiscent of MATLAB syntax.

2. Use the following steps

$$\mathbf{g} = [\mathbf{g} \ (M : 2 * M - 1) \ 0 \ \mathbf{g}(1 : M - 1)];$$

$$\mathbf{f} = [\mathbf{f} \ \text{zeros}(1, M)];$$

$$\mathbf{h} = \text{ifft}(\text{fft}(\mathbf{f}) .* \text{fft}(\mathbf{g}));$$

$$\mathbf{h} = \mathbf{h}(1 : M);$$

As noted in [14], the above algorithm requires applying the FFT and iFFT to arrays of length $2M$ rather than M . However, it is still much faster than evaluating (174) in a cycle (e.g., a `for` loop in MATLAB).

APPENDIX M

Technical calculations

M.1. Proof of Lemma 4.1

First, we calculate

$$J_{j,\ell} := \int_{x_j}^{x_{j+1}} e^{-ix\xi} \left(\frac{x - x_j}{x_{j+1} - x_j} \right)^\ell dx = e^{-ix_j\xi} (x_{j+1} - x_j) \cdot I_\ell(-i(x_{j+1} - x_j)\xi),$$

where $I_m(\alpha) = \int_0^1 e^{\alpha t} t^m dt$. Integrating by parts, we obtain

$$\begin{aligned} I_0(\alpha) &= \frac{e^\alpha - 1}{\alpha}, \\ I_1(\alpha) &= \frac{1}{\alpha} \int_0^1 t de^{t\alpha} = \frac{e^\alpha}{\alpha} - \frac{1}{\alpha} I_0(\alpha) = e^\alpha \frac{\alpha - 1}{\alpha^2} + \frac{1}{\alpha^2}, \\ I_2(\alpha) &= \frac{1}{\alpha} \int_0^1 t^2 de^{t\alpha} = \frac{e^\alpha}{\alpha} - \frac{2}{\alpha} I_1(\alpha) = e^\alpha \frac{\alpha^2 - 2\alpha + 2}{\alpha^3} - \frac{2}{\alpha^3}, \\ I_3(\alpha) &= \frac{1}{\alpha} \int_0^1 t^3 de^{t\alpha} = \frac{e^\alpha}{\alpha} - \frac{3}{\alpha} I_2(\alpha) = e^\alpha \frac{\alpha^3 - 3\alpha^2 + 6\alpha - 6}{\alpha^4} + \frac{6}{\alpha^4}. \end{aligned}$$

Therefore,

$$\begin{aligned}
J_{j,0} &= e^{-ix_j\xi}(x_{j+1} - x_j) \frac{e^{-i(x_{j+1}-x_j)\xi} - 1}{-i(x_{j+1} - x_j)\xi} = (-i\xi)^{-1} [e^{-ix_{j+1}\xi} - e^{-ix_j\xi}], \\
J_{j,1} &= e^{-ix_j\xi}(x_{j+1} - x_j) \left[e^{-i(x_{j+1}-x_j)\xi} \frac{-i(x_{j+1} - x_j)\xi - 1}{(-i(x_{j+1} - x_j)\xi)^2} + \frac{1}{(-i(x_{j+1} - x_j)\xi)^2} \right] \\
&= e^{-ix_{j+1}\xi} \frac{i(x_{j+1} - x_j)\xi + 1}{(x_{j+1} - x_j)\xi^2} - e^{-ix_j\xi} \frac{1}{(x_{j+1} - x_j)\xi^2}, \\
J_{j,2} &= e^{-ix_j\xi}(x_{j+1} - x_j) \left[e^{-i(x_{j+1}-x_j)\xi} \frac{-(x_{j+1} - x_j)^2\xi^2 + 2i(x_{j+1} - x_j)\xi + 2}{(-i(x_{j+1} - x_j)\xi)^3} \right. \\
&\quad \left. - \frac{2}{(-i(x_{j+1} - x_j)\xi)^3} \right] \\
&= e^{-ix_{j+1}\xi} \frac{-(x_{j+1} - x_j)^2\xi^2 + 2i(x_{j+1} - x_j)\xi + 2}{i(x_{j+1} - x_j)^2\xi^3} - e^{-ix_j\xi} \frac{2}{i(x_{j+1} - x_j)^2\xi^3}, \\
J_{j,3} &= e^{-ix_j\xi}(x_{j+1} - x_j) \left[\frac{6}{(-i(x_{j+1} - x_j)\xi)^4} \right. \\
&\quad \left. + e^{-i(x_{j+1}-x_j)\xi} \frac{(-i(x_{j+1} - x_j)\xi)^3 + 3(x_{j+1} - x_j)^2\xi^2 - 6i(x_{j+1} - x_j)\xi - 6}{(-i(x_{j+1} - x_j)\xi)^4} \right] \\
&= e^{-ix_{j+1}\xi} \frac{i(x_{j+1} - x_j)^3\xi^3 + 3(x_{j+1} - x_j)^2\xi^2 - 6i(x_{j+1} - x_j)\xi - 6}{(x_{j+1} - x_j)^3\xi^4} \\
&\quad + e^{-ix_j\xi} \frac{6}{(x_{j+1} - x_j)^3\xi^4}.
\end{aligned}$$

If the grid $x_j = h + (j - 1)\Delta$, $j = 1, 2, \dots, M$, is equally spaced, the expressions above simplify

$$\begin{aligned}
J_{j,1} &= e^{-ix_{j+1}\xi} \frac{i\Delta \cdot \xi + 1}{\Delta \cdot \xi^2} - e^{-ix_j\xi} \frac{1}{\Delta \cdot \xi^2}, \\
J_{j,2} &= e^{-ix_{j+1}\xi} \frac{-\Delta^2\xi^2 + 2i\Delta \cdot \xi + 2}{i\Delta^2\xi^3} - e^{-ix_j\xi} \frac{2}{i\Delta^2\xi^3}, \\
J_{j,3} &= e^{-ix_{j+1}\xi} \frac{i\Delta^3\xi^3 + 3\Delta^2\xi^2 - 6i\Delta \cdot \xi - 6}{\Delta^3\xi^4} + e^{-ix_j\xi} \frac{6}{\Delta^3\xi^4},
\end{aligned}$$

and we obtain

$$\begin{aligned}
\widehat{\mathcal{V}}_s(\xi) &= -e^{-ix_1\xi} \left\{ f_{1,0}^s \frac{1}{-i\xi} + f_{1,1}^s \frac{1}{\Delta \cdot \xi^2} + f_{1,2}^s \frac{2}{i\Delta^2\xi^3} - f_{1,3}^s \frac{6}{\Delta^3\xi^4} \right\} \\
&+ e^{-ix_M\xi} \left\{ f_{M-1,0}^s \frac{1}{-i\xi} + f_{M-1,1}^s \frac{i\Delta \cdot \xi + 1}{\Delta \cdot \xi^2} \right. \\
&\quad + f_{M-1,2}^s \frac{-\Delta^2\xi^2 + 2i\Delta \cdot \xi + 2}{i\Delta^2\xi^3} \\
&\quad \left. + f_{M-1,3}^s \frac{i\Delta^3\xi^3 + 3\Delta^2\xi^2 - 6i\Delta \cdot \xi - 6}{\Delta^3\xi^4} \right\} \\
&+ \sum_{j=2}^{M-1} e^{-ix_j\xi} \left\{ f_{j-1,0}^s \frac{1}{-i\xi} + f_{j-1,1}^s \frac{i\Delta \cdot \xi + 1}{\Delta \cdot \xi^2} \right. \\
&\quad + f_{j-1,2}^s \frac{-\Delta^2\xi^2 + 2i\Delta \cdot \xi + 2}{i\Delta^2\xi^3} \\
&\quad + f_{j-1,3}^s \frac{i\Delta^3\xi^3 + 3\Delta^2\xi^2 - 6i\Delta \cdot \xi - 6}{\Delta^3\xi^4} \\
&\quad \left. - f_{j,0}^s \frac{1}{-i\xi} - f_{j,1}^s \frac{1}{\Delta \cdot \xi^2} - f_{j,2}^s \frac{2}{i\Delta^2\xi^3} + f_{j,3}^s \frac{6}{\Delta^3\xi^4} \right\}.
\end{aligned} \tag{175}$$

The RHS of (175) can be simplified if we take into account that a reasonable approximation is continuous on $[h, x_M]$, and, if the approximation is chosen so that $\mathcal{V}_s(x_M) = 0$, then \mathcal{V}_s is continuous on $[h, \infty)$. Then the term of the slowest rate ξ^{-1} of decay at infinity comes from the only point of discontinuity at $x_1 = h$ (this can be verified directly by using the continuity condition $f_{j+1,0}^s = f_{j,0}^s + f_{j,1}^s + f_{j,2}^s + f_{j,3}^s$). The

result is

$$\begin{aligned}
\widehat{\mathcal{V}}_s(\xi) &= -e^{-ix_1\xi} \left\{ f_{1,0}^s \frac{1}{-i\xi} + f_{1,1}^s \frac{1}{\Delta \cdot \xi^2} + f_{1,2}^s \frac{2}{i\Delta^2\xi^3} - f_{1,3}^s \frac{6}{\Delta^3\xi^4} \right\} \\
&+ e^{-ix_M\xi} \left\{ f_{M-1,1}^s \frac{1}{\Delta \cdot \xi^2} + f_{M-1,2}^s \frac{2i\Delta \cdot \xi + 2}{i\Delta^2\xi^3} \right. \\
&\quad \left. + f_{M-1,3}^s \frac{3\Delta^2\xi^2 - 6i\Delta \cdot \xi - 6}{\Delta^3\xi^4} \right\} \\
&+ \sum_{j=2}^{M-1} e^{-ix_j\xi} \left\{ f_{j-1,1}^s \frac{1}{\Delta \cdot \xi^2} + f_{j-1,2}^s \frac{2i\Delta \cdot \xi + 2}{i\Delta^2\xi^3} \right. \\
&\quad \left. + f_{j-1,3}^s \frac{3\Delta^2\xi^2 - 6i\Delta \cdot \xi - 6}{\Delta^3\xi^4} \right. \\
&\quad \left. - f_{j,1}^s \frac{1}{\Delta \cdot \xi^2} - f_{j,2}^s \frac{2}{i\Delta^2\xi^3} + f_{j,3}^s \frac{6}{\Delta^3\xi^4} \right\}.
\end{aligned} \tag{176}$$

Collecting like terms, we derive (89), (90), (90).

M.2. Proof of Lemma 4.3

Use will be made of the following result.

Proposition M.1. *The truncation of the state space at $x = x_M$ in the backward induction procedure for the price of a DO option with terminal payoff $G(x)$ and barrier e^h is equivalent to killing the process X when it enters $[x_M, \infty)$, and the resulting loss in option value is less than the price of an up-and-in option with barrier e^{x_M} which, upon activation, becomes a European option with the payoff $\mathbb{1}_{(h,\infty)}(X_T)G(X_T)$.*

PROOF. Follows from the fact that the price calculated with truncation of the state space at $x = x_M$ at steps $N - 1, N - 2, \dots, 1$ is given by

$$V_0^{\text{tr}}(x) = e^{-r(T-t)} \mathbb{1}_{(h,\infty)}(x) \mathbb{E}^x \left[\mathbb{1}_{(h,x_M)}(X_{\bar{\Delta}}) \mathbb{1}_{(h,x_M)}(X_{2\bar{\Delta}}) \dots \mathbb{1}_{(h,x_M)}(X_{T-\bar{\Delta}}) \mathbb{1}_{(h,\infty)}(X_T) G(X_T) \right].$$

□

Denote by τ the first entrance time of process X into $[x_M, \infty)$. For any $\omega_+ \in (0, \lambda_+)$, the τ -price of the embedded European option admits an upper bound via

$$\begin{aligned}
& e^{-r(T-\tau)} \mathbb{E}_\tau \left[(K - e^{X_T})_+ \mathbb{1}_{[h, \infty)}(X_T) \right] \\
& \leq (K - e^h) e^{-r(T-\tau)} \mathbb{E}_\tau \left[e^{-\omega_+ X_{T-\tau}} \cdot e^{\omega_+ X_{T-\tau}} \cdot \mathbb{1}_{[h, \ln K]}(X_T) \right] \\
& \leq (K - e^h) e^{-r(T-\tau)} e^{-\omega_+(x_M - \ln K)} \mathbb{E}_\tau \left[e^{-\omega_+ X_{T-\tau}} \right] \\
& = (K - e^h) e^{-r(T-\tau)} e^{-\omega_+(x_M - \ln K) - (T-\tau)\psi(i\omega_+)}.
\end{aligned}$$

It follows that, at time 0 and $X_0 = x \in (h, x_M)$, the truncation error admits an upper bound via $\sup_{0 \leq \tau \leq T}$ of the following expression

$$\begin{aligned}
& \mathbb{E}^x \left[e^{-r\tau} (K - e^h) e^{-r(T-\tau)} e^{-\omega_+(x_M - \ln K) - (T-\tau)\psi(i\omega_+)} \mathbb{1}_{[x_M, \infty)}(X_\tau) \right] \\
& = e^{-rT} (K - e^h) e^{-r(T-\tau) - \omega_+(x_M - \ln K) - (T-\tau)\psi(i\omega_+)} \\
& \quad \times \mathbb{E}^x \left[e^{-\omega_-(X_\tau - x)} \cdot e^{\omega_-(X_\tau - x)} \mathbb{1}_{[x_M, \infty)}(X_\tau) \right] \\
& \leq e^{-rT} (K - e^h) e^{-\omega_+(x_M - \ln K) - (T-\tau)\psi(i\omega_+)} e^{\omega_-(x_M - x)} e^{-\tau\psi(i\omega_-)}.
\end{aligned}$$

M.3. Proof of Lemma 4.4

For simplicity, and without loss of generality, in the rest of this appendix we will use the barrier $H = e^h$ as the numéraire, setting $h = 0$. We will also set $g_0(x) := V_N(x)$ and, for $n = 1, 2, \dots, N-1$, define

$$g_{n+1}(x) = \mathbb{E}^x [g_n(X_{\bar{\Delta}}) \mathbb{1}_{(0, \infty)}(X_{\bar{\Delta}})]. \quad (177)$$

With this notation and convention, the time-0 option price is given by $e^{-rT} g_N(x)$. The following result will be used.

Lemma M.2. *Let X be a Lévy process such that its transition density $p_{\bar{\Delta}} \in C^m(\mathbb{R})$, for some $m \in \mathbb{Z}_+$, and its first m derivatives are in $L_1(\mathbb{R})$. If we define the operator $P_{\bar{\Delta}}^{(j)} : L_{\infty}(\mathbb{R}) \rightarrow L_{\infty}(\mathbb{R})$ by*

$$(P_{\bar{\Delta}}^{(j)} f)(x) = \frac{d^j}{dx^j} \mathbb{E}^x[f(X_{\bar{\Delta}})],$$

for $j = 0, 1, \dots, m$ (the case $j = 0$ corresponding to no differentiation), then the norm of the operator $P_{\bar{\Delta}}^{(j)}$ is bounded above by $\|p_{\bar{\Delta}}^{(j)}\|_{L_1}$ (and, in particular, by 1, for $j = 0$).

PROOF. If $f \in L_{\infty}(\mathbb{R})$, then

$$\left| \frac{d^j}{dx^j} \mathbb{E}^x[f(X_{\bar{\Delta}})] \right| = \left| \int_{\mathbb{R}} p_{\bar{\Delta}}^{(j)}(y-x) (-1)^j f(y) dy \right| \quad (178)$$

$$\leq \int_{\mathbb{R}} |p_{\bar{\Delta}}^{(j)}(y-x)| \cdot |f(y)| dy \leq \|f\|_{L_{\infty}} \cdot \int_{\mathbb{R}} |p_{\bar{\Delta}}^{(j)}(y-x)| dy = \|p_{\bar{\Delta}}^{(j)}\|_{L_1} \cdot \|f\|_{L_{\infty}}. \quad (179)$$

□

Remark M.3. The lemma applies to model processes, of order $\nu > 0$, and in general to all RLPEs (cf. Theorem A.10).

Remark M.4. From Lemma M.2, it follows that, if X satisfies the conditions in the lemma, for some $m \in \mathbb{Z}_+$, then the functions g_n , defined by (177), are such that $g_n^{(j)} \in C(\mathbb{R}) \cap L_{\infty}(\mathbb{R})$, for $j = 0, 1, \dots, m$, and $n = 1, 2, \dots, N$. Hence, there exist constants d_j , $j = 0, 1, \dots, m$, such that $\|g_0^{(j)}\|_{L_{\infty}} \leq d_j$. It also follows from Lemma M.2 (with $j = 0$) that the total interpolation error in the time-0 option price is bounded by the sum of the error at each single step of backward induction (the same applies to other sources of errors).

We can now prove the following result.

Lemma M.5. *For the functions g_n , $n = 1, 2, \dots, N$, and a Lévy process satisfying the conditions of Lemma M.2, for some $j \geq 0$, we have*

$$\|g_n^{(j)}\|_{L_\infty} \leq \|p_\Delta^{(j)}\|_{L_1} \cdot d_0,$$

for $j = 0, 1, \dots, m$, where d_0 is as defined in Remark M.4.

PROOF. Using (177) and Lemma M.2, we obtain, for $n = 0, 1, \dots, N$

$$\begin{aligned} |g_n^{(j)}(x)| &= \left| \frac{d^j}{dx^j} \mathbb{E}^x [g_{n-1}(X_\Delta) \mathbb{1}_{(0, \infty)}(X_\Delta)] \right| \\ &\leq \|p_\Delta^{(j)}\|_{L_1} \cdot \|g_{n-1}\|_{L_\infty} \leq \|p_\Delta^{(j)}\|_{L_1} \cdot d_0. \end{aligned}$$

□

Lemma 4.4 follows from Lemma M.5, together with the previous considerations.

Remark M.6. From Remark M.4 and Lemma M.2, it follows that we can set $d_j = \|p_\Delta^{(j)}\|_{L_1} \cdot \|V_N\|_{L_\infty}$, $j = 0, 1, \dots, m$. Note that for the DO put case, with $h = 0$, we have $\|V_N\|_{L_\infty} = K - 1$.

M.4. Proof of Proposition 4.6

Since the transition operator is translation-invariant, we may assume that $\mu = 0$ and $\psi = \psi^0$. If X is a model process of order $\nu > 0$, we can write

$$p_\Delta^{(n)}(x) = \frac{1}{2\pi} \int_{\text{Im } \xi = \omega} e^{-ix\xi - \bar{\Delta}\psi^0(\xi)} (-i\xi)^n d\xi, \quad (180)$$

for any $\omega \in (\lambda_-, \lambda_+)$. If $x < 0$, we take $\omega = \omega_+ \in (0, \lambda_+)$; if $x \geq 0$, we take $\omega = \omega_- \in (\lambda_-, 0)$. Define the contours $\mathcal{L}_{\omega_+, \phi}^+ = i\omega_+ + (e^{i\phi}\mathbb{R}_+ \cup e^{i(\pi-\phi)}\mathbb{R}_+)$ and $\mathcal{L}_{\omega_-, \phi}^- = i\omega_- + (e^{-i\phi}\mathbb{R}_+ \cup e^{i(-\pi+\phi)}\mathbb{R}_+)$, for $\phi \in (0, \min\{\pi/2, \pi/(2\nu)\})$. Since $\|p_\Delta^{(n)}\|_{L_1} =$

$\|p_{\bar{\Delta}}^{(n)} \mathbb{1}_{(-\infty, 0)}\|_{L_1} + \|p_{\bar{\Delta}}^{(n)} \mathbb{1}_{(0, \infty)}\|_{L_1}$, we can consider each term separately, obtaining similar estimates. For $x < 0$ ($x > 0$) we can deform the contour of integration in (180) into $\mathcal{L}_{\omega_+, \phi}^+$ ($\mathcal{L}_{\omega_-, \phi}^-$). Consider the case $x < 0$. We have

$$p_{\bar{\Delta}}^{(n)}(x) = \frac{1}{2\pi} \int_{\mathcal{L}_{\omega_+, \phi}^+} e^{-ix\xi - \bar{\Delta}\psi^0(\xi)} (-i\xi)^n d\xi.$$

Changing variable $\xi = i\omega_+ + e^{i\phi}\rho$, $\rho > 0$, and reducing the integral to \mathbb{R}_+ , we obtain

$$\begin{aligned} |p_{\bar{\Delta}}^{(n)}(x)| &\leq \frac{1}{\pi} \int_0^\infty |e^{(\omega_+ - ie^{i\phi}\rho)x - \bar{\Delta}\psi^0(i\omega_+ + e^{i\phi}\rho)}| \cdot |i\omega_+ + e^{i\phi}\rho|^n d\rho \\ &= \frac{1}{\pi} \int_0^\infty e^{(\omega_+ + \cos(\phi - \pi/2)\rho)x - \bar{\Delta} \operatorname{Re} \psi^0(i\omega_+ + e^{i\phi}\rho)} ((\omega_+ + \cos \phi \cdot \rho)^2 + (\sin \phi \cdot \rho)^2)^{n/2} d\rho. \end{aligned} \tag{181}$$

Since $\omega_+ > 0$ and $\cos(\phi - \pi/2) > 0$, we can integrate this over $x < 0$, applying Fubini's theorem, and obtain

$$\|p_{\bar{\Delta}}^{(n)} \mathbb{1}_{(-\infty, 0)}\|_{L_1} \leq \frac{1}{\pi} \int_0^\infty \frac{e^{-\bar{\Delta} \operatorname{Re} \psi^0(i\omega_+ + e^{i\phi}\rho)}}{\omega_+ + \cos(\phi - \pi/2)\rho} ((\omega_+ + \cos \phi \cdot \rho)^2 + (\sin \phi \cdot \rho)^2)^{n/2} d\rho. \tag{182}$$

From (5), it follows that there exists $C > 0$ such that, for $\rho > C$, $\operatorname{Re} \psi^0(i\omega_+ + e^{i\phi}\rho)$ is monotone. For $n \leq 4$, and ω_+ not too small (hence, λ_+ not too small), C is not large, for processes under consideration, hence we can replace the integral in (182) with one

over (C, ∞) and obtain an approximate bound. Put $y = \bar{\Delta} \operatorname{Re} \psi^0(i\omega_+ + e^{i\phi} \rho)$. Then

$$\rho = \left(\frac{y}{\bar{\Delta} d_+^0 \cos(\phi\nu)} \right)^{1/\nu} (1 + O(y^{-1/\nu})) \quad (183)$$

$$\frac{d\rho}{dy} \sim \nu^{-1} (\bar{\Delta} d_+^0 \cos(\phi\nu))^{-1/\nu} y^{1/\nu-1} \quad (184)$$

$$\begin{aligned} \frac{((\omega_+ + \cos \phi \cdot \rho)^2 + (\sin \phi \cdot \rho)^2)^{n/2}}{\omega_+ + \cos(\phi - \pi/2)\rho} &\sim \frac{\rho^{n-1}}{\cos(\phi - \pi/2)} \\ &\sim (\cos(\phi - \pi/2))^{-1} (\bar{\Delta} d_+^0 \cos(\phi\nu))^{(1-n)/\nu} y^{(n-1)/\nu}. \end{aligned} \quad (185)$$

Substituting into (182), we obtain the approximate bound

$$\|p_{\bar{\Delta}}^{(n)} \mathbb{1}_{(-\infty, 0)}\|_{L_1} \leq \frac{(\bar{\Delta} d_+^0)^{-n/\nu}}{\pi\nu D(n, \phi)} \int_{C\nu \bar{\Delta} d_+^0 \cos(\phi\nu)}^{\infty} e^{-y} y^{n/\nu-1} dy, \quad (186)$$

where $D(n, \phi) = (\cos(\phi\nu))^{n/\nu} \cos(\phi - \pi/2)$. From this, (112) follows.

M.5. Proof of Lemma 4.7

Write $v_N(x) = G(x)$, and

$$v_s(x) = \mathbb{E}^x[\mathbb{1}_{(h, \infty)}(X_{\bar{\Delta}}) v_{s+1}(X_{\bar{\Delta}})], \quad s = 0, 1, \dots, N-1.$$

Assume, for simplicity, that $r = 0$. Denote by $\tilde{I}_\ell(x)$ the approximation to $I_\ell(x)$ due to truncation and/or discretization in the dual space, i.e. $\tilde{I}_\ell(x) = I_\ell(x) + \mathcal{E}_{I_\ell}(x)$, where $\mathcal{E}_{I_\ell}(x)$ is the error in the computation of $I_\ell(x)$. Recall that the total error in the price at $t = 0$ due to approximations at time steps $s = 0, 1, \dots, N-1$ is bounded above by the sum of the (absolute) errors at each time step. In other words, the total error at $t = 0$ can be estimated by summing the bounds for the absolute errors at steps $s = 0, 1, \dots, N-1$, each time assuming that the price v_{s+1} is exact. With this

understanding, at each step $s = 0, 1, \dots, N - 2$, we have

$$\begin{aligned} v_s(x_k) &= \mathcal{W}_{1,0}^{s+1} \cdot \tilde{I}_0(x_k - h) + \Delta^{-1} \sum_{j=1}^M \mathcal{W}_{j,1}^{s+1} \cdot \tilde{I}_1(x_k - x_j) \\ &\quad + \Delta^{-2} \sum_{j=1}^M \mathcal{W}_{j,2}^{s+1} \cdot \tilde{I}_2(x_k - x_j), \end{aligned} \quad (187)$$

where $\mathcal{W}_{1,0}^{s+1} = -v_{s+1}(h)$. Hence, if we assume that v_{s+1} is error-free, it follows that the error in $v_s(x_k)$ is given by

$$\begin{aligned} \mathcal{E}_{v_s}(x_k) &= -\mathcal{E}_{I_0}(x_k - h) \cdot v_{s+1}(h) + \Delta^{-1} \sum_{j=1}^M \mathcal{W}_1^{s+1}(x_j) \cdot \mathcal{E}_{I_1}(x_k - x_j) \\ &\quad + \Delta^{-2} \sum_{j=1}^M \mathcal{W}_2^{s+1}(x_j) \cdot \mathcal{E}_{I_2}(x_k - x_j). \end{aligned} \quad (188)$$

If u is smooth on (x_1, x_M) and continuous on $[x_1, x_M]$, and we write $u_j = u(x_j)$, then the mean value theorem gives $(u_{j+1} - u_j)/\Delta = u'(x_j + \theta\Delta)$, for $j = 1, 2, \dots, M - 1$ and some $\theta \in (0, 1)$. Substituting this into the expression for the second order finite difference, one obtains

$$\frac{u_{j+1} - 2u_j + u_{j-1}}{\Delta^2} = \xi u''(x_j + \phi\Delta), \quad (189)$$

for some $\xi \in (0, 2)$, $\phi \in (-1, 1)$. Therefore

$$\left\| \frac{u_{j+1} - 2u_j + u_{j-1}}{\Delta^2} \right\|_{\ell_\infty} \leq 2 \|u''\|_{L_\infty}. \quad (190)$$

In a similar way, for the third order finite difference, one can write

$$\begin{aligned} \frac{u_{j+1} - 3u_j + 3u_{j-1} - u_{j-2}}{\Delta^3} &= \Delta^{-1}(\xi_1 - \xi_2)u''(x_j + \phi_1\Delta) \\ &\quad + \Delta^{-1}\xi_2 [u''(x_j + \phi_1\Delta) - u''(x_j - \Delta + \phi_2\Delta)], \end{aligned} \quad (191)$$

for some $\xi_j \in (0, 2)$, $\phi_j \in (-1, 1)$. It follows that

$$\left\| \frac{u_{j+1} - 3u_j + 3u_{j-1} - u_{j-2}}{\Delta^3} \right\|_{\ell_\infty} \leq \frac{2}{\Delta} \|u''\|_{L_\infty} + 6 \|u'''\|_{L_\infty}. \quad (192)$$

Using (103), together with (191) and (192), we obtain

$$\begin{aligned} \|\mathcal{W}_{j,1}^{s+1}\|_{L_\infty} &\leq \Delta^2 \|V_{s+1}''\|_{L_\infty} + 3\Delta^3 \|v_{s+1}'''\|_{L_\infty} \\ &\leq \Delta^2 \|V_{s+1}\|_{L_\infty} (\|p_\Delta''\|_{L_1} + 3\Delta \|p_\Delta'''\|_{L_\infty}) \\ &\leq \Delta^2 (K - H) (\|p_\Delta''\|_{L_1} + 3\Delta \|p_\Delta'''\|_{L_\infty}), \end{aligned}$$

where Lemma M.2 has been used, with a similar result holding for $\|\mathcal{W}_{j,2}^{s+1}\|_{L_\infty}$. Also, for small Δ , we have $\|\mathcal{E}_{I_\ell}\|_{\ell_1} \approx \Delta^{-1} \|\mathcal{E}_{I_\ell}\|_{L_1}$. The result then follows from the considerations above, together with the fact that, if $f = \{f_j\}$ and $g = \{g_j\}$ are sequences such that $f \in \ell_\infty$, $g \in \ell_1$, then $\|f * g\|_{\ell_\infty} \leq \|f\|_{\ell_\infty} \cdot \|g\|_{\ell_1}$, where $*$ denotes the discrete convolution.

M.6. Error bounds for the CDS price

The following result allows one to choose an error tolerance ϵ_P for the calculation of the survival probability P_s at each step of backward induction (cf. (121) in Section M.6) from the error tolerance ϵ for the CDS price. Recall that, for all sources of errors except the truncation in the state space, the total error is approximately proportional to the number of steps in the backward induction cycle.

Lemma M.7. *Consider a CDS contract with maturity T , spread c , recovery rate R and underlying notional Ω , with risk-free rate r , under a discrete time model with time step $\bar{\Delta}$. If ϵ is the error tolerance for the time-0 CDS price, then the maximum error ϵ_P in the calculation of each default probability $P_N = P(N\bar{\Delta})$, in the case of all*

sources of error except truncation in the state space, can be set as

$$\epsilon_P = \frac{\epsilon N \Omega^{-1}}{\left(\frac{c}{r} + 1 - R\right) \frac{1 - e^{-rT} - N e^{-rT} (e^{r\bar{\Delta}} - 1)}{e^{r\bar{\Delta}} - 1} + (1 - R) N e^{-rT}}, \quad (193)$$

where $N = T/\bar{\Delta}$. In the case of truncation in the state space, (M.7) is replaced by

$$\epsilon_P = \frac{\epsilon r \Omega^{-1}}{c(1 - e^{-rT}) + r(1 - R)}. \quad (194)$$

PROOF. Denote by ϵ_s the error in the calculation of $P(s\bar{\Delta})$. For all errors except the one due to truncation in the state space, we have $\epsilon_s \approx s\epsilon_1$. If we denote the corresponding error in the CDS price by $\text{Err}_{\text{CDS}}(T)$, then we can write, using (121)

$$\Omega^{-1} \text{Err}_{\text{CDS}}(T) = \epsilon_1 \left(\frac{c}{r} + 1 - R\right) (1 - e^{-r\bar{\Delta}}) \sum_{s=0}^{N-1} e^{-rs\bar{\Delta}} s + (1 - R) e^{-rT} N \epsilon_1.$$

Hence

$$|\epsilon_1 \Omega^{-1} \text{Err}_{\text{CDS}}(T) \epsilon_1^{-1}| \leq \left(\frac{c}{r} + 1 - R\right) \frac{1 - e^{-rT} - N e^{-rT} (e^{r\bar{\Delta}} - 1)}{e^{r\bar{\Delta}} - 1} + (1 - R) N e^{-rT},$$

from which (193) follows. The proof for the case of the truncation error in the state space is similar, except that one has $\epsilon_s \approx \epsilon_1$. \square

The following result can be used to find a suitable value of x_M so that the absolute error in the survival probability $P(T)$, for $T > 0$, lies below a given error tolerance ϵ .

Lemma M.8. *Let $P(T)$ denote the probability of survival from time 0 until time $T > 0$, calculated using (123). Then the error in the calculation of $P(T)$ due to the truncation of the state space at $x = x_M$ admits the upper bound $e^{-\omega_- x_M} \cdot \sup_{\tau \in [0, T]} e^{-\tau \psi(i\omega_-)}$, for any $\omega_- \in (\lambda_-, 0)$.*

PROOF. We use a similar approach to that for the case of barrier options in Appendix M.2. Recall from Section 5.1.1 that $P(T) = e^{rT}V_{DO}(T, 0)$, where $V_{DO}(T, x)$ is the time-0 price of a (discretely monitored) DO option with payoff $\mathbb{1}_{(h, \infty)}(x)$ and maturity T . Also recall from Appendix M.2 that the truncation of the state space at $x = x_M$ in the calculation of the price of a DO option results in a loss in the option value which is bounded above by the price of an UI option with barrier x_M , which, upon activation, becomes a European option with payoff $G(x) \equiv 1$, barrier e^h and maturity T . Let τ be the first-entrance time into the set $[x_M, \infty)$. Under the transformed measure \mathbb{Q}^γ (where $\gamma \in (0, -\lambda_-)$; cf. Section 5.1.1, Appendix A.3.2), the τ -price of the embedded European option admits the following upper bound

$$\begin{aligned} & e^{-r(T-\tau)} \mathbb{E}_\tau^{\mathbb{Q}^\gamma} [e^{-\gamma X_T} \mathbb{1}_{(h, \infty)}(X_T)] \\ &= e^{-r(T-\tau)} \mathbb{E}_\tau^{\mathbb{Q}^\gamma} [e^{-\gamma(X_\tau + X_T - X_\tau)} \mathbb{1}_{(h, \infty)}(X_T)] \\ &= e^{-r(T-\tau)} e^{-\gamma X_\tau} \mathbb{E}_\tau^{\mathbb{Q}^\gamma} [e^{-\gamma X_{T-\tau}} \mathbb{1}_{(h, \infty)}(X_T)] \\ &\leq e^{-r(T-\tau)} e^{-\gamma X_\tau} e^{-(T-\tau)\psi^\gamma(i\gamma)} = e^{-r(T-\tau)} e^{-\gamma X_\tau}, \end{aligned}$$

since the characteristic exponent of X under \mathbb{Q}^γ is $\psi^\gamma(\xi) = \psi(\xi - i\gamma)$. Hence, at step $t = 0$, the truncation error in the calculation of $V_{DO}(T, x)$, under \mathbb{Q} , is bounded above via the following expression, for any $\omega'_- \in (\lambda_- + \gamma, 0)$

$$\begin{aligned} & \sup_{\tau \in [0, T]} \left\{ e^{\gamma x} e^{-r\tau} \mathbb{E}^{\mathbb{Q}, x} \left[e^{-r(T-\tau) - \gamma x_M} \cdot \mathbb{1}_{[x_M, \infty)}(X_T) \right] \right\} \\ &= e^{-rT} e^{\gamma(x-x_M)} \cdot \sup_{\tau \in [0, T]} \mathbb{E}^{\mathbb{Q}, x} \left[e^{-\omega'_-(X_\tau - x)} \cdot e^{\omega'_-(X_\tau - x)} \mathbb{1}_{[x_M, \infty)}(X_T) \right] \\ &\leq e^{-rT} e^{\gamma(x-x_M) + \omega'_-(x_M - x)} \cdot \sup_{\tau \in [0, T]} e^{-\tau\psi^\gamma(i\omega'_-)} = e^{\omega'_-(x_M - x)} \cdot \sup_{\tau \in [0, T]} e^{-\tau\psi(i\omega'_-)}, \end{aligned}$$

where $\omega_- \in (\lambda_-, 0)$. The result follows from the fact $V_{DO}(T, x) = e^{\gamma x} V_{DO}^\gamma(T, x)$.

□

APPENDIX N

Benchmark prices used in numerical examples

Tables 1 and 2 show the benchmarks used for the numerical comparisons in Section 4.4.

TABLE 1. Benchmark prices used for numerical examples in Section 4.4. DO put option with $H = 80$, $K = 100$, $r = 0.03$, under KoBoL with $\lambda_- = -8$, $\lambda_+ = 9$, $\nu = 1.2$, $m_2 = 0.16$, $r = 0.03$, $q = 0$.

$x - h$	S	$T = 0.25$	$T = 0.5$	$T = 1$	$T = 2$
0.0198598	81.60466	0.7874795	0.3022111	0.1092502	0.0378899
0.0397196	83.24151	1.2045203	0.4655813	0.1688737	0.0586578
0.0595793	84.91120	1.5747130	0.6170645	0.2253475	0.0785302
0.0794391	86.61437	1.8976159	0.7583372	0.2796995	0.0979428
0.0992989	88.35171	2.1686511	0.8888220	0.3320719	0.1170169
0.1191587	90.12389	2.3836597	1.0073908	0.3823338	0.1357724
0.1390184	91.93162	2.5402448	1.1128661	0.4302551	0.1541880
0.1588782	93.77561	2.6382029	1.2042218	0.4755730	0.1722232
0.1787380	95.65659	2.6795476	1.2806787	0.5180235	0.1898282
0.1985978	97.57530	2.6682978	1.3417520	0.5573577	0.2069493
0.2184575	99.53249	2.6101161	1.3872690	0.5933527	0.2235316

TABLE 2. Benchmark prices used for numerical examples in Section 4.4. DO put option with $H = 80$, $K = 100$, $r = 0.03$, under KoBoL with $\lambda_- = -60$, $\lambda_+ = 50$, $\nu = 0.7$, $c = 4$, $r = 0.05$, $q = 0.02$.

$x - h$	S	$T = 0.25$	$T = 0.5$	$T = 1$	$T = 2$
0.0198598	81.60466	2.4672710	1.1678112	0.4804866	0.1775060
0.0397196	83.24151	3.8518309	1.8633295	0.7778474	0.2898515
0.0595793	84.91120	4.9223824	2.4597732	1.0493906	0.3961360
0.0794391	86.61437	5.6382276	2.9398467	1.2907212	0.4956579
0.0992989	88.35171	5.9914948	3.2912529	1.4972945	0.5873418
0.1191587	90.12389	6.0088954	3.5099061	1.6657565	0.6702021
0.1390184	91.93162	5.7438663	3.5998892	1.7942011	0.7434307
0.1588782	93.77561	5.2658178	3.5723590	1.8821954	0.8064230
0.1787380	95.65659	4.6493119	3.4438925	1.9307008	0.8587865
0.1985978	97.57530	3.9649264	3.2345642	1.9419230	0.9003412
0.2184575	99.53249	3.2727447	2.9659962	1.9191107	0.9311127

APPENDIX O

The iFT method for put-like options

In this appendix, we recall two methods for the calculation of integral (106) in Section 4.2.5 with $\omega \in (0, \lambda_+)$. Calculations in the case $\omega \in (\lambda_-, 0)$ can be reduced to the ones in the case $\omega \in (0, \lambda_+)$ by making the change of variables $\xi \mapsto -\xi$ and replacing $\psi(\xi)$ with $\tilde{\psi}(\xi) = \psi(-\xi)$ (cf. Appendix D). The same methods can be applied to integrals with more general functions $\widehat{G}(\xi)$ in place of $(-i\xi)^{-\ell-1}$. See [19] for more details.

O.1. Flat iFT method

We choose a uniformly spaced grid $\xi_j = \xi_1 + (j-1)\zeta$, $j = 1, 2, \dots, 2N+1$, where $\xi_1 = -N\zeta + i\omega$ on the line $\text{Im } \xi = \omega$, discretize the integral using the *infinite trapezoid rule* with grid $i\omega + \zeta\mathbb{Z}$, and truncate the sum

$$I(\omega; n, \ell) \approx \frac{e^{-r\bar{\Delta}}\zeta}{2\pi} \sum_{j=1}^{2N+1} e^{i\xi_j(n\Delta + \mu\bar{\Delta}) - \bar{\Delta}\psi^0(\xi_j)} (-i\xi_j)^{-\ell-1} d\xi. \quad (195)$$

As noted in Section 2.2.2, the number of operations decreases almost twofold using the equivalent expression

$$\begin{aligned} I(\omega; n, \ell) &\approx e^{-r\bar{\Delta} - \omega(n\Delta + \mu\bar{\Delta})} \frac{\zeta}{\pi} \\ &\times \text{Re} \sum_{j=1}^N e^{i\eta_j(n\Delta + \mu\bar{\Delta}) - \bar{\Delta}\psi^0(i\omega + \eta_j)} (\omega - i\eta_j)^{-\ell-1} (1 - \delta_{j=0}/2) d\eta. \end{aligned} \quad (196)$$

Recall that we need to evaluate (196) for $0 \leq n \leq M-1$ if $\ell = 0$, and for $-M+1 \leq n \leq M-1$, if $\ell = 1, 2, 3$. Hence, if M is large (e.g., about a hundred or more) then

the speed of calculations can be enhanced using the iFFT algorithm and its variations (cf. Appendix B, [14, 13, 19]).

O.1.1. Error analysis. As in [45], we start with Theorem 3.2.1 in [81], which we reformulate in accordance with our system of notation. Denote by $f_\ell(\xi)$ the integrand in (106) for a specific choice of ℓ , including the factor $(2\pi)^{-1}$ outside the integral, and choose $[\mu_-, \mu_+] \subset (0, \lambda_+)$ and set $\mathcal{D}(\mu_-, \mu_+) := \{\xi \mid \text{Im } \xi \in (\mu_-, \mu_+)\}$. Let $H^1(\mathcal{D}(0, \lambda_+))$ denote the Hardy space of functions analytic in the strip (μ_-, μ_+) such that

$$\int_{\mu_-}^{\mu_+} |f_\ell(\eta + i\omega)| d\omega \rightarrow 0 \quad \text{as } \eta \rightarrow \pm\infty,$$

and the Hardy norm is finite (cf. Appendix G, [81]):

$$\|f_\ell\|_{\mathcal{D}(\mu_-, \mu_+)} := \lim_{\omega \uparrow \mu_+} \int_{\mathbb{R}} |f_\ell(\eta + i\omega)| d\eta + \lim_{\omega \downarrow \mu_-} \int_{\mathbb{R}} |f_\ell(\eta + i\omega)| d\eta < \infty.$$

Denote by $\mathcal{E}^{\text{disc}}(\zeta; \infty)$ the error of the replacement of the exact option price (106) with the price calculated using the infinite trapezoid rule with mesh ζ , and, for $\omega \in (\mu_-, \mu_+)$, set $d(\omega) = \min\{\omega - \mu_-, \mu_+ - \omega\}$. The following result will be used.

Theorem O.1. ([81, Theorem 3.2.1]). *For $r = 0$, we have*

$$|\mathcal{E}^{\text{disc}}(\zeta; \infty)| \leq \frac{e^{-2\pi d(\omega)/\zeta}}{1 - e^{-2\pi d(\omega)/\zeta}} \|f_\ell\|_{\mathcal{D}(\mu_-, \mu_+)}. \quad (197)$$

Corollary O.1. *Let the error tolerance $\epsilon > 0$ for the discretization error be small so that $\epsilon_f := \epsilon / \|f_\ell\|_{\mathcal{D}(\mu_-, \mu_+)} < 1$. Then, for $r = 0$, the mesh ζ can be chosen as $\zeta = 2\pi d(\omega) / \ln((1 + \epsilon_f) / \epsilon_f)$.*

If $\epsilon \ll 1 / \|f_\ell\|_{\mathcal{D}(\mu_-, \mu_+)}$, then we may (and will) use the following approximation

$$\zeta = 2\pi d(\omega) / \ln(\|f_\ell\|_{\mathcal{D}(\mu_-, \mu_+)}/\epsilon). \quad (198)$$

Set $x' = n\Delta + \mu\bar{\Delta}$. The following estimates of the Hardy norm are derived similarly to Proposition 2.4 in [19].

Proposition O.2. *a) Consider the case of $I_\ell(x)$, $\ell \geq 1$. Then, for $r = 0$ and any $[\mu_-, \mu_+] \subset (0, \lambda_+)$, one can apply (197) and the bound*

$$\|f_\ell\|_{\mathcal{D}(\mu_-, \mu_+)} \leq 2 \max_{\gamma \in \{\mu_-, \mu_+\}} \frac{e^{-\gamma x' - \bar{\Delta}\psi^0(i\gamma)}}{(\ell + 1)\gamma^\ell}, \quad (199)$$

where $x' = x + \mu\bar{\Delta}$.

b) For the calculation of $I_0(x)$, (199) is replaced by

$$\|f_\ell\|_{\mathcal{D}(\mu_-, \mu_+)} \leq \frac{\Gamma(s/2)}{\sqrt{\pi} \Gamma((s+1)/2)} \max_{\gamma \in \{\mu_-, \mu_+\}} \gamma^{-s} e^{-\gamma x' - \bar{\Delta}\psi^0(i\gamma)}, \quad (200)$$

where $s > 0$, and $x' = x + \mu\bar{\Delta}$.

c) For the calculation of $v_{N-1}^{\text{put}}(x)$, (199) is replaced by

$$\|f_\ell\|_{\mathcal{D}(\mu_-, \mu_+)} \leq 2 \max_{\gamma \in \{\mu_-, \mu_+\}} \frac{K e^{-\gamma x' - \bar{\Delta}\psi^0(i\gamma)}}{(\ell + 1)\gamma^\ell}, \quad (201)$$

where $x' = x + \mu\bar{\Delta} - \ln K$.

d) For the calculation of $v_{N-1}^{\text{barr}}(x)$, (199) is replaced by

$$\|f_\ell\|_{\mathcal{D}(\mu_-, \mu_+)} \leq \frac{K\Gamma(s/2)}{\sqrt{\pi} \Gamma((s+1)/2)} \max_{\gamma \in \{\mu_-, \mu_+\}} \gamma^{-s} e^{-\gamma x' - \bar{\Delta}\psi^0(i\gamma)}, \quad (202)$$

where $s > 0$, and $x' = x + \mu\bar{\Delta} - h$.

e) For the calculation of $\Pi_{N-1}(x)$, (199) is replaced by

$$\|f_\ell\|_{\mathcal{D}(\mu_-, \mu_+)} \leq \frac{\Gamma(s/2)}{\sqrt{\pi} \Gamma((s+1)/2)} \max_{\gamma \in \{\mu_-, \mu_+\}} \gamma^{-s} e^{-\gamma x' - \bar{\Delta}\psi^0(i\gamma)}, \quad (203)$$

where $s > 0$, and $x' = x + \mu\bar{\Delta} - h$.

PROOF. Assume $r = 0$. Consider case (a) first. We have

$$\frac{1}{\pi} \int_0^\infty \frac{d\eta}{|\eta + i\omega|^{\ell+1}} = \frac{1}{\pi} \int_0^\infty \frac{d\eta}{(\omega^2 + \eta^2)^{\frac{\ell+1}{2}}} = \begin{cases} \frac{1}{2\omega}, & \ell = 1, \\ \frac{1}{\pi\omega^2}, & \ell = 2, \\ \frac{1}{4\omega^3}, & \ell = 3, \end{cases}$$

where the integral can be calculated using the substitution $\tan \theta = \eta/\omega$. Hence, in all three cases, $((\ell + 1)\omega^\ell)^{-1}$ is an upper bound. For $\omega \in (\lambda_-, \lambda_+)$, $\psi_1(\eta) := \psi^0(\eta + i\omega) - \psi^0(i\omega)$ is the characteristic exponent of a Lévy process, obtained from the process $X - \mu t$ via an Esscher transform (cf. Remark A.14, [18, §1.3.4]). Due to the properties of characteristic functions, $\operatorname{Re} \psi_1(\eta) \geq 0$, and therefore $\operatorname{Re} \psi^0(\eta + i\omega) \geq \psi^0(i\omega)$. It follows that

$$\frac{1}{\pi} \int_0^\infty |f_\ell(\eta + i\omega)| d\eta \leq \sup_{\eta \in \mathbb{R}} \left| e^{-\omega x' - \bar{\Delta} \psi^0(\eta + i\omega)} \right| \cdot \int_0^\infty \frac{d\eta}{|\eta + i\omega|^{\ell+1}} \leq \frac{e^{-\omega x' - \bar{\Delta} \psi^0(i\omega)}}{(\ell + 1)\omega^\ell}.$$

In case (b), with $\ell = 0$, we need a bound for $|I_0(x)|$. For some $s > 0$, we have

$$\begin{aligned} |I_0(x)| &\leq \frac{e^{-\omega x'}}{\pi} \int_0^\infty \frac{e^{-\bar{\Delta} \operatorname{Re} \psi^0(\eta + i\omega)}}{(\omega^2 + \eta^2)^{\frac{1}{2}}} d\eta \leq \frac{e^{-\omega x' - \bar{\Delta} \psi^0(i\omega)}}{\pi} \int_0^\infty \frac{|\eta + i\omega|^{-s}}{(\omega^2 + \eta^2)^{\frac{1}{2}}} d\eta \\ &= \frac{e^{-\omega x' - \bar{\Delta} \psi^0(i\omega)}}{\pi} \int_0^\infty \frac{d\eta}{(\eta^2 + \omega^2)^{\frac{s+1}{2}}} = \frac{e^{-\omega x' - \bar{\Delta} \psi^0(i\omega)}}{2\omega^s \sqrt{\pi}} \frac{\Gamma(s/2)}{\Gamma((s+1)/2)}. \end{aligned}$$

The last step can be proved as follows. Consider the integral

$$I = \int_0^\infty \frac{d\eta}{(\omega^2 + \eta^2)^{\frac{s+1}{2}}}.$$

Using the substitution $\tan \theta = \eta/\omega$, we obtain

$$I = \omega^{-s} \int_0^{\pi/2} (\cos \theta)^{s-1} d\theta. \quad (204)$$

Recall that the beta function, which can be defined by

$$B(x, y) = 2 \int_0^{\pi/2} (\sin \theta)^{2x-1} (\cos \theta)^{2y-1} d\theta \quad (205)$$

for $\operatorname{Re} x > 0$, $\operatorname{Re} y > 0$, satisfies

$$B(x, y) = \frac{\Gamma(x)\Gamma(y)}{\Gamma(x+y)}. \quad (206)$$

The result then follows from (204), (205), and (206). The proofs for cases (c)-(e) are similar. \square

The same argument as in [19, §2.7] can be used to derive from Proposition O.2 the following recommendation for a choice of ω and ζ .

O.1.1.1. *Choice of ω and ζ .* We assume that λ_+ is not small. Given a small discretization error tolerance $\epsilon > 0$, we can use Theorem O.1, Corollary O.1, and Proposition O.2 to choose ω and ζ . Consider first the calculation of $I_\ell(x)$, $\ell \geq 1$ (case (a) in Proposition O.2). We can choose

$$\zeta = \frac{2\pi d(\omega)}{\ln \|f_\ell\|_{D(\mu_-, \mu_+)} - \ln \epsilon}, \quad (207)$$

where $f_\ell(\eta + i\omega)$ again denotes the integrand in (106). We have $0 < \mu_- < \mu_+ < \lambda_+$, and $\omega \in (\mu_-, \mu_+)$. Set $\omega \in (\mu_+ + \mu_-)/2$, then $d = \omega \in (\mu_+ - \mu_-)/2$. Recall that, according to Proposition O.2, we have

$$\|f_\ell\|_{D(\mu_-, \mu_+)} \leq 2 \max_{\gamma \in \{\mu_-, \mu_+\}} \frac{e^{-\gamma x' - \bar{\Delta}\psi^0(i\gamma)}}{(\ell + 1)\gamma^\ell}.$$

It follows from (207) that we can take

$$\zeta = 2\pi d \left[\ln \left(\frac{1}{\epsilon_1} \right) + \min_{\gamma \in \{\mu_-, \mu_+\}} (-\gamma x' - \bar{\Delta}\psi^0(i\gamma) - \ell \ln \gamma) \right]^{-1}, \quad (208)$$

where $\epsilon_1 = (\ell + 1)\epsilon/2$. From the previous considerations, the following modification of the prescription in [19, §2.7] can be used¹

1. If $0.1 \ln(1/\epsilon_1) \geq -\bar{\Delta}\psi^0(i\lambda_+ - 0) - \ell \ln \lambda_+$, then set $\mu_+ = \lambda_+$, otherwise find μ_+ as the unique positive solution of equation $0.1 \ln(1/\epsilon_1) = -\bar{\Delta}\psi^0(i\mu_+) - \ell \ln \mu_+$.
2. Set $\omega = \mu_+/2$, $\mu_- = 0$, $\zeta = -\pi\mu_+/(1.1 \ln \epsilon_1)$.

For $\ell = 0$ (case (b) in Proposition O.2), we have

$$\|f_\ell\|_{D(\mu_-, \mu_+)} \leq \frac{\Gamma(s/2)}{\sqrt{\pi} \Gamma((s+1)/2)} \max_{\gamma \in \{\mu_-, \mu_+\}} \gamma^{-s} e^{-\gamma x' - \bar{\Delta}\psi^0(i\gamma)}.$$

Hence, (208) becomes

$$\zeta = 2\pi d \left[\ln \left(\frac{1}{\epsilon'_1} \right) + \min_{\gamma \in \{\mu_-, \mu_+\}} (-\gamma x' - \bar{\Delta}\psi^0(i\gamma) - s \ln \gamma) \right]^{-1},$$

where now $\epsilon'_1 = \sqrt{\pi}\epsilon\Gamma((s+1)/2)/\Gamma(s/2)$. Numerical testing for KoBoL parameters which typically arise from calibration to market data shows that, in practice, one can usually take $s \in (0, 0.1)$. The algorithm for the choice of ω and ζ is the same as the one for the case $\ell \geq 1$, except that we replace ϵ_1 by ϵ'_1 , and ℓ by s . The modifications for the remaining cases (c)-(e) in Proposition O.2 are straightforward.

Remark O.3. Since the discretization error decays exponentially, in applications, it is not always necessary to use an accurate bound for this error. An alternative procedure is to fix a very large value of the truncation parameter Λ (so that the truncation error is negligible), then start from an initial value of ζ , e.g., $\zeta = 2$, and, in a cycle, reduce it by a factor of 1.5 at each step, say, until the difference in price between two steps lies below a small error tolerance. This procedure works due to the fact that the discretization error in the price, without truncation, decays very fast, as $C \exp[-2\pi d(\omega)/\zeta]$, where C is a constant (cf. Section 3.5.1).

¹Typically, μ_- is close to zero, hence, one can use $\mu_- = 0$ as a good approximation.

Estimates for the truncation error and the choice of truncation parameter Λ under KoBoL for flat iFT, which are not relevant for our purposes, can be found in [19, §2.8].

O.2. Parabolic iFT method (case $x' \geq 0, \omega > 0$)

O.2.1. Deformation and change of variable. Let $x' := n\Delta + \mu\bar{\Delta} \geq 0$. As in Section 2.3.1, we deform the contour of integration in the formula (106) under the conformal map χ_α^+ , defined by (20) for $\alpha \in [1, 2]$. In the same way as (22) was obtained from (12), we obtain from (106)

$$I(\omega; n, \ell) = \frac{e^{-r\bar{\Delta}}}{2\pi} \int_{\text{Im}\xi=\omega} e^{ix'\chi_\alpha^+(\xi) - \bar{\Delta}\psi^0(\chi_\alpha^+(\xi))} (-i\chi_\alpha^+(\xi))^{-\ell-1} \alpha \left(\frac{\lambda_+ + i\xi}{\lambda_+} \right)^{\alpha-1} d\xi. \quad (209)$$

Finally, to decrease CPU time, we take into account that, for real η , $\overline{i(i\omega + \eta)} = i(i\omega - \eta)$, $\overline{i\chi_\alpha^+(i\omega + \eta)} = i\chi_\alpha^+(i\omega - \eta)$ and $\overline{\psi^0(\chi_\alpha^+(i\omega + \eta))} = \psi^0(\chi_\alpha^+(i\omega - \eta))$, and obtain

$$I(\omega; n, \ell) = \frac{e^{-r\bar{\Delta}}}{\pi} \text{Re} \int_{i\omega}^{i\omega+\infty} e^{ix'\chi_\alpha^+(\xi) - \bar{\Delta}\psi^0(\chi_\alpha^+(\xi))} (-i\chi_\alpha^+(\xi))^{-\ell-1} \alpha \left(\frac{\lambda_+ + i\xi}{\lambda_+} \right)^{\alpha-1} d\xi. \quad (210)$$

Recall that we term this variation of iFT conformal parabolic iFT method (or parabolic iFT) of order α , or Para(α) for short.

The larger the α parameter, the faster the integrand in (210) decays at infinity. Recall from Section 2.3.1 that we can consider the analytic continuation of the RHS in (210) w.r.t. α . The rightmost part of (20) admits the analytic continuation w.r.t. α in the whole plane. As noted in Section 2.3.1, $\psi^0(\chi_\alpha^+(\xi))$ for KoBoL with $\nu \in (0, 2)$, $\nu \neq 1$ can be written explicitly as in (24). Finally, it is necessary that the integrand in (209) be of class L_1 . Recall that, in order for this to be the case, we must have $\alpha \in [1, \alpha_0)$, where $\alpha_0 > 1$ depends on x' and the order of the process:

- if $x' > 0$ and $\nu \in [0, 1)$, then $\alpha_0 = \min\{3, 1 + 1/\nu\}$;
- if $x' = 0$ and $\nu \in [0, 1)$, then $\alpha_0 = \min\{4, 1 + 1/\nu\}$;
- if $x' \geq 0$ and $\nu \in [1, 2]$, then $\alpha_0 = 1 + 1/\nu$.

The integral on the RHS of (210) is calculated using the simplified trapezoid rule.

O.2.2. Recommendation for the choice of ω and ζ for parabolic iFT method. In Appendix O.1.1, we analyzed the discretization error for the flat iFT method, giving a procedure to find the mesh ζ and the offset ω in terms of the strip $\text{Im } \xi \in [\mu_-, \mu_+] \subset (0, \lambda_+)$, such that $\omega = (\mu_+ + \mu_-)/2$. We follow the exposition in [19, §5.2.1], which we reformulate in accordance with our system of notation, to outline the procedure for the case of parabolic iFT and put-like options. For parabolic iFT, we need to find σ_{\pm} such that $\chi_{\alpha}^+(i\sigma_{\pm}) = i\mu_{\pm}$, then set $\omega = (\sigma_+ + \sigma_-)/2$, $d = (\sigma_+ - \sigma_-)/2$. The σ_{\pm} can be found from $(\lambda_+ - \mu_{\pm})/\lambda_+ = ((\lambda_+ - \sigma_{\pm})/\lambda_+)^{\alpha}$, which gives

$$\sigma_{\pm} = \lambda_+ - \lambda_+ \left(\frac{\lambda_+ - \mu_{\pm}}{\lambda_+} \right)^{1/\alpha}.$$

If $\mu_- = 0$, then $\sigma_- = 0$, and if $\mu_+ = \lambda_+$, then $\sigma_+ = \lambda_+$. It follows that

$$d = \frac{\lambda_+}{2} \left[\left(\frac{\lambda_+ - \mu_-}{\lambda_+} \right)^{1/\alpha} - \left(\frac{\lambda_+ - \mu_+}{\lambda_+} \right)^{1/\alpha} \right], \quad (211)$$

$$\omega = \lambda_+ - \frac{\lambda_+}{2} \left[\left(\frac{\lambda_+ - \mu_-}{\lambda_+} \right)^{1/\alpha} + \left(\frac{\lambda_+ - \mu_+}{\lambda_+} \right)^{1/\alpha} \right]. \quad (212)$$

If we denote the transformed coordinate by $\eta = \chi_{\alpha}^+(\xi)$, then the domain of analyticity outside the imaginary axis extends to infinity as $\text{Im } \eta \rightarrow \pm\infty$, hence, one can expect the main contribution to the discretization error to come from the bottleneck between the two cuts. Therefore we can select the strip in the transformed η -coordinate which has the same intersection with the imaginary axis as the strip $\text{Im } \xi \in [\mu_-, \mu_+]$ in the

original ξ -coordinate. Similarly to (198), we have

$$\zeta = \frac{2\pi d}{\ln(\|f_\ell(\chi_\alpha^+(\cdot))\|_{D(\sigma_-, \sigma_+)}/\epsilon)},$$

where, e.g., for the calculation of $I_\ell(x)$, we have

$$f_\ell(\chi_\alpha^+(\xi)) = \frac{e^{-r\bar{\Delta}}}{2\pi} e^{ix'\chi_\alpha^+(\xi) - \bar{\Delta}\psi^0(\chi_\alpha^+(\xi))} (-i\chi_\alpha^+(\xi))^{-\ell-1} \alpha \left(\frac{\lambda_+ + i\xi}{\lambda_+} \right)^{\alpha-1}.$$

Since the exponential factor decays very fast as $\text{Re } \xi \rightarrow \pm\infty$ along the lines $\text{Im } \xi = \sigma_\pm$, we can expect to obtain a reasonably good upper bound for it via the modulus of its value at $\xi = i\sigma_\pm$, i.e., at $\chi_\alpha^+(\xi) = i\mu_\pm$. It follows that the Hardy norm in the flat iFT case is approximately equal to the Hardy norm in the parabolic iFT case. Therefore, the following modification of the algorithm in Appendix O.1.1.1 can be used for the choice of ω and ζ , for a given small error tolerance ϵ

1. If $0.1 \ln(1/\epsilon_1) \geq -\bar{\Delta}\psi^0(i\lambda_+ - 0) - \ell \ln \lambda_+$, then set $\mu_+ = \lambda_+$, otherwise find μ_+ as the unique positive solution of equation $0.1 \ln(1/\epsilon_1) = -\bar{\Delta}\psi^0(i\mu_+) - \ell \ln \mu_+$.
2. Set $\mu_- = 0$, calculate d and ω according to (211) and (212), respectively, and set $\zeta = -\pi d/(1.1 \ln \epsilon_1)$.

O.2.3. Recommendations for the choice of truncation parameter Λ . We give the recommendations for KoBoL and VG models, which are straightforward generalizations of those in [19] for the case $\ell = 1$; therein, the reader can also find the recommendation for NIG, and detailed error estimates for the case $\ell = 1$.

Proposition O.4. *Let $\nu \in (0, 2), \nu \neq 1$, and either $x' > 0$ and $\alpha \in (1, \min\{1 + 1/\nu, 3\})$, or $x' = 0$ and $\alpha \in (1, \min\{1 + 1/\nu, 4\})$. If $\epsilon > 0$ is the tolerance for the truncation error in the dual space, and $r = 0$, then*

a) For the calculation of $I_\ell(x)$, Λ can be chosen as the smallest number which satisfies

$$\frac{\alpha}{\alpha\ell + s} \frac{e^{x'A(\Lambda)\Lambda^\alpha + \bar{\Delta}B(\Lambda)\Lambda^{\alpha\nu}}}{\Lambda^{\ell\alpha + s}} < \epsilon\pi\lambda_+^{\ell(1-\alpha)} \exp[c\bar{\Delta}\Gamma(-\nu)(\lambda_+^\nu + (-\lambda_-)^\nu)], \quad (213)$$

where $x' = x + \mu\bar{\Delta}$ and $s = 0$ if $\ell \geq 1$; if $\ell = 0$, then we require that (213) holds for some $s > 0$ (this recommendation is applicable only in the region of sufficiently large Λ , where the LHS is monotone or very close to a monotone function). The functions $A(\Lambda)$ and $B(\Lambda)$ are defined by (25) and (26), respectively.

b) For the calculation of $v_{N-1}^{\text{put}}(x)$, equation (213) is replaced by

$$\frac{Ke^{x'A(\Lambda)\Lambda^\alpha + \bar{\Delta}B(\Lambda)\Lambda^{\alpha\nu}}}{\Lambda^\alpha} < \epsilon\pi\lambda_+^{1-\alpha} \exp[c\bar{\Delta}\Gamma(-\nu)(\lambda_+^\nu + (-\lambda_-)^\nu)], \quad (214)$$

where $x' = x + \mu\bar{\Delta} - \ln K$.

c) For the calculation of v_{N-1}^{barr} , equation (213) is replaced by

$$\frac{2\alpha Ke^{x'A(\Lambda)\Lambda^\alpha + \bar{\Delta}B(\Lambda)\Lambda^{\alpha\nu}}}{s\Lambda^s} < \epsilon\pi \exp[c\bar{\Delta}\Gamma(-\nu)(\lambda_+^\nu + (-\lambda_-)^\nu)], \quad (215)$$

where $x' = x + \mu\bar{\Delta} - h$.

d) For the calculation of $\Pi_{N-1}(x)$, equation (213) is replaced by

$$\frac{\alpha e^{x'A(\Lambda)\Lambda^\alpha + \bar{\Delta}B(\Lambda)\Lambda^{\alpha\nu}}}{s\Lambda^s} < \epsilon\pi \exp[c\bar{\Delta}\Gamma(-\nu)(\lambda_+^\nu + (-\lambda_-)^\nu)], \quad (216)$$

where $x' = x + \mu\bar{\Delta} - h$.

PROOF. Consider case (a) with $\ell \geq 1$. Then (213) follows from Proposition 2.5, together with the fact that, for a decreasing positive function f and any $\Lambda > 0$, we have

$$\int_\Lambda^\infty f(x)\alpha x^{-\ell\alpha-1} dx \leq \frac{f(\Lambda)}{\ell\Lambda^{\alpha\ell}}.$$

If $\ell = 0$, then the proof is similar to that of case (b) in Proposition O.2. \square

Remark O.5. As noted in [19, §5.2], in practice, a good approximation can be obtained by simply neglecting the $O(\Lambda^{-1})$ terms in the definitions of $A(\Lambda)$ and $B(\Lambda)$, i.e., using $A(\infty)$ and $B(\infty)$ instead of $A(\Lambda)$ and $B(\Lambda)$.

O.2.3.1. *Estimates for the L_1 -norms of $\mathcal{E}_{I_\ell}^{\text{disc}}$ and $\mathcal{E}_{I_\ell}^{\text{tr}}$, $\ell \geq 1$.* Since each calculation of $I_\ell(x)$ over the grid $x = n\Delta$, $n = -M + 1, -M + 2, \dots, M - 1$, actually involves two separate parabolic iFT procedures, one for $x' = x + \mu\bar{\Delta} \geq 0$ and the other for $x' < 0$ (cf. Appendix O.3), we need separate bounds for the L_1 -norms of $\mathcal{E}_{I_\ell}^{\text{disc}} \cdot \mathbb{1}_{\{x' \geq 0\}}$ and $\mathcal{E}_{I_\ell}^{\text{disc}} \cdot \mathbb{1}_{\{x' < 0\}}$, and similarly for $\mathcal{E}_{I_\ell}^{\text{tr}}$. The following results can be derived from the bounds for the discretization and truncation errors for parabolic iFT.

Proposition O.6. *Denote by $\mathcal{E}_{I_\ell}^{\text{disc}}(x)$ the discretization error in the calculation of $I_\ell(x)$, $\ell \geq 1$, with mesh ζ , using flat iFT. Then, if $r = 0$, the L_1 -norm of its restriction to $x + \mu\bar{\Delta} \geq 0$ satisfies the following upper bound (cf. (199))*

$$\left\| \mathcal{E}_{I_\ell}^{\text{disc}} \cdot \mathbb{1}_{\{x' \geq 0\}} \right\|_{L_1} \leq \frac{2e^{-2\pi d(\omega)/\zeta}}{1 - e^{2\pi d(\omega)/\zeta}} \max_{\gamma = \{\mu_-, \mu_+\}} \frac{e^{-\bar{\Delta}\psi^0(i\gamma)}}{(\ell + 1)\gamma^{\ell+1}}. \quad (217)$$

Remark O.7. The bound for the case $x' < 0$ is similar, except that instead of the original process one considers the “dual” process (cf. Appendix D). For the case of KoBoL or VGP, this is obtained by replacing λ_\pm with $-\lambda_\mp$, and $\psi^0(\xi)$ with $\tilde{\psi}^0(\xi) := \psi^0(-\xi)$.

Remark O.8. If ϵ is the maximum tolerance for $\left\| \mathcal{E}_{I_\ell}^{\text{disc}} \cdot \mathbb{1}_{\{x' \geq 0\}} \right\|_{L_1}$, then the pair (ω, ζ) can be chosen using the algorithm in Appendix O.2.2, only with $x' = 0$ and the same choice $\epsilon'_1 = (\ell + 1)\epsilon/2$, but replacing ℓ with $\ell + 1$ in Step 1.

Proposition O.9. *If ϵ is the maximum tolerance for $\left\| \mathcal{E}_{I_\ell}^{\text{tr}} \cdot \mathbb{1}_{\{x' \geq 0\}} \right\|_{L_1}$, where $\mathcal{E}_{I_\ell}^{\text{tr}}(x)$ is the truncation error in the calculation of $I_\ell(x)$, $\ell \geq 1$, using parabolic iFT, with truncation parameter Λ , then, in the case where $r = 0$ and the underlying follows a*

KoBoL process of order $\nu \in (0, 2)$, $\nu \neq 1$, Λ can be chosen as the smallest number, which satisfies

$$\frac{e^{\bar{\Delta}B(\infty)\Lambda^{\alpha\nu}}}{\Lambda^{\alpha(\ell+1)}|A(\infty)|} < \epsilon\pi\ell\lambda_+^{\ell(1-\alpha)} \exp[c\bar{\Delta}\Gamma(-\nu)(\lambda_+^\nu + (-\lambda_-)^\nu)]. \quad (218)$$

(This recommendation is applicable only in the region of sufficiently large Λ , where the LHS is monotone or very close to a monotone function).

Remark O.10. The bound for the $x' < 0$ case is similar, except that the absolute values of the steepness parameters are interchanged, $\lambda_\pm \mapsto -\lambda_\mp$, including when calculating the expressions for $A(\Lambda)$ and $B(\Lambda)$ (cf. Appendix D).

O.3. General implementation scheme for parabolic iFT

We give the algorithm for the calculation of the price of a put-like or call-like option using $\text{Para}(\alpha)$, according to (210). We only give the details for the case of OTM and ATM put-like options, since call-like options can be priced using (the equivalent of) put-call parity² (PCP), if needed (e.g., (108) for the calculation of $I(\omega; n, \ell)$).

O.3.1. Choice of α and general scheme for put-like options. We set $\alpha_\nu = 1 + 1/\nu$ for KoBoL with $\nu \in (0, 1)$ or $\nu \in (1, 2)$. The recommended choice of α is as follows

1. $x' > 0$ (OTM). Use $\text{Para}(\alpha)$ with $\alpha \in (1, \min\{3, \alpha_\nu\})$;
2. $x' = 0$ (ATM) Use $\text{Para}(\alpha)$ with $\alpha \in (1, \min\{4, \alpha_\nu\})$;
3. $x' < 0$ (ITM). Price the equivalent (OTM) call-like option, with the same x' , using $\text{Para}(\alpha)$ with $\alpha \in (1, \min\{3, \alpha_\nu\})$, using the symmetry of Appendix D, hence, replacing x' by $-x'$. Finally, apply PCP to recover the price of the original option.

²I.e., the relationship between the price of a call-like option and that of the equivalent put-like option, which can be obtained by using the residue theorem in the iFT expression for the price.

O.3.1.1. *Procedure for the choice of error tolerances ϵ_{\pm} for each subgrid $\mathbf{x}' \geq 0$ and $\mathbf{x}' < 0$, given an overall error tolerance ϵ at a point x'_0 .* This procedure is an initial step which should be performed in order to determine the appropriate error tolerances, as well as the optional output x'_{\pm} , which are used in order to calculate the iFT settings Λ , (ω, ζ) .

1. Take grid \mathbf{x}' , error tolerance ϵ , and point x'_0 (the latter is optional), such that x'_0 lies on \mathbf{x}' .
2. Set³ $\mathbf{x}'_- = \mathbf{x}'(\text{find}(\mathbf{x}' < 0))$ and $\mathbf{x}'_+ = \mathbf{x}'(\text{find}(\mathbf{x}' \geq 0))$.
3. If $x'_0 \in \mathbf{x}'_+$, and \mathbf{x}'_- is empty, then set $x'_+ = x'_0$, $\epsilon_+ = \epsilon$. If $x'_0 \in \mathbf{x}'_-$, and \mathbf{x}'_+ is empty, then set $x'_- = x'_0$, $\epsilon_- = \epsilon$. If x'_0 is not provided, then set $x'_+ = \min(\mathbf{x}'_+)$ and $\epsilon_+ = \epsilon$ if \mathbf{x}'_- is empty, or $x'_- = \max(\mathbf{x}'_-)$ and $\epsilon_- = \epsilon$ if \mathbf{x}'_+ is empty.
4. If neither \mathbf{x}'_- nor \mathbf{x}'_+ is empty, then
 - a. If $x'_0 \in \mathbf{x}'_+$, then set $x'_+ = x'_0$, $x'_- = \max(\mathbf{x}'_-)$, $\epsilon_+ = \epsilon_- = \epsilon/2$.
 - b. If $x'_0 \in \mathbf{x}'_-$, then set $x'_- = x'_0$, $x'_+ = \min(\mathbf{x}'_+)$, $\epsilon_+ = \epsilon_- = \epsilon/2$.
 - c. If x'_0 is not provided, then set $x'_+ = \min(\mathbf{x}'_+)$, $x'_- = \max(\mathbf{x}'_-)$, $\epsilon_+ = \epsilon_- = \epsilon/2$.

O.3.2. Algorithm for parabolic iFT. We describe the algorithm for the implementation of $\text{Para}(\alpha)$, for a given function $\widehat{G}(\xi)$ (the Fourier transform of the payoff) and “driftless” characteristic exponent function $\psi^0(\xi)$, over a grid $\mathbf{x}' = \mathbf{x} + \mu\tau$. We assume that the grid \mathbf{x}' has already been broken into the subgrids \mathbf{x}'_{\pm} (cf. Step 2 of the algorithm in Appendix O.3.1.1), and that the iFT settings Λ_{\pm} and $(\omega_{\pm}, \zeta_{\pm})$ for each subgrid have already been calculated.

The algorithm is as follows

³In this appendix, we use a notation reminiscent of MATLAB syntax.

1. Computation of $\text{Para}(\alpha)$ over the grid \mathbf{x}'_+

a. Create the grids

$$\boldsymbol{\eta} = i\omega_+(0 : N_+ - 1) \cdot \zeta_+,$$

$$\boldsymbol{\eta}_\alpha = i\lambda_+ - i\lambda_+^{1-\alpha} \exp[\alpha \cdot \ln(\lambda_+ + i\boldsymbol{\eta})],$$

$$d\boldsymbol{\eta}_\alpha = \alpha\lambda_+^{1-\alpha} \exp[(\alpha - 1) \cdot \ln(\lambda_+ + i\boldsymbol{\eta})],$$

$$\boldsymbol{\psi}_\alpha = \psi(\chi_\alpha^+(\boldsymbol{\eta})),$$

where $\psi(\chi_\alpha^+(\boldsymbol{\eta}))$ is given by (24) for KoBoL with $\nu \in (0, 1)$ or $\nu \in (1, 2)$.

b. Create the grid $\mathbf{H} = \exp(-\tau(r + \boldsymbol{\psi}_\alpha)) .* d\boldsymbol{\eta}_\alpha .* \widehat{G}(\boldsymbol{\eta}_\alpha)$, then replace $H(1)$ with $H(1)/2$.c. Create the result grid $\mathbf{V}_+ = \text{zeros}(1, M)$.d. In a loop⁴ w.r.t. $j = 1, \dots, M$, set $\mathbf{V}_+ = \exp(ix'(j)\boldsymbol{\eta}_\alpha) .* \mathbf{H} * \text{ones}(1, N_+)$.e. Finally, replace \mathbf{V}_+ with $\zeta_+/\pi \cdot \text{real } \mathbf{V}_+$.2. Repeat the procedure in step 1 over the grid \mathbf{x}'_- , replacing $\widehat{G}(\xi)$ by $\widetilde{G}(\xi) := \widehat{G}(-\xi)$ and $\psi^0(\xi)$ by $\widetilde{\psi}^0(\xi) := \psi^0(-\xi)$. Call the result \mathbf{V}_- .3. Apply PCP to either \mathbf{V}_- or \mathbf{V}_+ , if needed.4. The grid $\mathbf{V} = [\mathbf{V}_- \ \mathbf{V}_+]$ stores the result of the calculation.

⁴This step can be parallelized, rather than run in a loop. However, in the case of discrete barrier options, one typically needs to use rather large grids \mathbf{x}' , hence such a parallelization is usually not feasible.

APPENDIX P

Hilbert transform method

P.1. General idea

This method follows from the approximation theory in Hardy spaces of analytical functions, first applied in finance by Feng and Linetsky [45].

Recall that [18, §15.5.3]

$$\mathcal{F}(\mathbb{1}_{(0,\infty)}f)(\xi) = \frac{1}{2\pi i} \int_{\mathbb{R}} \frac{\hat{f}(\eta)}{\xi - i0 - \eta} d\eta,$$

where $f \in L_1(\mathbb{R})$, and \hat{f} is the Fourier transform of f . By applying the residue theorem, this can be re-written as

$$\mathcal{F}(\mathbb{1}_{(0,\infty)}f)(\xi) = \frac{1}{2}\hat{f}(\xi) + \frac{1}{2i}\mathcal{H}\hat{f}(\xi),$$

where $\mathcal{H}\hat{f}$ is the Hilbert transform of \hat{f} , defined by

$$\mathcal{H}\hat{f}(\xi) = \frac{1}{\pi} P \int_{\mathbb{R}} \frac{\hat{f}(\eta)}{\xi - \eta} d\eta,$$

and P denotes the Cauchy principal value of the integral. From this we obtain

$$\mathcal{F}(\mathbb{1}_{(h,\infty)}f)(\xi) = \frac{1}{2}\hat{f}(\xi) + \frac{1}{2i}e^{-ih\xi}\mathcal{H}(e^{ih\eta}\hat{f}(\eta))(\xi). \quad (219)$$

Similarly,

$$\mathcal{F}(\mathbb{1}_{(-\infty,h)}f)(\xi) = \frac{1}{2}\hat{f}(\xi) - \frac{1}{2i}e^{-ih\xi}\mathcal{H}(e^{ih\eta}\hat{f}(\eta))(\xi). \quad (220)$$

Finally, using $\mathbb{1}_{(h_-, h_+)} = \mathbb{1}_{(h_-, \infty)} - \mathbb{1}_{[h_+, \infty)}$, and noticing that (219) is valid with $[h, \infty)$ instead of (h, ∞) , we obtain

$$\begin{aligned} \mathcal{F}(\mathbb{1}_{(h_-, h_+)} f)(\xi) &= \frac{1}{2i} (e^{-ih_-\xi} \mathcal{H}(e^{ih_-\eta} \hat{f}(\eta)) - e^{-ih_+\xi} \mathcal{H}(e^{ih_+\eta} \hat{f}(\eta)))(\xi) \\ &= \int_{\mathbb{R}} \frac{e^{-ih_-(\xi-\eta)} - e^{-ih_+(\xi-\eta)}}{2\pi i(\xi-\eta)} \hat{f}(\eta) d\eta \\ &= \int_{\mathbb{R}} e^{-i(\xi-\eta)(h_++h_-)/2} \frac{\sin(\frac{(\xi-\eta)(h_+-h_-)}{2})}{\pi(\xi-\eta)} \hat{f}(\eta) d\eta. \end{aligned} \quad (221)$$

P.2. Algorithms

P.2.1. Down-and-out barrier option with terminal payoff G .

1. Put¹ $\widehat{V}_N(\xi) = \mathcal{F}(\mathbb{1}_{(h, \infty)} G)(\xi)$.
2. In a cycle w.r.t. $s = N, N-1, \dots, 1$, calculate

$$\widehat{V}_{s-1}(\xi) = \frac{1}{2} e^{-\bar{\Delta}\psi(\xi)} \widehat{V}_s(\xi) + \frac{e^{-ih\xi}}{2i} \mathcal{H}(e^{ih\eta - \bar{\Delta}\psi(\eta)} \widehat{V}_s(\eta))(\xi). \quad (222)$$

3. Set $V(0, x) = e^{-rT} \mathbb{1}_{(h, \infty)}(x) \cdot V_0(x)$.

P.2.2. Up-and-out barrier option with the terminal payoff G . The algorithm is similar to that of Appendix P.2.1, except that in the first step we put $\widehat{V}_N(\xi) = \mathcal{F}(\mathbb{1}_{(-\infty, h)} G)(\xi)$, in the second step we use (222) with the minus sign in front of the second term on the RHS, and in the third step we use $V(0, x) = e^{-rT} \mathbb{1}_{(-\infty, h)}(x) \cdot V_0(x)$.

P.2.3. Double knock-out barrier options with the terminal payoff G and barriers $H_{\pm} = e^{h_{\pm}}$.

1. Put $\widehat{V}_N(x) = \mathcal{F}(\mathbb{1}_{(h_-, h_+)} G)(\xi)$.

¹In this appendix, we denote by G the terminal payoff without the barrier.

2. In a cycle w.r.t. $s = N, N - 1, \dots, 1$, calculate

$$\widehat{V}_{s-1}(\xi) = \int_{\mathbb{R}} e^{-i(\xi-\eta)(h_++h_-)/2} \frac{\sin(\frac{(\xi-\eta)(h_+-h_-)}{2})}{\pi(\xi-\eta)} e^{-\bar{\Delta}\psi(\eta)} \widehat{V}_s(\eta) d\eta. \quad (223)$$

3. Set $V(0, x) = e^{-rT} \mathbb{1}_{(h_-, h_+)}(x) \cdot V_0(x)$.

P.2.4. Numerical realization of the Hilbert transform. The method, introduced to finance in [41], approximates the Hilbert transform of a function f by the multiplication of the vector of function values \mathbf{f} , of dimension² M , by a Toeplitz matrix T . Since it is known that any $M \times M$ Toeplitz matrix can be embedded into a wider circulant matrix C , and that the multiplication of a circulant matrix C by a vector \mathbf{x} can be realized as follows³ [34, 45]

$$C\mathbf{x} = \text{ifft}(\text{fft}(\mathbf{c}) .* \text{fft}(\mathbf{x}));$$

where \mathbf{c} is first column of C , we end up with the following algorithm for the calculation of the discrete Hilbert transform

1. Compute the entries of the vector $\mathbf{t} = (t_j)_{j=1}^M$, given by

$$t_j = \frac{1 - (-1)^{1-j}}{\pi(1-j)},$$

for $k = 2, \dots, M$, and $t_1 = 0$.

2. Let N denote the smallest power of 2 such that $N \geq 2M - 1$. If M is already a power of 2, then set $N = 2M$.

3. Construct the vector \mathbf{c} such that

$$\mathbf{c} = [-\mathbf{t} \text{ zeros}(1, N - 2 * M + 1) \mathbf{t}(\text{end} : -1 : 2)].$$

²For consistency with the exposition in [45], in this appendix we denote by M the number of points on the dual space grid, rather than the state space grid.

³In this appendix, we use a notation reminiscent of MATLAB syntax.

4. Augment the vector \mathbf{f} by appending $N - M$ zeros to it

$$\mathbf{f}_1 = [\mathbf{f} \text{ zeros}(1, N - M)].$$

5. Calculate

$$\mathbf{g}_1 = \text{ifft}(\text{fft}(\mathbf{c}) .* \text{fft}(\mathbf{f}_1)).$$

6. Finally, discard the last $N - M$ elements in the vector \mathbf{g}_1 to obtain the result vector

$$\mathbf{g} = \mathbf{g}_1(1 : M).$$

We note that the vector $\text{fft}(\mathbf{c})$ can be computed in advance, for several values of M , therefore this method only involves the calculation of one FFT and one inverse FFT of dimensions $2M$ each. For the numerical realization, we used the refined FFT setup of M. Boyarchenko and Levendorskii (cf. Section 2.2.1.1, Appendix B, [14]).

P.2.5. Error estimates. We recall the following error bounds, which follow from a fairly non-trivial approximation theory for functions analytic in a strip around the real axis (see [45] for details and references). Let $V_N(\xi)$ and $\psi(\xi)$ be analytic in a strip $\text{Im } \xi \in (\lambda_-, \lambda_+)$, where $\lambda_- < 0 < \lambda_+$, and let, for some $\nu \in (0, 2]$ and⁴ $\kappa, C > 0$

$$\text{Re } \psi(\xi) \geq \kappa |\xi|^\nu - C, \quad \xi \in \mathbb{R}. \quad (224)$$

Choose $d > 0$ such that $[-d, d] \subset (\lambda_-, \lambda_+)$. Feng and Linetsky [45, §6], proved the following bounds

Proposition P.1. *a) Set*

$$\zeta = \left(\frac{\pi d}{\kappa \Delta} \right)^{\frac{1}{1+\nu}} M^{-\frac{\nu}{1+\nu}}. \quad (225)$$

⁴In [45], the notation c is used instead of κ . Recall that, in our notation, $\kappa = -2c\Gamma(-\nu) \cos(\pi\nu/2)$ for KoBoL with $\nu > 0$, $\nu \neq 1$.

There exists $C > 0$ independent of M such that the error of approximation of the Hilbert transform by the discrete Hilbert transform in (222) admits the bound

$$CM^{\frac{1}{1+\nu}} \exp \left[-(\kappa\bar{\Delta})^{\frac{1}{1+\nu}} (\pi dM)^{\frac{\nu}{1+\nu}} \right]. \quad (226)$$

b) Set

$$\zeta = \left(\frac{2\pi d}{\kappa\bar{\Delta}} \right)^{\frac{1}{1+\nu}} M^{-\frac{\nu}{1+\nu}}. \quad (227)$$

There exists $C > 0$ independent of M such that the error of approximation of the Hilbert transform by the discrete Hilbert transform in (223) admits the bound

$$C \max\{1, M^{\frac{1-\nu}{1+\nu}}\} \exp \left[-(\kappa\bar{\Delta})^{\frac{1}{1+\nu}} (2\pi dM)^{\frac{\nu}{1+\nu}} \right]. \quad (228)$$

c) Define ζ by (225). There exists $C > 0$ independent of M such that the error of approximation of $\mathcal{F}_{\xi \rightarrow x}^{-1} e^{-\bar{\Delta}\psi(\xi)} \widehat{V}^1(\xi)$ by the simplified trapezoid rule admits the bound

$$C \max\{1, M^{\frac{1-\nu}{1+\nu}}\} \exp \left[-(\kappa\bar{\Delta})^{\frac{1}{1+\nu}} (2\pi dM)^{\frac{\nu}{1+\nu}} \right]. \quad (229)$$

APPENDIX Q

COS method

Q.1. Main details

The COS method for vanilla options is based on the following result. The time $t = 0$ price for a European option with maturity T , strike K and underlying spot S_0 following an exponential Lévy process is approximated by

$$V(x, t) = e^{-rT} \sum_{k=0}^{N-1} \operatorname{Re} \left[e^{-(T-t)\psi\left(\frac{k\pi}{b-a}\right)} e^{ik\pi\frac{x-a}{b-a}} \right] U_k(t), \quad (230)$$

where $x = \ln(S_0/K)$, ψ is the characteristic exponent of the underlying Lévy process, and expressions for a , b and the coefficients $U_k(t)$ can be found in [43].

The method can be generalized to the case of discretely monitored barrier options. Denote the barrier by H and the monitoring dates by $0 = t_0 < t_1 < \dots < t_M = T$. Following the conventions in [44], in this appendix we will write $h = \ln(H/K)$. The terminal payoff is given by $G(x) = [\alpha K(e^x - 1)]_+$, where $\alpha = 1$ for a call and $\alpha = -1$ for a put. For simplicity, we also assume that $t_{m+1} - t_m = \bar{\Delta}$, $m = 0, \dots, M - 1$. The generalization of the method to the case of discrete barrier options, which is relevant for our purposes, is based on the following result.

Lemma Q.1 (Lemma 2.1 in [44]). *The time-0 price of an up-and-out (UO) discretely monitored barrier option with no rebate can be approximated using (230) with $T - t$ replaced by $\bar{\Delta}$, and the coefficients U_k calculated by the following backward induction*

procedure. At steps $m = M - 1, M - 2, \dots, 1$, calculate

$$U_k(t_m) = C_k(x_1, x_2, t_m),$$

where

$$\mathbf{C}(x_1, x_2, t_m) = \frac{e^{-r\bar{\Delta}}}{\pi} \text{Im}[(\mathbf{M}_c + \mathbf{M}_s)\mathbf{u}], \quad (231)$$

and in turn

$$\begin{aligned} u_0 &= \frac{1}{2}\varphi(0)U_0(t_{m+1}), \\ u_j &= \varphi\left(\frac{j\pi}{b-a}\right)U_j(t_{m+1}), \end{aligned}$$

where $\varphi(\xi) = e^{-\bar{\Delta}\psi(\xi)}$. The matrices \mathbf{M}_c and \mathbf{M}_s in (231) are given by

$$M_{k,j}^c = \begin{cases} \frac{x_2 - x_1}{b-a}\pi i & k = j = 0, \\ (j+k)^{-1} \left[\exp\left(i(j+k)\frac{x_2-a}{b-a}\pi\right) - \exp\left(i(j+k)\frac{x_1-a}{b-a}\pi\right) \right] & \text{otherwise,} \end{cases} \quad (232)$$

$$M_{k,j}^s = \begin{cases} \frac{x_2 - x_1}{b-a}\pi i & k = j = 0, \\ (j-k)^{-1} \left[\exp\left(i(j-k)\frac{x_2-a}{b-a}\pi\right) - \exp\left(i(j-k)\frac{x_1-a}{b-a}\pi\right) \right] & \text{otherwise,} \end{cases} \quad (233)$$

where $i = \sqrt{-1}$. For the step $t = t_M$, if $h < 0$, $U_k(t_M)$ is given by

$$U_k(t_M) = \begin{cases} 0 & \text{for a call,} \\ G_k(a, h) & \text{for a put.} \end{cases} \quad (234)$$

For $h \geq 0$, on the other hand, $U_k(t_M)$ is given by

$$U_k(t_M) = \begin{cases} G_k(0, h) & \text{for a call,} \\ G_k(a, 0) & \text{for a put.} \end{cases} \quad (235)$$

Finally, the function $G_k(x_1, x_2)$ is given by

$$G_k(x_1, x_2) = \frac{2}{b-a} \alpha K [\chi_k(x_1, x_2) - \psi_k(x_1, x_2)], \quad (236)$$

with

$$\begin{aligned} \chi_k(x_1, x_2) = & \frac{1}{1 + \left(\frac{k\pi}{b-a}\right)^2} \left[\cos\left(k\pi \frac{x_2 - a}{b-a}\right) e^{x_2} - \cos\left(k\pi \frac{x_1 - a}{b-a}\right) e^{x_1} \right. \\ & \left. + \frac{k\pi}{b-a} \sin\left(k\pi \frac{x_2 - a}{b-a}\right) e^{x_2} - \frac{k\pi}{b-a} \sin\left(k\pi \frac{x_1 - a}{b-a}\right) e^{x_1} \right], \end{aligned} \quad (237)$$

and

$$\psi_k(x_1, x_2) = \begin{cases} \left[\sin\left(k\pi \frac{x_2 - a}{b-a}\right) - \sin\left(k\pi \frac{x_1 - a}{b-a}\right) \right] \frac{b-a}{k\pi} & k \neq 0, \\ x_2 - x_1 & k = 0. \end{cases} \quad (238)$$

The $N \times N$ matrices $M_{k,j}^c(x_1, x_2)$ and $M_{k,j}^s(x_1, x_2)$ can be calculated using the FFT. One has

$$\mathbf{M}_c = \begin{bmatrix} m_0 & m_1 & m_2 & \dots & m_{N-1} \\ m_1 & m_2 & \dots & \dots & m_N \\ \vdots & & & & \vdots \\ m_{N-2} & m_{N-1} & \dots & & m_{2N-3} \\ m_{N-1} & \dots & m_{2N-3} & m_{2N-2} \end{bmatrix},$$

$$\mathbf{M}_s = \begin{bmatrix} m_0 & m_1 & \dots & m_{N-2} & m_{N-1} \\ m_{-1} & m_0 & m_1 & \dots & m_{N-2} \\ \vdots & & \ddots & & \vdots \\ m_{2-N} & \dots & m_{-1} & m_0 & m_1 \\ m_{1-N} & m_{2-N} & \dots & m_{-1} & m_0 \end{bmatrix},$$

where the m_j are given by

$$m_j = \begin{cases} \frac{x_2 - x_1}{b - a} \pi i & j = 0, \\ j^{-1} \left[\exp\left(i j \frac{x_2 - a}{b - a} \pi \right) - \exp\left(i j \frac{x_1 - a}{b - a} \pi \right) \right] & j \neq 0, \end{cases}$$

for $j = 0, 1, \dots, 2N - 1$. Note that \mathbf{M}_c is a Hankel matrix and \mathbf{M}_s is a Toeplitz matrix. The matrix-vector products in (231) can be calculated using the FFT. The product $\mathbf{M}_s \mathbf{u}$ is equal, in MATLAB notation, to the first N elements of the vector

$$\text{ifft}(\text{fft}(\mathbf{m}_s) .* \text{fft}(\mathbf{u}_s)),$$

where $\mathbf{u}_s = [u_0, u_1, \dots, u_{N-1}, 0, \dots, 0]$, and

$$\mathbf{m}_s = [m_0, m_{-1}, m_{-2}, \dots, m_{1-N}, 0, m_{N-1}, m_{N-2}, \dots, m_1].$$

The product $\mathbf{M}_c \mathbf{u}$ is given by the first N elements of the vector $\text{ifft}(\text{fft}(\mathbf{m}_c) .* \text{fft}(\mathbf{u}_c))$, in reverse order, where $\mathbf{u}_c = [0, \dots, 0, u_0, u_1, \dots, u_{N-1}]$, and

$$\mathbf{m}_c = [m_{2N-1}, m_{2N-2}, \dots, m_1, m_0].$$

Finally, there is no need to compute the FFTs of both \mathbf{u}_s and \mathbf{u}_c , since

$$\text{fft}(\mathbf{u}_c) = [-1, 1, -1, 1, \dots] .* \text{fft}(\mathbf{u}_s).$$

Q.2. Algorithm

Consider a discretely monitored barrier option with no rebate, barrier H , strike K , spot S_0 , time to maturity T , monitoring interval $\bar{\Delta}$. We use the COS method with N terms. The algorithm is as follows (cf. [44, §2.4]):

1. Set $x = \ln(S_0/K)$, $L = 8$ (cf. Section 3.3 in *op. cit.*) and

$$a = c_1 + x - L\sqrt{c_2 + \sqrt{c_4}}, \quad (239)$$

$$b = c_1 + x + L\sqrt{c_2 + \sqrt{c_4}}, \quad (240)$$

where c_1, c_2, c_4 are the first, second and fourth cumulants of the process, with maturity $\bar{\Delta}$, respectively¹.

2. Calculate the coefficients $U_k(t_M) = G_k(x_1, x_2)$, using (236) with

- $x_1 = 0, x_2 = h$, for an UO call option;
- $x_1 = a, x_2 = h$, for an UO put option;
- $x_1 = 0, x_2 = b$, for a DO call option;
- $x_1 = h, x_2 = 0$, for a DO put option.

3. For $j = 0, 1, \dots, 2N - 1$, set

$$m_j = \begin{cases} \frac{x_2 - x_1}{b - a} \pi i & j = 0, \\ j^{-1} \left[\exp\left(ij \frac{x_2 - a}{b - a} \pi \right) - \exp\left(ij \frac{x_1 - a}{b - a} \pi \right) \right] & j \neq 0, \end{cases}$$

where

- $x_1 = a, x_2 = h$, for an UO option;
- $x_1 = h, x_2 = b$, for a DO option.

¹Expressions for the first four cumulants of VG, KoBoL and NIG processes can be found in [43].

4. Using the fact that $m_{-j} = -\overline{m_j}$, set

$$\mathbf{m}_s = [m_0, m_{-1}, m_{-2}, \dots, m_{1-N}, 0, m_{N-1}, m_{N-2}, \dots, m_1].$$

5. Set

$$\mathbf{m}_c = [m_{2N-1}, m_{2N-2}, \dots, m_1, m_0].$$

6. Calculate

$$\mathbf{d}_1 = \text{fft}(\mathbf{m}_s),$$

$$\mathbf{d}_2 = \mathbf{s} \cdot \text{fft}(\mathbf{m}_c),$$

where $\mathbf{s} = [1, -1, 1, -1, \dots]$.

7. In a cycle w.r.t. $m = M - 1, \dots, m = 1$,

a. Compute $\mathbf{u} = (u_j)_{j=0}^{N-1}$, such that

$$u_0 = \frac{1}{2}\varphi(0)U_0,$$

$$u_j = \varphi\left(\frac{j\pi}{b-a}\right)U_j, \quad j \neq 0.$$

b. Create the vector \mathbf{u}_s by padding N zeros to the right in \mathbf{u} .

c. Calculate the vector \mathbf{M}_s , given by the first N elements of the vector $\text{ifft}(\mathbf{d}_1 \cdot \text{fft}(\mathbf{u}_s))$.

d. Calculate the vector \mathbf{M}_c , given by the first N elements, *in reverse order*, of the vector $\text{ifft}(\mathbf{d}_2 \cdot \text{fft}(\mathbf{u}_s))$.

e. Replace $\mathbf{U} = (U_k)_{k=0}^{N-1}$ by $\pi^{-1}e^{-r\bar{\Delta}} \text{Im}(\mathbf{M}_s + \mathbf{M}_c)$.

8. Replace U_0 by $U_0/2$.

9. Calculate the approximation to the option price via

$$V(x) \approx e^{-r\bar{\Delta}} \sum_{k=0}^{N-1} \operatorname{Re} \left[\varphi \left(\frac{k\pi}{b-a} \right) \cdot \exp \left(ik\pi \frac{x-a}{b-a} \right) \right] U_k.$$

The modification of the COS algorithm for the CDS case can be found in [42].

Bibliography

- [1] M. Abramowitz and I. Stegun (eds.). *Handbook of Mathematical Functions, with Formulas, Graphs and Mathematical Tables*. Dover Publications, Mineola, NY, 1965.
- [2] D. Applebaum. *Lévy processes and infinitely divisible distributions*, volume 116 of *Cambridge Stud. Adv. Math.* Cambridge University Press, Cambridge, second edition, 2009.
- [3] S. Asmussen, D. Madan, and M.R. Pistorius. Pricing Equity Default Swaps under an approximation to the CGMY Lévy model. *Journal of Computational Finance*, 11:79–93, 2008.
- [4] D.H. Bailey and P.N. Swartztrauber. The fractional Fourier transform and applications, 1991.
- [5] O.E. Barndorff-Nielsen. Processes of normal inverse Gaussian type. *Finance and Stochastics*, 2:41–68, 1998.
- [6] C. Becker and U. Wystup. On the cost of delayed currency fixing announcements. *Annals of Finance*, 5:161–174, March 2009.
- [7] J. Bertoin. *Lévy Processes*, volume 121 of *Cambridge Tracts in Mathematics*. Cambridge University Press, 1996.
- [8] T. Björk. *Arbitrage Theory in Continuous Time*. Oxford University Press, Oxford, third edition, 2009.
- [9] F. Black and J.C. Cox. Valuing corporate securities: some effects of bonds indenture provisions. *Journal of Finance*, 31:351–367, 1976.
- [10] F. Black and M. Scholes. The pricing of options and corporate liabilities. *Journal of Political Economy*, 81:637–659, May/June 1973.
- [11] M. Boyarchenko and S. Boyarchenko. Double barrier options in regime-switching hyper-exponential jump-diffusion models. *International Journal of Theoretical and Applied Finance*, 14(7):1005–1043, 2011.

- [12] M. Boyarchenko, M. de Innocentis, and S.Z. Levendorskiĭ. Prices of barrier and first-touch digital options in Lévy-driven models, near barrier. *International Journal of Theoretical and Applied Finance*, 14(7):1045–1090, 2011.
- [13] M. Boyarchenko and S.Z. Levendorskiĭ. Prices and sensitivities of barrier and first-touch digital options in Lévy-driven models. *International Journal of Theoretical and Applied Finance*, 12(8):1125–1170, December 2009.
- [14] M. Boyarchenko and S.Z. Levendorskiĭ. Refined and enhanced fast Fourier transform techniques, with an application to the pricing of barrier options. Working paper, June 2009. Available at SSRN: <http://papers.ssrn.com/abstract=1142833>.
- [15] N. Boyarchenko and S.Z. Levendorskiĭ. On errors and bias of Fourier transform methods in quadratic term structure models. *International Journal of Theoretical and Applied Finance*, 10(2):273–306, 2007.
- [16] S.I. Boyarchenko and S.Z. Levendorskiĭ. On rational pricing of derivative securities for a family of non-Gaussian processes. Preprint 98/7, Institut für Mathematik, Universität Potsdam, 1998. Available at <http://opus.kobv.de/ubp/volltexte/2008/2519>.
- [17] S.I. Boyarchenko and S.Z. Levendorskiĭ. Option pricing for truncated Lévy processes. *International Journal of Theoretical and Applied Finance*, 3(3):549–552, July 2000.
- [18] S.I. Boyarchenko and S.Z. Levendorskiĭ. *Non-Gaussian Merton-Black-Scholes Theory*, volume 9 of *Adv. Ser. Stat. Sci. Appl. Probab.* World Scientific Publishing Co., River Edge, NJ, 2002.
- [19] S.I. Boyarchenko and S.Z. Levendorskiĭ. New efficient versions of Fourier transform method in applications to option pricing. *Journal of Computational Finance*, 2012. (Forthcoming).
- [20] M. Broadie, P. Glasserman, and S.G. Kou. A continuity correction for discrete barrier options. *Mathematical Finance*, 7(4):325–348, October 1997.
- [21] M. Broadie and Y. Yamamoto. Application of the fast Gauss transform to option pricing. *Management Science*, 49(8):1071–1088, 2003.
- [22] M. Broadie and Y. Yamamoto. A double-exponential fast Gauss transform algorithm for pricing discrete path-dependent options. *Operation Research*, 53(5):764–779, 2005.
- [23] J. Cariboni and W. Schoutens. Pricing credit default swaps under Lévy models. *Journal of Computational Finance*, 10(4):1–21, 2007.

- [24] P. Carr. Two extensions to barrier option valuation. *Applied Mathematical Finance*, 2(3):173–209, September 1995.
- [25] P. Carr. Randomization and the American put. *Review of Financial Studies*, 11(3):597–626, Fall 1998.
- [26] P. Carr, H. Geman, D.B. Madan, and M. Yor. The fine structure of asset returns: an empirical investigation. *Journal of Business*, 75:305–332, 2002.
- [27] P. Carr, A. Hogan, and H. Stein. Time for a change: The Variance Gamma model and option pricing. Working paper, January 2007. Available at SSRN: <http://papers.ssrn.com/abstract=956625>.
- [28] P. Carr and D.B. Madan. Option valuation using the Fast Fourier Transform. *Journal of Computational Finance*, 2(4):61–73, 1999.
- [29] A. Castagna. The Hedging Costs of Discrete Monitoring of FX Barrier Options. Working paper, January 2009. Available at SSRN: <http://papers.ssrn.com/abstract=1335302>.
- [30] G. Chacko and S. Das. Pricing interest rate derivatives: a general approach. *Review of Financial Studies*, 15(1):195–241, 2002.
- [31] Iain J. Clark. *Foreign Exchange Option Pricing: A Practitioner's Guide*. The Wiley Finance Series. John Wiley & Sons, Ltd, Chichester, 2010.
- [32] R. Cont and P. Tankov. *Financial Modelling with Jump Processes*. CRC Financ. Math. Ser. Chapman & Hall, Boca Raton, FL, 2004.
- [33] J.W. Cooley and J.W. Tukey. An algorithm for the machine calculation of complex Fourier series. *Mathematical Computing*, 19:297–301, 1965.
- [34] P.J. Davis. *Circulant Matrices*. Chelsea Publishing Company, New York, second edition, 1994.
- [35] M. de Innocentis. Fast calculation of prices and sensitivities of European options under Variance Gamma. Working paper, August 2011. Available at SSRN: <http://papers.ssrn.com/abstract=1916020>.
- [36] M. de Innocentis and S. S.Z. Levendorskii. Pricing discrete barrier options and credit default swaps under Lévy processes. Working paper, June 2012. Available at SSRN: <http://papers.ssrn.com/abstract=2080215>.
- [37] F. Delbaen and W. Schachermayer. A general version of the fundamental theorem of asset pricing. *Math. Ann.*, 300:463–520, 1994.

- [38] D. Duffie, J. Pan, and K. Singleton. Transform Analysis and Asset Pricing for Affine Jump Diffusions. *Econometrica*, 68:1343–1376, 2000.
- [39] E. Eberlein and U. Keller. Hyperbolic distributions in finance. *Bernoulli*, 1:281–299, 1995.
- [40] E. Eberlein and F. Özkan. The Lévy Libor model. *Finance and Stochastics*, 9:327–348, 2005.
- [41] A. Eydeland. A fast algorithm for computing integrals in function spaces: financial applications. *Computational Economics*, 7:277–285, 1994.
- [42] F. Fang, H. Jönsson, C.W. Oosterlee, and W. Schoutens. Fast valuation and calibration of credit default swaps under Lévy dynamics. *Journal of Computational Finance*, 14(2):57–86, Winter 2010.
- [43] F. Fang and C.W. Oosterlee. A novel pricing method for european options based on Fourier-cosine series expansions. *SIAM Journal on Scientific Computing*, 31(2):826–848, 2008.
- [44] F. Fang and C.W. Oosterlee. Pricing early-exercise and discrete barrier options by Fourier-cosine series expansions. *Numerische Mathematik*, 114(1):27–62, 2009.
- [45] L. Feng and V. Linetsky. Pricing discretely monitored barrier options and defaultable bonds in Lévy process models: a fast Hilbert transform approach. *Mathematical Finance*, 18(3):337–384, July 2008.
- [46] W. Gander and W. Gautschi. Adaptive quadrature – revisited. *BIT*, 40(1):84–101, March 1993.
- [47] H. Geman and D.B. Madan. Risks in returns: a pure jump perspective. In *Exotic Option Pricing and Advanced Lévy Models*. Wiley, 2005.
- [48] J.M. Harrison and D.M. Kreps. Martingales and arbitrage in multiperiod securities markets. *Journal of Economic Theory*, 20, 1979.
- [49] J.M. Harrison and S. R. Pliska. Martingales and stochastic integrals in the theory of continuous trading.
- [50] J.M. Harrison and S. R. Pliska. A stochastic calculus model of continuous trading: complete markets. *Stochastic Processes and their Applications*, 15:313–316, 1983.
- [51] S. L. Heston. A closed-form solution for options with stochastic volatility with applications to bond and currency options. *The Review of Financial Studies*, 6(2):327–343, 1993.
- [52] M. Jeannin and M.R. Pistorius. A transform approach to calculate prices and greeks of barrier options driven by a class of Lévy processes. *Quantitative Finance*, 10(6):629–644, 2010.

- [53] I. Koponen. Analytic approach to the problem of convergence of truncated Lévy flights towards the Gaussian stochastic process. *Physics Review E*, 52:1197–1199, 1995.
- [54] S.G. Kou. A jump-diffusion model for option pricing. *Management Science*, 48(8):1086–1101, August 2002.
- [55] S.G. Kou and H. Wang. First passage times of a jump diffusion process. *Advances in Applied Probability*, 35(2):504–531, 2003.
- [56] S.G. Kou and H. Wang. Option pricing under a double exponential jump diffusion model. *Management Science*, 50(9):1178–1192, September 2004.
- [57] O. Kudryavtsev and S.Z. Levendorskiĭ. Fast and accurate pricing of barrier options under Lévy processes. *Finance and Stochastics*, 13(4):531–562, 2009.
- [58] A. Kuznetsov. Wiener-Hopf factorization and distribution of extrema for a family of Lévy processes. *Annals of Applied Probability*, 20, 2009.
- [59] S. Levendorskiĭ. Convergence of Carr’s Randomization Approximation Near Barrier. *SIAM J. Finan. Math.*, 2:79–111, 2011.
- [60] S. Levendorskiĭ and J. Xie. Fast pricing and calculation of sensitivities of OTM European options under Lévy processes. *Journal of Computational Finance*, 15(3):71–133, 2012.
- [61] S.Z. Levendorskiĭ. Pricing of the American put under Lévy processes. *International Journal of Theoretical and Applied Finance*, 7(3):303–335, May 2004.
- [62] A. Lipton. Assets with jumps. *Risk*, pages 149–153, September 2002.
- [63] A. Lipton. Path-dependent options on assets with jumps. 5th Columbia-Jaffe Conference, April 2002. Available at <http://www.math.columbia.edu/~lrb/columbia2002.pdf>.
- [64] R. Lord, F. Fang, F. Bervoets, and C.W. Oosterlee. A fast and accurate FFT-based method for pricing early-exercise options under Lévy processes. *SIAM Journal on Scientific Computing*, 30(4):1678–1705, 2008.
- [65] R. Lord and C. Kahl. Optimal Fourier inversion in semi-analytical option pricing. *Journal of Computational Finance*, 10(4):1–30, Summer 2007.
- [66] D.B. Madan, P. Carr, and E.C. Chang. The Variance Gamma process and option pricing. *European Finance Review*, 2:79–105, 1998.
- [67] D.B. Madan and F. Milne. Option pricing with V.G. martingale components. *Mathematical Finance*, 1(4):39–55, 1991.

- [68] D.B. Madan and W. Schoutens. Break on through the single side. Technical report 07-07, July 2007. Available at: SSRN: <http://papers.ssrn.com/abstract=1003144>.
- [69] D.B. Madan and E. Seneta. The Variance Gamma (V.G.) model for share market returns. *Journal of Business*, 63:511–524, 1990.
- [70] B. Mandelbrot. The variation of certain speculative prices. *Journal of Business*, 36(4):394–419, October 1963.
- [71] R.C. Merton. Theory of rational option pricing. *Bell Journal of Economics and Management Science*, 4:141–183, Spring 1973.
- [72] R.C. Merton. Option pricing when underlying stock returns are discontinuous. *Journal of Financial Economics*, 3:125–144, 1976.
- [73] F.W.J. Olver, D.W. Lozier, R.F. Boisvert, and C.W. Clark (eds.). *NIST Handbook of Mathematical Functions*. National Institute of Science and Technology and Cambridge University Press, New York, 2010.
- [74] W.H. Press, S.A. Teukolsky, W.T. Vetterling, and B.P. Flannery. *Numerical Recipes in C*. Cambridge University Press, New York, second edition, 1992.
- [75] W.H. Press, S.A. Teukolsky, W.T. Vetterling, and B.P. Flannery. *Numerical Recipes – The Art of Scientific Computing*. Cambridge University Press, New York, third edition, 2007.
- [76] R. Rebonato. *Volatility and Correlation – The Perfect Hedger and the Fox*. The Wiley Finance Series. John Wiley & Sons, Ltd., Chichester, 2004.
- [77] K. Sato. *Lévy Processes and Infinitely Divisible Distributions*, volume 68 of *Cambridge Stud. Adv. Math.* Cambridge University Press, Cambridge, 1999.
- [78] L.F. Shampine. Vectorized adaptive quadrature in MATLAB. *Journal of Computational and Applied Mathematics*, 211(2):131–140, January 2008.
- [79] A. Shleifer. *Inefficient Markets: An Introduction to Behavioral Finance*. Clarendon Lectures in Economics. Oxford University Press, Oxford, 2000.
- [80] S.E. Shreve. *Stochastic Calculus for Finance II – Continuous-Time Models*. Springer Verlag, New York, Berlin, 2004.
- [81] F. Stenger. *Numerical Methods based on Sinc and Analytic functions*. Springer Verlag, New York, 1993.

- [82] P. Tankov. Lévy processes in finance and risk management. *Wilmott Magazine*, pages 89–97, September 2007.
- [83] N. M. Temme. Computational aspects of incomplete gamma functions with large complex parameters. In R. V. M. Zahar, editor, *Approximation and Computation. A Festschrift in Honor of Walter Gautschi.*, volume 119 of *International Series of Numerical Mathematics*, pages 551–562. Birkhäuser Boston, Boston, MA, 1994.
- [84] N. Wiener and E. Hopf. Über eine Klasse singulärer Integralgleichungen. *Sitzungsberichte der Preußischen Akademie der Wissenschaften, Mathematisch-Physikalische Klasse*, 30:696–706, 1931.
- [85] S. Winitzki. Computing the incomplete Gamma function to arbitrary precision. *Lecture Notes in Computer Science*, 2667:790–798, 2003.
- [86] U. Wystup. *FX Options and Structured Products*. The Wiley Finance Series. John Wiley & Sons, Ltd., Chichester, 2006.